Alma Mater Studiorum – Università di Bologna

DOTTORATO DI RICERCA IN

INGEGNERIA BIOMEDICA, ELETTRICA E DEI SISTEMI

Ciclo XXXII

Settore Concorsuale: 09 / G1 - AUTOMATICA

Settore Scientifico Disciplinare: ING-INF / 04 - AUTOMATICA

ADVANCED COMPUTATIONAL-EFFECTIVE CONTROL AND OBSERVATION SCHEMES FOR CONSTRAINED NONLINEAR SYSTEMS

Presentata da: Alessandro Bosso

Coordinatore Dottorato | **Supervisore**

Prof. Daniele Vigo | **Prof. Andrea Tilli**

Esame finale anno 2020

Abstract

Constraints are one of the most common challenges that must be faced in control systems design. The sources of constraints in engineering applications are several, ranging from actuator saturations to safety restrictions, from imposed operating conditions to trajectory limitations. Their presence cannot be avoided, and their importance grows even more in high performance or hazardous applications. As a consequence, a common strategy to mitigate their negative effect is to oversize the components. This conservative choice could be largely avoided if the controller was designed taking all limitations into account. Similarly, neglecting the constraints in system estimation often leads to suboptimal solutions, which in turn may negatively affect the control effectiveness. Therefore, with the idea of taking a step further towards reliable and sustainable engineering solutions, based on more conscious use of the plants' dynamics, we decide to address in this thesis two fundamental challenges related to constrained control and observation.

In the first part of this work, we consider the control of uncertain nonlinear systems with input and state constraints, for which a general approach remains elusive. In this context, we propose a novel closed-form solution based on Explicit Reference Governors and Barrier Lyapunov Functions. Notably, it is shown that adaptive strategies can be embedded in the constrained controller design, thus handling parametric uncertainties that often hinder the resulting performance of constraint-aware techniques.

The second part of the thesis deals with the global observation of dynamical systems subject to topological constraints, such as those evolving on Lie groups or homogeneous spaces. Here, general observability analysis tools are overviewed, and the problem of sensorless control of permanent magnets electrical machines is presented as a case of study. Through simulation and experimental results, we demonstrate that the proposed formalism leads to high control performance and simple implementation in embedded digital controllers.

Sommario

La presenza di vincoli è probabilmente una delle più comuni sfide affrontate nella progettazione dei sistemi di controllo. Nelle tipiche applicazioni ingegneristiche i vincoli possono scaturire da molteplici cause, come saturazioni degli attuatori, restrizioni per la sicurezza, l'imposizione di punti di lavoro o limiti sulle traiettorie. La presenza di questi vincoli è ancor più rilevante quando si considerano applicazioni ad elevate prestazioni o pericolose, e molte volte il loro effetto viene mitigato attraverso il sovradimensionamento dei componenti in fase di progettazione. Questa scelta conservativa, molto comune nella pratica ingegneristica, è spesso evitabile attraverso una progettazione consapevole degli algoritmi di controllo. Allo stesso modo, trascurare l'effetto dei vincoli nella ricostruzione dello stato e dei parametri dei sistemi porta a soluzioni inefficienti, di cui inevitabilmente risentono i controllori che ne fanno uso. Per queste motivazioni, lo scopo di questa tesi è affrontare due importanti sfide legate alla gestione dei vincoli nei sistemi di controllo e osservazione, con l'obiettivo di favorire lo sviluppo di soluzioni ingegneristiche sostenibili e affidabili.

La prima parte della tesi è dedicata al problema di stabilizzazione e tracking di sistemi soggetti a vincoli di input e stato. Mentre nel contesto dei sistemi lineari le tecniche di controllo predittivo (Model Predictive Control) stanno sempre più emergendo come standard di fatto nelle applicazioni industriali, civili e militari, lo stesso non si può affermare nel caso di dinamiche nonlineari, per le quali soluzioni generali restano tuttora elusive. L'oggetto dell'attività di ricerca qui presentata consiste, in particolare, nell'esplorazione di una nuova strategia per i sistemi nonlineari soggetti a incertezze, combinando tecniche come gli Explicit Reference Governor e le funzioni barriera. In questo contesto, verrà mostrato come sia possibile includere opportune strategie di adattamento dei parametri all'interno della progettazione del controllo vincolato, gestendo così incertezze che spesso contribuiscono a invalidare tecniche basate su una conoscenza perfetta della dinamica.

La seconda parte di questo lavoro si concentra invece sull'osservazione globale in presenza di vincoli topologici, particolari restrizioni della dinamica che emergono ad esempio in sistemi definiti su gruppi di Lie o spazi omogenei. In seguito alla descrizione di opportune tecniche per lo studio globale dell'osservabilità, verrà considerato come rilevante esempio applicativo il controllo sensorless di macchine elettriche a magneti permanenti. Attraverso risultati numerici simulativi e sperimentali, sarà possibile mostrare come il formalismo qui adottato consenta di ottenere elevate prestazioni e, allo stesso tempo, garantisca una semplice implementazione in sistemi di elaborazione digitale embedded.

Acknowledgements

Firstly, I would like to thank my supervisor Andrea for his constant support, great ideas and deep understanding of so many topics. Thank you for your attention to our group and for constantly keeping us in the loop. Thank you for all the entertaining conversations we had and for being always ready to make hilarious jokes with us. Thank you for believing in me, this has been very important to me and for my life decisions.

I want to deeply thank my parents for their support in this path as a PhD student. Thank you for enduring my bad temper and excessively rational mindset. I could not feel more lucky for the encouragement you gave me, and for the understanding you felt for my desire to chase my dreams instead of immediate certainties. I will do my best not to let you down.

I would like to thank Andrea Serrani for his huge knowledge, incredible intuition and for having improved my skills so much. Thank you for having been so welcoming in Columbus and for always being supportive. Finally, a special thanks goes to all people I met during these years as a PhD. Thank you Christian and Matteo for being so welcoming and inclusive in the team, our lab would not be the same without you. Thank you Davide, Matteo (Burger to the friends) and Ilario for being the best colleagues I could ever imagine. Thanks to all lab mates, you guys are awesome.

Contents

Abstract iii

Sommario v

Acknowledgements vii

I Constrained Control of Uncertain Nonlinear Systems 1

1 Constrained Control of Nonlinear Systems: an Overview 3

1.1 A General Framework for Constrained Control . . . 5
1.2 Model Predictive Control - based Approaches . . . 7
1.2.1 Reference and Command Governors . . . 8
Reference Governors for Linear Systems . . . 9
Robustness to Unmeasured Disturbances . . . 10
Reference Governors for Nonlinear Systems . . . 11
1.2.2 The Explicit Reference Governors . . . 12
1.3 Barrier Functions Approaches . . . 14
1.3.1 Barrier Lyapunov Functions . . . 14
1.3.2 Barrier Lyapunov Function Construction . . . 17
Case 1: $\mathcal{X}$ is a symmetric compact interval . . . 17
Case 2: $\mathcal{X}$ is an asymmetric compact interval . . . 18
Case 3: $\mathcal{X}$ is specified with respect to a function $\psi(x)$ . . . 18
1.3.3 QP Problems based on Barrier Lyapunov Functions . . . 19
1.3.4 Barrier Lyapunov Function Backstepping . . . 21
1.4 Other Techniques . . . 24

2 Constrained-Inversion Model Reference Adaptive Control 25

2.1 Problem Statement . . . 26
2.2 Constrained-Inversion MRAC: Systems in Normal Form . . . 29
2.2.1 Augmented Zero-Dynamics Construction . . . 29
2.2.2 A Preliminary Constrained Controller for the Known-Parameter Case . . . 31
2.2.3 Constrained-Inversion MRAC Design . . . 35
2.3 Application of Constrained-Inversion MRAC to an Euler-Lagrange System . . . 42
2.4 Constrained-Inversion MRAC: Systems in Strict-Feedback Normal Form 47
2.4.1 Challenges in the Design of a Robust Constrained Stabilizer . . . 49
2.4.2 Robust Stabilization: BLF Backstepping with Nonlinear Damping . . . 50
2.4.3 Asymptotic Regulation: x-Swapping Identifier Design . . . 57
2.4.4 State Constraints Feasibility: Right-Inverse Design . . . 60

2.4.5 Tuning Procedure to Enforce Constraint Feasibility: Scalar Relative Degree 1 Example . . . 64
2.5 Concluding Remarks . . . 66

II Observers for Nonlinear Systems on Manifolds **67**

3 Dynamical Systems and Observability on Manifolds **69**
3.1 Dynamical Systems on Manifolds . . . 70
3.1.1 Lie Groups . . . 72
3.1.2 Notable Examples of Lie Groups . . . 73
3.2 Global Observability of Dynamical Systems on Manifolds . . . 76
3.3 Global Observability of Inertial Navigation Systems . . . 78
3.3.1 Inertial Navigation Equations . . . 79
3.3.2 Example 1: 2D Car Navigation . . . 81
3.3.3 Example 2: 3D Vehicle Navigation - Calibrated Sensors . . . 81
3.3.4 Example 3: 3D Vehicle Navigation - Biased Sensors . . . 83
3.4 Observer Design for Systems on Manifolds: State of the Art and Challenges . . . 84

4 Sensorless Observers for PMSMs with no Mechanical Model **87**
4.1 PMSM Dynamics and Observability Analysis . . . 89
4.1.1 Global Observability Analysis through the Indistinguishable Dynamics Approach . . . 90
4.2 A Sensorless Observer with Unknown Mechanical Model . . . 92
4.2.1 Problem Statement . . . 92
4.2.2 Observer Definition . . . 93
4.2.3 A High-Gain Observer for Back-EMF Reconstruction . . . 94
4.2.4 Sensorless Observer with Unknown Mechanical Model: Complete Stability Analysis . . . 96
4.2.5 Sensorless Observer with Unknown Mechanical Model: Domain of Attraction . . . 100
4.3 Advanced UAV Electric Propulsion . . . 103
4.3.1 Open Loop Simulation of the Observer . . . 104
4.3.2 A Computational-Effective Nested Speed Controller . . . 105
4.3.3 Error System Analysis and Tuning . . . 107
4.3.4 The Experimental Setup . . . 109
4.3.5 Closed Loop Experimental Results . . . 110
4.4 Advanced Topics . . . 112
4.4.1 A Controller-Observer for Robust Resistance Estimation . . . 112
4.4.2 A Hybrid Sensorless Observer for Semi-Global Practical Stability 117
A Mini-Batch Identifier for Enhanced Initial Convergence . . . 122
Numerical Comparison of the Proposed Observers . . . 123
4.5 Future Directions . . . 126

A Elements of Lyapunov Stability Theory for Time-Varying Systems **127**

B Proofs **133**
B.1 Proof of Lemma 4.2 . . . 133
B.2 Proof of Theorem 4.3 . . . 135

Bibliography **139**

List of Figures

1.1 Limits imposed to the trajectories as a consequence of the constrained control design. . . . 6
1.2 Typical control scheme arising in Reference Governor design. 9

2.1 Overall Scheme for the Constrained-Inversion MRAC and its interconnection with the plant. . . . 35
2.2 CAD model of a four-bar linkage used as test bench for the proposed Constrained-Inversion MRAC. . . . 41
2.3 Steady-state feedforward input maps associated to system (2.69). . . . 43
2.4 Feasible sets for the right-inverse of system (2.69). . . . 44
2.5 Output tracking performance. The constraints are indicated in red. . . 45
2.6 Internal dynamics behavior of system (2.69). The constraints are indicated in red. . . . 45
2.7 Control input fed to system (2.69). The constraints are indicated in red. 46
2.8 Parameter estimates behavior. The observer variables are solid, while corresponding true values are dashed. . . . 46

3.1 Example of a smooth manifold (2-torus). . . . 70
3.2 Graphical representation of two indistinguishable points, p_1 and p_2. . . 76

4.1 Representation of the domain of attraction of system (4.31), along with some meaningful sets and trajectories. . . . 102
4.2 Speed estimation performance of the proposed sensorless observer. . . 104
4.3 Position and rotor flux amplitude estimation performance of the proposed sensorless observer. . . . 105
4.4 Back-EMF estimation performance of the proposed sensorless observer. 105
4.5 UAV actuator scheme for sensorless FOC. . . . 106
4.6 UAV propeller experimental setup. . . . 110
4.7 Sensorless controller response to some benchmark reference signals (yellow). . . . 111
4.8 Sensorless controller response to an aggressive sinusoidal reference (yellow). . . . 111
4.9 Speed estimation performance of the sensorless controller-observer. . . 116
4.10 Stator resistance and rotor flux amplitude estimation performance of the proposed sensorless controller-observer. . . . 117
4.11 Torque tracking performance of the sensorless controller-observer, and relation with the position estimation error. . . . 117
4.12 Stator currents tracking performance of the sensorless controller-observer. 118
4.13 Speed estimation comparison. (Top): continuous-time observer. (Center): hybrid observer (4.105). (Bottom): hybrid observer with mini-batch identifier. . . . 124

4.14 Position estimation error comparison. (Top): continuous-time observer. (Center): hybrid observer (4.105). (Bottom): hybrid observer with mini-batch identifier. 124
4.15 Inverse flux estimation comparison. (Top): continuous-time observer. (Center): hybrid observer (4.105). (Bottom): hybrid observer with mini-batch identifier. 125
4.16 Back-EMF estimation error comparison. (Top): continuous-time observer. (Center): hybrid observer (4.105). (Bottom): hybrid observer with mini-batch identifier. 125

List of Tables

4.1 Simulation PMSM parameters 104
4.2 T-Motor-Antigravity-4006-KV380 parameters 109
4.3 Tuning Parameters of the Proposed Controller 111

Notation

$\emptyset$	empty set
$\mathbb{N}$	set of natural numbers
$\mathbb{Z}$	set of integer numbers
$\mathbb{Z}_{\geq i}$	set of integer numbers greater than or equal to $i \in \mathbb{Z}$
$\mathbb{Z}_{\leq i}$	set of integer numbers less than or equal to $i \in \mathbb{Z}$
$\mathbb{R}$	set of real numbers
$\mathbb{R}_{\geq s}$	set of real numbers greater than or equal to $s \in \mathbb{R}$
$\mathbb{R}_{\leq s}$	set of real numbers less than or equal to $s \in \mathbb{R}$
$GL(n, \mathbb{R})$	general linear group of $n \times n$ real-valued matrices
$\mathbb{S}^1$	unit circle set (1-torus)
$\mathbb{S}^n$	n-sphere
$SO(n)$	special orthogonal group of $n \times n$ real-valued rotation matrices
$SE(n)$	special Euclidean group in $\mathbb{R}^n$
$\mathbb{B}^n$	closed n-ball of radius 1
I_n	identity matrix of size n
$\in$	belonging to
$\notin$	not belonging to
$\forall$	for all
$\exists$	there exists
$\circ$	function composition
$\subset$	subset of
$\supset$	superset of
$:=$	defined as
$\cup$	union of sets
$\cap$	intersection of sets
$A + B$	sum of sets: $\{a + b, a \in A, b \in B\}$
$A \backslash B$	set difference
$A \sim B$	Pontryagin set difference
A/B	quotient set
$\mathrm{Int}(A)$	interior of the set A
$\partial(A)$	boundary of the set A
M^T	transpose of a matrix M
M^{-1}	inverse of a square matrix M
$\mathrm{Tr}\, M$	trace of a square matrix M
$\mathcal{C}^0$	set of continuous functions
$\mathcal{C}^1$	set of continuously differentiable functions
$\lvert \cdot \rvert$	vector norm or matrix induced norm
$\lVert \cdot \rVert_\infty$	$\mathcal{L}$-infinity norm
$\lVert \cdot \rVert_2$	$\mathcal{L}$-2 norm
$\langle u, v \rangle$	scalar product between u and v
D^+	upper right Dini derivative
$\nabla \phi$	gradient of the scalar function ϕ

$\mathcal{C}[\zeta]$	map from $\zeta \in \mathbb{S}^1$ to its corresponding element in $SO(2)$
CLF	Control Lyapunov Function
BLF	Barrier Lyapunov Function
UCO	uniformly completely observable
PE	persistently exciting
MRAC	model reference adaptive control
PMSM	permanent magnets synchronous machine

Part I

Constrained Control of Uncertain Nonlinear Systems

Chapter 1

Constrained Control of Nonlinear Systems: an Overview

Pointwise-in-time input and state constraints are ubiquitous in control systems, and naturally arise as a crucial element in many high performance engineering applications. Their presence can be appreciated even in the most basic examples of "linear" systems, where linearity is actually just an approximation of the real behavior. Considering a basic introductory example, most steel springs are typically modeled through a linear relation between stress and strain (Hooke's law), but this is true as long as the proportionality limit is not reached, and if then the stress goes beyond the elastic limit, permanent deformation or even rupture will occur. Indeed, in many (actually, most) physical systems, the model that is used to describe the dynamics requires similar "small signals" approximations, meaning that when the involved physical quantities assume large values, undesirable and possibly disruptive phenomena occur. In addition, when considering in particular control systems, the actuator and sensor technologies inevitably lead to saturations and rate limits. We cite (Slotine and Li, 1991; Mazenc and Iggidr, 2004): "saturation is probably the most commonly encountered nonlinearity in control engineering". Nowadays, as further complication of this landscape, the ever growing importance of decision making in large scale or open systems, where there is continuous interaction with humans (autonomous vehicles, cooperative robotics) or vital man-related processes (electric and water distribution, finance), leads to impose safety, reliability and time limitations.

Indeed, the presence of constraints poses significant complications in all the engineering design workflow, from the initial concept to the final application, and in many industrial contexts this is mitigated by oversizing the components. Roughly speaking this conservative choice, that very naturally occurs in engineering decision-making, stems from two sources. On the one hand, the control tools for the usually nonlinear and uncertain plant dynamics are still unavailable or, if present, possibly too complex for implementation in fast real-time architectures. In fact, most of the challenging control problems that are still open for research are associated with uncertain and "aggressive" nonlinear dynamics, thus the algorithms not only need to provide formal guarantees of safety and stability, but also need to be fast and work with limited computational resources available. On the other hand, one very essential issue is that the control design mostly occurs *after* the components/technological design is completed. The decision process of most engineering projects, however, should not be thought as a "series process", but with a feedback itself. In other words, the knowledge of the control engineer should be accounted for *since* the components/technological design, so that not only far better performance can be achieved, but also new behaviors can be unlocked. In this sense, we should move towards applications where, without automatic controls, the proposed solution would not even exist.

This part of the thesis focuses on the first of the aforementioned issues, that is, to provide rigorous mathematical tools to combine the regulation of nonlinear uncertain systems with the problem of hard constraint satisfaction. We believe that this represents one of the main stepping stones towards the second, most ambitious goal. Historically, the problem of constraint handling in control design dates back to the 1940s/1950s, when the problem of input saturation emerged in industrial applications (Lozier, 1956; Galeani et al., 2009) and as early as the 1960s/1970s for the first examples of Model Predictive Control (MPC) in petrochemical and process industries (Propoi, 1963; Richalet et al., 1978), accounting for fully constrained systems. Those methods would become the precursors of the modern Anti-Windup (Grimm et al., 2003; Galeani et al., 2009; Zaccarian and Teel, 2011) and MPC (Mayne et al., 2000) strategies.

From a very general point of view, the methodologies found in the literature explicitly dealing with constraints can be classified according to two key properties. On the one hand, we can separate the control strategies in optimization-based (e.g. MPC) and closed form solutions, where the latter are clearly more oriented towards implementation in fast/embedded architectures, even if the speed advantage often comes at the expense of increased conservativeness. Note that sometimes this distinction is very thin, as is the case of implicit MPC for linear systems, where the heavy optimization routines are moved offline, leading to a static look-up table containing the desired control law. On the other hand, we distinguish between solutions that solve, at the same time, both stabilization/regulation and constraint satisfaction problems, and strategies that augment a nominal "unconstrained" controller with constraint handling features. To the former category belong all main MPC techniques and most methods in the literature employing the so-called Barrier Lyapunov Functions, while in the latter we find Reference Governors (Garone, Cairano, and Kolmanovsky, 2017) and Anti-Windup. Note that Reference Governors share most of the tools with MPC, and indeed they can be regarded as a subclass of it.

With respect to the above strategies, our specific interest is also in accounting for the severe complication given by model uncertainties, typically given in parametric form. The problem of designing controllers that guarantee some degree of robustness with respect to uncertain model parameters has found wide success in automatic control history, and has given birth to the very popular adaptive control techniques (Krstic, Kanellakopoulos, and Kokotovic, 1995; Sastry and Bodson, 2011; Ioannou and Sun, 2012). Because of the inherent properties of these techniques, though, special care is required in the design of constrained controllers with parameters adaptation, in order to effectively preserve feasibility and robustness.

To summarize the above discussion, the contribution of this part of the thesis will be to combine three objectives, which are usually in contrast between each other:

- to guarantee hard constraint satisfaction at all times;
- to preserve an "unconstrained" behavior as much as possible, thus reducing the conservativeness deriving from the above requirement;
- to include adaptive control strategies, guaranteeing at the same time speculative behavior to comply with uncertainties, and preserving a relatively simple structure for implementation with limited computational resources.

We will refer to the approach developed in the next chapter as Constrained-Inversion Model Reference Adaptive Control (briefly, Constrained-Inversion MRAC), because of its distinctive features that allow the combination of all the aforementioned objectives.

The content of this chapter, instead, is aimed at presenting a literature overview, focusing on the tools required for the development of Constrained-Inversion MRAC. In order to remain consistent with the proposed solution, we will mainly concentrate on the two techniques that inspired our design, namely Reference Governors and Barrier Lyapunov Functions.

1.1 A General Framework for Constrained Control

We begin by stating more precisely the general objective of constrained control problems. Since the literature on constrained control is highly heterogeneous, and it is often formulated either in continuous-time or discrete-time, depending on the specific research community, we opt to present an initial formulation based on the formalism of hybrid dynamical systems (Goebel, Sanfelice, and Teel, 2009; Goebel, Sanfelice, and Teel, 2012). In order to make this introduction more direct and explanatory, we will often choose to sacrifice the mathematical formalism to provide a more intuitive understanding of the problem. Consider a generic hybrid system with inputs, given by

$$\mathcal{H}_{\mathrm{P}} : \begin{cases} \dot{x} \in F_{\mathrm{P}}(x,u,w) & (x,u,w) \in C_{\mathrm{P}} \\ x^{+} \in G_{\mathrm{P}}(x,u,w) & (x,u,w) \in D_{\mathrm{P}} \end{cases} \tag{1.1}$$

where $x \in \mathbb{R}^{n}$ is the state vector, $u \in \mathbb{R}^{m}$ is the control input, while $w \in \mathcal{W} \subset \mathbb{R}^{p}$ is an exogenous unknown input, taking values in a compact set $\mathcal{W}$ containing the origin. Furthermore, F_{P} and G_{P} are set valued maps and C_{P}, D_{P} are some subsets of $\mathbb{R}^{n} \times \mathbb{R}^{m} \times \mathcal{W}$. The unknown input w can be in principle used to model several behaviors, such as process noise (perturbations on the actuator commands), parametric uncertainties and/or disturbances that can be generated, for instance, by some kind of exosystem, as in the literature of output regulation (Isidori and Byrnes, 1990; Serrani, Isidori, and Marconi, 2001). In such case, we indicate with $\mathcal{H}_{\mathrm{W}}$ a generic (usually autonomous) model of w, and therefore we can consider the augmented plant given by the interconnection of $\mathcal{H}_{\mathrm{P}}$ and $\mathcal{H}_{\mathrm{W}}$. The concept of interconnection of hybrid systems is not precisely stated here, but it is defined very naturally considering all possible jump combinations for the two systems (either $\mathcal{H}_{\mathrm{P}}$ or $\mathcal{H}_{\mathrm{W}}$ is jumping, or both systems are jumping). We stress since now that this overview will focus on the case of full-state feedback, meaning that x is completely available for measurement. The significantly more complex problem of output feedback is out of the purpose of this thesis, and it will be the content of future research activities.

Define two sets of outputs, given by:

$$\begin{aligned} y &= h(x) \\ y_{\mathrm{c}} &= \gamma(x,u), \end{aligned} \tag{1.2}$$

with $y \in \mathbb{R}^{n_y}$ and $y_{\mathrm{c}} \in \mathbb{R}^{n_{\mathrm{c}}}$, representing the output for tracking and the constrained variables, respectively. In particular, y is required to track a known bounded signal $y_{\mathrm{r}} \in \mathbb{R}^{n_y}$, possibly through some form of projection, whereas y_{c} is imposed to satisfy, whenever solutions exist, a condition of the form $y_{\mathrm{c}} \in \mathcal{Y}_{\mathrm{c}}$, with $\mathcal{Y}_{\mathrm{c}} \subset \mathbb{R}^{n_{\mathrm{c}}}$ an opportune set (clearly the choice $\mathcal{Y}_{\mathrm{c}} = \mathbb{R}^{n_{\mathrm{c}}}$ restores an unconstrained problem formulation). In many applications, it is also common practice to assume that a "nominal" controller is already available, and given by a structure of the form

$$\begin{aligned}&\mathcal{H}_\mathrm{K}:\begin{cases}\dot{\eta}\in F_\mathrm{K}(x,\eta,v) & (x,\eta,v)\in C_\mathrm{K}\\ \eta^+\in G_\mathrm{K}(x,\eta,v) & (x,\eta,v)\in D_\mathrm{K}\end{cases}\\ &u^*=\kappa(x,\eta,v),\end{aligned}\tag{1.3}$$

and with $v\in\mathbb{R}^{n_y}$ a generic input signal to be designed. This type of controller, usually referred to as precompensator, is supposed to guarantee some form of desirable closed loop behavior when the condition $v=y_\mathrm{r}$, $u=u^*$ is satisfied at all times. For instance, it is common to assume that some attractor, satisfying the condition $y-y_\mathrm{r}=0$, is preasymptotically stable (for $w=0$) or input-to-state stable (with input w) for the closed loop interconnection of $\mathcal{H}_\mathrm{P}$ and $\mathcal{H}_\mathrm{K}$. Such attractor is often defined as a set of steady-state equilibria corresponding to constant references in $\mathbb{R}^{n_y}$ (Garone and Nicotra, 2015), but much more general formulations can be provided (see e.g. Byrnes and Isidori, 2003). The role of v, intended as a proxy of y_r, is clearly to adjust the closed loop behavior to account for the constraints, which are in principle completely disregarded in the design of system (1.3). Indeed, the precompensator is often a priori given and can only be manipulated at the terminal v (this commonly occurs, for instance, in industrial applications).

Thus, the problem of constrained control can be summarized as follows: design a dynamical system such that, given any reference y_r belonging to some specific class (e.g. constant or periodic bounded signals), it generates a corresponding feedback law $u(x,y_\mathrm{r},\cdot)$ (resp. $v(x,\eta,y_\mathrm{r},\cdot)$) such that the trajectories of the feedback interconnection satisfy the following properties, for any $w(0,0)=w_0\in\mathcal{W}$ (we consider for simplicity $(0,0)$ as the initial time of the system):

- given the aforementioned set $\mathcal{Y}_\mathrm{c}\subset\mathbb{R}^{n_\mathrm{c}}$, it holds $y_\mathrm{c}\in\mathcal{Y}_\mathrm{c}$ for all the time domain of trajectories originating in a set Ω_0, with Ω_0 that can be a priori computed or approximated (through an appropriate subset) without a priori information on w_0;

- for all initial conditions contained in Ω_0, the output y approaches the reference y_r (or some a priori known set valued map $P(y_\mathrm{r})$), as long as this requirement is not in contrast with the above point.

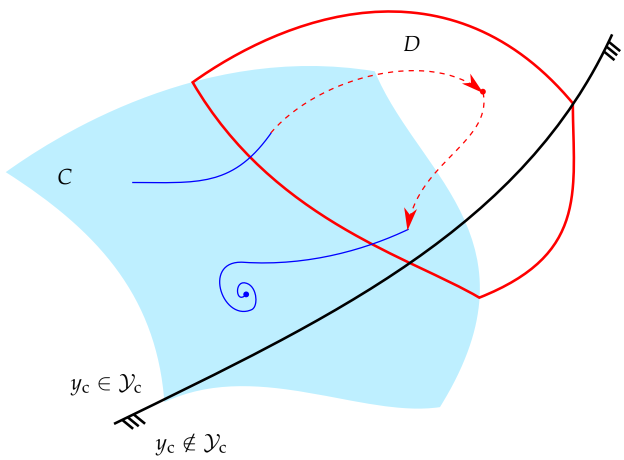

FIGURE 1.1: Limits imposed to the trajectories as a consequence of the constrained control design.

See Figure 1.1 for the intuitive meaning of the problem, where the trajectories of the overall closed loop system, indicated with $\mathcal{H} := (C, F, D, G)$, are constrained in a subset of $C \cup D$.

This problem, in particular if presented in the hybrid formulation, appears in general a formidable task. As a consequence, to the best of the author's knowledge, the literature mainly deals only with the respective continuous- or discrete-time formulations, usually with unrestricted flow sets/jump sets (thus only $\mathcal{Y}_c$ imposes a restriction on the trajectories), and with significant simplifications of the flow maps/jump maps. For practical reasons, it is important to require that some safe initial conditions are known, i.e. a subset of Ω_0 can be numerically computed for trajectory initialization: this requirement is tightly related to the concept of recursive feasibility in optimization-based control, which we will recall in the section dedicated to MPC and Reference Governors. Moreover, the set-valued map P is often inevitable since not all references y_r may be steady-state admissible, meaning that their corresponding attractor is at least in part unfeasible. We can thus employ the above general "directives" as a key for a unifying interpretation of the topic, so that we can proceed now with a coherent overview of the works of interest from the literature.

1.2 Model Predictive Control - based Approaches

This family of controllers is based on the idea of solving, at each sample time, an optimization problem embedding tracking error and input energy in its cost function, over a specific prediction (possibly time-varying) horizon. As a consequence of its optimization-based philosophy, MPC is in principle very convenient to enforce hard constraints at all times, since they can be embedded as constraints in the optimization problem.

We present a brief introduction of MPC in the discrete-time case, since it is the traditional context in which it is treated. For this purpose, consider the following difference equation:

$$x^+ = g(x, u, w), \qquad x(j_0) = x_0 \tag{1.4}$$

where $x \in \mathbb{R}^n$ is the state of the system, $u \in \mathbb{R}^m$ is the control input, and $w \in \mathbb{R}^p$ is an unknown disturbance. For any pair of initial conditions (j_0, x_0), denote with $x(j) = x(j; j_0, x_0, u_{j_0}^{j-1}, w_{j_0}^{j-1})$ the corresponding trajectory, evaluated at time $j \geq j_0$, and related to the input sequences $u_{j_0}^{j-1} = (u(j_0), \ldots, u(j-1))$, $w_{j_0}^{j-1} = (w(j_0), \ldots, w(j-1))$. This notion of solutions will be applied, mutatis mutandis, in the following subsections involving discrete-time systems. Additionally, given a number $N \in \mathbb{Z}_{\geq 1}$, indicate with $\hat{x}(i|\bar{x}, \bar{u})$ an appropriate prediction of system (1.4), with $i \in \{0, \ldots, N\}$, computed from the initial condition $\bar{x}$ and the input sequence $\bar{u} = (u_0, \ldots, u_{N-1})$. Note that it holds $\hat{x}(0|\bar{x}, \bar{u}) = \bar{x}$.

Then, exploiting the above notation, we can define a cost function of the form:

$$V_N(x, \bar{u}) = \sum_{i=0}^{N-1} l(\hat{x}(i|x, \bar{u}), u_i) + J(\hat{x}(N|x, \bar{u})), \tag{1.5}$$

where l is a positive semidefinite loss function embedding the tracking error (given, similarly to the previous section, as $h(\hat{x}(i|x, \bar{u}), u_i)) - y_r$) and, possibly, some penalization of the input amplitude, while J is a function representing the terminal cost. The resulting MPC feedback law, at time j, is then given by the first component

$u_{MPC}(j) = \kappa(x(j)) = u_0^*$ of the optimal input sequence $\bar{u}^*$, which is computed as

$$\begin{aligned} \bar{u}^* &= \arg\min_{\bar{u}} V_N(x(j), \bar{u}) \\ \text{subj. to: } & \gamma(\hat{x}(i|x(j), \bar{u}), u_i) \in \mathcal{Y}_c, \\ & i = 0, \ldots, N. \end{aligned} \tag{1.6}$$

For this specific MPC setup we have defined a prediction horizon, N, which coincides with the size of the input sequence that can be assigned in the optimization problem, referred to as control horizon and indicated with N_c. Otherwise, if N_c is strictly less that N, the remaining $N - N_c$ elements of $\bar{u}$ are kept fixed and coincident with the last term of the decision variable $\bar{u}$, that is $\bar{u} = (u_0, \ldots, u_{N_c-1}, u_{N_c} = u_{N_c-1}, \ldots, u_{N-1} = u_{N_c-1})$. Similar arguments can be used to introduce the continuous-time counterpart of (1.6). It is known from the literature that (1.6) or one of its variants cannot a priori guarantee stability (Mayne et al., 2000) (this is actually the case also for infinite horizon problems, as shown in Kalman, 1960), unless some additional conditions are satisfied. Another important issue is to provide formal guarantees that, if (1.6) is feasible at time j, then the problem is also feasible at time $j+1$. If this condition is verified, then the MPC controller is said to be recursively feasible. This property is often achieved by shaping the optimization problem with specific additional constraints, while we refer to (Löfberg, 2012) for an optimization-based test to verify recursive feasibility with formal guarantees.

We omit here an in-depth description of the stability properties of general formulations of MPC, with the related standing assumptions: for an interested reader, we refer to the reviews (Camacho and Bordons, 2007; Mayne et al., 2000) and references therein. Instead, we are interested in a particular class of predictive controllers, given by Reference Governors, which are specifically designed to efficiently handle constraints in the presence of a nominal precompensator.

1.2.1 Reference and Command Governors

As already mentioned, a very popular strategy to handle input and state constraints is that of Reference Governors, which show many features in common with MPC. Indeed, following the main concepts of MPC, Reference Governors are usually based on (online-) optimization to compute the required control action, thus including the constraints directly within the optimization problem. The main distinctive element however is that, in this case, a precompensator is already feedback interconnected with the plant, and is supposed to provide the optimal behavior. As a consequence, the Reference Governor is introduced solely for the purpose of preserving this nominal behavior as much as possible, while enforcing constraint feasibility at all times. To perform this task, the Reference Governor acts, as the name suggests, on the reference trajectory fed to the inner closed loop system (v in the precompensator in (1.3)) with a role similar to that of a nonlinear filter, i.e. with the purpose of "slowing down" the reference. A representative scheme of the Reference Governor approach is presented in Figure 1.2, where we used the same notation of the introduction and identified the governor with system $\mathcal{H}_{RG}$. Although the initial formulation of the Reference Governor approach was proposed in continuous-time (Kapasouris, Athans, and Stein, 1990), we prefer to present here the results given in the discrete time framework, both for simplicity and to be more consistent with the main literature on the topic.

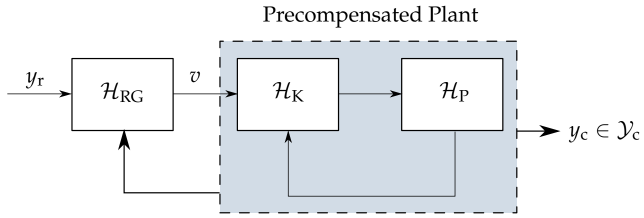

FIGURE 1.2: Typical control scheme arising in Reference Governor design.

Reference Governors for Linear Systems

Consider a linear discrete time system of the form

$$\begin{aligned} x^+ &= Ax + Bv \\ y_\mathrm{c} &= Cx + Dv, \end{aligned} \tag{1.7}$$

where $x \in \mathbb{R}^n$ is the state vector, now including both plant and controller states, $v \in \mathbb{R}^m$ is the input reference, which is required to track $y_\mathrm{r} \in \mathcal{Y}_\mathrm{r} \subset \mathbb{R}^m$, while $y_\mathrm{c} \in \mathbb{R}^{n_\mathrm{c}}$ is the output of the system. We assume that the nominal closed loop system (1.7) is asymptotically stable, i.e. the matrix A is Schur. Here, we consider for simplicity $j_0 = 0$ as initial time of solutions. Similarly to the general framework, the constraints are imposed through the output vector as follows:

$$y_\mathrm{c}(j) \in \mathcal{Y}_\mathrm{c}, \qquad \text{for all } j \in \mathbb{Z}_{\geq 0}, \tag{1.8}$$

where $\mathcal{Y}_\mathrm{c} \subset \mathbb{R}^{n_\mathrm{c}}$ is in this case a compact convex set. In the classical Reference Governor literature, the optimization strategy considers an infinite prediction horizon, and a single step control horizon, so with the above MPC notation, it holds $N = \infty$, $N_\mathrm{c} = 1$. In other words, the goal of Reference Governors is to compute, at each time j, the reference input $v(j)$ that, if kept constant, will never lead to constraint violations. A crucial role in this context is played by the maximum output admissible set, defined as:

$$\mathcal{O}_\infty := \{(x, v) : \hat{y}(i|x, v) \in \mathcal{Y}_\mathrm{c}, \text{ for all } i \in \mathbb{Z}_{\geq 0}\}, \tag{1.9}$$

with the predicted output sequence computed as

$$\begin{aligned} \hat{y}(i|x, v) &= CA^i x + C\sum_{l=1}^{i} A^{l-1}Bv + Dv \\ &= CA^i x + C(I - A)^{-1}(I - A^i)Bv + Dv. \end{aligned} \tag{1.10}$$

Even though $\mathcal{O}_\infty$ could be used to compute v as a function of x, usually a smaller set is introduced for computational simplicity. Let $\epsilon > 0$ be an arbitrary (small) scalar, and denote the steady-state value of system (1.7), for a given constant reference v, with $\bar{y}(v) = (C(I - A)^{-1}B + D)v$, then let the set $\tilde{\mathcal{O}}_\infty$ be defined as follows:

$$\begin{aligned} \tilde{\mathcal{O}}_\infty &:= \mathcal{O}_\infty \cap \mathcal{O}^\epsilon \\ \mathcal{O}^\epsilon &:= \{(x, v) : \bar{y}(v) \in (1 - \epsilon)\mathcal{Y}_\mathrm{c}\}. \end{aligned} \tag{1.11}$$

The advantage of this choice is that, if A is Schur, (C, A) is observable and $\mathcal{Y}_c$ is compact, then $\tilde{\mathcal{O}}_\infty$ is finitely determined, that is there exists $i^* \in \mathbb{Z}_{\geq 0}$ such that

$$\tilde{\mathcal{O}}_\infty = \{(v, x) : \hat{y}(i|v, x) \in \mathcal{Y}_c, i = 0, \ldots, i^*\} \cap \mathcal{O}^\epsilon. \tag{1.12}$$

In addition $\tilde{\mathcal{O}}_\infty$ is positively invariant for constant references v (i.e. $(x, v) \in \tilde{\mathcal{O}}_\infty \implies (x^+, v) \in \tilde{\mathcal{O}}_\infty$) and convex if $\mathcal{Y}_c$ is convex. These considerations easily lead to the Scalar Reference Governor, which involves the solution of an optimization problem of the form

$$\begin{aligned} k(j) = &\max_{k\in[0,1]} k \\ &\text{subj. to: } v = v(j-1) + k(y_r(j) - v(j-1)) \\ &\qquad\qquad (x(j), v) \in \tilde{\mathcal{O}}_\infty, \end{aligned} \tag{1.13}$$

with output of the governor given by $v(j) = v(j-1) + k(j)(y_r(j) - v(j-1))$. Loosely speaking, the Scalar Reference Governor computes the best (closest to y_r) feasible reference value along the line that connects the previous reference $v(j-1)$ and the current target set-point $y_r(j)$. The above optimization problem, due to the properties of $\tilde{\mathcal{O}}_\infty$, is recursively feasible and it can be proven (Gilbert, Kolmanovsky, and Tan, 1995) that any steady-state admissible constant reference y_r leads to finite-time convergence. A similar although more computationally-intesive generalization is that of Command Governors, which solve the following optimization problem, for a given positive definite matrix Q:

$$\begin{aligned} v(j) = &\arg\min_v (v - y_r(j))^T Q (v - y_r(j)) \\ &\text{subj. to: } (x(j), v) \in \tilde{\mathcal{O}}_\infty. \end{aligned} \tag{1.14}$$

For more details on further extensions of these basic schemes, as well as their convergence and computational properties, we refer to (Garone, Cairano, and Kolmanovsky, 2017) and references therein.

Robustness to Unmeasured Disturbances

Consider now a modified version of system (1.7) by including input w:

$$\begin{aligned} x^+ &= Ax + Bv + B_w w \\ y_c &= Cx + Dv + D_w w, \end{aligned} \tag{1.15}$$

where $w \in \mathcal{W}$ is used in particular to model a bounded unknown disturbance, and $\mathcal{W}$ is a set which contains the origin. The previously defined sets can now be reformulated to account for the presence of the disturbance, in particular let

$$\mathcal{O}_\infty := \{(x, v) : \hat{y}_w(i|x, v) \subset \mathcal{Y}_c, \text{ for all } i \in \mathbb{Z}_{\geq 0}\}, \tag{1.16}$$

where $\hat{y}_w(i|v, x)$ is a set-valued map that takes into account all values of the disturbance:

$$\begin{aligned} \hat{y}_w(i|x, v) &:= \hat{y}(i|x, v) + \hat{\mathcal{Y}}_i \\ \hat{\mathcal{Y}}_i &:= C \left(\sum_{l=0}^{i-1} A^{i-l-1} B_w \mathcal{W} \right) + D_w \mathcal{W}. \end{aligned} \tag{1.17}$$

Additionally, we can rewrite $\mathcal{O}_\infty$ employing the Pontryagin set difference:

$$\mathcal{O}_\infty = \{(x,v) : \hat{y}(i|x,v) \in \mathcal{Y}_\mathrm{c} \sim \hat{\mathcal{Y}}_i, \text{ for all } i \in \mathbb{Z}_{\geq 0}\}. \tag{1.18}$$

Due to the fact that A is Schur, then the sequence $\lim_{i\to\infty} \hat{\mathcal{Y}}_i$ converges. Therefore, it is possible to prove that if in addition $\mathcal{Y}_\mathrm{c}$ is convex, the pair (C, A) is observable and $\mathcal{W}$ is compact, then the set $\tilde{\mathcal{O}}_\infty = \mathcal{O}_\infty \cap \mathcal{O}^\epsilon$ is finitely determined and positively invariant as before. It follows that the aforementioned strategies can be applied with no modification except for the increased conservativity. In a similar fashion, the case of output feedback control can be dealt with the addition of the unmeasurable states uncertainty, possibly in combination with an observer to recover the state feedback properties asymptotically.

Reference Governors for Nonlinear Systems

Different approaches can be found in the literature, both dealing with linearized models or directly with the nonlinear dynamics. Among the former category, we find techniques that either perform the linear approximation of the dynamics, treating the mismatch as a disturbance, or feedback linearization. Note that feedback linearization can possibly lead to non-convex constraints, even in the case of convex original constraints. Another similar technique consists of representing the nonlinear dynamics with a family of linear time-varying or parameter-varying models.

Since we are more interested in approaches working directly with the nonlinear dynamics, consider the nominal closed loop system:

$$\begin{aligned} x^+ &= g(x,v) \\ y_\mathrm{c} &= \gamma(x,v), \end{aligned} \tag{1.19}$$

where, for any constant reference v, it is assumed that there exists a unique globally asymptotically stable equilibrium. We want to impose constraints given, for simplicity, by the condition

$$y_\mathrm{c}(j) \in \mathcal{Y}_\mathrm{c} := \{y = (y_1, \dots, y_{n_\mathrm{c}}) \in \mathbb{R}^{n_\mathrm{c}} : y_i \leq 0, i = 1, \dots, n_\mathrm{c}\}, \qquad \text{for all } j \in \mathbb{Z}_{\geq 0}. \tag{1.20}$$

The simplest approach in this context is similar to the aforementioned Scalar Reference Governor, and involves the solution of the following optimization problem:

$$\begin{aligned} k(j) = \max_{k\in[0,1]} & k \\ \text{subj. to: } & v = v(j-1) + k(y_\mathrm{r}(j) - v(j-1)), \\ & \hat{x}(i+1|x(j),v) = g(\hat{x}(i|x(j),v),v), \\ & \hat{y}(i|x(j),v) = \gamma(\hat{x}(i|x(j),v),v) \in \mathcal{Y}_\mathrm{c}, \quad i \in \mathbb{Z}_{\geq 0}. \end{aligned} \tag{1.21}$$

Let $\bar{y}(v) = h(\bar{x}, v)$ denote the output steady-state value, and suppose that for any v satisfying $\bar{y}(v) \in \mathcal{Y}_\mathrm{c}$ the condition $\gamma(\bar{x}, v) \in \mathcal{Y}_\mathrm{c}$ defines a compact set, then the above governor can be recast into a finite prediction horizon problem:

$$\begin{aligned} k(j) = &\max_{k\in[0,1]} k \\ &\text{subj. to: } v = v(j-1) + k(y_\mathrm{r}(j) - v(j-1)), \\ &\qquad\quad \hat{x}(i+1|x(j),v) = g(\hat{x}(i|x(j),v),v), \\ &\qquad\quad \hat{y}(i|x(j),v) = \gamma(\hat{x}(i|x(j),v),v) \in \mathcal{Y}_\mathrm{c}, \quad i \in \{0,\dots,i^*\}, \\ &\qquad\quad \bar{y}(v) = \gamma(\bar{x},v) \le -\epsilon, \end{aligned} \tag{1.22}$$

with $\epsilon > 0$ a sufficiently small scalar and $i^* \in \mathbb{Z}_{\ge 0}$ a sufficiently large integer. In this context, it is once again possible to prove that the sequence of constraint sets as $i^* \to \infty$ is finitely determined. In addition, recursive feasibility can be proven if an initial feasible solution is known. Further details are provided in (Garone, Cairano, and Kolmanovsky, 2017) and references therein. Note that an explicit knowledge of i^* can be avoided if some invariance property that ensures constraints feasibility at all times is known, e.g., when a Lyapunov function $V(x,v)$ is known.

A relevant modification that more actively exploits a Lyapunov characterization is described in the following. Let $\mu(v)$ be a function satisfying

$$V(x,v) \le \mu(v) \implies \gamma(x,v) \in \mathcal{Y}_\mathrm{c}, \tag{1.23}$$

then a simple Reference Governor design is given by

$$\begin{aligned} k(j) = &\max_{k\in[0,1]} k \\ &\text{subj. to: } v = v(j-1) + k(y_\mathrm{r}(j) - v(j-1)), \\ &\qquad\quad V(x(j),v) \le \mu(v) \\ &\qquad\quad \bar{y}(v) = \gamma(\bar{x},v) \le -\epsilon, \end{aligned} \tag{1.24}$$

with nice recursive feasibility, convergence and robustness properties. One main drawback of this approach is the increased conservativity caused by the reformulation of the constraints. This scheme represents the starting point for the construction of the Explicit Reference Governors, which are the main topic of the next subsection. For further details on other discrete-time and optimization-based Reference Governors, we once again refer to (Garone, Cairano, and Kolmanovsky, 2017). We also remark that many other governor structures can be found in the literature. Among these, we find Parameter Governors (Kolmanovsky and Sun, 2006) and output feedback schemes (Hatanaka and Takaba, 2005), to recall some relevant examples.

1.2.2 The Explicit Reference Governors

Resuming from the convenient structure in (1.24), it is possible to consider an analogous closed-form solution for continuous time systems, which we present in the following. Consider a nominal closed loop system of the form

$$\begin{aligned} \dot{x} &= f(x,v) \\ y_\mathrm{c} &= \gamma(x,v), \end{aligned} \tag{1.25}$$

where, as usual, $x \in \mathbb{R}^n$ is the state vector, $v \in \mathbb{R}^{n_y}$ is the reference fed to the inner loop and $y_\mathrm{c} \in \mathbb{R}^{n_\mathrm{c}}$ is an output vector. As usual, the signal v must be chosen to approximate as well as possible a target reference y_r, while preserving feasibility at all times. The above system is subject to the constraints (cf. (1.20)):

$$y_c(t) \in \mathcal{Y}_c := \{y = (y_1, \ldots, y_{n_c}) \in \mathbb{R}^{n_c} : y_i \leq 0, i = 1, \ldots, n_c\}, \qquad \text{for all } t \geq 0. \tag{1.26}$$

Suppose that, for all constant references $v = \bar{v}$, there exists a unique equilibrium point $\bar{x}(v)$ which is globally asymptotically stable under the flows of $\dot{x} = f(x, \bar{v})$. Let in addition $\bar{y}(v) = \gamma(\bar{x}(v), v)$ be the associated constant steady-state output. Related to the given stability property, it is assumed that a Lyapunov function $V(x, v)$, parametrized in the reference vector v, exists and is available for control. As before, let $\mu(v)$ be a function satisfying

$$V(x, v) \leq \mu(v) \implies \gamma(x, v) \in \mathcal{Y}_c, \tag{1.27}$$

then a natural strategy to define the reference trajectory is to generate it through the following simple dynamics (Garone, Cairano, and Kolmanovsky, 2017):

$$\dot{v} = k[\mu(v) - V(x, v)] \frac{y_r - v}{\max\{|y_r - v|, \epsilon\}}, \tag{1.28}$$

with positive scalars k, ϵ. Note that this structure can be directly interpreted as a nonlinear filter of the target reference y_r. A more general solution can be provided if, in addition to the map μ, there exists a map ρ satisfying:

$$\dot{V}\left(x, v, c\frac{\dot{v}}{|\dot{v}|}\right) \leq \dot{\mu}\left(v, c\frac{\dot{v}}{|\dot{v}|}\right), \qquad \forall c \text{ s.t. } 0 \leq c \leq \rho. \tag{1.29}$$

In other words, we assume that there exists an upper bound to the norm of $\dot{v}$ such that it holds $\dot{V} \leq \dot{\mu}$. This requirement, in particular, should be necessary just when the condition $V = \mu$ is satisfied. With all these elements available, the following result defines the general structure of (Lyapunov-based) Explicit Reference Governors (Garone and Nicotra, 2015).

Theorem 1.1. *If the initial conditions $(x(0), v(0))$ satisfy $V(x(0), v(0)) \leq \mu(v(0))$ and if v is designed according to*

$$\dot{v} = \lambda(x, v, y_r) \frac{y_r - v}{|y_r - v|}, \tag{1.30}$$

with $\lambda(\cdot)$ a map such that

$$\begin{aligned} |\lambda(x, v, y_r)| &= 0, & & v = y_r \\ |\lambda(x, v, y_r)| &\leq \rho, & & V(x, v) = \mu(v) \\ |\lambda(x, v, y_r)| &> 0, & & v \neq y_r \text{ and } V(x, v) < \mu(v), \end{aligned} \tag{1.31}$$

then for any bounded reference signal $y_r(\cdot)$ the constraints are always satisfied. In addition, for any constant reference Y_r such that $\bar{y}(Y_r) \in \mathcal{Y}_c$, v converges asymptotically to Y_r.

We refer to (Nicotra and Garone, 2018) for further generalizations of Explicit Reference Governor strategies not involving Lyapunov functions but more general invariance properties.

1.3 Barrier Functions Approaches

Inspired by the use of barrier functions in optimization algorithms, similar structures have emerged in the recent years in the context of automatic controls, due to the evident connection between barriers and Lyapunov functions for constrained systems. Indeed, the basic idea is to construct a function whose level sets are directly related to the shape of the feasible set. According to the nomenclature introduced in (Ames et al., 2017), it is possible to distinguish between two different types of barriers, depending on their behavior as the level sets approach the constraints: the Reciprocal Barrier Functions, whose values tend to infinity, and the Zeroing Barrier Functions, which instead tend to zero. In general, no requirement of convexity is required, thus leading to feasibility without guaranteeing the existence of a unique or stable equilibrium. Other strategies, e.g. those related to (Tee, Ge, and Tay, 2009), embed the barrier properties in the construction of some specific Lyapunov functions, thus giving a precise characterization of the behavior with respect to a desired attractor.

Attempting to provide a unifying description of several strategies encountered in the literature, we present a general definition which employs as main mathematical instrument functions that are proper on the constraint set, thus allowing to consider proper indicator functions as a special case. We refer to the resulting structure as Barrier Lyapunov Functions (BLFs), and from their general definition we derive some interesting properties, as well as methods for their systematic construction. For further insight on how Barrier Lyapunov Functions can be used, some notable control approaches from the recent literature are recalled in the final part of this section.

1.3.1 Barrier Lyapunov Functions

Consider a time-invariant nonlinear system of the form

$$\dot{x} = f(x), \qquad x(0) = x_0. \tag{1.32}$$

where $x \in \mathbb{R}^n$ is the state vector and $f : \mathbb{R}^n \to \mathbb{R}^n$ is a smooth vector field. In the following, we will always let the maps be sufficiently differentiable unless specified otherwise, yet analogous results could be obtained under relaxed regularity assumptions. We want to identify conditions, not based on the explicit computation of the system's trajectories, that allow to analyze the forward invariance properties of a given connected set $\mathcal{X} \subset \mathbb{R}^n$. To support the next developments, let $\mathcal{U}$ be an open set such that $\mathcal{X} \subset \mathcal{U}$ and let $H : \mathcal{U} \to \mathbb{R}$ be such that:

$$\begin{aligned} &H(x) > 0, && x \in \operatorname{Int}(\mathcal{X}) \\ &H(x) = 0, && x \in \partial\mathcal{X} \\ &H(x) < 0, && x \in (\mathcal{X} + \rho\mathbb{B}) \cap (\mathcal{U}/\mathcal{X}), \end{aligned} \tag{1.33}$$

for some positive scalar ρ. The set $(\mathcal{X} + \rho\mathbb{B}) \cap (\mathcal{U}/\mathcal{X})$ is a generalization of $\mathbb{R}^n/\mathcal{X}$, and can be used as a technical instrument for constraints that lead to a feasible set with several connected components. This is the case, for instance, when considering input constraints of nonlinear systems, in particular when they are reformulated as constraints depending directly on the vector field.

Definition 1.1 (Barrier Lyapunov Function)**.** *Consider system* (1.32)*, subject to the constraint $x(t) \in \mathcal{X}$, for all $t \geq 0$. Suppose that* $\operatorname{Int}(\mathcal{X}) \neq \emptyset$*, and let a continuous function $\omega : \operatorname{Int}(\mathcal{X}) \to \mathbb{R}_{\geq 0}$ be proper on* $\operatorname{Int}\mathcal{X}$*. Then, a continuously differentiable function $B : \operatorname{Int}(\mathcal{X}) \to \mathbb{R}_{\geq 0}$ is a Barrier Lyapunov Function for system* (1.32) *on $\mathcal{X}$ if there exist* *class $\mathcal{K}_\infty$ functions $\underline{\alpha}$, $\overline{\alpha}$, χ and a positive scalar c such that, for all $x \in \mathrm{Int}(\mathcal{X})$:*

$$\begin{aligned} \underline{\alpha}(\omega(x)) \leq B(x) &\leq \overline{\alpha}(\omega(x)) \\ L_f B(x) &\leq \frac{1}{\chi(\omega(x)+c)}. \end{aligned} \tag{1.34}$$

The next statement is the main result of this section, and is a reformulation of (Ames et al., 2017, Theorem 1).

Theorem 1.2. *If there exists a Barrier Lyapunov Function B for system (1.32) on $\mathcal{X}$, then the set $\mathrm{Int}(\mathcal{X})$ is forward invariant.*

Proof. Let $[0, t_f)$ be the maximal interval of existence of the solutions. Since χ is increasing, it holds $\chi(\omega(x)+c) \geq \chi(\overline{\alpha}^{-1}(B(x))+c) = \chi(\overline{\alpha}^{-1}(B(x))+\overline{\alpha}^{-1}(\overline{\alpha}(c)))$, and in addition note that for any s_1, $s_2 \geq 0$ it holds $\overline{\alpha}^{-1}(s_1+s_1) \leq \overline{\alpha}^{-1}(2s_1)+\overline{\alpha}^{-1}(2s_2)$, hence we can prove that there exist a positive scalar c_1 and a class $\mathcal{K}_\infty$ function α such that $\chi(\omega(x)+c) \geq \alpha(B(x)+c_1)$. Let $B_1 = B + c_1 > 0$, so there exists a class $\mathcal{K}$ function α_1 such that, for all $t \in [0, t_f)$

$$\dot{B}_1 \leq \alpha_1\left(\frac{1}{B_1}\right). \tag{1.35}$$

Indeed, this is verified by taking α_1 satisfying $\alpha_1(0) = 0$, $\alpha_1(s) = 1/(\alpha(1/s))$, for $s > 0$, and in particular it can be verified that the so-defined function is continuous in its domain and monotonically increasing. We want now to employ the Comparison Lemma in order to characterize the solutions of B_1. From (Ames et al., 2017, Lemma 1) we have that the solution of

$$\dot{y} = \alpha_1\left(\frac{1}{y}\right), \qquad y(0) = y_0 \in \mathbb{R}_{>0} \tag{1.36}$$

is unique and satisfies

$$y = \frac{1}{\beta\left(\frac{1}{y_0}, t\right)}, \qquad t \in [0, t_f) \tag{1.37}$$

for some class $\mathcal{KL}$ function β. It is possible then to recall the Comparison Lemma (with relaxation of the Lipschitz continuity requirement due to the already proven uniqueness of solutions) to show that

$$\underline{\alpha}(\omega(x)) + c_1 \leq B_1(x) \leq \frac{1}{\beta\left(\frac{1}{B_1(x_0)}, t\right)}, \tag{1.38}$$

Note that the left hand side of the inequality chain is positive for all $x \in \mathrm{Int}(\mathcal{X})$ and, thus, there exist a class $\mathcal{K}$ function α_2 and a map H satisfying (1.33) such that

$$\frac{1}{\alpha_2(H(x))} \leq B_1(x), \tag{1.39}$$

thus it follows immediately that

$$\alpha_2^{-1} \circ \beta\left(\frac{1}{B_1(x_0)}, t\right) \leq H(x). \tag{1.40}$$

Since $B_1(x_0) > 0$, it holds that $H(x) > 0$ in $[0, t_f)$. As a consequence, $\mathrm{Int}(\mathcal{X})$ is forward invariant under the dynamics (1.32). □

Note that if $\mathcal{X}$ is compact, then x is bounded with bounds which do not depend on t_f in the proof of the Theorem, and therefore it is possible to pick $t_f = \infty$ and show that the solutions are forward complete. This fact, together with the above result, will be used extensively in the developments of the next chapter. Clearly, the condition $\dot{B}(x) \leq 0$, for all $x \in \mathcal{X}$, is a stronger sufficient condition to guarantee invariance of the set $\mathcal{X}$, and in general it will not be imposed because too restrictive. Indeed the following case, dealing with situations where the dynamics is affected by bounded disturbances, is a simple example where Theorem 1.2 is sufficient to prove invariance.

Corollary 1.1. *Suppose that there exist a continuously differentiable function B, a positive scalar c, a continuous function ω proper on $\mathrm{Int}(\mathcal{X})$ and class $\mathcal{K}_\infty$ functions $\underline{\alpha}$, $\overline{\alpha}$, α such that, for all $x \in \mathrm{Int}(\mathcal{X})$:*

$$\begin{aligned} \underline{\alpha}(\omega(x)) \leq B(x) \leq \overline{\alpha}(\omega(x)) \\ L_f B(x) \leq -\alpha(\omega(x)) + c. \end{aligned} \tag{1.41}$$

Then, $\mathrm{Int}(\mathcal{X})$ is forward invariant.

It is easy to show that Lyapunov functions for $\mathcal{KL}$-stable systems (see Teel and Praly, 2000 and references therein) are indeed Barrier Lyapunov Functions. Assume there exist a compact set $\mathcal{A} \subset \mathrm{Int}(\mathcal{X})$, a proper indicator of $\mathcal{A}$ on $\mathrm{Int}(\mathcal{X})$, a continuously differentiable function V and class $\mathcal{K}_\infty$ functions α_1, α_2 satisfying:

$$\begin{aligned} \alpha_1(\omega(x)) \leq V(x) \leq \alpha_2(\omega(x)) \\ L_f V(x) \leq -V(x). \end{aligned} \tag{1.42}$$

Direct verification shows that V is a Barrier Lyapunov Function.

Similarly, Reciprocal Barrier Functions can be included in the definition.

Definition 1.2 (Reciprocal Barrier Function)**.** *Consider system (1.32), subject to the constraint $x(t) \in \mathcal{X}$, for all $t \geq 0$. Let $H : \mathcal{U} \to \mathbb{R}$ be defined according to (1.33). A continuously differentiable function $B : \mathrm{Int}(\mathcal{X}) \to \mathbb{R}_{\geq 0}$ is a Reciprocal Barrier Function for system (1.32) on $\mathcal{X}$ if there exist class $\mathcal{K}$ functions α_1, α_2, α_3 such that, for all $x \in \mathrm{Int}(\mathcal{X})$:*

$$\begin{aligned} \frac{1}{\alpha_1(H(x))} \leq B(x) \leq \frac{1}{\alpha_2(H(x))} \\ L_f B(x) \leq \alpha_3(H(x)). \end{aligned} \tag{1.43}$$

For completeness, we briefly provide the definition of Zeroing Barrier Functions as well, without however aiming at a full presentation of their properties and their relation with the above Barrier Lyapunov Functions.

Definition 1.3 (Zeroing Barrier Function)**.** *Let $\mathcal{X} \subset \mathbb{R}^n$ be a closed connected set such that $\mathrm{Int}(\mathcal{X}) \neq \emptyset$, and let $H : \mathcal{U} \to \mathbb{R}$ be a continuously differentiable function defined according to (1.33). Then, H is a Zeroing Barrier Function for system (1.32), relative to the set $\mathcal{X}$, if there exist an extended class $\mathcal{K}$ function α, such that, for all $x \in \mathcal{U}$:*

$$L_f H(x) \geq -\alpha(H(x)). \tag{1.44}$$

An invariance property, similar to that in Theorem 1.2, is given next without proof.

Proposition 1.1 (Ames et al., 2017)**.** *If there exists a Zeroing Barrier Function H for system* (1.32)*, relative to the set $\mathcal{X}$, then the set* $\mathrm{Int}(\mathcal{X})$ *is forward invariant.*

Note that the boundedness of Zeroing Barrier Functions makes them better suited for implementation in a digital controller with respect to Reciprocal Barrier Functions. In (Xu et al., 2015) some properties, also related to robustness, are provided for Zeroing Barrier Functions. To conclude this description, we provide (without proof) a converse result which holds provided that the constraint set $\mathcal{X}$ is compact.

Theorem 1.3. *Consider system* (1.32) *and a compact connected set $\mathcal{X}$ such that* $\mathrm{Int}(\mathcal{X}) \neq \emptyset$*, and let $H : \mathcal{U} \to \mathbb{R}$ be defined according to* (1.33)*. Let $\dot{H} > 0$ for all $x \in \partial\mathcal{X}$, then $B = 1/H$, defined in* $\mathrm{Int}(\mathcal{X})$*, and H, defined in $\mathcal{X}$, are a Reciprocal Barrier Function and a Zeroing Barrier Function, respectively.*

1.3.2 Barrier Lyapunov Function Construction

It seems profitable to provide some Barrier Lyapunov Function structures, to be used depending on the context, in a hope to provide some tools for the systematic application of constrained control strategies. We will distinguish the design according to the form of the constraint set $\mathcal{X}$ and that of the attractor, which we limit for simplicity to the case of an equilibrium point x^*. In general, we will show that a simple construction that ensures global convexity and a global minimum in $B(x^*)$ is hard to achieve. This can be often mitigated, however, requiring that the convexity and minimization property are satisfied "sufficiently far" from the constraint boundaries.

Case 1: $\mathcal{X}$ is a symmetric compact interval

This case applies for the barriers employed in (Tee, Ge, and Tay, 2009). The constraint to be imposed is of the form $x \in [x^* - \mu, x^* + \mu]$, for some positive scalar μ. Let $z := x - x^*$ and $p \in \mathbb{N}_{>0}$, then an easy structure is as follows:

$$B(x, x^*) = V(z) = \frac{1}{2p} \log\left(\frac{\mu^{2p}}{\mu^{2p} - z^{2p}}\right) \tag{1.45}$$

A useful property of this function is the following.

Lemma 1.1. *For all $z \in (-\mu, \mu)$, it holds*

$$\log\left(\frac{\mu^{2p}}{\mu^{2p} - z^{2p}}\right) \leq \frac{z^{2p}}{\mu^{2p} - z^{2p}}. \tag{1.46}$$

Proof. Let $w = z^{2p}$, then consider, for $w \in [0, \mu^{2p})$:

$$\phi(w) = \frac{w}{\mu^{2p} - w} - \log\left(\frac{\mu^{2p}}{\mu^{2p} - w}\right). \tag{1.47}$$

Clearly,

$$\frac{d}{dw}\phi(w) = \frac{w}{(\mu^{2p} - w^2)^2}, \tag{1.48}$$

which is 0 only if $w = 0$, while it is positive in $(0, \mu^{2p})$. Note that $\phi(0) = 0$, therefore $\phi(w) \geq 0$ in $[0, \mu^{2p})$. The claim follows immediately. □

Lemma 1.1 is instrumental to establish local exponential stability, and in fact it can be noticed that

$$-z\frac{\partial V}{\partial z} = -z\frac{1}{2p}\frac{\mu^{2p}-z^{2p}}{\mu^{2p}}\frac{2pz^{2p-1}}{(\mu^{2p}-z^{2p})^2} = -\frac{z^{2p}}{\mu^{2p}-z^{2p}} \leq -2pV \leq -V. \tag{1.49}$$

Case 2: $\mathcal{X}$ is an asymmetric compact interval

Firstly, suppose $x^* \in \operatorname{Int}(\mathcal{X})$. Suppose that the constraint takes the form $x \in [x^* - \underline{\mu}; x^* + \overline{\mu}]$. The strategy adopted in (Tee, Ge, and Tay, 2009) is to consider a structure of the form (let $z := x - x^*$)

$$B(x,x^*) = V(z) = \frac{1}{2p}\lambda(z)\log\left(\frac{\underline{\mu}^{2p}}{\underline{\mu}^{2p}-z^{2p}}\right) + \frac{1}{2p}(1-\lambda(z))\log\left(\frac{\overline{\mu}^{2p}}{\overline{\mu}^{2p}-z^{2p}}\right), \tag{1.50}$$

where $p \in \mathbb{N}_{>0}$ is a positive arbitrarily large integer which can be used to make $V(z)$ arbitrarily smooth, and $\lambda(\cdot)$ satisfies:

$$\lambda(z) = \begin{cases} 1, & z > 0 \\ 0, & z \leq 0. \end{cases} \tag{1.51}$$

We consider now the case $x^* \in \mathcal{X}_\mathrm{r} \subset \mathbb{R}$, where $\mathcal{X}_\mathrm{r}$ is a compact set not necessarily included in $\operatorname{Int}(\mathcal{X})$. This case is conceptually important, because in general a constrained control technique should also automatically consider reference "projection" in case it takes unfeasible values. Let $\tau : \operatorname{Int}\mathcal{X} \to \mathcal{R}$ be a diffeomorphism satisfying the following properties:

- $\frac{d\tau}{dx} \geq 1$, for all $x \in \operatorname{Int}\mathcal{X}$;
- $\tau(x) = x$ for all $x \in \overline{\mathcal{X}} \subset \operatorname{Int}\mathcal{X}$, with $\overline{\mathcal{X}}$ compact.

Note that the structure of τ is qualitatively that of a tangent function. A natural selection for the Barrier Lyapunov Function is then as follows:

$$B(x,x^*) = \frac{1}{2}(\tau(x) - x^*)^2. \tag{1.52}$$

As simple as it may seem, this structure allows to embed reference projection, a barrier certificate depending on x and not the tracking error, and a zero tracking error property as long as the reference is sufficiently contained in the constraints, i.e. in the set $\overline{\mathcal{X}}$. This structure was employed in the context of Barrier Lyapunov Functions in (Bosso et al., 2019), partly inspired by the backstepping techniques in (Mazenc and Iggidr, 2004). Note that, regardless of the value of x^*, the unique global minimum of B is, due to the invertibility properties of τ, $\bar{x} = \tau^{-1}(x^*)$, which qualitatively takes the form of a saturation function (or sigmoid, due to smoothness).

Case 3: $\mathcal{X}$ is specified with respect to a function $\psi(x)$

Let ψ be a uniformly continuous function, and suppose that we want to impose a constraint of the form $\underline{\psi} \leq \psi(x) \leq \overline{\psi}$, without a specific attractor. This case is considered for instance in the works (Ames et al., 2017; Serrani and Bolender, 2016; Bosso et al., 2019) and is based on (Boyd and Vandenberghe, 2004, Chapter 11), where the logarithmic barrier function is introduced as an approximator of the indicator function (considered here for the non-negative reals):

$$I_+(s) = \begin{cases} 0, & s \geq 0 \\ +\infty, & s < 0. \end{cases} \tag{1.53}$$

Indeed, consider for this purpose the function

$$H(x) = (\psi(x) - \underline{\psi})(\overline{\psi} - \psi(x)). \tag{1.54}$$

The map $H(x)$ satisfies the conditions presented in (1.33), and can be used to construct an inverse or logarithmic barrier:

$$B_1(x) = \frac{1}{H(x)}, \qquad B_2(x) = -\log\left(\frac{H(x)}{1+H(x)}\right). \tag{1.55}$$

Clearly, these barriers do not enforce asymptotic properties with respect to any attractor, nor are they guaranteed to be convex. Some modifications can be employed, though, to mitigate this undesirable property. Consider a generic Lyapunov function V, then the sum $V(x) + \varepsilon B_i(x)$, $i \in \{1,2\}$, with ε sufficiently small, allows to make the effect of B_i negligible when the constraint is far from active. It is possible to further improve this behavior by considering a modification of H:

$$\begin{aligned} H(x) &= \sigma[\psi(x) - \underline{\psi}]\sigma[\overline{\psi} - \psi(x)] \\ \sigma(s) &= \begin{cases} \lambda\varepsilon, & s \geq \varepsilon \\ \lambda s, & -\varepsilon/2 \leq s \leq \varepsilon/2 \\ -\lambda\varepsilon, & s \leq -\varepsilon, \end{cases} \end{aligned} \tag{1.56}$$

with σ a continuously differentiable function, $\varepsilon > 0$ a sufficiently small scalar and $\lambda > 0$ an arbitrarily large scalar (e.g. $\lambda = 1/\varepsilon$ for simplicity). The idea is that if the differences of both $\psi(x) - \underline{\psi}$ and $\overline{\psi} - \psi(x)$ are larger than a small scalar ε, then $B(x)$ becomes flat. As a consequence, any Lyapunov function V defined with respect to an attractor $\mathcal{A}$ "sufficiently feasible" with respect to the constraint on ψ, will lead to a Barrier Lyapunov Function $V(x) + B_i(x)$, $i \in \{1,2\}$, with a global minimum in $\mathcal{A}$ and locally convex in a neighborhood of $\mathcal{A}$. Note that σ in the above structure can be a sigmoid, and can be approximated e.g. with an arctangent function.

1.3.3 QP Problems based on Barrier Lyapunov Functions

Several examples can be found in the literature that exploit universal formulas, similar to Sontag's formula (Sontag, 1989) or the Pointwise Minimum Norm (PMN) formula (Freeman and Kokotovic, 1996) in order to compute a stabilizing control law through an optimization problem. Let for simplicity a nonlinear control-affine system of the form

$$\dot{x} = f(x) + g(x)u, \tag{1.57}$$

with $x \in \mathbb{R}^n$ the state vector, and $u \in \mathbb{R}^m$ the input vector. Let f and g be smooth vector fields. We recall that a positive definite, radially unbounded, continuously differentiable function V is a Control Lyapunov Function (CLF) if it satisfies, for some class $\mathcal{K}$ function α:

$$\inf_{u \in \mathbb{R}^m} \{L_f V(x) + L_g V(x)u + \alpha(|x|)\} < 0 \tag{1.58}$$

for all $x \neq 0$. We also recall for convenience the Small Control Property.

Definition 1.4. *A CLF V satisfies the Small Control Property if, in a neighborhood of the origin, there exists a continuous control law $u(x)$ such that $u(0) = 0$ and*

$$\dot{V} = L_f V(x) + L_g V(x) u(x) \leq -\alpha(|x|). \tag{1.59}$$

With these definitions, it is possible to recall some universal formulas, starting with Sontag's formula.

Theorem 1.4 (Sontag's formula Sontag, 1989)**.** *Suppose that system* (1.57) *has a CLF V and satisfies the Small Control Property. Then the control law*

$$u(x) = \begin{cases} -\dfrac{L_f V(x) + \sqrt{(L_f V(x))^2 + |L_g V(x)|^4}}{|L_g V(x)|^2} (L_g V(x))^T, & L_g V(x) \neq 0, \\ 0, & \text{otherwise}, \end{cases} \tag{1.60}$$

is smooth in $\mathbb{R}\backslash\{0\}$, continuous at the origin and such that the closed-loop system is globally asymptotically stable.

Another strategy that exploits CLFs is the PMN formula, which involves the solution, for every x, of an optimization problem to retrieve the controller $u(x)$ (see e.g. Freeman and Kokotovic, 1996):

$$\begin{aligned} &\min |u|^2 \\ &\text{subj. to:} L_f V(x) + L_g V(x) u + \alpha(|x|) \leq 0. \end{aligned} \tag{1.61}$$

Similar regularity properties, in conjunction with the Small Control Property, can be inferred for this controller as well. In (Primbs, Nevistic, and Doyle, 2000) a suggestive connection between the PMN formula, Sontag's formula and optimal control through HJB computation is presented. In a fashion inspired by these techniques, it is possible to find in the literature both closed-form and optimization-based solutions that exploit barrier functions. For the latter, the most notable case is the QP problem in (Ames, Grizzle, and Tabuada, 2014; Ames et al., 2017), based on Reciprocal Barrier Functions. Suppose that a function $B(x)$ is a Reciprocal Barrier Function satisfying, for some class $\mathcal{K}$ function α_B (for simplicity we do not show the computations with the map $H(x)$, but the extension is straightforward):

$$\min_{u \in \mathbb{R}^m} \{L_f B(x) + L_g B(x) u - \alpha_B(1/B)\} < 0, \tag{1.62}$$

then a QP problem like the one presented below can be set up (Jankovic, 2018):

$$\begin{aligned} &\min |u|^2 + m\delta^2 \\ &\text{subj. to:} L_f V(x) + L_g V(x) u + \alpha(|x|) + \delta \leq 0 \\ &\qquad L_f B(x) + L_g B(x) u - \alpha_B(1/B) \leq 0, \end{aligned} \tag{1.63}$$

where $m \geq 1$ and δ is a relaxation variable, intended to remain as small as possible, used to satisfy the CLF decrease constraint at all times. One main drawback of the controller in (1.63) is that there is no value of m which guarantees global boundedness or local asymptotic stability. Still, it can be shown that as $m \to \infty$, the QP problem approximates the PMN controller (which guarantees asymptotic stability). This means, intuitively, that the stabilizing properties can be approximately recovered for large m. In (Jankovic, 2018), a modified QP problem is shown to guarantee local asymptotic stability, if the constraints are inactive around the desired equilibrium:

$$\begin{aligned} &\min |u|^2 + m|\delta|^2 \\ \text{subj. to:} &\gamma_f(L_f V(x) + \alpha(|x|)) + L_g V(x) u + L_g V(x)\delta \leq 0 \\ &L_f B(x) + L_g B(x) u - \alpha_B(1/B) \leq 0, \end{aligned} \tag{1.64}$$

where $\gamma_f(\cdot)$ is a Lipschitz function satisfying:

$$\gamma_f(s) = \begin{cases} \lambda s, & s \geq 0 \\ s, & s < 0, \end{cases} \tag{1.65}$$

for some scalar $\lambda \geq 1$. We refer to (Jankovic, 2018) for a detailed analysis of the algorithm, as well as the modifications for systems with disturbances.

1.3.4 Barrier Lyapunov Function Backstepping

Moving in a different direction with respect to the techniques of the previous section, in (Tee, Ge, and Tay, 2009) and related works, systems in strict feedback nonlinear form with box constraints on each state variable are considered. We present in this context a simplified example to show the design principle, without intending to be exhaustive on the topic. In particular, we consider a relative degree 2 system, with unitary gains on the virtual controls, and constraints directly imposed on the output for tracking. The technique can be easily shown to apply to higher relative degrees with just an increased notational burden. Let the nonlinear system

$$\begin{aligned} \dot{x}_1 &= f_1(x_1) + x_2 \\ \dot{x}_2 &= f_2(x_1, x_2) + u \\ y &= h(x) = x_1, \end{aligned} \tag{1.66}$$

where $x_i \in \mathbb{R}$, $i \in \{1, 2\}$, $u \in \mathbb{R}$ and f_i are smooth functions, for $i \in \{1, 2\}$. Let y_r be an output reference satisfying $|y_\mathrm{r}| \leq \overline{Y} < \kappa$, for some positive scalars κ, $\overline{Y}$, and consider a constraint of the form

$$|y(t)| \leq \kappa, \qquad \text{for all } t \geq 0. \tag{1.67}$$

Suppose that $\dot{y}_\mathrm{r}(t)$, $\ddot{y}_\mathrm{r}(t)$ exist and are bounded for all $t \geq 0$. Let $\mu := \kappa - \overline{Y}$ and $z_1 := x_1 - y_\mathrm{r}$, then consider a Barrier Lyapunov Function as in (1.50) (with $p = 1$ for simplicity):

$$V_1(z_1) = \frac{1}{2} \log \left(\frac{\mu^2}{\mu^2 - z_1^2} \right). \tag{1.68}$$

After simple computations, it follows that

$$\dot{V}_1 = \frac{z_1}{\mu^2 - z_1^2} (f_1(x_1) + x_2 - \dot{y}_\mathrm{r}). \tag{1.69}$$

Employing standard backstepping, define the virtual control

$$\alpha := -f_1(x_1) - k_1 z_1 \tag{1.70}$$

which leads to, defining $z_2 := x_2 - \alpha - \dot{y}_r$:

$$\dot{V}_1 = -k_1 \frac{z_1^2}{\mu^2 - z_1^2} + \frac{z_1 z_2}{\mu^2 - z_1^2}, \tag{1.71}$$

with the second term which will be canceled in the next step. Note that another virtual control that can be employed is, as in (Tee, Ge, and Tay, 2009):

$$\alpha_1 := -f_1(x_1) - k_1 z_1 (\mu^2 - z_1^2). \tag{1.72}$$

Clearly, any (possibly state dependent) gain $k(z_1)$ that ensures strict decrease of V_1 whenever $z_2 = 0$ can be employed in the stabilizing term of α. Let

$$V := V_1 + \frac{1}{2} z_2^2, \tag{1.73}$$

it follows that its derivative along the solutions yields:

$$\dot{V} = -k_1 \frac{z_1^2}{\mu^2 - z_1^2} + \frac{z_1 z_2}{\mu^2 - z_1^2} + z_2 (f_2(x_1, x_2) + u - \dot{\alpha} - \ddot{y}_r). \tag{1.74}$$

The natural choice for the control is then

$$u = -f_2(x_1, x_2) + \dot{\alpha} + \ddot{y}_r - \frac{z_1}{\mu^2 - z_1^2} - k_2 z_2. \tag{1.75}$$

This leads to (apply Lemma 1.1):

$$\dot{V} = -k_1 \frac{z_1^2}{\mu^2 - z_1^2} - k_2 z_2^2 \leq -k_1 V_1(z_1) - 2k_2 \frac{1}{2} z_2^2 \leq -\rho V, \tag{1.76}$$

for some scalar $\rho > 0$. The above arguments show that not only that $\dot{V} \leq 0$, which leads to constraint feasibility at all times if $|z_1(0)| < \mu$, but also that an exponential decrease of V can be ensured in a neighborhood of the origin, thus leading, following the arguments in (Tee and Ge, 2011), to regional asymptotic stability and local exponential stability. It is easy to show that the same technique can be coupled with adaptive control, when the above system is affected by parametric uncertainties:

$$\begin{aligned} \dot{x}_1 &= \phi_1^T(x_1)\vartheta + x_2 \\ \dot{x}_2 &= \phi_2^T(x_1, x_2)\vartheta + u \\ y &= h(x) = x_1, \end{aligned} \tag{1.77}$$

where $\vartheta \in \mathbb{R}^p$ is a vector of unknown parameters and $\phi_1 : \mathbb{R} \to \mathbb{R}^p$, $\phi_2 : \mathbb{R}^2 \to \mathbb{R}^p$ are smooth functions. Employing for simplicity the overparameterization technique instead of tuning functions (note that extended matching could also be exploited in this case), let

$$V_1(z_1) = \frac{1}{2} \log \left(\frac{\mu^2}{\mu^2 - z_1^2} \right) + \frac{1}{2} \tilde{\vartheta}_1^T \Gamma^{-1} \tilde{\vartheta}_1, \tag{1.78}$$

where $\Gamma = \Gamma^T > 0$, $\tilde{\vartheta}_1 := \hat{\vartheta}_1 - \vartheta$ and $\hat{\vartheta}_1$ is an estimate of the unknown parameters. Let

$$\begin{aligned} \alpha(x_1, y_r, \hat{\vartheta}_1) &:= -\phi_1^T(x_1)\hat{\vartheta}_1 - k_1 z_1 \\ \dot{\hat{\vartheta}}_1 &= \Gamma\phi_1(x_1)\frac{z_1}{\mu^2 - z_1^2}, \end{aligned} \tag{1.79}$$

which leads to ($z_2 := x_2 - \alpha - \dot{y}_r$):

$$\dot{V}_1 = -k_1\frac{z_1^2}{\mu^2 - z_1^2} + \frac{z_1 z_2}{\mu^2 - z_1^2}. \tag{1.80}$$

Proceeding as before, let

$$V := V_1 + \frac{1}{2}z_2^2 + \frac{1}{2}\tilde{\vartheta}_2^T\Gamma^{-1}\tilde{\vartheta}_2, \tag{1.81}$$

with $\tilde{\vartheta}_2 := \hat{\vartheta}_2 - \vartheta$ ($\hat{\vartheta}_2$ is the second estimate of the parameters), then it follows that:

$$\dot{V} = \dot{V}_1 + z_2\left(\phi_2^T\vartheta - \frac{\partial\alpha}{\partial x_1}(\phi_1^T\vartheta + x_2) - \frac{\partial\alpha}{\partial y_r}\dot{y}_r - \frac{\partial\alpha}{\partial\hat{\vartheta}_1}\dot{\hat{\vartheta}}_1 - \ddot{y}_r + u\right) + \tilde{\vartheta}_2^T\Gamma^{-1}\dot{\hat{\vartheta}}_2. \tag{1.82}$$

As a consequence, choose the control

$$\begin{aligned} u &= -\left(\phi_2^T - \frac{\partial\alpha_1}{\partial x_1}\phi_1^T\right)\hat{\vartheta}_2 + \frac{\partial\alpha}{\partial x_1}x_2 + \frac{\partial\alpha}{\partial y_r}\dot{y}_r + \frac{\partial\alpha}{\partial\hat{\vartheta}_1}\dot{\hat{\vartheta}}_1 + \ddot{y}_r - \frac{z_1}{\mu^2 - z_1^2} - k_2 z_2 \\ \dot{\hat{\vartheta}}_2 &= \Gamma\left(\phi_2(x_1, x_2) - \frac{\partial\alpha_1}{\partial x_1}\phi_1(x_1)\right)z_2, \end{aligned} \tag{1.83}$$

to yield as before

$$\dot{V} = -k_1\frac{z_1^2}{\mu^2 - z_1^2} - k_2 z_2^2 \leq 0, \tag{1.84}$$

which ensures regional stability and, recalling LaSalle-Yoshizawa's Theorem (see Theorem A.1 or alternatively Khalil, 2002, Theorem 8.4), that $(z_1(t), z_2(t)) \to 0$ as $t \to \infty$. Note that this control solution is only valid for the nominal case, since no robustness at all is ensured with this method, unless ϕ_1 and ϕ_2 are individually persistently exciting (PE). Indeed, for what concerns Barrier Lyapunov Function - based backstepping, few cases can be found in the literature (to the author's best knowledge) dealing with the robustness issue with some form of update law modification. Several generalizations based on the previous arguments can be found in the literature. In (Tee and Ge, 2009; Tee and Ge, 2011) the technique is directly extended to constraints on multiple states of systems in strict-feedback form. The main issue of this extension is that, while all the tracking errors are kept bounded with the barrier functions, the virtual controls are growing unbounded as the errors approach the constraints. As a consequence, it is necessary to introduce cumbersome optimization problems to find gains of the controller to guarantee at least the existence of a feasible domain of attraction. The work (Ngo, Mahony, and Jiang, 2005) shows that for the simple case of a system in the Brunovsky normal form this problem can be mitigated by removing the cross-terms cancelations, relying on the choice of the stabilizing gains to guarantee that the structure preserves stability. In an attempt to reduce the conservativeness of the aforementioned methods, Integral Barrier Lyapunov Functionals are used in (Tee and Ge, 2012) to define the barriers in the original coordinates. Additionally, in (Tee, Ren, and Ge, 2011) time-varying constraints are considered, while on a somewhat different note in (Ren et al., 2009) and related works the problem of output feedback is considered. Finally, we recall that a notable example where a robust modification is required is (Ren et al., 2010), where Artificial Neural Networks are used to develop an output feedback adaptive controller.

1.4 Other Techniques

We conclude the chapter with a list of other relevant control strategies that appear in the literature. In (Burger and Guay, 2010), stability and feasibility are achieved through a switching policy between two controllers: a nominal controller used for stabilization, and an "invariance controller" to enforce feasibility through a particular type of barrier certificate. This is performed assuming a well-defined relative degree between the input of the plant and the constraint, seen as the output $y_c = \gamma(x) \leq 0$ (in analogy with the literature of nonlinear Reference Governors). This idea is based on the so-called invariance control presented in (Wolff and Buss, 2004; Kimmel, Jähne, and Hirche, 2016) and the related works.

An interesting method applied on linear systems, also based on a suitable modification of a pre-existing nominal controller, is that shown in (Blanchini and Miani, 2000), where a stabilization solution is elegantly converted into a constrained tracking one. The problem of designing backstepping with bounded inputs has received some attention in the works (Freeman and Praly, 1998; Mazenc and Iggidr, 2004; Mazenc and Bowong, 2004), where it is shown that under some growth properties of the system a Lyapunov function that leads to bounded inputs can be found. For systems in feedforward form with input constraints we refer to the nested saturations technique in (Teel, 1992; Gayaka, Lu, and Yao, 2012) and the results in (Mazenc and Praly, 1996). We also mention the technique known as funnel control (Hopfe, Ilchmann, and Ryan, 2010), which imposes some time-varying constraints to the tracking error of input-saturated nonlinear systems. An extension of funnel control to the case of higher relative degrees is also reported in (Chowdhury and Khalil, 2017). In (Hauser and Saccon, 2006) logarithmic barriers are employed for constrained trajectory functionals optimization, performed with a Newton-based projection operator.

Finally, we highlight that we did not overview the control techniques employed for equality or dynamic constraints, such as nonholonomic constraints, to name a notable example. These and other constrained control problems fall outside the topic of this work, however they will be possibly addressed, in part, as focus of future activities.

Chapter 2

Constrained-Inversion Model Reference Adaptive Control

This chapter introduces a novel approach for the control of nonlinear systems with input and state constraints. In particular, we show that the proposed strategy is specifically intended to handle parametric uncertainties with adaptive control, while enforcing hard constraints at all times. Due to the possibly high computational complexity of online-optimization solutions, we opt to focus on closed-form techniques, in an attempt to enable application of the algorithms to systems with fast dynamics, even with low-cost digital controllers.

Our strategy presents some peculiar features that make it differ from both typical Barrier Lyapunov Function and Reference Governor approaches. Indeed, in contrast with the BLF adaptive backstepping literature, the desired set-point is processed through a nonlinear system that "slows down" the actual reference fed to the controller, thus enhancing the feasibility properties, even when the set-point is unfeasible. On the other hand however, differently from the Reference Governor philosophy, we present a design that solves the stabilization and feasibility problems altogether. On this topic of designing a stabilizer, it is worth quoting the comments about Reference Governors in (Blanchini and Miani, 2000): "the resulting constructed invariant sets depend on the precompensator", thus "an unsuitable choice of the compensator can produce a very small domain of attraction" making the overall solution conservative. With the interest in defining a solution capable of enabling implementation in embedded digital controllers, and considering in particular systems with fast dynamics, we opt to focus on closed-form techniques or where optimization, if necessary, is only computed offline. From these considerations, firstly a separation between trajectory planning and adaptive tracking is introduced to simplify the design, and enable a certainty equivalence-like strategy. The reference trajectories are generated taking into account the right-inverse of the dynamics, which is thus shaped to guarantee constraint feasibility. Indeed, the reference is explicitly computed only for a subset of the states, the so-called flat-dynamics (denoting the output and its derivatives, up to the relative degree minus 1). From a different perspective, this additional dynamics of the adaptive controller replaces the traditional reference model, which in classic adaptive literature is simply a transfer function between an input reference and the trajectory that the output of the plant is required to track. Finally, an adaptive stabilizer is employed to restrict the system's states within sufficiently small "tubes" around the inverse trajectories. Due to the properties of the parameters update law, asymptotic convergence to the inverse trajectories is ensured. The proposed solution, aptly named Constrained (right-)Inversion Model Reference Adaptive Control (briefly, Constrained-Inversion MRAC), can be interpreted as a special class of MRAC design strategy for nonlinear systems.

To easily introduce this new tool we restrict first the discussion to systems which, after a parameter-independent change of coordinates, can be written in the so-called normal form, with a special minimum-phase property. To prove the effectiveness of the presented strategy, we show the application of the algorithm to a significant case of study, consisting of the constrained position control of a four-bar linkage. A treatment of a more general strategy, where the arbitrary relative degree cannot be reduced through such transformation, is presented in the second part of this chapter, which deals with systems in strict-feedback normal form.

2.1 Problem Statement

In the work that we use as a reference (Bosso et al., 2019), the control problem was introduced for relative degree 1 systems with convergent zero-dynamics (see Pavlov, Van De Wouw, and Nijmeijer, 2007 for details concerning convergent systems). Here, to begin the discussion, we provide a generalization of that framework, and we point out which assumptions are needed to recover it. Consider a single-input single-output linearly parameterized nonlinear system of the form

$$\begin{aligned} \dot{\zeta} &= f_0(\zeta) + F(\zeta)\vartheta + [g_0(\zeta) + G(\zeta)\vartheta]u, \qquad \zeta(0) = \zeta_0 \\ y &= h(\zeta), \end{aligned} \tag{2.1}$$

where $\zeta \in \mathbb{R}^n$ is the state vector, $u \in \mathbb{R}$ is the control input, $y \in \mathbb{R}$ is the output for tracking and $\vartheta \in \mathbb{R}^p$ is a vector of unknown parameters. In addition, assume that h is smooth and $F := (f_1, \dots, f_p)$, $G := (g_1, \dots, g_p)$, with $f_i : \mathbb{R}^n \to \mathbb{R}^n$, $g_i : \mathbb{R}^n \to \mathbb{R}^n$, $0 \le i \le p$, smooth vector fields. Suppose that $f_i(0) = 0$, $0 \le i \le p$ so that the origin is an equilibrium of system (2.1) as $u(t) = 0$, for all t. We assume that $\vartheta \in \Theta$, where Θ is a known compact convex set. Let $\mathcal{P}$ be a convex subset of $\mathbb{R}^p$ which contains Θ in its interior. The role of of $\mathcal{P}$ will become clear in the design of the adaptive controllers. Furthermore, we require a well-defined relative degree property, formally stated in the following assumptions.

Assumption 2.1. *There exists a open set containing the origin, $\mathcal{N}_\zeta \subset \mathbb{R}^n$ such that $g_0(\zeta) + G(\zeta)\vartheta \neq 0$, for all $\zeta \in \mathcal{N}_\zeta$ and all $\vartheta \in \mathcal{P}$.*

Assumption 2.2. *There exist $n - r$ smooth functions φ_i, $1 \le i \le n - r$ such that the change of coordinates*

$$\begin{aligned} z_i &= \varphi_i(\zeta) \qquad 1 \le i \le n - r \\ x_j &= L_{f_0}^{j-1} h(\zeta) \qquad 1 \le j \le r \end{aligned} \qquad x = (x_1, \dots, x_r) \tag{2.2}$$

is a diffeomorphism of the form $(z, x) = T(\zeta)$ in an open set $\mathcal{R}$ such that $\mathcal{N}_\zeta \subset \mathcal{R}$, transforming system (2.1) into:

$$\begin{aligned} \dot{z} &= \psi_0(z, x_1) + \Psi(z, x_1)\vartheta \\ \dot{x}_i &= x_{i+1} + \phi_i^T(z, x_1, \dots, x_i)\vartheta, \qquad 1 \le i \le r - 1 \\ \dot{x}_r &= \phi_0(z, x) + \phi_r^T(z, x)\vartheta + \left[\beta_0(z, x) + \beta^T(z, x)\vartheta\right] u \\ y &= x_1. \end{aligned} \tag{2.3}$$

From Assumptions 2.1-2.2, it follows that there exists a positive scalar b_0 such that $\beta_0(z, x) + \beta^T(z, x)\vartheta \ge b_0$, for all $T^{-1}(z, x) \in \mathcal{N}_\zeta$ and all $\vartheta \in \mathcal{P}$.

Remark 2.1. *It is known that the existence of the diffeomorphism $(z, x) = T(\zeta)$ can be derived from the following conditions (see Kanellakopoulos, Kokotovic, and Morse, 1991 for similar requirements in the context of unconstrained adaptive control):*

- *there exists a diffeomorphism of the form (2.2) transforming system*

$$\dot{\zeta} = f_0(\zeta) + g_0(\zeta)u, \qquad y = h(\zeta) \tag{2.4}$$

  into the normal form

$$\begin{aligned} \dot{z} &= \psi_0(z, x_1) \\ \dot{x}_i &= x_{i+1}, \qquad 1 \le i \le r-1 \\ \dot{x}_r &= \phi_0(z, x) + \beta_0(z, x)u \\ y &= x_1; \end{aligned} \tag{2.5}$$

- *let $\mathcal{G}^i := \operatorname{span}\left\{g_0, \operatorname{ad}_{f_0} g_0, \ldots, \operatorname{ad}^i_{f_0} g_0\right\}$, then for $1 \le i \le p$:*

$$\begin{aligned} &g_i \in \mathcal{G}^0 \\ &[X, f_i] \in \mathcal{G}^j \qquad \forall X \in \mathcal{G}^j, \;\; 0 \le j \le r-2. \end{aligned} \tag{2.6}$$

For the solvability of our control problem we need to set up some properties tightly related to the z-sybsystem, which we summarize in the following statement.

Assumption 2.3. *There exists a $\mathcal{C}^1$ manifold of the form*

$$\mathcal{M} := \{\zeta = T^{-1}(z, x) \in \mathcal{N}_\zeta \subset \mathbb{R}^n : z = \pi_z(x_1, \vartheta), x_i = 0, \; 2 \le i \le r-1\}, \tag{2.7}$$

where $\pi_z(x_1, \vartheta)$ is the unique solution of the following equation, for all x_1 and all $\vartheta \in \mathcal{P}$ such that $T^{-1}(\pi_z(x_1, \vartheta), x) \in \mathcal{N}_\zeta$:

$$\psi_0(\pi_z, x_1) + \Psi(\pi_z, x_1)\vartheta = 0. \tag{2.8}$$

Assumption 2.3, in other terms, requires that the solution of the regulator equation (2.8), associated to the trivial exosystem

$$\dot{w} = 0, \qquad w(0) = w_0 \in \mathbb{R}, \tag{2.9}$$

and system (2.1), with regulation output $e = h(\zeta) - w = x_1 - w$, is unique and differentiable. Furthermore, we consider the restriction of the solution to the states where the well-defined relative degree assumptions are satisfied. To summarize, as soon as a unique $\mathcal{C}^1$ solution of the FBI equation for the ζ-system exists and is differentiable in a neighborhood of the origin, Assumption 2.3 is verified. This is the case, for instance, if for each (x_1, ϑ) the point $\pi_z(x_1, \vartheta)$ is a hyperbolic isolated equilibrium of the z-subsystem. Indeed, it is well-known (Isidori and Byrnes, 1990) that the solvability of the FBI equation is a property of the zero dynamics of the plant and, as a consequence of the center manifold theorem, a hyperbolic equilibrium is a sufficient condition for the existence of a $\mathcal{C}^k$ ($k \ge 2$) solution. The map π_z can be conveniently used to define the error $\tilde{z} := z - \pi_z(x_1, \vartheta)$ which is associated to the off-manifold dynamics:

$$\dot{\tilde{z}} = \psi_0(z, x_1) + \Psi(z, x_1)\vartheta - \frac{\partial \pi_z}{\partial x_1}\dot{x}_1. \tag{2.10}$$

System (2.10) plays an important role for what concerns stabilization, hence constrained stabilization of system (2.1): some special minimum-phase properties will be imposed in the control design in order to preserve generality of the solution. In particular, in the following sections we will require that the equilibrium $\tilde{z} = 0$, for constant x_1, is either asymptotically stable, for any constant x_1, or ISS with respect to the input $\dot{x}_1$.

In addition to the differential equation in (2.1), we consider constraints given by:

$$y_{\mathrm{c}} = \gamma(\zeta, u) \in \mathcal{Y}_{\mathrm{c}} := \{Y = (Y_1, \dots, Y_{n_{\mathrm{c}}}) : Y_i \leq 0, i = 1, \dots, n_{\mathrm{c}}\}, \tag{2.11}$$

where for all $u^* \in \mathbb{R}$, the (possibly empty) set $\mathcal{F}_{u^*} := \{\zeta : \gamma(\zeta, u^*) \in \mathcal{Y}_{\mathrm{c}}\}$ is connected and satisfies $\mathcal{F}_{u^*} \subset \mathcal{N}_\zeta$. Let in addition $\gamma(0,0) \in \mathrm{Int}(\mathcal{Y}_{\mathrm{c}})$ so to ensure feasibility in a neighborhood of the origin. As a special case and in the light of the previous changes of coordinates, the above constraint can be transformed into a "box form", which can be more easily exploited for control purposes:

$$z \in \mathcal{Z}, \qquad x \in \mathcal{X}, \qquad u \in \mathcal{U} \tag{2.12}$$

where $\mathcal{Z} \subset \mathbb{R}^{n-r}$, $\mathcal{X} \subset \mathbb{R}^r$, $\mathcal{U} \subset \mathbb{R}$ are some compact connected sets containing the and origin defined, e.g., as $\mathcal{Z} := \{|z_i| \leq Z_i, 1 \leq i \leq n-r\}$, $\mathcal{X} = \mathcal{X}_1 \times \ldots \times \mathcal{X}_r$, with $\mathcal{X}_i := \{\xi \in \mathbb{R} : |\xi| \leq X_i\}$, and $\mathcal{U} = \{u \in \mathbb{R} : |u| \leq U\}$, for some positive scalars $Z_1, \dots, Z_{n-r}, X_1, \dots, X_r$ and U.

Similarly to the general formulation of the previous chapter, we require the output of the system, y, to track a given known reference y_{r}, belonging to a class of constant signals ranging in an arbitrary compact set $\mathcal{Y}_{\mathrm{r}} \subset \mathbb{R}$. We are now ready to state the control problem.

Problem 2.1. *Consider system (2.1)-(2.12), with unknown parameter vector $\vartheta \in \Theta \subset \mathcal{P}$, and let $y_{\mathrm{r}} \in \mathcal{Y}_{\mathrm{r}} \subset \mathbb{R}$. Design a state-feedback controller of the form*

$$\begin{aligned} \dot{\eta} &= \varphi(\zeta, \eta, y_r), \qquad \eta(0) = \eta_0 \\ u &= \kappa(\zeta, \eta, y_r), \end{aligned} \tag{2.13}$$

where $\eta \in \mathbb{R}^{n_\eta}$, such that the closed loop interconnection (2.1)-(2.13) satisfies the following properties:

- *there exists a set $\Omega_0 \subset \mathcal{N}_\zeta \times \mathbb{R}^{n_\eta}$, with the origin contained in the interior of Ω_0, such that for all $y_{\mathrm{r}} \in \mathcal{Y}_{\mathrm{r}}$, all $\vartheta \in \Theta$ and all $(\zeta_0, \eta_0) \in \Omega_0$, the trajectories are forward complete and satisfy the constraints*

$$\gamma(\zeta(t), \kappa(\zeta(t), \eta(t), y_{\mathrm{r}})) \in \mathcal{Y}_{\mathrm{c}}, \tag{2.14}$$

  for all $t \geq 0$;

- *the set Ω_0 is independent of ϑ, hence it can be computed explicitly as a set of feasible initial conditions;*

- *there exists a set-valued map $P(\cdot) : \mathbb{R} \rightrightarrows \mathbb{R}$ such that, for all $y_{\mathrm{r}} \in \mathcal{Y}_{\mathrm{r}}$ and all $\vartheta \in \Theta$, the closed-loop system possesses an ω-limit satisfying $y = h(\zeta) \in P(y_r)$.*

Compare this problem statement with the general formulation in the previous chapter. In this respect, we remark that not only a set of safe initial conditions is required to exist, but this has to be non-trivial ($\Omega_0 \neq \{0\}$) and computable a priori, at least in some approximated form, without any information of the actual value of

ϑ. These considerations yield a problem whose solution cannot be the trivial choice $u(t) = 0$, for all t.

2.2 Constrained-Inversion MRAC: Systems in Normal Form

In order to retrieve the framework of (Bosso et al., 2019), we could let for simplicity $r = 1$ in Assumption 2.2, however a more general class of systems can be cast into the same structure. This class, in particular, corresponds to those models that can be represented in the well-known normal form, with additionally a minimum-phase property.

2.2.1 Augmented Zero-Dynamics Construction

It can be shown that the following two hypotheses are instrumental to achieve the relative degree 1 property.

Assumption 2.4. *For all (z, x) such that $T^{-1}(z, x) \in \mathcal{N}_\zeta$ and all $\vartheta \in \mathcal{P}$, it holds*

$$\phi_i^T(z, x_1, \ldots, x_i)\vartheta = 0, \qquad 1 \leq i \leq r-1. \tag{2.15}$$

Assumption 2.5. *There exist a continuously differentiable function $V_0 : \mathbb{R}^{n-r} \times \mathbb{R} \times \mathcal{P} \to \mathbb{R}_{\geq 0}$ and class $\mathcal{K}_\infty$ functions $\underline{\alpha}$, $\overline{\alpha}$, α such that, for all (z, x_1) satisfying $T^{-1}(z, x) \in \mathcal{N}_\zeta$ (with $x = (x_1, \bar{x})$, $\bar{x} \in \mathbb{R}^{r-1}$) and all $\vartheta \in \mathcal{P}$, it holds:*

$$\begin{aligned}\underline{\alpha}(|\tilde{z}|) \leq V_0(\tilde{z}, x_1, \vartheta) \leq \overline{\alpha}(|\tilde{z}|)\\ \frac{\partial V_0}{\partial \tilde{z}}(\tilde{z}, x_1, \vartheta)\left[\psi_0(z, x_1) + \Psi(z, x_1)\vartheta\right] \leq -\alpha(|\tilde{z}|).\end{aligned} \tag{2.16}$$

In other words, we require that for any constant x_1, the z-subsystem is asymptotically stable in a subset of the feasible states. This assumption is quite standard, see e.g. (Isidori, 2013), where it is exploited to achieve semiglobal stabilization with partial state feedback. A stronger requirement can be found in (Isidori, 2012, Corollary 12.1.2), (Serrani, Isidori, and Marconi, 2001), where local exponential stability is imposed to semiglobally stabilize the entire vector (z, x) with partial state feedback. Indeed, we see that system (2.3) can be written as follows, indicating with $\bar{x} := (x_1, \ldots, x_{r-1})$ the concatenated first $r-1$ components of x:

$$\begin{aligned}\dot{z} &= \psi_0(z, C\bar{x}) + \Psi(z, C\bar{x})\vartheta, \qquad C = \begin{pmatrix}1 & 0 & \ldots & 0\end{pmatrix}\\ \dot{\bar{x}} &= \left(\begin{array}{c|c} 0 & \\ \vdots & I_{r-1} \\ 0 & \\ \hline 0 & 0 \;\; \ldots \;\; 0 \end{array}\right)\bar{x} + \begin{pmatrix}0\\ \vdots\\ 0\\ 1\end{pmatrix} x_r = A\bar{x} + Bx_r\\ \dot{x}_r &= \phi_0(z, \bar{x}, x_r) + \phi_r^T(z, \bar{x}, x_r)\vartheta + \left[\beta_0(z, \bar{x}, x_r) + \beta^T(z, \bar{x}, x_r)\vartheta\right] u,\end{aligned} \tag{2.17}$$

where in particular (A, B) is controllable and (C, A) is observable. Consider a new output of the form

$$\chi := \frac{1}{d_0 k^{r-1}}\left(x_r + k d_{r-2} x_{r-2} + \cdots + k^{r-1} d_0 x_1\right), \tag{2.18}$$

with k a positive scalar and d_i, $i \in \{0, \dots, r-2\}$ such that the polynomial in λ,

$$p(\lambda) = \lambda^{r-1} + d_{r-2}\lambda^{r-2} + \cdots + d_1\lambda + d_0, \tag{2.19}$$

is Hurwitz. Then, selecting as state of the new augmented z-subsystem the vector z_{a}, given by:

$$z_{\mathrm{a}} := \begin{pmatrix} z \\ \varkappa \end{pmatrix} = \begin{pmatrix} z \\ D_k^{-1}\bar{x} \end{pmatrix}, \qquad \varkappa_i = \frac{x_i}{k^{i-1}},\ i \in \{1, \dots, r-1\}, \tag{2.20}$$

with $D_k = \mathrm{diag}\{1, k, \dots, k^{r-2}\}$, it follows that system (2.17) becomes:

$$\begin{aligned} \dot{z}_{\mathrm{a}} &= \psi_{\mathrm{a}}(z_{\mathrm{a}}, \chi) + \Psi_{\mathrm{a}}(z_{\mathrm{a}})\vartheta \\ \dot{\chi} &= \phi^T(z_{\mathrm{a}}, \chi)\vartheta + \left[b^T(z_{\mathrm{a}}, \chi)\vartheta\right] u, \end{aligned} \tag{2.21}$$

with new output for tracking given by $y_\chi = \chi = h(\zeta)$. In particular, we defined:

$$\psi_{\mathrm{a}} = \begin{pmatrix} \psi_0(z, CD_k\varkappa) \\ kA_\lambda\varkappa + d_0kB\chi \end{pmatrix}, \qquad \Psi_{\mathrm{a}} = \begin{pmatrix} \Psi(z, CD_k\varkappa) \\ 0_{r-1\times 1} \end{pmatrix}, \tag{2.22}$$

with A_λ a Hurwitz matrix, whose characteristic polynomial coincides with $p(\lambda)$ in (2.19). Additionally, it can be noted that, for any constant χ, there exists unique equilibrium of the z_a-subsystem which takes the form

$$\pi_{\mathrm{a}}(\chi, \vartheta) = \begin{pmatrix} \pi_z(\chi, \vartheta) \\ \chi \\ 0 \\ \vdots \\ 0 \end{pmatrix}. \tag{2.23}$$

A very important stability property can be inferred for the error $\tilde{z}_{\mathrm{a}} := z_{\mathrm{a}} - \pi_{\mathrm{a}}(\chi, \vartheta) = (\tilde{z}, \tilde{\varkappa})$, whose dynamics can be in general described by:

$$\dot{\tilde{z}}_{\mathrm{a}} = \tilde{\psi}(\tilde{z}_{\mathrm{a}}, \chi) + \tilde{\Psi}(\tilde{z}_{\mathrm{a}}, \chi)\vartheta - \frac{\partial \pi_{\mathrm{a}}}{\partial \chi}\dot{\chi}. \tag{2.24}$$

Proposition 2.1. *Suppose $\dot{\chi} = 0$. Then, there exists a positive scalar k^* such that, for all $k > k^*$, the origin of system (2.24) is locally asymptotically stable, for any $(\chi, \vartheta) \in \mathbb{R} \times \mathcal{P}$ such that $T^{-1}(\pi_{\mathrm{a}}(\chi, \vartheta), 0) \in \mathcal{N}_\zeta$ and with bounds which hold uniformly in $(\zeta, \vartheta) \in \mathcal{N}_\zeta \times \mathcal{P}$, that is, there exists a class $\mathcal{KL}$ function β_z such that it holds:*

$$|\tilde{z}_{\mathrm{a}}(t)| \leq \beta_z(|\tilde{z}_{\mathrm{a}}(0)|, t). \tag{2.25}$$

The proof follows from direct application of (Isidori, 2013, Theorem 9.3.1), so we omit the details here for brevity. Note that an explicit Lyapunov function is available, and is given by:

$$V_{\mathrm{a}}(\tilde{z}_{\mathrm{a}}, \chi, \vartheta) = V_0(\tilde{z}, \chi, \vartheta) + \tilde{\varkappa}^T P_\lambda \tilde{\varkappa}, \tag{2.26}$$

where $P_\lambda = P_\lambda^T > 0$ is such that:

$$P_\lambda A_\lambda + A_\lambda^T P_\lambda = -I. \tag{2.27}$$

Furthermore, note that in case $n = r$ we obtain the so-called Brunovsky normal form.

In that context, the choice of k is arbitrary and may become instrumental to reduce the conservativeness of this approach by appropriately shaping the trajectories.

2.2.2 A Preliminary Constrained Controller for the Known-Parameter Case

For the solution of Problem 2.1 under the assumptions from 2.1 to 2.5, we derive a dynamic controller from a structure designed in the known-parameters case. The complete solution is developed from this simplified scenario with a certainty-equivalence approach. Consider system (2.21), which we rewrite here for convenience (considering also the case $r = 1$ by including χ in the arguments of Ψ_{a}):

$$\begin{aligned} \dot{z}_{\mathrm{a}} &= \psi_{\mathrm{a}}(z_{\mathrm{a}}, \chi) + \Psi_{\mathrm{a}}(z_{\mathrm{a}}, \chi)\vartheta \\ \dot{\chi} &= \phi^T(z_{\mathrm{a}}, \chi)\vartheta + \left[b^T(z_{\mathrm{a}}, \chi)\vartheta\right] u \\ y_\chi &= \chi, \end{aligned} \tag{2.28}$$

with $z_{\mathrm{a}} \in \mathbb{R}^{n-1}$, $\chi \in \mathbb{R}$, $u \in \mathbb{R}$, $\vartheta \in \Theta \subset \mathcal{P}$, and for simplicity we endow the system with box input and state constraints of the form:

$$|u| \le U, \qquad z_{\mathrm{a}} \in \mathcal{Z}_{\mathrm{a}} := \{\underline{Z}_i \le z_{\mathrm{a},i} \le \overline{Z}_i, 1 \le i \le n-1\}, \qquad |\chi| \le Y, \tag{2.29}$$

for some positive scalars U and Y, and for some numbers $\underline{Z}_i$, $\overline{Z}_i$ satisfying $\underline{Z}_i < 0 < \overline{Z}_i$, for all $1 \le i \le n-1$. Note that from the given assumptions, the constraints (2.11) can always be recast in the form (2.29), clearly with some degree of conservativeness. Suppose here that ϑ is available for control design, and let $y_{\mathrm{r}} \in \mathcal{Y}_{\mathrm{r}}$ be a reference that y_χ is required to track. A simple strategy to handle the constraints (2.29) can be summarized in the following steps:

1. to manage $|u| \le U$, a policy of input allocation is adopted: in particular, part of the control authority is employed to compensate the nonlinearity of the dynamics, while the remaining authority is used to let $|\chi(t)| \le Y$ by assigning its derivative $\dot{\chi}$;

2. $\dot{\chi}$ is shaped through a BLF, embedding both the constraint $|\chi| \le Y$ and the limitations imposed to the nonlinearity compensation, evaluated at $z_{\mathrm{a}} = \pi_{\mathrm{a}}(\chi, \vartheta)$;

3. a nonlinear gain is introduced in the control law to handle (by reducing $|\dot{\chi}|$) the remaining constraints, arising from $z_{\mathrm{a}} \ne \pi_{\mathrm{a}}(\chi, \vartheta)$.

Step 1

Denote, for compactness of notation, the map

$$q(z_{\mathrm{a}}, \chi, \vartheta) := -\frac{\phi^T(z_{\mathrm{a}}, \chi)\vartheta}{b^T(z_{\mathrm{a}}, \chi)\vartheta}. \tag{2.30}$$

By assumption on the smoothness of the vector field, $q(z_{\mathrm{a}}, \chi, \vartheta)$ is well-defined and continuously differentiable as a function of χ and z_{a}, for all $\vartheta \in \mathcal{P}$. Consider a generic Barrier Lyapunov Function of the form $W(\chi, y_{\mathrm{r}}, \vartheta)$, with the corresponding control law:

$$u = q(z_{\mathrm{a}}, \chi, \vartheta) - \frac{1}{b^T(z_{\mathrm{a}}, \chi)\vartheta}\kappa\left(z_{\mathrm{a}}, \chi, \vartheta, y_{\mathrm{r}}\right), \tag{2.31}$$

where $\kappa(\cdot)$ is a locally Lipschitz function, designed according to the gradient of $W(\chi, y_{\mathrm{r}}, \vartheta)$, that will be provided in the subsequent steps. Pick a scalar $\delta \in (0, 1)$

and define $U_\delta := U(1-\delta)$ and $k_u := U\delta b_0$. The proposed input allocation consists of requiring $|q(z_{\rm a}, \chi, \vartheta)| \le U_\delta$ and $|\kappa(\cdot)| \le k_u$, for all $t \ge 0$. This way, the worst case scenario will lead to the norm of the control input in (2.31) to be exactly equal to U.

Step 2

Consider, in place of $q(z_{\rm a}, \chi, \vartheta)$, the value of the map evaluated at the steady-state of the augmented zero dynamics, that is, $c(\chi, \vartheta) = q(\pi_{\rm a}(\chi, \vartheta), \chi, \vartheta)$. As a consequence of Assumption 2.3 and from the regulator equation for system (2.28), given by:

$$\begin{aligned} 0 &= \psi_{\rm a}(\pi_{\rm a}, w) + \Psi_{\rm a}(\pi_{\rm a}, w)\vartheta \\ 0 &= \phi^T(\pi_{\rm a}, \chi)\vartheta + \left[b^T(\pi_{\rm a}, w)\vartheta \right] c, \end{aligned} \tag{2.32}$$

we have that the feedforward map $c(\cdot)$ is $\mathcal{C}^1$, for all $\vartheta \in \mathcal{P}$. As a consequence, we design of the BLF embedding the condition $|c| \le U_\delta$ as follows:

$$W(\chi, y_{\rm r}, \vartheta) := \frac{1}{2}\left(\omega(\chi) - y_{\rm r}\right)^2 + k_B B(H(\chi, \vartheta)), \tag{2.33}$$

with k_B a positive scalar and $B(H(\chi, \vartheta))$ defined as

$$\begin{aligned} B(H) &= -\ln\left(\frac{H}{1+H}\right), \\ H(\chi, \vartheta) &= (c(\chi, \vartheta) + U_\delta)(U_\delta - c(\chi, \vartheta)) \prod_{i=1}^{n-1} (\pi_{{\rm a},i}(\chi, \vartheta) - \underline{Z}_i)(\overline{Z}_i - \pi_{{\rm a},i}(\chi, \vartheta)), \end{aligned} \tag{2.34}$$

and $\omega(\cdot) : (-Y, Y) \to \mathbb{R}$ a diffeomorphism such that $(\partial\omega/\partial\chi) > 0$ (e.g. a tangent function). Alternatively, if a compact set $\mathcal{X}_z \subset (-Y, Y)$ is known such that $\pi_{\rm a}(\chi, \vartheta) \in \mathrm{Int}(\mathcal{Z}_{\rm a})$, for all $\chi \in \mathcal{X}_z$, then the terms depending on $\pi_{\rm a}$ can be omitted in H and $\omega(\cdot) : \mathrm{Int}(\mathcal{X}_z) \to \mathbb{R}$ can be defined as consequence to account for this modification. This is the case, e.g. when $r = n$ and thus the constraints on $\pi_{\rm a}(\chi, \vartheta)$ can be explicitly recast into the set $\mathcal{X}_z$ with no particular effort. Regardless of these choices, the above design of the BLF $W(\chi, y_{\rm r}, \vartheta)$ yields the control law:

$$u = q(z_{\rm a}, \chi, \vartheta) - \frac{1}{b^T(z_{\rm a}, \chi)\vartheta}\sigma\left(\frac{\partial W}{\partial \chi}(\chi, y_{\rm r}, \vartheta)\right), \tag{2.35}$$

with $\sigma(\cdot)$ a sigmoid function, chosen as an odd function such that $\sigma(0) = 0$, $0 < (\partial\sigma/\partial s) \le 1$ and $|\sigma| \le k_u$ (e.g., an arctangent function, with suitable gains). As a consequence, $\dot{W}(\chi, y_{\rm r}, \vartheta) \le 0$, for all $\vartheta \in \Theta$ and all $\chi(0) \in \mathcal{X}_0$, with $\mathcal{X}_0 := \{\chi : \exists d > 0 \text{ s.t. } W(\chi, y_{\rm r}, \vartheta) \le d\}$, for $y_{\rm r} \in \mathcal{Y}_{\rm r}$.

Step 3

Intuitively, from a two time scales analysis viewpoint, the above control law could be effective also for the original constraints, as long as the zero-dynamics were sufficiently fast to converge to $\pi_{\rm a}(\chi, \vartheta)$ or, from the opposite perspective, the χ-dynamics was maneuvered sufficiently slowly to almost remain on the steady state manifold after the initial transient is complete. This intuition suggests to embed in the controller an Explicit Reference Governor in order to enforce the original constraints. Considering $V_{\rm a}(\tilde{z}_{\rm a}, \chi, \vartheta)$ as in (2.26), let $\mu(\cdot) : [-Y, Y] \times \Theta \to \mathbb{R}_{\ge 0}$ be a $\mathcal{C}^1$ map such that:

$$V_{\mathrm{a}}(\tilde{z}_{\mathrm{a}}, \chi, \vartheta) \le \mu(\chi, \vartheta) \implies z_{\mathrm{a}} \in \mathcal{Z}_{\mathrm{a}}, \quad |q(z_{\mathrm{a}}, \chi, \vartheta)| \le U_{\delta}. \tag{2.36}$$

By continuity of $q(\cdot)$, $\mu(\cdot)$ can be designed such that $\mu(\chi, \vartheta) > 0$ for all $\chi \in \mathcal{X}_0$. Therefore, since $q(0, 0, \vartheta) = 0$, there exists a positive scalar $\bar{\Delta}$ such that the set $\mathcal{X}_\Delta := \{\chi \in [-Y, Y] : \mu(\chi, \vartheta) \ge \Delta\}$ is non-empty, for $0 < \Delta < \bar{\Delta}$. These considerations suggest the following modification of (2.35):

$$u = q(z_{\mathrm{a}}, \chi, \vartheta) - \frac{1}{b^T(z_{\mathrm{a}}, \chi)\vartheta}\sigma\left(\lambda(z_{\mathrm{a}}, \chi, \vartheta, y_{\mathrm{r}})\frac{\partial W}{\partial \chi}(\chi, y_{\mathrm{r}}, \vartheta)\right), \tag{2.37}$$

with $\lambda(\cdot)$ a nonlinear gain provided in the following Lemma.

Lemma 2.1. *Consider the constrained system (2.28)-(2.29), with $\vartheta \in \Theta$ available for feedback. Select $\Delta > 0$ such that the set $\mathcal{X}_\Delta := \{\chi : \mu(\chi, \vartheta) \ge \Delta\}$ is not empty. Let $\lambda(\cdot)$ be defined as*

$$\lambda(z_{\mathrm{a}}, \chi, \vartheta, y_{\mathrm{r}}) = \frac{k_{\mathrm{g}}\left[\mu(\chi, \vartheta) - V_{\mathrm{a}}(\tilde{z}_{\mathrm{a}}, \chi, \vartheta)\right] + \nu(\chi, \vartheta)}{1 + \left(\frac{\partial W}{\partial \chi}(\chi, y_{\mathrm{r}}, \vartheta)\right)^2}, \tag{2.38}$$

with k_{g} a positive scalar, and $\nu(\cdot) : [-Y, Y] \times \Theta \to \mathbb{R}_{\ge 0}$ a locally Lipschitz function such that $|\dot{\chi}| \le \nu(\chi, \vartheta)$ implies $\dot{V}_{\mathrm{a}} \le \dot{\mu}$ whenever $\mu = V_0$. Then, there exists a set $\Omega_0 \subset \mathcal{Z}_{\mathrm{a}} \times \mathcal{X}_\Delta$ such that, for all $(z_a(0), \chi(0)) \in \Omega_0$ and all constant $y_{\mathrm{r}} \in \mathcal{Y}_{\mathrm{r}}$, the solutions of the closed loop system are forward complete, and satisfy the constraints (2.29), for all $t \ge 0$. Furthermore, the ω-limit set of the closed-loop system has the form $(\pi_a(P(y_{\mathrm{r}}), \vartheta), P(y_{\mathrm{r}}))$, where $P(\cdot)$ is the set valued map that associates, to each $y_{\mathrm{r}} \in \mathcal{Y}_{\mathrm{r}}$, the solutions p of:

$$\frac{\partial \omega}{\partial \chi}(\omega(p) - y_{\mathrm{r}}) + k_B \frac{\partial B}{\partial H}\frac{\partial H}{\partial \chi}(p, \vartheta) = 0. \tag{2.39}$$

Proof. Part of the procedure is similar to (Garone and Nicotra, 2015, Theorem 1), although presented here in a different setup. Firstly, we show the form of the map $\nu(\cdot)$. Let the function $\tilde{\mu} = \mu - V_a$, and consider the condition $\dot{\tilde{\mu}} \ge 0$, yielding

$$\left(\frac{\partial \mu}{\partial \chi} - \frac{\partial V_{\mathrm{a}}}{\partial \chi} + \frac{\partial V_{\mathrm{a}}}{\partial \tilde{z}_{\mathrm{a}}}\frac{\partial \pi_{\mathrm{a}}}{\partial \chi}\right)\dot{\chi} - \frac{\partial V_{\mathrm{a}}}{\partial \tilde{z}_{\mathrm{a}}}\left[\psi_{\mathrm{a}} + \Psi_{\mathrm{a}}\vartheta\right] = a_1\dot{\chi} - a_0 \ge 0. \tag{2.40}$$

As a consequence, for all χ, z_{a} such that $\tilde{\mu} = 0$, it is possible to ensure $\dot{\tilde{\mu}} \ge 0$ by finding the solution $\nu(\chi, \vartheta)$ of the inequality $a_1(\tilde{z}_{\mathrm{a}}, \chi, \vartheta)\nu \ge a_0(\tilde{z}_{\mathrm{a}}, \chi, \vartheta)$ for all $\tilde{z}_{\mathrm{a}}$ satisfying the condition $V_{\mathrm{a}}(\tilde{z}_{\mathrm{a}}, \chi, \vartheta) = \mu(\chi, \vartheta)$. Note that from the construction of W, it follows that $a_0 < 0$ because of the minimum-phase assumption. Therefore, $\nu = 0$ always belongs to the solution of the above inequality, even though it is clearly in general a conservative choice. Due to the continuity of $\tilde{\mu}$, $\tilde{\mu} < 0$ can only occur if, at some time, $\tilde{\mu} = 0$. When the equality is satisfied, however, we have:

$$\dot{\chi} = -\sigma\left(\nu(\chi, \vartheta)\frac{\frac{\partial W(\chi, y_{\mathrm{r}}, \vartheta)}{\partial \chi}}{1 + \left(\frac{\partial W(\chi, y_{\mathrm{r}}, \vartheta)}{\partial \chi}\right)^2},\right) \tag{2.41}$$

which means $|\dot{\chi}| \le \nu(\chi, \vartheta)$, since $(\partial\sigma/\partial s) \le 1$, and the argument of the saturation function is a term less than 1, multiplied by $\nu(\chi, \vartheta)$. This way, the constraints (2.29) are always satisfied, and the solutions are forward complete in the compact sets imposed by the constraints.

Since $\dot{W} \leq 0$, and because the trajectories are contained in a positively invariant compact set, direct application of LaSalle's Invariance Theorem (Khalil, 2002, Theorem 4.4) implies that the trajectories converge to the maximum invariant set $\mathcal{E}$ contained in the set such that $\lambda(z_a, \chi, \vartheta, y_r)\frac{\partial W}{\partial \chi}(\chi, y_r, \vartheta) = 0$. From the construction of W, $\mu(\chi, \vartheta) \to 0 \implies \left|\frac{\partial W}{\partial \chi}\right| \to \infty$. Choose initial conditions in $\mathcal{Z}_a \times \mathcal{X}_\Delta$ such that $\tilde{\mu} \geq 0$: W and $\frac{\partial W}{\partial \chi}$ are bounded for $t \geq 0$ so, by contradiction of the above implication, there exists a positive scalar δ such that $\mu(\chi, \vartheta) > \delta$, for all $t \geq 0$. It follows that $\frac{\partial W}{\partial \chi} = 0$ on the set $\mathcal{E}$, thus $\chi = P(y_r)$ and $\tilde{z}_a = 0$. □

Remark 2.2. *The solutions of (2.39) exist for all $y_r \in \mathcal{Y}_r$ if $\mathcal{Y}_r$ is compact. On the other hand, uniqueness of these solutions is only guaranteed if B is convex, because in that case W would be a sum of convex functions. Intuitively, it is possible to make $P(y_r)$ close to $\omega^{-1}(y_r)$ by reducing k_B. However, a clearly more elaborate yet rigorous approach is to ensure convexity in an opportune subset of $(-Y, Y)$, exploiting the techniques briefly summarized in chapter 1 concerning Barrier Lyapunov Function construction.*

To summarize, we obtained the convergence of χ to a solution of (2.39) by means of the gradient descent of the Control (Barrier) Lyapunov Function $W(\chi, y_r, \vartheta)$, while preserving input and state feasibility. As a consequence, the trajectories converge to a set (corresponding to $\chi \in P(y_r)$) which is internally stable. This is sufficient to imply local asymptotic stability of the attractor $(\pi_a(P(y_r), \vartheta), P(y_r))$, since uniform stability can be shown appealing to the ε-δ definition. Indeed, consider an isolated solution of (2.39) and indicate it with χ_r, and recallling the notation in (2.24), we can write $\dot{\tilde{z}}_a = \tilde{\psi}_a + \tilde{\Psi}_a\vartheta + \tilde{g}(\tilde{z}_a, \chi, \vartheta)$, with $\tilde{g}$ a continuous function which vanishes as $\chi \to \chi_r$. We omit the analysis for non-isolated equilibra of the χ-subsystem, even though similar considerations could be inferred with some increase of notation. Note that in the domain of attraction of $(\pi_a(\chi_r, \vartheta), \chi_r)$, we can state the following facts:

- by the properties of the gradient descent of $W(\chi, y_r, \vartheta)$, for any $\varepsilon_\chi > 0$ there exists $\delta_\chi > 0$ such that $|\chi(0) - \chi_r| \leq \delta_\chi \implies |\chi(t) - \chi_r| \leq \varepsilon_\chi$;
- by continuity for π_a, for any $\varepsilon_\pi > 0$ there exists $\delta_\pi > 0$ such that $|\chi(0) - \chi_r| \leq \delta_\pi \implies |\pi_a(\chi(t), \vartheta) - \pi_a(\chi_r, \vartheta)| \leq \varepsilon_\pi$;
- by the theorem of total stability applied to the $\tilde{z}_a$-subsystem, with $\tilde{g}$ that acts bounded disturbance, for any $\varepsilon_z > 0$ there exist $\delta_{z1} > 0$, $\delta_{z2} > 0$ such that $|\tilde{z}_a(0)| \leq \delta_{z1}, |\chi(t) - \chi_r| \leq \delta_{z2} \implies |\tilde{z}_a(t)| \leq \varepsilon_z$.

Finally, apply the triangle inequality to show that

$$|z_a(t) - \pi_a(\chi_r, \vartheta)| = |\tilde{z}_a(t) + \pi_a(\chi(t)) - \pi_a(\chi_r)| \leq |\tilde{z}_a(t)| + |\pi_a(\chi(t), \vartheta) - \pi_a(\chi_r, \vartheta)|. \tag{2.42}$$

Choose, and fix, $\varepsilon > 0$, then let $\varepsilon_\pi = \varepsilon/2$, $\varepsilon_z = \varepsilon/2$, then choose δ_π, δ_{z1}, δ_{z2} accordingly. Finally, let $\varepsilon_\chi = \min\{\delta_{z2}, \varepsilon\}$ and select δ_χ accordingly. Therefore, as $|\tilde{z}_a(0)| \leq \delta_{z1}$ and $|\chi(0) - \chi_r| \leq \min\{\delta_\chi, \delta_\pi\}$, it holds $|z_a(t) - \pi_a(\chi_r, \vartheta)| \leq \varepsilon$, $|\chi(t) - \chi_r| \leq \varepsilon$, which is exactly the condition that we seeked. We summarize this result in the following Corollary.

Corollary 2.1. *Let the assumptions of Lemma 2.1 hold, then the attractor $(\pi_a(\chi_r, \vartheta), \chi_r)$, for any isolated solution $\chi_r \in P(y_r)$ of (2.39), is locally asymptotically stable. Furthermore, if W is strictly convex, the domain of attraction of $(\pi_a(\chi_r, \vartheta), \chi_r)$ is the maximal open feasible subset of $\mathcal{Z}_a \times [-Y, Y]$.*

2.2.3 Constrained-Inversion MRAC Design

As anticipated in the introductory discussion, we propose to separate the design into two subproblems: a trajectory planning based on the right-inverse of system (2.28), and adaptive stabilization of the computed trajectories. This design principle is shown in Figure 2.1, where the two subsystems are highlighted for clarity. Intuitively, the idea is to design a feasible trajectory that, as long as the adaptive tracking error is contained within a certain ball, leads to feasible "tubes" of trajectories. This, of course, requires to apply to the right-inverse trajectories suitable subsets of the original constraints. In this perspective, the feasible inverse represents a particular reference model for the adaptive controller.

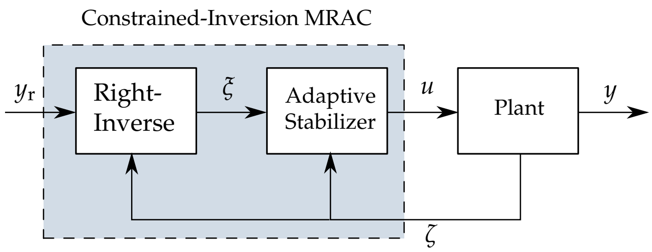

FIGURE 2.1: Overall Scheme for the Constrained-Inversion MRAC and its interconnection with the plant.

Adaptive Stabilizer

The linearly parameterized structure of system (2.28) can be used to design a stabilizer appealing to classic adaptive control techniques. We choose an indirect, observer-based structure of the form:

$$\begin{aligned}
\dot{\hat{\chi}} &= \left[\phi^T(z_a,\chi) + b^T(z_a,\chi)u\right]\hat{\vartheta} + k_o\tilde{\chi} \\
\dot{\hat{\vartheta}} &= \underset{\hat{\vartheta}\in\bar{\Theta}}{\mathrm{Proj}}\left\{\Gamma\left[\phi(z_a,\chi) + b(z_a,\chi)u\right]\tilde{\chi}\right\} \\
u &= \frac{-\phi^T(z_a,\chi)\hat{\vartheta} + \dot{\xi} - k_{st}e}{b^T(z_a,\chi)\hat{\vartheta}},
\end{aligned} \tag{2.43}$$

where k_o and k_{st} are positive scalars, $\Gamma = \Gamma^T$ is a positive-definite matrix, while $\tilde{\chi} = \chi - \hat{\chi}$, $e = \hat{\chi} - \xi$, and ξ is the output of the right-inverse subsystem. Finally, $\mathrm{Proj}\{\cdot\}$ is a locally Lipschitz parameter projection operator that enforces $\hat{\vartheta}(t) \in \bar{\Theta} \subset \mathcal{P}$, with $\Theta \subset \bar{\Theta}$, as long as $\hat{\vartheta}(0) \in \bar{\Theta}$. Let the boundary of $\bar{\Theta}$ be smooth, for simplicity. To provide more insight on a possible construction of such operator, we show the quite general construction in (Krstic, Kanellakopoulos, and Kokotovic, 1995, Appendix E), and similar procedures can be found for more specific classes of sets. Suppose that the set Θ is defined through a convex smooth map Π as follows:

$$\Theta := \{\hat{\vartheta} \in \mathbb{R}^p : \Pi(\hat{\vartheta}) \leq 0\} \subset \mathcal{P}. \tag{2.44}$$

The smoothness of Q ensures that the boundary of Θ is smooth. Similarly, let

$$\bar{\Theta} := \{\hat{\vartheta} \in \mathbb{R}^p : \Pi(\hat{\vartheta}) \leq c\} \subset \mathcal{P}, \tag{2.45}$$

for some positive scalar c, be a slightly enlarged set. Note that by assumption, there exists a sufficiently small $c > 0$ which guarantees the existence of $\bar{\Theta}$. Let

$g(\hat{\vartheta}) = \Gamma \min\{1, \Pi(\hat{\vartheta})/c\}$, and let $\nabla\Pi$ be the gradient of Π with respect to $\hat{\vartheta}$, then the projector operator can be defined as follows:

$$\underset{\hat{\vartheta}\in\bar{\Theta}}{\operatorname{Proj}}\{\tau\} = \begin{cases} \tau & \hat{\vartheta} \in \operatorname{Int}(\Theta) \text{ or } \nabla\Pi^T\tau \leq 0 \\ \left(I_p - g(\hat{\vartheta})\frac{\nabla\Pi\nabla\Pi^T}{\nabla\Pi^T\Gamma\nabla\Pi}\right)\tau & \hat{\vartheta} \in \bar{\Theta}\backslash \operatorname{Int}(\Theta) \text{ and } \nabla\Pi^T\tau > 0. \end{cases} \tag{2.46}$$

It can be proved that this operator is locally Lipschitz in its arguments (Krstic, Kanellakopoulos, and Kokotovic, 1995), so that classic results on existence and uniqueness of solutions can be used as a consequence. Furthermore, the following useful properties hold:

- for all $\vartheta \in \Theta$ and all $\hat{\vartheta} \in \bar{\Theta}$, with $\tilde{\vartheta} = \hat{\vartheta} - \vartheta$, $\tilde{\vartheta}^T\Gamma^{-1}\operatorname{Proj}_{\hat{\vartheta}\in\bar{\Theta}}\{\tau\} \leq \tilde{\vartheta}^T\Gamma^{-1}\tau$;
- the differential equation $\dot{\hat{\vartheta}} = \operatorname{Proj}_{\hat{\vartheta}\in\bar{\Theta}}\{\tau\}$, for differentiable $\tau(t)$, is such that $\hat{\vartheta} \in \bar{\Theta}$ in its domain of existence.

We refer to (Cai, Queiroz, and Dawson, 2006) for a differentiable (up to the desired order) construction of parameter projection, which can prove useful, e.g., in backstepping design. The following classical result can be inferred for the properties of the nominal closed loop system.

Lemma 2.2. *Consider the closed loop interconnection (2.28)-(2.43), with ξ, $\dot{\xi}$ bounded signals. Denote with $\tilde{\vartheta} := \hat{\vartheta} - \vartheta$ the parameter estimation error. Suppose that $\xi(t)$ is contained in a proper subset of $[-Y, Y]$, while $z_a \in \mathcal{Z}_a$, for all t in the domain of existence of solutions. Then, the origin of the tracking error system, with state variables given by the stack $(\tilde{\chi}, e, \tilde{\vartheta})$, is locally uniformly stable, and there exists a ball with radius δ such that $|(\tilde{\chi}(0), e(0), \tilde{\vartheta}(0))| \leq \delta$ guarantees that the trajectories are forward complete and satisfy $|\chi(t)| \leq Y$, for all $t \geq 0$. Furthermore, for all forward complete trajectories, satisfying the constraints (2.29) at all times, the set $\bar{\Theta}$ is forward invariant and it holds:*

$$\lim_{t\to\infty} |\tilde{\chi}(t)| = \lim_{t\to\infty} |e(t)| = \lim_{t\to\infty} |\chi(t) - \xi(t)| = 0. \tag{2.47}$$

Proof. The procedure is analogous to LaSalle-Yoshizawa's Theorem (see Appendix A.1 and Khalil, 2002, Theorem 8.4), and we revisit here some of the main steps accounting for the constraints (2.29). Let the Lyapunov function:

$$W_{\mathrm{st}} = \frac{1}{2}\tilde{\chi}^2 + \frac{1}{2\gamma_W}e^2 + \frac{1}{2}\tilde{\vartheta}^T\Gamma^{-1}\tilde{\vartheta}, \tag{2.48}$$

whose derivative along the solutions of the error system are the following:

$$\begin{aligned} \dot{W}_{\mathrm{st}} = & -k_{\mathrm{o}}\tilde{\chi}^2 - \frac{e}{\gamma_W}(k_{\mathrm{st}}e - k_{\mathrm{o}}\tilde{\chi}) - \tilde{\vartheta}^T\left[\phi(z_{\mathrm{a}},\chi) + b(z_{\mathrm{a}},\chi)u\right]\tilde{\chi} \\ & + \tilde{\vartheta}^T\Gamma^{-1}\underset{\hat{\vartheta}\in\bar{\Theta}}{\operatorname{Proj}}\{\Gamma\left[\phi(z_{\mathrm{a}},\chi) + b(z_{\mathrm{a}},\chi)u\right]\tilde{\chi}\} \\ \leq & -k_{\mathrm{o}}\tilde{\chi}^2 + \frac{k_{\mathrm{o}}}{\gamma_W}\tilde{\chi}e - \frac{k_{\mathrm{st}}}{\gamma_W}e^2 \\ \leq & -k_{\mathrm{o}}\tilde{\chi}^2 + \frac{k_{\mathrm{o}}}{\gamma_W}\frac{\rho}{2}\tilde{\chi}^2 + \frac{k_{\mathrm{o}}}{\gamma_W}\frac{1}{2\rho}e^2 - \frac{k_{\mathrm{st}}}{\gamma_W}e^2, \qquad \rho > 0, \end{aligned} \tag{2.49}$$

which yields $\dot{W}_{\mathrm{st}} \leq -M(\tilde{\chi}, e) \leq 0$ as long as the condition

$$\frac{k_{\mathrm{o}}}{2k_{\mathrm{st}}} < \rho < 2\gamma_W, \tag{2.50}$$

is satisfied, i.e. as long as $\gamma_W > k_o/(4k_{st})$. For a generic initial condition, let $[0, t_f)$ be the domain of existence of the solution originating from it. Since $\xi(t)$ is contained, for all $t \in [0, t_f)$, in a proper subset of the interval $[-Y, Y]$, there exists a positive scalar ε_ξ such that, if $|\chi(t) - \xi(t)| = |\tilde{\chi}(t) + e(t)| \le \varepsilon_\xi$, then $|\chi(t)| \le Y$, for all $t \in [0, t_f)$. Note that $|\tilde{\chi}(t) + e(t)| \le \sqrt{2}|(\chi, e)|$. Therefore, let $\varepsilon = \varepsilon_\xi/\sqrt{2}$, $\delta = \underline{\alpha} \circ \overline{\alpha}^{-1}(\varepsilon)$: since for all $t \in [0, t_f)$ it holds $\dot{W}_{st} \le 0$, it follows simmediately that, as long as $|\eta(0)| \le \delta$ ($\eta = (\tilde{\chi}, e, \tilde{\vartheta})$):

$$\frac{|\chi(t) + e(t)|}{\sqrt{2}} \le |\eta(t)| \le \underline{\alpha}^{-1}(W_{st}(t)) \le \underline{\alpha}^{-1} \circ \overline{\alpha}(|\eta(0)|) \le \varepsilon, \tag{2.51}$$

which also proves local uniform stability from the upper bound on $|\eta(t)|$. Since the bounds that we found do not depend on t_f, and the previous arguments show that $|\chi(t)| \le Y$ if $|\eta(0)| \le \delta$, then this means that the trajectories originating from such ball are forward complete. The remainder of the proof, dealing with convergence of χ to ξ, follows the same arguments of the LaSalle-Yoshizawa's Theorem. We refer to Appendix A.1 for all involved computations. □

The above lemma confirms the intuitive idea that the controller should enforce the trajectories, at each time, to be sufficiently close to the profile generated by ξ. If this is guaranteed, then the trajectories are forward complete and the tracking problem is satisfied, by means of classical adaptive control tools.

Note that the indirect structure was chosen for more versatility in the actual implementation, but a direct scheme can be used to derive the same results. Indeed, with an indirect controller it is possible to easily include an Anti-Windup strategy, by considering $\text{sat}_U(u)$ in the observer in place of u. This simple modification can be used to correctly compute the parameter estimate update law, also in case an input constraint violation occurred and corresponded to actuator saturation. On the other hand, it is not possible to guarantee, without further assumptions of the vector field of the plant, that the corresponding trajectories are bounded or the unconstrained condition can be actually recovered.

Right-Inverse Design

We propose a right-inverse of the form

$$\begin{aligned}\dot{\xi} &= \phi^T(z_a, \xi)\hat{\vartheta} + b^T(z_a, \xi)\hat{\vartheta} \underbrace{\left[q(z_a, \xi, \hat{\vartheta}) + \frac{v(\xi, z_a, \chi, y_r)}{b^T(z_a, \xi)\hat{\vartheta}}\right]}_{u_\xi(\xi, z_a, \chi, \hat{\vartheta})} \\ &= v(\xi, z_a, \chi, y_r).\end{aligned} \tag{2.52}$$

The dynamics of ξ can be interpreted as a known-parameters copy of the χ-dynamics, in a certainty-equivalence sense for χ and ϑ, replaced by ξ and $\hat{\vartheta}$, respectively. Considering the structure of u_ξ, we see that an analogous control scheme to the known-parameter case (2.37) can be pursued, with a crucial role played by the corresponding nonlinear gain (2.38).

Consider a modified set of constraints, given by proper subsets of the original ones in (2.29):

$$|u_\xi| \le U' < U, \qquad |\xi| \le Y' < Y, \tag{2.53}$$

Relative to the newly defined constraints, let U'_δ and k'_u denote the parameters of the input allocation strategy. Note that we did not require a modification of the constraint set $\mathcal{Z}_{\mathrm{a}}$, since we are not replicating the dynamics of z_{a} through the right-inverse design, as we shall see more clearly in the stability analysis. In place of (2.33), consider the CBLF

$$W_{\xi}(\xi, y_r) := \frac{1}{2}\left(\omega(\xi) - y_r\right)^2 + k_B B(H(\xi)), \tag{2.54}$$

with k_B a positive scalar for tuning and $B(\cdot)$ such that

$$\begin{aligned}
B(H) &= -\ln\left(\frac{H}{1+H}\right), \\
H(\xi, \vartheta) &= (c_{\mathrm{m}}(\xi) + U_\delta)(U_\delta - c_{\mathrm{M}}(\xi)) \prod_{i=1}^{n-1} (\pi_{\mathrm{m},i}(\xi) - \underline{Z}_i)(\overline{Z}_i - \pi_{\mathrm{M},i}(\xi)), \\
c_{\mathrm{m}}(\xi) &= \min_{\hat{\vartheta} \in \bar{\Theta}} c(\xi, \hat{\vartheta}), \qquad c_{\mathrm{M}}(\xi) = \max_{\hat{\vartheta} \in \bar{\Theta}} c(\xi, \hat{\vartheta}) \\
\pi_{\mathrm{m},i}(\xi) &= \min_{\hat{\vartheta} \in \bar{\Theta}} \pi_{a,i}(\xi, \hat{\vartheta}), \qquad \pi_{\mathrm{M},i}(\xi) = \max_{\hat{\vartheta} \in \bar{\Theta}} \pi_{a,i}(\xi, \hat{\vartheta}),
\end{aligned} \tag{2.55}$$

where now the maps are taken accounting for the worst-case scenario, while $\omega(\cdot) : (-Y', Y') \to \mathbb{R}$ is as before a diffeomorphism such that $(\partial \omega / \partial s) > 0$ (the same considerations can be given for the simplified constraint set $\mathcal{X}_z$, now indicated with $\mathcal{X}_z'$). Note that the set $\Xi_0 := \{\xi : \exists d > 0 \text{ s.t. } W_{\xi}(\xi, y_{\mathrm{r}}) \le d\}$, for $y_{\mathrm{r}} \in \mathcal{Y}_{\mathrm{r}}$, is non-empty, because we assumed a small control property of the origin, for any possible value of $\bar{\Theta}$. Clearly, the extension of the set Ξ_0 heavily depends on the problem at hand, and intuitively a connection can be established between the "size" of $\bar{\Theta}$ and that of the constraint sets. From an engineering application point of view, this strongly depends on the plant design and its uncertainties. In the current framework, where the uncertainties are set to belong to a fixed compact set, the degrees of freedom available to reduce this source of conservativeness are limited, and future research activity will be dedicated to address this particular challenge. Clearly, we did not consider the case of soft constraints, where the techniques can be inherently more speculative. The development of this particular framework will be pursued as well in the future, since many control applications actually fall within this category (see, e.g. constraints on the root mean square of electric currents, related to the active power losses contributing to component heating and, possibly, consequent breakdown).

Consider now the map

$$S(\rho) = \begin{cases} \rho, & \rho > 0 \\ 0, & \rho \le 0 \end{cases}, \quad \rho(z_{\mathrm{a}}, \chi) = \min_{\hat{\vartheta} \in \bar{\Theta}} \left(\mu(\chi, \hat{\vartheta}) - V_{\mathrm{a}}(\tilde{z}_{\mathrm{a}}, \chi, \hat{\vartheta})\right), \tag{2.56}$$

with $\mu(\cdot)$ such that:

$$V_{\mathrm{a}}(\tilde{z}_{\mathrm{a}}, \chi, \hat{\vartheta}) \le \mu(\chi, \hat{\vartheta}) \implies z_{\mathrm{a}} \in \mathcal{Z}_a, \quad |q(z_{\mathrm{a}}, \chi, \hat{\vartheta})| \le U_\delta'. \tag{2.57}$$

From the properties of W_{ξ}, $\mu(\cdot)$ can be designed such that $\mu(\chi, \hat{\vartheta}) > 0$, for all $\chi \in \Xi_0$ and all $\hat{\vartheta} \in \bar{\Theta}$, for $y_{\mathrm{r}} \in \mathcal{Y}_{\mathrm{r}}$. We propose, hence, the following right-inverse dynamics:

$$\dot{\xi} = -\sigma\left(\lambda(z_{\mathrm{a}}, \chi, \xi, y_{\mathrm{r}}) \frac{\partial W_{\xi}}{\partial \xi}(\xi, y_{\mathrm{r}})\right), \tag{2.58}$$

with nonlinear gain $\lambda(\cdot)$ given by

$$\lambda(z_{\mathrm{a}},\chi,\xi,y_{\mathrm{r}}) = \frac{k_{\mathrm{g}} S\left(\rho(z_{\mathrm{a}},\chi)\right) + \nu(\chi)}{1 + \left(\frac{\partial W_{\xi}}{\partial \xi}(\xi,y_{\mathrm{r}})\right)^2}, \tag{2.59}$$

with k_{g} a positive gain for tuning and $\nu(\chi) \geq 0$ such that, whenever $\rho \leq 0$, $|\dot{\chi}| \leq \nu(\chi)$ implies $\dot{\rho} \geq 0$, for all $\hat{\vartheta} \in \bar{\Theta}$. The following result shows that the interconnection of the right-inverse and the adaptive stabilizer solves Problem 2.1.

Theorem 2.1. *Consider the constrained system (2.28)-(2.29), and let the controller be defined as the interconnection (2.43)-(2.58)-(2.59). Choose, and fix, the modified set of constraints (2.53) and a positive scalar Δ such that the set $\mathcal{X}_{\xi\Delta} := \{x \in \Xi_0 : \mu(x,\hat{\vartheta}) \geq \Delta, \hat{\vartheta} \in \Theta\}$ is non-empty. Pick $\Gamma = \gamma_\vartheta \Gamma_0$, with γ_ϑ a positive scalar and Γ_0 an arbitrary positive definite matrix. Let Assumptions from 2.1 to 2.5 hold. Then, there exist positive gains k_{o}, k_{st}, γ_ϑ and a set $\Omega_0 \subset \mathcal{Z}_{\mathrm{a}} \times (-\Upsilon,\Upsilon)^2 \times \mathcal{X}_{\xi\Delta}$ such that, for all $(z_{\mathrm{a}}(0),\chi(0),\hat{\chi}(0),\xi(0),\hat{\vartheta}) \in \Omega_0 \times \bar{\Theta}$ and all $y_{\mathrm{r}} \in \mathcal{Y}_{\mathrm{r}}$, the solutions of the closed-loop system are forward complete, and satisfy the constraints (2.29), for all $t \geq 0$. Furthermore, the ω-limit set of the closed-loop system has the form $(\pi_{\mathrm{a}}(P(y_{\mathrm{r}})), P(y_{\mathrm{r}}), P(y_{\mathrm{r}}), P(y_{\mathrm{r}}), \vartheta^*)$, where $\vartheta^* \in \bar{\Theta}$ is an arbitrary parameter vector and $P(\cdot)$ is defined as the map that associates, to each $y_{\mathrm{r}} \in \mathcal{Y}_{\mathrm{r}}$, the solutions p of:*

$$\frac{\partial \omega}{\partial \chi}(\omega(p) - y_{\mathrm{r}}) + k_B \frac{\partial B}{\partial H}\frac{\partial H}{\partial \chi}(p) = 0.$$

Proof. We divide the proof into two steps. Firstly, we prove that there exists a set of initial conditions, independent of $\hat{\vartheta}(0) \in \bar{\Theta}$, that ensures constraint satisfaction at all times, then we analyze the ω-limit set of the closed-loop system.

Feasibility and Forward Completeness

We recall that the tracking error dynamics is given by:

$$\begin{aligned}
\dot{e} &= -k_{\mathrm{st}} e + k_{\mathrm{o}} \tilde{\chi} \\
\dot{\tilde{\chi}} &= -k_{\mathrm{o}} \tilde{\chi} - \left[\phi^T(z_{\mathrm{a}},\chi) + b^T(z_{\mathrm{a}},\chi) u\right] \tilde{\vartheta} \\
\dot{\hat{\vartheta}} &= \underset{\hat{\vartheta}\in\bar{\Theta}}{\mathrm{Proj}} \left\{\gamma_\vartheta \Gamma_0 \left[\phi(z_{\mathrm{a}},\chi) + b(z_{\mathrm{a}},\chi) u\right] \tilde{\chi}\right\}.
\end{aligned} \tag{2.60}$$

Adopting a two time scales perspective as in (Teel, Moreau, and Nešić, 2003), it can be shown that the dynamics of $x_{\mathrm{f}} = (e,\tilde{\chi})$ can be expressed as $\varepsilon \dot{x}_{\mathrm{f}} = A_{\mathrm{f}}(x_{\mathrm{f}},\cdot)x_{\mathrm{f}} + \varepsilon d_f(\cdot)$, with $\varepsilon > 0$ that can be made arbitrarily small by selecting k_{o}, k_{st} sufficiently large and γ_ϑ sufficiently small. This is done by replacing the control input u in the above system and noticing that, with the adaptation sufficiently small, the tuning gains of the x_{f}-dynamics can be used to dominate the nonlinearities, since it holds:

$$\dot{x}_{\mathrm{f}} = \underbrace{\begin{pmatrix} -k_{\mathrm{st}} & k_{\mathrm{o}} \\ (1-\Delta)k_{\mathrm{st}} & -k_{\mathrm{o}} \end{pmatrix}}_{A_{\mathrm{f}}^{\varepsilon}} x_{\mathrm{f}} + d_{\mathrm{f}}(x_{\mathrm{f}},\xi,\vartheta,\tilde{\vartheta}), \tag{2.61}$$

with d_{f} which does not depend on the gains k_{o}, k_{st} and $\Delta = (b^T(z_{\mathrm{a}},\chi)\vartheta)/(b^T(z_{\mathrm{a}},\chi)\hat{\vartheta}) \geq \Delta_0 > 0$. The first term in the right-hand side can be seen as linear time-varying, for any feasible trajectory of the closed loop system. Indeed, for any feasible $x_{\mathrm{f}},\xi,z_{\mathrm{a}}$, the characteristic polynomial of $A_{\rm f}^{\varepsilon}$, $p(\lambda)$, is given by

$$p(\lambda) = (\lambda + k_{\rm st})(\lambda + k_{\rm o}) + (\Delta - 1)k_{\rm o}k_{\rm st} = \lambda^2 + (k_{\rm o} + k_{\rm st})\lambda + \Delta k_{\rm o}k_{\rm st}, \tag{2.62}$$

which is Hurwitz for any positive $k_{\rm o}$, $k_{\rm st}$, uniformly in the arguments of Δ. Furthermore, for $k = k_{\rm o} = k_{\rm st}$ the real part of the eigenvalues is upper bounded by $-k\Delta_0/2$, hence it is possible to pick $k = \varepsilon^{-1}$, $\gamma_{\vartheta} = \varepsilon$ to yield the desired time scales separation, with $A_{\rm f}^{\varepsilon} = \varepsilon^{-1}A_{\rm f}$. The boundary-layer system $d\bar{x}_{\rm f}/d\tau = A_{\rm f}(\bar{x}_{\rm f}, \cdot)\bar{x}_{\rm f}$ (with $t = \varepsilon\tau$) is exponentially stable, as long as the trajectories exist (as before, note that forward completeness is guaranteed only for trajectories satisfying constraints at all times). Indeed, from the above arguments we have that there exists a symmetric positive definite matrix P such that $PA_{\rm f} + A_{\rm f}^T P \leq -I_2$. The overline notation is used here to distinguish the boundary-layer trajectories from the actual ones. From the selection of Y' it follows that, for all $\xi \in (-Y', Y')$, there exist positive constants $m_{\rm f}$, $a_{1\rm f}$, $a_{2\rm f}$ such that, for all $|x_{\rm f}(0)| \leq m_{\rm f}$, $|\bar{x}_{\rm f}(t)| \leq a_{1\rm f}\exp(-a_{2\rm f}\tau)|x_{\rm f}(0)|$.

Let $x_{\rm s} := (z_{\rm a}, \xi, \hat{\vartheta})$. The reduced-order system (obtained from $\varepsilon = 0$), indicated again with the overline notation, is the following:

$$\begin{aligned}
\dot{\bar{z}}_{\rm a} &= \psi(\bar{z}_{\rm a}, \bar{\chi}) + \Psi(\bar{z}_{\rm a}, \bar{\chi})\vartheta \\
\dot{\bar{\xi}} &= -\sigma\left(\lambda(\bar{z}_{\rm a}, \bar{\chi}, \bar{\xi}, y_{\rm r})\frac{\partial W_{\xi}}{\partial \bar{\xi}}(\bar{\xi}, y_{\rm r})\right) \\
\dot{\bar{\hat{\vartheta}}} &= 0, \quad \bar{\hat{\vartheta}} \in \bar{\Theta}, \quad \bar{\xi} = \bar{\hat{\chi}} = \bar{\chi}.
\end{aligned} \tag{2.63}$$

System (2.63) has the same form of the closed loop system (2.28)-(2.29)-(2.37)-(2.38), therefore from Lemma 2.1 we have that $\bar{u} \in [-U', U']$, $\bar{z}_{\rm a} \in \mathcal{Z}_{\rm a}$ and $\bar{\xi} \in (-Y', Y')$, for all $\bar{\hat{\vartheta}} \in \bar{\Theta}$. Note that it holds $\bar{u}\,(\bar{z}_{\rm a}, \bar{\chi}, \vartheta) = q(\bar{z}_{\rm a}, \bar{\chi}, \vartheta) + \dot{\bar{\xi}}/(b(\bar{\chi}, \bar{z}_{\rm a})^T\vartheta)$ for any $\vartheta \in \Theta$ and $\bar{\hat{\vartheta}} \in \bar{\Theta}$. From Corollary 2.1, it follows that there exists a locally asymptotically stable attractor of the form $\mathcal{A}_{\rm s} = (\pi_{\rm a}(\chi_{\rm r}), \chi_{\rm r}) \times \bar{\Theta}$. Denote with $\mathcal{R}_{\rm s}$ its domain of attraction, and pick a proper indicator $\omega_{\rm s}(\cdot)$ of $\mathcal{A}_{\rm s}$ in $\mathcal{R}_{\rm s}$. The trajectories of the reduced-order system satisfy $\omega_{\rm s}(\bar{x}_{\rm s}(t)) \leq \beta_{\rm s}(\omega_{\rm s}(x_s(0)), t)$, for some class $\mathcal{KL}$ function $\beta_{\rm s}$. Following the remaining steps in (Teel, Moreau, and Nešić, 2003), it is possible to show that for any $\delta > 0$, $0 < c_{\rm f} < m_{\rm f}$, $c_{\rm s} > 0$, there exists $\varepsilon^* > 0$ such that, for all $0 < \varepsilon < \varepsilon^*$, and all $|x_{\rm f}(0)| \leq c_{\rm f}$ and all $\omega_{\rm s}(x_{\rm s}(0)) \leq c_{\rm s}$, the trajectories of the closed-loop system exist, and satisfy:

$$\begin{aligned}
|x_{\rm f}(t)| &\leq a_{1\rm f}\exp\left(-a_{2\rm f}\frac{t}{\varepsilon}\right)|x_{\rm f}(0)| + \delta \\
\omega_{\rm s}(x_{\rm s}(t)) &\leq \beta_{\rm s}(\omega_{\rm s}(x_{\rm s}(0)), t) + \delta.
\end{aligned} \tag{2.64}$$

Choose ε sufficiently small, then $z_{\rm a}(t) \in \mathcal{Z}_{\rm a}$ and $|\chi(t)| \leq Y$, for all the domain of existence of the solutions $[0, t_{\rm f})$, hence the trajectories exist and are contained in a compact set, $t \in [0, t_{\rm f})$. Since the bounds of the compact set do not depend on $t_{\rm f}$, then forward completeness of trajectories follows. Finally, in order to ensure input feasibility, u can be factorized as $u = \bar{u} + \Omega_{\rm f}(x_{\rm f}, x_{\rm s}, \varepsilon)x_{\rm f}$, with $\Omega(\cdot)$ a continuous function, bounded for feasible $x_{\rm f}$, $x_{\rm s}$. Let ε sufficiently small to ensure state feasibility, and let $\bar{u}(\bar{z}_{\rm a}, \bar{\chi}, \vartheta)$ be feasible for all ξ in an enlarged interval (with respect to $[-Y', Y']$) accounting for $\omega_{\rm s}(x_{\rm s}) \leq \delta$. Then, proper selection of initial conditions, for some positive scalars $c_{\rm f}$ and $c_{\rm s}$ possibly smaller than the ones in (2.64), yields $u \in [-U, U]$. This means that, if input and state feasibility in a possibly small tube around the right-inverse trajectories is ensured, then there exists a region of possible initializations leading to input and state feasibility.

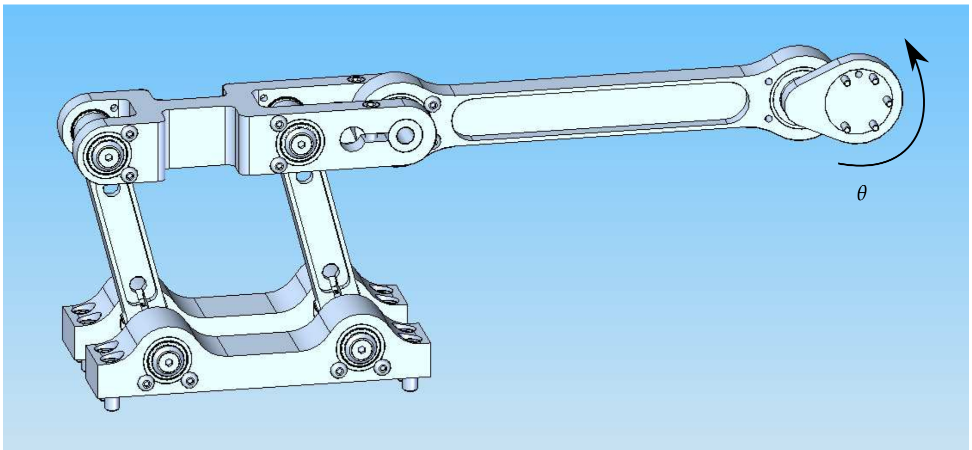

FIGURE 2.2: CAD model of a four-bar linkage used as test bench for the proposed Constrained-Inversion MRAC.

Convergence

Since the overall closed-loop system is autonomous, (2.64) implies that the trajectories converge to a non-empty compact invariant set. From $\dot{W}_\xi$, $\dot{W}_{\mathrm{st}}$ being non-positive, it follows that W_ξ and W_{st} (which are continuous and bounded from below) have constant limits as $t \to \infty$. It is possible to show, by Lemma 2.2 and similar arguments applied to $\dot{W}_\xi$, that $\chi \to \xi$, $\lambda \frac{\partial W_\xi}{\partial \xi} \to 0$. Since χ, ξ converge to a constant in Ξ_0 and $\hat{\vartheta}$ converges to a constant in $\bar{\Theta}$ by properties of the projection operator, we have that the trajectories converge to a set which is internally stable by Proposition 2.1, hence $\tilde{z}_{\mathrm{a}} \to 0$ asymptotically. From the properties of $\rho(\cdot)$, the same arguments of Lemma 2.1 can be used to show that the trajectories converge to $(\pi_{\mathrm{a}}(P(y_{\mathrm{r}})), P(y_{\mathrm{r}}), P(y_{\mathrm{r}}), P(y_{\mathrm{r}}), \vartheta^*)$. □

Some important considerations are due. Firstly, note that by choosing ε sufficiently small, the initial condition $\xi(0) = \hat{\chi}(0) = \chi(0)$, which is always possible due to $\chi(0)$ available for control, guarantees feasibility at all times. Note that such choice is not limiting at all, as the asymptotic behavior is always given by the right-inverse, and hence convergence to the target (projected) reference $P(y_{\mathrm{r}})$ is always ensured. The domain of attraction of the stabilizer, when the above initialization is not satisfied, is however strongly affected by the selection of ε, and indeed it can be easily shown that it shrinks as $\varepsilon \to 0$. This undesirable behavior cannot be avoided if a two time scales perspective is adopted to prove feasibility of the above structure, and it is seriously detrimental for the proposed strategy in case measurement errors are present. One of the main goals in the following will be to remove this restriction by an appropriate selection of the adaptive stabilizer structure, and by means of appropriate tuning choices. Interestingly, the intuition that adaptation must be slow in order to ensure feasibility will be confirmed also in the new controller. A general procedure for a tuning to yield a feasible and non-trivial domain of attraction is currently under investigation.

2.3 Application of Constrained-Inversion MRAC to an Euler-Lagrange System

In this section, we apply the Constrained-Inversion MRAC on the case of study of a planar four-bar linkage, whose mechanical structure is depicted in Figure 2.2. Let $\theta \in \mathbb{R}$ denote the angular configuration of the mechanism, which is limited, for convenience, in an interval with amplitude smaller than 2π. Note that in general the correct formalism to describe this state variable would be to employ the unit circle manifold, which displays a notable topological structure. The next chapters will deeply analyze this specific representation in the context of observability analysis and observer design.

Let $J(\theta)$ and $U(\theta)$ denote the inertia and the potential energy of the mechanism. Then, by standard considerations, it is possible to derive the model from the Lagrangian of the system, given by:

$$L = K - U = \frac{1}{2}J(\theta)\dot{\theta}^2 - U(\theta), \tag{2.65}$$

with K used to denote the kinetic energy. Let $u \in \mathbb{R}$ denote an input torque, applied at the same joint that we consider as generalized coordinate. Assuming negligible friction, it is possible to link the Lagrangian and the applied input torque u as follows:

$$\frac{d}{dt}\left(\frac{\partial L}{\partial \dot{\theta}}\right) - \frac{\partial L}{\partial \theta} = u, \tag{2.66}$$

which yields, after straightforward computations, the well-known model:

$$J(\theta)\ddot{\theta} + \frac{1}{2}\frac{\partial J}{\partial \theta}(\theta)\dot{\theta}^2 + \frac{\partial U}{\partial \theta}(\theta) = u. \tag{2.67}$$

In the following, use ω to indicate $\dot{\theta}$, so that it is possible to write:

$$\begin{aligned} \dot{\theta} &= \omega \\ \dot{\omega} &= J^{-1}(\theta)\left[-\frac{1}{2}\frac{\partial J}{\partial \theta}(\theta)\omega^2 - \frac{\partial U}{\partial \theta}(\theta) + u\right] \end{aligned} \tag{2.68}$$

For simplicity, the model for control and simulation was obtained, through curve-fitting optimization, approximating the data of the CAD mechanical model simulator by considering only the main harmonic contributions, and considering the vector field (2.68). The straightforward process that was employed is omitted for brevity. Note that a more precise process would involve to approximate the maps $J(\theta)$, $\partial J(\theta)/\partial\theta$, $\partial U(\theta)/\partial\theta$: this clearly would introduce a mismatch, whose effects are removed for simplicity in the numerical simulations that we present here.

Consider, then, the following system for control and simulation

$$\begin{aligned} \dot{\theta} &= \omega \\ \dot{\omega} &= f_\omega(\theta, \omega, u) - \Phi_{dU}^T(\theta)p_{dU} - \frac{\omega^2}{2}\Phi_{dJ}^T(\theta)p_{dJ} + \Phi_{J\mathrm{inv}}^T(\theta)p_{J\mathrm{inv}}u, \end{aligned} \tag{2.69}$$

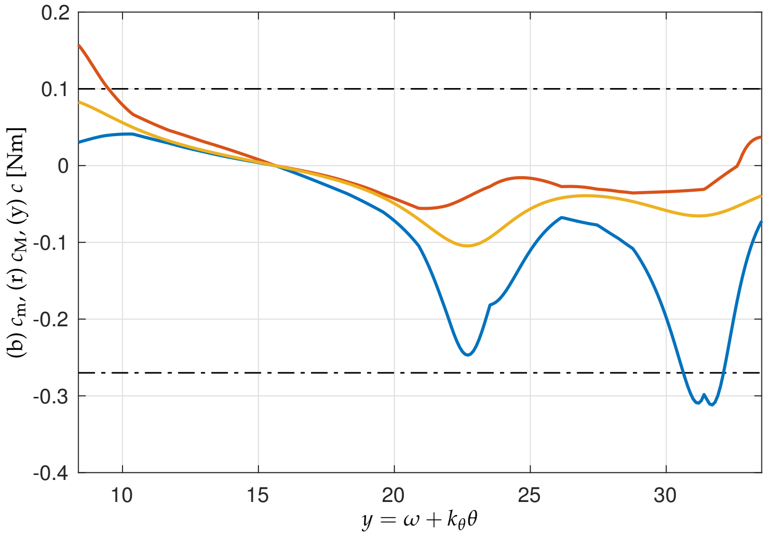

FIGURE 2.3: Steady-state feedforward input maps associated to system (2.69).

with the vector field defined by the data:

$$
\begin{aligned}
f_\omega &= -(86.73\sin(2\theta) + 128.75\cos(\theta) - 2.6) \\
&\quad - 0.5\omega^2(-2.16\sin(2\theta) - 86\times 10^{-3}\cos(2\theta) + 4\times 10^{-4}) \\
&\quad + 1000(0.22\sin(2\theta) - 4.91\cos(2\theta) + 4.98)u \\
\Phi_{dU} &= (\sin(4\theta), \sin(6\theta), \cos(3\theta), \cos(5\theta)) \\
\Phi_{dJ} &= (\sin(4\theta), \sin(6\theta), \cos(4\theta), \cos(6\theta)) \\
\Phi_{J\mathrm{inv}} &= (\sin(4\theta), \cos(4\theta), \cos(5\theta), \cos(5\theta)) \\
p_{dU} &= (-47.74, 25.55, -68.25, 37.44) \\
p_{dJ} &= (1.26, -0.67, 0.28, -0.23) \\
p_{J\mathrm{inv}} &= 1000(-0.46, 3.06, 0.27, -1.31).
\end{aligned}
\tag{2.70}
$$

The parameters p_{dU}, p_{dJ} and $p_{J\mathrm{inv}}$ are unknown and supposed to belong to a hypercube, ranging, component-wise, between the the values of the following vectors:

$$
\begin{aligned}
p_{dU,\min} &= (-55.44, 21.01, -76.98, 31.61) \\
p_{dU,\max} &= (-41.93, 32.01, -61.39, 45.42) \\
p_{dJ,\min} &= (1.12, -0.82, 0.25, -0.28) \\
p_{dJ,\max} &= (1.44, -0.56, 0.31, -0.2) \\
p_{J\mathrm{inv},\min} &= 1000(-0.6, 2.47, 0.23, -1.83) \\
p_{J\mathrm{inv},\max} &= 1000(-0.37, 3.92, 0.31, -0.97).
\end{aligned}
\tag{2.71}
$$

For the purpose of tracking, select the output $y = \omega + k_\theta \theta$, with k_θ a positive scalar (we selected, for implementation, $k_\theta = 10$). This yields the following dynamics:

$$\dot{\theta} = -k_\theta \theta + y, \tag{2.72}$$

which is exponentially stable, with Lyapunov Function given by

$$V_\theta(\tilde{\theta}, y) = \tilde{\theta}^2 = \left(\theta - \frac{y}{k_\theta}\right)^2. \tag{2.73}$$

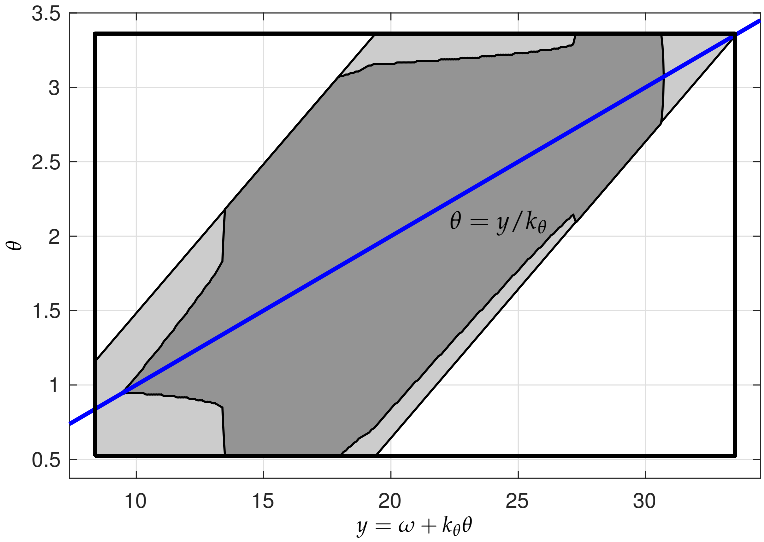

FIGURE 2.4: Feasible sets for the right-inverse of system (2.69).

The constraints that we impose for the right-inverse design are of the form

$$\begin{aligned} \theta &\in [0.52, 3.35] \\ \xi &\in [8.38, 33.5] \\ u_\xi &\in [-0.52, 0.35], \end{aligned} \tag{2.74}$$

which are related to the maps c, c_m and c_M as depicted in Figure 2.3, where the limits imposed on the restriction of u_ξ for BLF design (cf. U'_δ in the previous developments) are shown as dashed lines. Note that, in addition, the vector field and the constraints are such that in the feasible set there exists a point (clearly seen in Figure 2.3 at the intersection of c_m, c_M and c) satisfying the Small Control Property, which ensures the solvability of the problem, as long as all remaining assumptions hold (and indeed they can be immediately verified). The CBLF that we select is then given by

$$W_\xi = \frac{1}{2}\left(\overline{\tan}(\xi - 20.94) - y_\mathrm{r} + 20.94\right)^2 - \ln\left(\frac{(c_\mathrm{m}(\xi) + 0.27)(0.1 - c_\mathrm{M}(\xi))}{1 + (c_\mathrm{m}(\xi) + 0.27)(0.1 - c_\mathrm{M}(\xi))}\right)$$

$$\overline{\tan}(s) = \begin{cases} 9.43 + \dfrac{6.29}{\pi}\tan\left(\dfrac{\pi}{6.29}(s - 9.43)\right), & s \geq 9.43 \\ s, \qquad -9.43 < s < 9.43 \\ -9.43 + \dfrac{6.29}{\pi}\tan\left(\dfrac{\pi}{6.29}(s + 9.43)\right), & s \leq -9.43. \end{cases} \tag{2.75}$$

Note that the diffeomorphism, $\overline{\tan}(\cdot)$, used to construct the reference tracking error, is linear in an opportune interior of the feasible set, this way guaranteeing improved tracking performance. The sigmoid was chosen as $\sigma(\cdot) = k'_u(2/\pi)\arctan(\cdot)$ (we did not impose unitary gain as we chose $\nu = 0$ for simplicity), with $k'_u = 0.25 b_0 = 375$. We assigned the nonlinear gain of the right-inverse as $k_\mathrm{g} = 1000$. As a result, the corresponding feasible set for the right-inverse trajectories is represented in Figure 2.4, from which $\rho(\theta, y)$ can be computed and stored for the Explicit Reference Governor implementation. In particular, the large box in Figure 2.4 denotes the original constraints, the light grey set is the feasible set only accounting for the state constraints

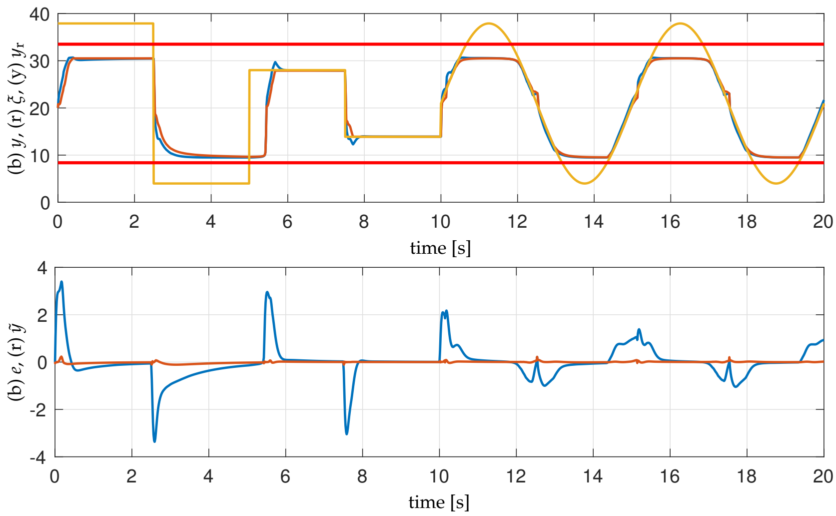

FIGURE 2.5: Output tracking performance. The constraints are indicated in red.

(see how symmetric it is due to the shape of V_θ), while the dark grey set is the computed domain of attraction, obtained after an opportune reduction accounting for the uncertainty set deriving from (2.71). On the other hand, the blue line across all the sets is the steady-state manifold of the zero-dynamics. As a final step for the Constrained-Inversion MRAC design, the observer and stabilizer gains were chosen as $k_o = 150$, $k_{st} = 25$ and $\Gamma = 50\,\mathrm{diag}\{I_8, 200I_4\}$.

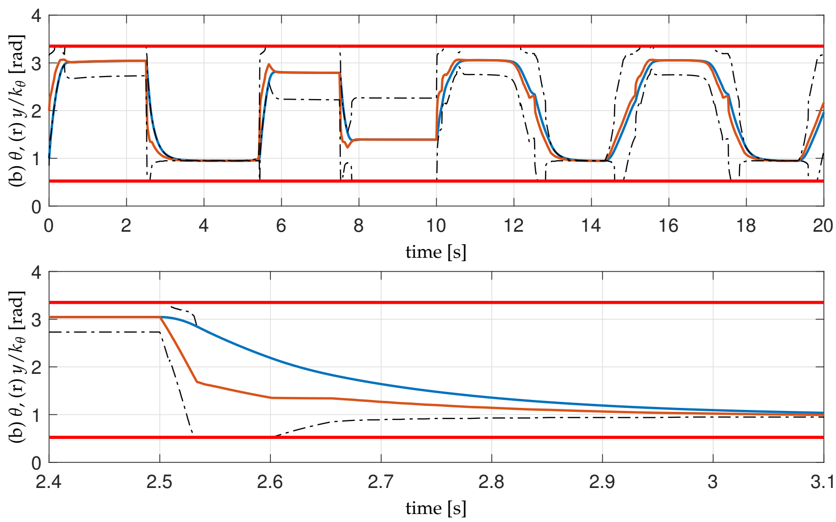

FIGURE 2.6: Internal dynamics behavior of system (2.69). The constraints are indicated in red.

In the simulation results that we present, we tested the proposed controller imposing a sequence of heterogeneous signal references, consisting of feasible and unfeasible set-points, followed by a (partially) unfeasible sinusoidal reference, thus showing the performance of the Constrained-Inversion MRAC in some challenging scenarios. In Figure 2.5 is given the output tracking performance, while in Figure 2.6 we see the corresponding behavior of the internal variable θ, which is contained within the specified limits by means of the Explicit Reference Governor strategy (the dash-dotted profiles correspond to the limits where the ERG is activated). As

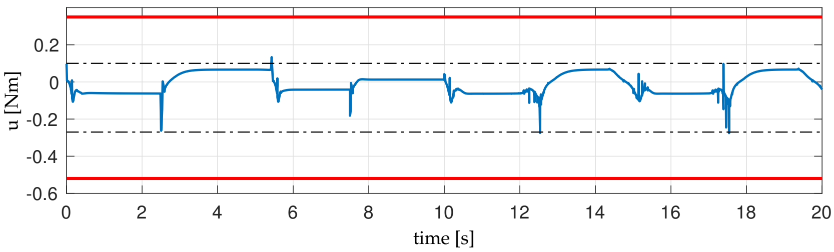

FIGURE 2.7: Control input fed to system (2.69). The constraints are indicated in red.

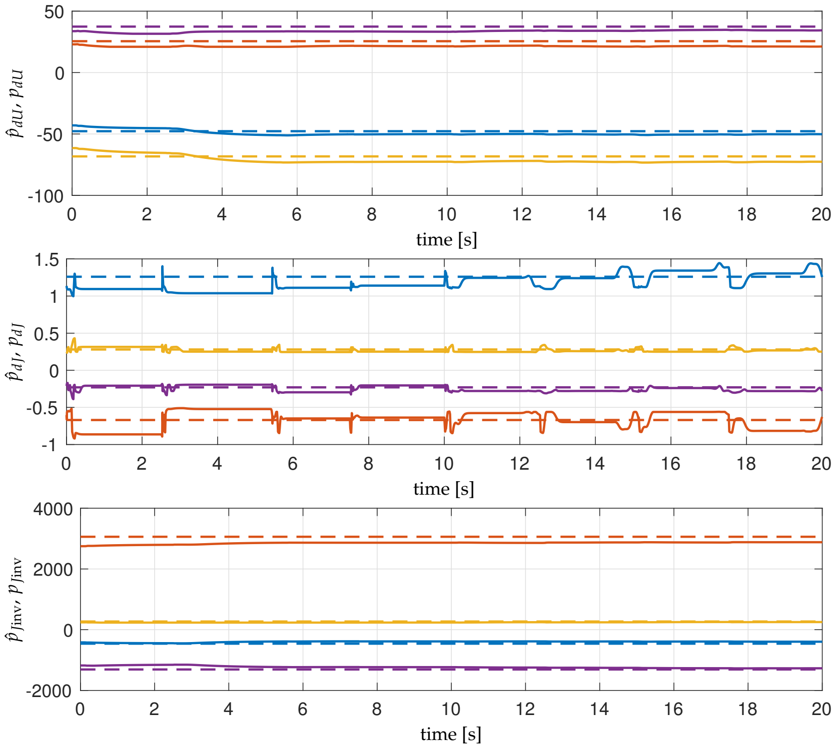

FIGURE 2.8: Parameter estimates behavior. The observer variables are solid, while corresponding true values are dashed.

expected, it can be noticed that the references are projected in the feasible set preserving, as much as possible, the original shape. In Figure 2.7 on the other hand we see the input behavior, which is contained, with some conservativeness, within the bounds. This limitation is largely due to the input allocation strategy and, at the same time, the fact that the parameters worst case scenario is not satisfied by the true vector field. Finally, we see the adaptive gains of the observer in 2.8. In particular, notice how the relatively fast adaptation occurs in some of the gains: this is due to the fact that the theoretical time-scale separation is not particularly stringent for good performance, so it is possible to employ not too small adaptation gains and, as a direct consequence, ensure a faster tracking response.

2.4 Constrained-Inversion MRAC: Systems in Strict-Feedback Normal Form

In this section, we no longer require that Assumption 2.4 holds, thus addressing a more general problem characterized by perturbations on each step of the chain of integrators. Still, we need to impose a set of hypotheses on the structure of the vector field, so to ensure a simple a stability analysis, with the aid a special minimum-phase assumption. Firstly, recall the general structure introduced at the beginning of the chapter:

$$\begin{aligned}
\dot{z} &= \psi_0(z, x_1) + \Psi(z, x_1)\vartheta \\
\dot{x}_i &= x_{i+1} + \phi_i^T(z, x_1, \dots, x_i)\vartheta, \qquad 1 \le i \le r-1 \\
\dot{x}_r &= \phi_0(z, x) + \phi_r^T(z, x)\vartheta + \left[\beta_0(z, x) + \beta^T(z, x)\vartheta\right] u \\
y &= x_1.
\end{aligned} \tag{2.76}$$

For simplicity, we let $\mathcal{N}_\zeta = \mathbb{R}^n$, then we impose the following assumption.

Assumption 2.6. *For all $T^{-1}(z, x) \in \mathbb{R}^n$ and all $\vartheta \in \mathcal{P}$, it holds $\phi_i(z, x_1, \dots, x_i) = \phi_i(x_1, \dots, x_i)$, for $1 \le i \le r-1$, and $\beta_0(z, x) + \beta^T(z, x)\vartheta = 1$.*

This way, we can rewrite system (2.76) as follows:

$$\begin{aligned}
\dot{z} &= \psi_0(z, x_1) + \Psi(z, x_1)\vartheta =: \psi_\vartheta(z, x_1, \vartheta) \\
\dot{x}_i &= x_{i+1} + \phi_i^T(x_1, \dots, x_i)\vartheta, \qquad 1 \le i \le r-1 \\
\dot{x}_r &= \phi_0(z, x) + \phi_r^T(z, x)\vartheta + u = \phi^T(z, x)\vartheta + u \\
y &= x_1,
\end{aligned} \tag{2.77}$$

where once again the dynamics of the last integrator state, x_r, fully depends on all states of the system. Note, however, that the structure cannot be easily reduced to a relative degree 1 system with a parameter-independent change of coordinates, as for the case of systems in normal form. For this reason, we need to perform some form of adaptive backstepping in order to successfully stabilize the system. This will prove a particularly delicate aspect, as we will show in detail in the following. In addition to the dynamics (2.77), consider for simplicity constraints of the form

$$z \in \mathcal{Z} := \{z : \underline{Z}_i \le z_i \le \overline{Z}_i, 1 \le i \le n-r\}, \;\; x \in \{x : |x_i| \le X_i, 1 \le i \le r\}, \tag{2.78}$$

for some positive scalars X_i, $1 \le i \le r$ and some numbers $\underline{Z}_i$, $\overline{Z}_i$ satisfying $\underline{Z}_i < 0 < \overline{Z}_i$, for $1 \le i \le n-r$. Note that in the special case $n = r$ these constraints can be used to include also input limitations. Indeed, consider in this case constraints given by $|x_i| \le X_i$, $1 \le i \le n$, $|u| \le U$, then it is sufficient to augment the system with an additional integrator:

$$\begin{aligned}
\dot{x}_i &= x_{i+1} + \phi_i^T(x_1, \dots, x_i)\vartheta, \qquad 1 \le i \le n-1 \\
\dot{x}_n &= \phi^T(x)\vartheta + u \\
u &= \eta, \qquad \dot{\eta} = \varphi,
\end{aligned} \tag{2.79}$$

where φ is an unconstrained control input. This way, the dynamics of (x, η) is in strict-feedback form, subject only to state constraints.

To guarantee solvability of Problem 2.1, we decide to introduce the following robust minimum phase assumption.

Assumption 2.7. *There exists a symmetric positive definite matrix $P = P^T > 0$ and positive scalars α, c_0 such that, for all $T^{-1}(z,x) \in \mathbb{R}^n$ and all $\vartheta \in \mathcal{P}$, it holds:*

$$\frac{1}{2}\left[P\frac{\partial\psi_\vartheta}{\partial z}(z,x_1,\vartheta) + \left(\frac{\partial\psi_\vartheta}{\partial z}(z,x_1,\vartheta)\right)^T P\right] =: J(z,x_1,\vartheta) \leq -\alpha I_{n-r}, \tag{2.80}$$

$$\sup_{x_1\in\mathbb{R},\vartheta\in\mathcal{P}} |\psi_\vartheta(0,x_1,\vartheta)| < c_0. \tag{2.81}$$

The above conditions are well-known in the literature of convergent systems (Pavlov et al., 2004; Pavlov, Van De Wouw, and Nijmeijer, 2007), and they are sufficient for (uniform) exponential convergence and input-to-state convergence of the z-subsystem. This means, generally speaking, that for any bounded input signal $\bar{x}_1(\cdot)$ defined on $(-\infty,\infty)$ and any $\theta \in \mathcal{P}$, there exists a unique bounded solution $\bar{z}(\cdot)$, defined on on $(-\infty,\infty)$, that is globally exponentially stable. Furthermore, such solution is input-to-state stable with respect to perturbations to $\bar{x}_1(\cdot)$ and ϑ. We formally collect these arguments in the following result, which recalls the properties stated in (Pavlov and Wouw, 2017, Definition 3.4, Theorem 3.1).

Lemma 2.3. *Consider system*

$$\dot{z} = \psi_\vartheta(z,x_1,\vartheta), \tag{2.82}$$

parameterized in $\vartheta \in \Theta \subset \mathcal{P}$, and with input x_1. Let Assumption 2.7 hold. Then, system (2.82) is exponentially convergent and input-to-state convergent, i.e., for any piecewise continuous input defined for all $t \in \mathbb{R}$, $\bar{x}_1(\cdot) \in \mathcal{L}_\infty$, the following properties hold:

- *there exists a unique solution $\bar{z}(\cdot)$ that is defined and bounded for $t \in \mathbb{R}$;*
- *the trajectory $\bar{z}(\cdot)$ is globally exponentially stable;*
- *there exist a class $\mathcal{KL}$ function β and a class $\mathcal{K}_\infty$ function σ such that, for any input of the form $x(t) = \bar{x}_1(t) + \Delta x(t)$, for $t \geq 0$, and for any initial condition $z(0) = z_0 \in \mathbb{R}^{n-r}$, it holds:*

$$|z(t) - \bar{z}(t)| \leq \beta(|z(0) - \bar{z}(0)|,t) + \sigma\left(\sup_{t\in[0,t]} |\Delta x(t)|\right). \tag{2.83}$$

In addition, a robust characterization also applies to the manifold in Assumption 2.3, written explicitly as $z = \pi_z(x_1,\vartheta)$. Notably, let $\tilde{z} := z - \pi_z(x_1,\vartheta)$ and consider the Lyapunov function

$$V_z(\tilde{z}) = \frac{1}{2}\tilde{z}^T P\tilde{z}. \tag{2.84}$$

Clearly, the dynamics of $\tilde{z}$, for generic inputs x_1, $\dot{x}_1$, is given by:

$$\dot{\tilde{z}} = \psi_\vartheta(z,x_1,\vartheta) - \frac{\partial\pi_z}{\partial x_1}\dot{x}_1, \tag{2.85}$$

therefore the derivative of V_z along the solutions of the $\tilde{z}$-subsystem becomes (apply the same arguments in (Pavlov et al., 2004) based on the mean value theorem):

$$\begin{aligned}\dot{V}_z &= \tilde{z}^T P \psi_\vartheta(z, x_1, \vartheta) - \tilde{z}^T P \frac{\partial \pi_z}{\partial x_1} \dot{x}_1 \\ &\leq -c_z V_z + |P^{1/2}\tilde{z}||P^{1/2}| \left| \frac{\partial \pi_z}{\partial x_1} \right| |\dot{x}_1| \\ &\leq -c_z V_z + d_z |P^{1/2}\tilde{z}||\dot{x}_1|,\end{aligned} \tag{2.86}$$

for some positive scalars c_z, d_z, where d_z was established exploiting the compact sets of the constraints (2.29), combined with the continuity assumption on $\partial\pi/\partial x_1$ (recall from the introductory section that the vector field is assumed smooth in the feasible domain). These computations easily show that system (2.85) is ISS with respect to the input $\dot{x}_1$, and in fact rewrite $V_z = |\bar{z}|^2/2$, $\bar{z} = P^{1/2}\tilde{z}$, so that

$$\dot{V}_z \leq -\frac{c_z}{2}|\bar{z}|^2 + d_z|\bar{z}||\dot{x}_1| = -\frac{c_z}{2}|\bar{z}| \left(|\bar{z}| - \frac{2d_z}{c_z}|\dot{x}_1| \right). \tag{2.87}$$

It is sufficient then that $|\bar{z}| \geq (2d_z/c_z)|\dot{x}_1|$ to yield $\dot{V}_z \leq 0$. This fact helps simplifying the design of the right-inverse.

2.4.1 Challenges in the Design of a Robust Constrained Stabilizer

Before proceeding with the control design, we point out a few comments, taking advantage of the experience gained from the solution for systems in the canonical normal form. The result that was provided by Theorem 2.1 embeds an important intuition: if a feasible trajectory compatible with the right-inverse of the plant exists, and it is feasible for any value of the uncertainties, then a stabilizer can be designed both to stay "close" to the inverse trajectory, and to ensure asymptotic convergence. This closeness of trajectories can be enforced through appropriate selection of the gains for tracking, so the resulting strategy can be seen as something in-between high gain and adaptive control. The adaptive update law, however, significantly complicates the analysis, and in the context of Theorem 2.1, the interconnection with the control input required a sufficiently small adaptation gain. Here, we intend to propose a solution belonging to the family of the well-known adaptive backstepping strategies (Krstic, Kanellakopoulos, and Kokotovic, 1995), where the virtual controllers usually (but not always) contain the derivative of the estimated parameters. In addition, it is known that adaptive control based on Lyapunov terms cancelation, as in the context of overparameterization or tuning functions, yields in general tuning laws that are related to the size of the regressor vector, and they cannot have any a priori restriction on their potential growth. Roughly speaking, this means that the tuning law, in order to "catch up" with the possibly destabilizing disturbance of parametric uncertainties on the tracking error, may take very large values during the transient. This qualitative behavior explains why nonlinear adaptive control designs rarely allow adaptation normalization, and shows that the virtual controllers in the backstepping process may be associated with undesirably large virtual control signals, especially when combined with high stabilizing gains. As a consequence, even if the tracking error with respect to virtual controllers is bounded, the actual trajectories potentially do not have a priori bounds that can be imposed through Barrier Lyapunov Functions.

For these reasons, we decide to move away from typical overparameterization or tuning functions approaches, and we suggest to employ a variant of the so-called modular design (Krstic, Kanellakopoulos, and Kokotovic, 1995; Krstic and Kokotovic, 1995). The modular design approach, basically, exploits a set of filters to asymptotically construct an algebraic parameter prediction error, which can be then processed as in classic continuous-time system identification. In order to guarantee an arbitrarily small "learning rate", the classic stabilizers with linear damping cannot be used with nonlinear systems. This is due to the fact that, even when the parameter estimation error is bounded at all times, if the regressor vector contains terms that grow faster-than-linear, then there may be finite escape times: differently than for linear systems, it cannot be guaranteed that the trajectories of an unstable nonlinear system are bounded in bounded time intervals. As a consequence, the stabilizer must ensure input-to-state stability with respect to the parameter estimation error and its derivative. This way, we can theoretically perform Constrained-Inversion MRAC design as a three-step modular design, involving separate structures for the stabilizer, the identifier and the right-inverse. Even though this discussion may suggest a complete design separation principle, special care must be paid to the tuning process, which is highly interconnected between the various blocks, relatively to the constraints imposed to the system. We begin the presentation with the novel robust stabilizer.

2.4.2 Robust Stabilization: BLF Backstepping with Nonlinear Damping

We begin with the problem of requiring the output x_1 of system (2.77) to track a reference trajectory generated by the right-inverse module, with the tracking errors contained in some form of "tube" that will be defined in the following. Denote such reference trajectory with ξ_1. Clearly, we suppose that the derivatives of ξ_1, up to the r-th order, are bounded and available for control purposes. Let for this purpose $\xi_1^{(i)} = \xi_{i+1}$, $\xi = (\xi_1, \dots, \xi_r)$ and $v := \xi_1^{(r)}$. For simplicity, we propose a certainty equivalence backstepping controller, based on designing initially a feedback law $u^* = \kappa(z, x, \xi, v, \vartheta)$ under the assumption of full parameter knowledge, to be then implemented as $u = \kappa(z, x, \xi, v, \hat{\vartheta})$, with $\hat{\vartheta}$ an appropriate parameter estimate. In the following, denote with $\tilde{\vartheta} = \vartheta - \hat{\vartheta}$ the parameter estimation error. Let α_i be the i-th virtual control law of the backstepping recursive design, for $i \in \{1, \dots, r-1\}$, then pick a collection of positive scalars μ_i, $i \in \{1, \dots, r\}$. We require the following properties:

- for all signals $\tilde{\vartheta}(\cdot)$ satisfying $\|\tilde{\vartheta}(\cdot)\|_\infty \le R$, $\|\dot{\tilde{\vartheta}}(\cdot)\|_\infty \le S$, for some positive scalars R, S, then the backstepping tracking errors, defined as:

$$e_i = x_i - \xi_i - \alpha_{i-1}, \qquad i \in \{1, \dots, r\}, \tag{2.88}$$

  with $\alpha_0 = 0$, are such that

$$|e_i(0)| < \mu_i \implies |e_i(t)| < \mu_i, \qquad i \in \{1, \dots, r\}, \forall t \ge 0; \tag{2.89}$$

- for any $x(0)$, $\xi(0)$ such that $|e_i(0)| < \mu_i$, $i \in \{1, \dots, r\}$, the known-parameters controller $u^* = \kappa(z, x, \xi, v, \vartheta)$ is such that $x_1(t) \to \xi_1(t)$ as $t \to \infty$.

In other words, we require the certainty equivalence controller to ensure a strong form of robustness to parametrization errors and parametric variations, while guaranteeing in the nominal case asymptotic convergence to the reference trajectory. To accomplish this task, we use Barrier Lyapunov Functions of the form (1.50), where $p = 1$ for simplicity:

$$V(\eta) = \frac{1}{2}\log\frac{\mu^2}{\mu^2 - \eta^2} \tag{2.90}$$

and we follow similar arguments to (Ngo, Mahony, and Jiang, 2005), where the cross terms of the backstepping design are not canceled but dominated by opportune gain selection. Note that the same Barrier Lyapunov Function structure is adopted in (Tee, Ge, and Tay, 2009; Tee and Ge, 2011) in connection with overparameterization adaptive techniques, with all the technical drawbacks that we overviewed before. Our design relies on Corollary 1.1, reproposed in the form of the following result.

Lemma 2.4. *Let $\mathcal{D} \subset \mathbb{R}^r$ be a compact set, and consider $V : \mathrm{Int}(\mathcal{D}) \to \mathbb{R}_{\geq 0}$ a Barrier Lyapunov Function (see Definition 1.1) on $\mathcal{X}$ for a dynamic system $\dot{\eta} = f(t,\eta)$ such that, for all $(t,\eta) \in \mathbb{R}_{\geq 0} \times \mathrm{Int}(\mathcal{D})$:*

$$\begin{aligned} &\left|\frac{\partial V}{\partial \eta}\right| \geq \alpha(\omega(\eta)) \\ &\dot{V} \leq \left|\frac{\partial V}{\partial \eta}\right| (-\kappa(t,\eta) + \delta(t,\eta)) + \Delta(t,\eta), \\ &|\delta(t,\eta)| \leq D, \quad |\Delta(t,\eta)| \leq M, \end{aligned} \tag{2.91}$$

with $\omega(\cdot)$ a proper indicator function of $\eta^* \in \mathrm{Int}(\mathcal{D})$ in $\mathcal{D}$, α a class $\mathcal{K}_\infty$ function and the map κ satisfying, for some positive scalar d:

$$\omega(\eta) \geq d \implies \kappa(\eta,t) > D. \tag{2.92}$$

Then, $\mathrm{Int}(\mathcal{D})$ is forward invariant.

Proof. Let $K = \min_{\omega(\eta)\geq d} \kappa(\eta)$. There exists a positive constant a such that $K - D \geq a$, therefore, for $\omega(\eta) \geq d$:

$$\dot{V} \leq -\left|\frac{\partial V}{\partial \eta}\right| a + M \leq -a\alpha(\omega(\eta)) + M. \tag{2.93}$$

On the other hand, if $\omega(\eta) < d$:

$$\dot{V} \leq \left|\frac{\partial V}{\partial \eta}\right| D + M \leq \max_{\omega(\eta)<d} \left|\frac{\partial V}{\partial \eta}\right| D + M = c_1 + M, \tag{2.94}$$

so we can write

$$\dot{V} \leq -a\alpha(\omega(\eta)) + c, \tag{2.95}$$

with $c = c_1 + M + a\alpha(d)$. From Corollary 1.1 the statement follows directly. □

Applying Lemma 1.1 to (2.90), it holds

$$\left|\frac{\partial V}{\partial \eta}\right| = \frac{|\eta|}{\mu^2 - \eta^2} \geq \frac{1}{\mu}\frac{\eta^2}{\mu^2 - \eta^2} \geq \frac{1}{\mu}\log\left(\frac{\mu^2}{\mu^2 - \eta^2}\right), \tag{2.96}$$

so we can select

$$\omega(\eta) = \frac{1}{2}\log\frac{\mu^2}{\mu^2 - \eta^2}, \qquad \alpha(|s|) = \frac{2}{\mu}|s|, \tag{2.97}$$

both for Definition 1.1 and Lemma 2.4. The same arguments can be thus applied to the BLF we will employ for our robust stabilizer, given by:

$$V_r(\eta_1, \ldots, \eta_r) := \frac{1}{2} \sum_{i=1}^{r} c_i \log \frac{\mu_i^2}{\mu_i^2 - \eta_i^2}, \tag{2.98}$$

for positive scalars c_i, $i \in \{1, \ldots, r\}$, such that $c_i = 1$ without loss of generality. In particular, note that

$$\left|\frac{\partial V_r}{\partial \eta}\right| = \sqrt{\sum_{i=1}^{r} \left(c_i \frac{\eta_i}{\mu_i^2 - \eta_i^2}\right)^2} \geq \frac{1}{\sqrt{r}} \sum_{i=1}^{r} \left| c_i \frac{\eta_i}{\mu_i^2 - \eta_i^2} \right| \geq \frac{1}{\sqrt{r}} \sum_{i=1}^{r} \frac{c_i}{\mu_i} \log\left(\frac{\mu_i^2}{\mu_i^2 - \eta_i^2}\right). \tag{2.99}$$

This way we proved that V_r is suitable to ensure forward completeness of the set $(-\mu_1, \mu_1) \times \ldots \times (-\mu_r, \mu_r)$ even in the presence of perturbations, as long as we can ensure negativity of the derivative in all points neighboring the boundary of such set. We can now proceed with the backstepping design.

Step 1

Consider the tracking error $e_1 := x_1 - \xi_1$, which yields the dynamics

$$\dot{e}_1 = \phi_1^T(x_1)\vartheta + x_2 - \xi_2. \tag{2.100}$$

Note that by the mean value theorem the map ϕ_1, denoted with w_1 in the following, can be factorized as $w_1(x_1) = w_1(\xi_1) + \Omega_1(\xi_1, e_1)e_1$, where $|\Omega_1(\xi, e_1)| \leq L$ for $|e_1| \leq \mu_1$ and due to boundedness of ξ_1 by assumption. Consider the BLF

$$V_1 := \frac{1}{2} \log \frac{\mu_1^2}{\mu_1^2 - e_1^2}, \tag{2.101}$$

and select the virtual controller

$$\begin{aligned} \alpha_1(x_1, \xi_1, \hat{\theta}) &= -s_1 e_1 - w_1^T(x_1)\hat{\vartheta} \\ s_1(x_1, \xi_1) &= k_1 + d_1 |\Omega_1|^2 \geq 0, \end{aligned} \tag{2.102}$$

with positive scalars k_1, d_1, which yields (recall that $e_2 := x_2 - \xi_2 - \alpha_1$):

$$\dot{V}_1 = \frac{1}{\mu_1^2 - e_1^2} \left[-(k_1 - d_1 |\Omega_1|^2) e_1^2 + e_1 w_1^T \tilde{\vartheta} + e_1 e_2 \right]. \tag{2.103}$$

Apply Young's inequality to obtain, for some positive scalars λ, ρ:

$$\begin{aligned} \dot{V}_1 \leq \frac{1}{\mu_1^2 - e_1^2} \Bigg(&-k_1 e_1^2 - d_1 |\Omega_1|^2 e_1^2 + \frac{\lambda}{2} e_1^2 + \frac{1}{2\lambda} (w_1^T(\xi_1)\tilde{\vartheta})^2 + \\ &+ \frac{\rho}{2} |\Omega_1|^2 e_1^2 + \frac{1}{2\rho} |\tilde{\vartheta}|^2 e_1^2 + e_1 e_2 \Bigg) \\ \leq -\frac{e_1^2}{\mu_1^2 - e_1^2} &\left(\frac{k_1}{4} - \frac{1}{4d_1} |\tilde{\vartheta}|^2 \right) + \frac{1}{2k_1} \frac{(w_1^T(\xi_1)\tilde{\vartheta})^2}{\mu_1^2 - e_1^2} + \frac{e_1 e_2}{\mu_1^2 - e_1^2} - \frac{k_1}{4} \frac{e_1^2}{\mu_1^2 - e_1^2}, \end{aligned} \tag{2.104}$$

where the last negative term will be required in the next step. Assuming $\|\tilde{\vartheta}\|_\infty \leq R$ and $\|w_1^T(\xi_1)\tilde{\vartheta}\|_\infty \leq \Xi_1$, then k_1 and d_1 must satisfy

$$\mu_1^2\left(k_1 - \frac{R^2}{d_1}\right) - 2\frac{\Xi_1^2}{k_1} > 0 \tag{2.105}$$

in order to guarantee that the term

$$W_1(\cdot) := -\frac{e_1^2}{\mu_1^2 - e_1^2}\left(\frac{k_1}{4} - \frac{1}{4d_1}|\tilde{\vartheta}|^2\right) + \frac{1}{2k_1}\frac{(\phi_{1\xi}^T\tilde{\vartheta})^2}{\mu_1^2 - e_1^2} \tag{2.106}$$

is negative as $0 < \underline{\mu}_1 < |e_1| < \mu_1$, for some number $\underline{\mu}_1$. As a consequence, if $e_2 = 0$, it holds by Lemma 2.4:

$$\dot{V}_1 \leq -\chi_1(\omega_1(e_1)) + \epsilon_1, \tag{2.107}$$

with χ_1 and ϵ_1 a class $\mathcal{K}_\infty$ function and a positive scalar, respectively.

Step 2

The dynamics of the second tracking error component, $e_2 = x_2 - \xi_2 - \alpha_1$, is given by:

$$\dot{e}_2 = \phi_2^T\vartheta + x_3 - \xi_3 - \frac{\partial\alpha_1}{\partial x_1}\left(x_2 + \phi_1^T\vartheta\right) - \frac{\partial\alpha_1}{\partial\xi_1}\xi_2 - \frac{\partial\alpha_1}{\partial\hat{\vartheta}}\dot{\hat{\vartheta}}. \tag{2.108}$$

Similarly to the previous step, we propose the factorizations $w_2 := \phi_2 - (\partial\alpha_1/\partial x_1)\phi_1 = w_{2\xi}(\xi_1, \xi_2) + \Omega_{21}e_1 + \Omega_{22}e_2$ and $q_2 := \partial\alpha_1/\partial\hat{\vartheta} = q_{2\xi}(\xi_1) + Q_2e_1$. To proceed with the backstepping procedure, choose

$$V_2 := V_1 + \frac{1}{2}c_2\log\frac{\mu_2^2}{\mu_2^2 - e_2^2}, \tag{2.109}$$

with positive scalar c_2, and select the virtual controller

$$\begin{aligned} \alpha_2(x_1, x_2, \xi_1, \xi_2, \hat{\vartheta}) &= -s_2e_2 - w_2^T\hat{\vartheta} + \frac{\partial\alpha_1}{\partial x_1}x_2 + \frac{\partial\alpha_1}{\partial\xi_1}\xi_2, \\ s_2(x_1, x_2, \xi_1, \xi_2, \hat{\vartheta}) &= k_2 + d_2\left(|\Omega_{21}e_1|^2 + |\Omega_{22}|^2\right) + l_2|Q_2e_1|^2 \geq 0 \end{aligned} \tag{2.110}$$

where k_2, d_2, l_2 are positive scalars. Recall that $e_3 := x_3 - \xi_3 - \alpha_2$, so that it holds:

$$\begin{aligned} \dot{V}_2 \leq{}& \dot{V}_1 - \frac{c_2}{4}\frac{1}{\mu_2^2 - e_2^2}\left[\left(k_2 - \frac{1}{d_2}|\tilde{\vartheta}|^2\right)e_2^2 - \frac{4}{k_2}|w_{2\xi}^T\tilde{\vartheta} + q_{2\xi}\dot{\hat{\vartheta}}|^2 - \left(\frac{|\tilde{\vartheta}|^2}{d_2} + \frac{|\dot{\hat{\vartheta}}|^2}{l_2}\right)\right] \\ &+ c_2\frac{e_2e_3}{\mu_2^2 - e_2^2} - c_2\frac{k_2}{2}\frac{e_2^2}{\mu_2^2 - e_2^2} \\ ={}& W_1(\cdot) + W_{1,2}(\cdot) + W_2(\cdot) + c_2\frac{e_2e_3}{\mu_2^2 - e_2^2} - c_2\frac{k_2}{4}\frac{e_2^2}{\mu_2^2 - e_2^2}, \end{aligned} \tag{2.111}$$

where we indicated

$$
\begin{aligned}
W_{1,2} &:= \frac{e_1 e_2}{\mu_1^2 - e_1^2} - \frac{k_1}{4}\frac{e_1^2}{\mu_1^2 - e_1^2} - c_2 \frac{k_2}{4}\frac{e_2^2}{\mu_2^2 - e_2^2}, \\
W_2 &:= -\frac{c_2}{4}\frac{1}{\mu_2^2 - e_2^2}\left[\left(k_2 - \frac{1}{d_2}|\tilde{\vartheta}|^2\right) e_2^2 - \frac{4}{k_2}|w_{2\xi}^T \tilde{\vartheta} + q_{2\xi}\dot{\hat{\vartheta}}|^2 - \left(\frac{|\tilde{\vartheta}|^2}{d_2} + \frac{|\dot{\hat{\vartheta}}|^2}{l_2}\right)\right].
\end{aligned}
\tag{2.112}
$$

Completing the squares for the cross term we obtain:

$$
\begin{aligned}
W_{1,2} = &-\frac{k_1}{4}\frac{e_1^2}{\mu_1^2 - e_1^2} + \frac{e_1^2}{2(\mu_1^2 - e_1^2)} + \frac{e_2^2}{2(\mu_1^2 - e_1^2)} + \\
&- c_2 \frac{k_2}{4}\frac{e_2^2}{\mu_2^2 - e_2^2} - \frac{c_2}{2}\frac{(e_1 - e_2)^2}{\mu_1^2 - e_1^2}.
\end{aligned}
\tag{2.113}
$$

It is easy to see that

$$
\frac{k_1}{4} \geq \frac{1}{2} + \frac{\mu_2^2}{\mu_1^2 \delta_1^2}, \qquad \delta_1 \in (0, 1) \tag{2.114}
$$

yields $W_{1,2} \leq 0$ if $|e_1| \geq \mu_1 \delta_1$. To handle the case where $|e_1| < \mu_1 \delta_1$, select

$$
\frac{c_2 k_2}{\mu_2^2} \geq \frac{2}{\mu_1^2 (1 - \delta_1^2)}. \tag{2.115}
$$

In other words, it is possible to pick k_1, k_2 sufficiently high in order to dominate the cross term. Finally, to ensure that W_2 is negative as $0 < \underline{\mu}_2 < |e_2| < \mu_2$, for some number $\underline{\mu}_2$, the same computations as before yield the inequality (recall $\|\dot{\hat{\vartheta}}(\cdot)\|_\infty \leq S$)

$$
\mu_2^2 \left(k_2 - \frac{R^2}{d_2}\right) - 4\frac{\Xi_2^2}{k_2} - \frac{R^2}{d_2} - \frac{S^2}{l_2} > 0. \tag{2.116}
$$

As a consequence, by Lemma 2.4, if $e_3 = 0$:

$$
\dot{V}_2 \leq -\chi_1(\omega_1(e_1)) + \epsilon_1 - \chi_2(\omega_2(e_2)) + \epsilon_2. \tag{2.117}
$$

Step i, (2 $\leq$ i $\leq$ r-2)

applying recursively the procedure in step 2, let

$$
\begin{aligned}
\alpha_i &:= -s_i e_i - w_i^T \hat{\vartheta} + \sum_{j=1}^{i-1} \frac{\partial \alpha_{i-1}}{\partial x_j} x_{j+1} + \sum_{j=1}^{i-1} \frac{\partial \alpha_{i-1}}{\partial \xi_j} \xi_{j+1} \\
s_i &:= k_i + d_i \left(|\Omega_{ii}|^2 + \left|\sum_{j=1}^{i-1} \Omega_{ij} e_j\right|^2\right) + l_i \left|\sum_{j=1}^{i-1} Q_{ij} e_j\right|^2 \geq 0 \\
w_i &:= \phi_i - \sum_{j=1}^{i-1} \frac{\partial \alpha_{i-1}}{\partial x_j} \phi_j = w_{i\xi}(\xi_1, \ldots, \xi_i) + \sum_{j=1}^{i} \Omega_{ij} e_j \\
q_i &:= -\frac{\partial \alpha_{i-1}}{\partial \hat{\vartheta}} = q_{i\xi}(\xi_1, \ldots, \xi_{i-1}) + \sum_{j=1}^{i-1} Q_{ij} e_j.
\end{aligned}
\tag{2.118}
$$

This way, imposing the bounds:

$$
\begin{aligned}
\mu_i^2\left(k_i-\frac{R^2}{d_i}\right)-4\frac{\Xi_i^2}{k_i}-\frac{R^2}{d_i}-\frac{S^2}{l_i}>0\\
\frac{k_{i-1}}{4}\geq\frac{1}{2}+\frac{\mu_i^2}{\mu_{i-1}^2\delta_{i-1}^2},\qquad \delta_{i-1}\in(0,1)\\
\frac{c_ik_i}{\mu_i^2}\geq\frac{2c_{i-1}}{\mu_{i-1}^2(1-\delta_{i-1}^2)}
\end{aligned}
\tag{2.119}
$$

yields, as long as $e_{i+1}=0$, the bound

$$
\dot{V}_i\leq\sum_{j=1}^{i}\left[-\chi_j(\omega_j(e_j))+\epsilon_j\right]
\tag{2.120}
$$

Step r-1

The main difference with respect to the previous step is in the selection of the bounds:

$$
\begin{aligned}
\mu_{r-1}^2\left(2k_{r-1}-\frac{R^2}{d_{r-1}}\right)-4\frac{\Xi_{r-1}^2}{k_{r-1}}-\frac{R^2}{d_{r-1}}-\frac{S^2}{l_{r-1}}>0,\\
\frac{k_{r-2}}{4}\geq\frac{1}{2}+\frac{\mu_{r-1}^2}{\mu_{r-2}^2\delta_{r-2}^2},\qquad \delta_{r-2}\in(0,1)\\
\frac{c_{r-1}k_{r-1}}{\mu_{r-1}^2}\geq\frac{3}{2}\frac{c_{r-2}}{\mu_{r-2}^2(1-\delta_{r-2}^2)}.
\end{aligned}
\tag{2.121}
$$

This choice is motivated by the fact that in the following step there is no need to dominate the cross terms, as they can be directly canceled as in standard backstepping.

Step r

Finally, let $e_r:=x_r-\xi_r-\alpha_{r-1}$ and consider the controller

$$
\begin{aligned}
u(z,x,\xi,v,\hat{\vartheta})=&v-s_re_r-w_r^T\hat{\vartheta}+\sum_{j=1}^{r-1}\frac{\partial\alpha_{r-1}}{\partial x_j}x_{j+1}+\sum_{j=1}^{r-1}\frac{\partial\alpha_{r-1}}{\partial\xi_j}\xi_{j+1}-e_{r-1}\frac{c_{r-1}}{c_r}\frac{\mu_r^2-e_r^2}{\mu_{r-1}^2-e_{r-1}^2}\\
s_r:=&k_r+\frac{d_r}{\mu_r^2-e_r^2}|w_r|^2+\frac{l_r}{\mu_r^2-e_r^2}\left|\frac{\partial\alpha_{r-1}}{\partial\hat{\vartheta}}\right|^2\geq 0\\
w_r:=&\phi-\sum_{j=1}^{r-1}\frac{\partial\alpha_{i-1}}{\partial x_j}\phi_j,
\end{aligned}
\tag{2.122}
$$

with arbitrary positive gains k_r, d_r, l_r. This choice yields the following bound to $\dot{V}_r$:

$$
\dot{V}_r\leq-\sum_{i=1}^{r}\chi_i(\omega_i(e_i))+\epsilon,
\tag{2.123}
$$

with ϵ a positive scalar and χ_i a set of class $\mathcal{K}_\infty$ functions. As a direct consequence of Lemma 2.4, it follows that if $|e_i(0)|<\mu_i$, then $|e_i(t)|<\mu_i$ for $i\in\{1,\dots,r\}$. The properties of the resulting controller can be summarized in the following Theorem.

Theorem 2.2. *Consider system (2.77), subject to the control law (2.122). Let $\mathcal{D} := \{|e_i(0)| \leq \mu_i, i = 1, \ldots, r\}$ and denote with $e = (e_1, \ldots, e_r)$ the tracking error. Fix $\mu_i > 0$, $d_i > 0$, $l_i > 0$, for $i = 1, \ldots, r$, and $\delta_j \in (0, 1)$, with $j = 1, \ldots, r-2$. Let $\xi_i(\cdot) \in \mathcal{L}_\infty$, $i = 1, \ldots, r$, $v(\cdot) \in \mathcal{L}_\infty$ and $\tilde{\vartheta}(\cdot), \dot{\tilde{\vartheta}}(\cdot) \in \mathcal{L}_\infty$. Then, there exist gains k_i^* such that, for $k_i \geq k_i^*$, $i = 1, \ldots, r-1$, the following properties hold:*

1. *if $e(0) \in \mathrm{Int}(\mathcal{D})$, then the trajectories of system (2.77) are forward complete and, in addition, $e(t) \in \mathrm{Int}(\mathcal{D})$, for all $t \geq 0$;*
2. *there exist scalars $R_x > 0$ and $R_z > 0$ such that $x(t) \in R_x \mathbb{B}^r$, $z(t) \in R_z \mathbb{B}^{n-r}$, for all $e(0) \in \mathrm{Int}(\mathcal{D})$ and all $t \geq 0$.*
3. *if $\tilde{\vartheta} = \dot{\tilde{\vartheta}} = 0$, then the origin of the tracking error system, $e = 0$, is asymptotically stable with domain of attraction $\mathrm{Int}(\mathcal{D})$ and locally exponentially stable;*

Proof. For an arbitrary initial condition satisfying $|e_i(0)| < \mu_i$, $i = 1, \ldots, r$, let $[0, t_f)$ be the maximal interval of existence of the solution originating from it. Using the bound (2.123), which holds as long as the gains k_i are chosen sufficiently high according to the above backstepping design, it can be shown that there exists a proper indicator $\omega(\cdot)$ of the origin of the tracking error in $\mathcal{D}$ and a class $\mathcal{K}_\infty$ function $\bar{\chi}(\cdot)$ satisfying

$$\dot{V}_r \leq -\bar{\chi}(\omega(e)) + C.$$

By Corollary 1.1 and Lemma 2.4, the set $\mathrm{Int}(\mathcal{D})$ is forward invariant.

From this, we can prove boundedness of x. Since ξ_1 and e_1 are bounded by hypothesis and from forward invariance of $\mathrm{Int}(\mathcal{D})$, respectively, it follows that x_1 is bounded. Being a continuous function of signals living in compact sets, α_1 is uniformly bounded in its arguments, hence so is x_2 from $e_2 = x_2 - \xi_2 - \alpha_1$. Apply this procedure recursively to show that the full vector x is bounded, for any initial tracking error in $\mathrm{Int}(\mathcal{D})$ (i.e. for any initialization arbitrarily close to the boundary of $\mathcal{D}$). In addition, by Assumption 2.7, we have that to each unperturbed bounded input signal of the z-subsystem, $\xi_1(\cdot)$, corresponds a unique bounded trajectory $z_\xi(\cdot)$ that is ISS with respect to the perturbations of $\xi_1(\cdot)$. Consider now $x_1(\cdot) = \xi_1(\cdot) + e_1(\cdot)$, then from Assumption 2.7 the corresponding trajectory, $z(\cdot)$ is bounded for all $t \in [0, t_f)$, with bounds that do not depend on t_f. Hence by contradiction $t_f = \infty$.

Finally, asymptotic stability of the origin is a direct consequence of the above result, since the condition $\tilde{\vartheta} = \dot{\tilde{\vartheta}} = 0$ implies $C = 0$, and thus V_r is a Lyapunov function for the tracking error dynamics. Exponential stability can be proven exploiting Lemma 1.1 in the same fashion as in (Tee and Ge, 2011), noticing that each diagonal term of $\dot{V}_r$, W_i, for $i = 1, \ldots, r$, satisfies, as long as $\tilde{\vartheta} = \dot{\tilde{\vartheta}} = 0$:

$$W_i \leq -\kappa_i \frac{e_i^2}{\mu_i^2 - e_i^2} \leq -\kappa_i \log \frac{\mu_i^2}{\mu_i^2 - e_i^2}, \tag{2.124}$$

while the cross terms of the form $W_{i,i+1}$ are all non-positive. Therefore, it is easy to establish that there exists a positive scalar ρ such that:

$$\dot{V}_r \leq -\rho V_r, \tag{2.125}$$

hence for all $e(0) \in \mathrm{Int}(\mathcal{D})$, it holds:

$$\frac{1}{2} c_i \log \frac{\mu_i^2}{\mu_i^2 - e_i^2(t)} \leq V_r(t) \leq V_r(0) \exp(-\rho t), \tag{2.126}$$

therefore:

$$|e_i(t)| \leq \mu_i \sqrt{1 - \exp\left(-\frac{2}{c_i} V_r(0) \exp(-\rho t)\right)}. \tag{2.127}$$

Note that

$$1 - \exp\left(-\frac{2}{c_i} V_r(0) \exp(-\rho t)\right) \leq \frac{2}{c_i} V_r(0) \exp(-\rho t), \tag{2.128}$$

hence we finally get:

$$|e_i(t)| \leq \mu_i \sqrt{\frac{2}{c_i} V_r(0)} \exp\left(-\frac{\rho}{2} t\right), \tag{2.129}$$

which implies local exponential stability. □

Remark 2.3. *The existence of the balls with radius R_x, R_z in the second point of the above theorem, which depends on the selection of the tuning gains, cannot be guaranteed to exist for all initial conditions in $\mathcal{D}$ if a control of the form presented in (Tee and Ge, 2011) is employed. In that work, in fact, if the initial error conditions approach the boundary of $\mathcal{D}$, the virtual controllers tend to infinity.*

2.4.3 Asymptotic Regulation: x-Swapping Identifier Design

To achieve the desired tracking properties, we exploit an x-swapping identifier applied to system (2.77) (note that a similar design applies to system (2.1), although with increased computational complexity). For this purpose, rewrite the dynamics (2.77) as follows

$$\begin{aligned} \dot{z} &= \psi_\vartheta(z, x_1, \vartheta) \\ \dot{x} &= \begin{pmatrix} x_2 \\ \vdots \\ x_r \\ u \end{pmatrix} + \begin{pmatrix} \phi_1^T(x_1) \\ \vdots \\ \phi_{r-1}^T(x_1, \ldots, x_{r-1}) \\ \phi^T(z, x_1, \ldots, x_r) \end{pmatrix} \vartheta = f_x(x, u) + \Phi^T(z, x)\vartheta. \end{aligned} \tag{2.130}$$

Consider the filters (note that the use of the notation χ in this context is not related to the Hurwitz polynomial used for systems in normal form):

$$\begin{aligned} \dot{\chi}^T &= A\chi^T + \Phi^T(z, x) \\ \dot{\chi}_0 &= A(\chi_0 + x) - f_x(x, u), \end{aligned} \tag{2.131}$$

with A such that

$$PA + A^T P = -I, \qquad P = P^T > 0. \tag{2.132}$$

It is possible to show that the prediction error $\epsilon := x + \chi_0 - \chi^T \hat{\vartheta}$ converges exponentially to $\chi^T \tilde{\vartheta}$. Indeed, consider an observer of the form

$$\dot{\hat{x}} = A(\hat{x} - x) + f_x(x, u) + \Phi^T(z, x)\hat{\vartheta}, \tag{2.133}$$

leading to an error dynamics ($\tilde{x} := x - \hat{x}$):

$$\dot{\tilde{x}} = A\tilde{x} + \Phi^T(z, x)\tilde{\vartheta}. \tag{2.134}$$

Following the nonlinear Swapping Lemma (Krstic, Kanellakopoulos, and Kokotovic, 1995, Appendix F), (Krstic and Kokotovic, 1995) we can design the filters

$$\begin{aligned}\dot{\chi}^T &= A\chi^T + \Phi^T(z,x)\\ \dot{\chi}_d &= A\chi_d + \chi^T\dot{\hat{\vartheta}}\end{aligned} \tag{2.135}$$

to construct a signal converging to a linear regression of the parameter errors. Consider the prediction error $\tilde{\epsilon} := \tilde{x} + \chi_d - \chi^T\tilde{\vartheta}$, it is easy to see that

$$\begin{aligned}\dot{\tilde{\epsilon}} &= A\tilde{x} + \Phi^T(z,x)\tilde{\vartheta} + A\chi_d +\\ &\quad + \chi^T\dot{\hat{\vartheta}} - (A\chi^T + \Phi^T(z,x))\tilde{\vartheta} - \chi^T\dot{\hat{\vartheta}}\\ &= A\tilde{\epsilon}.\end{aligned} \tag{2.136}$$

In order to be able to implement the above structure, select $\chi_0 = \chi_d + \chi^T\hat{\vartheta} - \hat{x}$, thus recovering the filters (2.131). This way, we have that if the trajectories of (2.131) and $\tilde{\epsilon}$ exist, they satisfy $\epsilon = \tilde{\epsilon} + \chi^T\tilde{\vartheta} \to \chi^T\tilde{\vartheta}$, thus suggesting a normalized projected gradient descent for the parameter update:

$$\dot{\hat{\vartheta}} = \operatorname*{Proj}_{\hat{\vartheta}\in\bar{\Theta}}\left\{\Gamma\frac{\chi\epsilon}{1+\gamma_0\,\mathrm{Tr}(\chi^T\Gamma\chi)}\right\}, \qquad \Gamma = \Gamma^T > 0, \quad \gamma_0 > 0, \tag{2.137}$$

with $\Theta \subset \bar{\Theta} \subset \mathcal{P}$, as we showed for the case of systems in normal form. Let such projection operator be at least once differentiable, following e.g. the techniques in (Cai, Queiroz, and Dawson, 2006) (this technical aspect will be required in the stability analysis). The stability properties of this identifier are provided in the following Lemma. Let in the following $\mathcal{L}_\infty[0,t_f)$ and $\mathcal{L}_2[0,t_f)$ indicate the spaces of bounded and square-integrable functions over $[0,t_f)$, respectively.

Lemma 2.5. *Let ζ, u be defined on $[0,t_f)$. Then the update law (2.137) yields $\tilde{\vartheta} \in \mathcal{L}_\infty[0,t_f)$, $\dot{\hat{\vartheta}} \in \mathcal{L}_\infty[0,t_f) \cap \mathcal{L}_2[0,t_f)$, $\epsilon/\sqrt{1+\gamma_0\,\mathrm{Tr}(\chi^T\Gamma\chi)} \in \mathcal{L}_\infty[0,t_f) \cap \mathcal{L}_2[0,t_f)$.*

Proof. If ζ and u are defined on $[0,t_f)$, then so are χ, χ_0 since they are driven by a perturbed stable linear dynamics. Pick the Lyapunov function

$$V_\epsilon := \frac{1}{2}\tilde{\vartheta}^T\Gamma^{-1}\tilde{\vartheta} + \tilde{\epsilon}^T P\tilde{\epsilon}. \tag{2.138}$$

Applying the properties of parameter projection it follows that

$$\begin{aligned}\dot{V}_\epsilon &= -\tilde{\vartheta}\Gamma^{-1}\operatorname*{Proj}_{\hat{\vartheta}\in\bar{\Theta}}\left\{\Gamma\frac{\chi\epsilon}{1+\gamma_0\,\mathrm{Tr}(\chi^T\Gamma\chi)}\right\} + \tilde{\epsilon}(PA + A^TP)\tilde{\epsilon}\\ &\le -\frac{\epsilon^T\epsilon - \tilde{\epsilon}^T\epsilon}{1+\gamma_0\,\mathrm{Tr}(\chi^T\Gamma\chi)} - |\tilde{\epsilon}|^2\\ &= -\frac{3}{4}\frac{|\epsilon|}{1+\gamma_0\,\mathrm{Tr}(\chi^T\Gamma\chi)} - \left|\frac{1}{2}\frac{\epsilon}{1+\gamma_0\,\mathrm{Tr}(\chi^T\Gamma\chi)} - \tilde{\epsilon}\right|^2\\ &\le -\frac{3}{4}\frac{|\epsilon|}{1+\gamma_0\,\mathrm{Tr}(\chi^T\Gamma\chi)} \le 0.\end{aligned} \tag{2.139}$$

As a consequence, since $V_\epsilon(t) \le V_\epsilon(0)$, we have that $\tilde{\vartheta} \in \mathcal{L}_\infty[0,t_f)$, $\tilde{\epsilon} \in \mathcal{L}_\infty[0,t_f)$. Note that the norm of $\Gamma^{1/2}\chi/\sqrt{1+\gamma_0\,\mathrm{Tr}(\chi^T\Gamma\chi)}$ is bounded by its Frobenius norm as follows:

$$\left| \frac{\Gamma^{1/2}\chi}{\sqrt{1+\gamma_0 \operatorname{Tr}(\chi^T \Gamma \chi)}} \right| \le \left| \frac{\Gamma^{1/2}\chi}{\sqrt{1+\gamma_0 \operatorname{Tr}(\chi^T \Gamma \chi)}} \right|_{\mathcal{F}} = \sqrt{\frac{\operatorname{Tr}(\chi^T \Gamma \chi)}{1+\gamma_0 \operatorname{Tr}(\chi^T \Gamma \chi)}} \le 1, \quad (2.140)$$

with a bound which holds regardless of χ, which is instead allowed to grow unbounded as $t \to t_f$. Note that $0 < \lambda_{\min}|\chi|^2 \le \chi^T \Gamma \chi$, with $\lambda_{\min}$ the smallest eigenvalue of Γ, so a uniform bound holds on $\chi / \sqrt{1+\gamma_0 \operatorname{Tr}(\chi^T \Gamma \chi)}$ as well. Then, it follows that:

$$\begin{aligned} |\dot{\hat{\vartheta}}| &\le |\Gamma| \left| \frac{\chi}{\sqrt{1+\gamma_0 \operatorname{Tr}(\chi^T \Gamma \chi)}} \right|^2 |\tilde{\vartheta}| + \\ &\quad + \frac{|\Gamma|}{\sqrt{1+\gamma_0 \operatorname{Tr}(\chi^T \Gamma \chi)}} \left| \frac{\chi}{\sqrt{1+\gamma_0 \operatorname{Tr}(\chi^T \Gamma \chi)}} \right| |\tilde{\varepsilon}| \\ &\le c < \infty \end{aligned} \quad (2.141)$$

with c which depends on the initial conditions and x, but not explicitly on t_f. From this uniform bound, it holds $\dot{\hat{\vartheta}} \in \mathcal{L}_\infty[0, t_f)$ and therefore $\epsilon / \sqrt{1+\gamma_0 \operatorname{Tr}(\chi^T \Gamma \chi)} \in \mathcal{L}_\infty[0, t_f)$. Recalling standard arguments,

$$-\int_0^{t_f} \dot{V}_\epsilon(\tau) d\tau = V_\epsilon(0) - V_\epsilon(t_f) \le V_\epsilon(0), \quad (2.142)$$

so $\epsilon / \sqrt{1+\gamma_0 \operatorname{Tr}(\chi^T \Gamma \chi)} \in \mathcal{L}_2[0, t_f)$ and, due to the above bound on $\chi / \sqrt{1+\gamma_0 \operatorname{Tr}(\chi^T \Gamma \chi)}$, also $\dot{\hat{\vartheta}} \in \mathcal{L}_2[0, t_f)$. □

With the properties of Lemma 2.5, we can state the stability properties of the closed-loop interconnection between stabilizer and identifier.

Theorem 2.3. *Consider system* (2.77)*, subject to the control law* (2.122)*, combined with the x-swapping identifier* (2.131)-(2.137)*. Let $\xi_i(\cdot) \in \mathcal{L}_\infty$ with $i \in \{1, \dots, r\}$ and $v(\cdot) \in \mathcal{L}_\infty$. Then, for all $e(0) \in \operatorname{Int}(\mathcal{D})$ and all $\hat{\vartheta}(0) \in \bar{\Theta}$ there exist positive gains k_i^*, $1 \le i \le r-1$ such that, for $k_i \ge k_i^*$, the trajectories are forward complete and uniformly bounded, $e(t) \in \operatorname{Int}(\mathcal{D})$ for all $t \ge 0$, and asymptotic tracking is achieved:*

$$\lim_{t\to\infty} x_1(t) - \xi_1(t) = 0. \quad (2.143)$$

Proof. Firstly, we prove forward completeness and boundedness of all trajectories. Consider $[0, t_f)$ the maximal interval of existence of the trajectories of the closed-loop system. In $[0, t_f)$, Lemma 2.5 implies $\tilde{\vartheta}(\cdot), \dot{\hat{\vartheta}}(\cdot) \in \mathcal{L}_\infty[0, t_f)$. From Theorem 2.2, we have that $\dot{V}_n \le -\bar{\chi}(\omega(e)) + C$, hence $e(\cdot) \in \mathcal{L}_\infty[0, t_f)$, and $x(\cdot), z(\cdot) \in \mathcal{L}_\infty[0, t_f)$. For any compact set of feasible initial conditions, we have that $u(\cdot) \in \mathcal{L}_\infty[0, t_f)$, so $\chi^T(\cdot) \in \mathcal{L}_\infty[0, t_f)$, $\chi_0(\cdot) \in \mathcal{L}_\infty[0, t_f)$ as they are exponentially stable linear systems driven by bounded inputs. This way, we proved that all trajectories are bounded in $[0, t_f)$, with a bound that does not depend on t_f. Thus, $t_f = \infty$ by contradiction.

From boundedness of all signals, we have that $\epsilon(\cdot) \in \mathcal{L}_2[0, \infty)$. In addition, it holds

$$\dot{\epsilon} = \left[A\chi^T + \Phi^T(z, x) \right] \tilde{\vartheta} + \chi^T \dot{\hat{\vartheta}} + A\tilde{\epsilon}, \quad (2.144)$$

hence $\dot{\epsilon}$ is uniformly bounded, and therefore a straightforward application of Barbalăt's Lemma (see Appendix A.1) yields $\epsilon(t) \to 0$ as $t \to \infty$. The same arguments are employed to prove that $\dot{\tilde{\vartheta}} \to 0$ asymptotically. Since $\epsilon \to 0$ it holds

$$\lim_{t\to\infty} \int_0^s \dot{\epsilon}(s)ds = \lim_{t\to\infty} \epsilon(t) - \epsilon(0) = -\epsilon(0) < \infty, \tag{2.145}$$

hence from the boundedness of $\ddot{\epsilon}$ (which can be readily verified with straightforward computations), apply once again Barbalăt's Lemma to yield $\dot{\epsilon}(t) \to 0$ asymptotically. Note that the tracking error dynamics can be rewritten as

$$\dot{e} = A_e(e,\hat{\vartheta},t)e + W_e^T(e,\hat{\vartheta},t)\tilde{\vartheta} + Z_e^T(e,\hat{\vartheta},t)\dot{\hat{\vartheta}}, \tag{2.146}$$

with W_e^T that can be decomposed as

$$W_e^T = \begin{pmatrix} 1 & 0 & \cdots & 0 \\ -\frac{\partial\alpha_1}{\partial x_1} & 1 & \ddots & \vdots \\ \vdots & \ddots & \ddots & 0 \\ -\frac{\partial\alpha_{r-1}}{\partial x_1} & \cdots & -\frac{\partial\alpha_{r-1}}{\partial x_{r-1}} & 1 \end{pmatrix} \begin{pmatrix} \phi_1^T \\ \vdots \\ \phi^T \end{pmatrix} = N\Phi^T. \tag{2.147}$$

Additionally, the swapping identifier dynamics can be conveniently rewritten as

$$\dot{\epsilon} = A\epsilon + \Phi^T(z,x)\tilde{\vartheta} - \chi^T\dot{\hat{\vartheta}}. \tag{2.148}$$

It follows immediately that

$$\Phi^T(z,x)\tilde{\vartheta} \to 0, \tag{2.149}$$

which yields $W_e^T\tilde{\vartheta} \to 0$ from invertibility of N. From the same arguments in Theorem 2.2, it follows that

$$\dot{V}_r \le -\rho V_r + C(t), \tag{2.150}$$

where $C(t)$ converges to zero as $\tilde{\vartheta} \to 0$, $\dot{\tilde{\vartheta}} \to 0$. Therefore, as a final step of the proof, recall (Krstic, Kanellakopoulos, and Kokotovic, 1995, Lemma B.8) to yield $e \to 0$. □

2.4.4 State Constraints Feasibility: Right-Inverse Design

Finally, we focus on the problem of generating the reference trajectory ξ. The considerations deriving from the above stabilizer provide some valuable insights on how to design it. Indeed, Theorem 2.2 guarantees that not only the error coordinates, but also the original coordinates are contained in a compact set, which depends on the choice of the gains for tuning and the reference ξ. This suggests that, to impose state constraints feasibility, ξ must be shaped to fit the compact set of trajectories within the desired set. Following the notation in the previous subsections, we consider a system of the form

$$\begin{aligned} \dot{\xi}_1 &= \xi_2 \\ &\vdots \\ \dot{\xi}_r &= v, \end{aligned} \tag{2.151}$$

with v a feedback law to be appropriately designed.

Our first step is to show how the ξ-dynamics can be effectively mapped into a unique, globally defined right-inverse of system (2.77). In particular, we intend to find the input sequence u that guarantees that the output $y = x_1$ is matched with the first element of the above chain, ξ_1. For, suppose $y = x_1 = \xi_1$ at all times, then

$$x_2 = \xi_2 - \phi_1^T(\xi_1)\vartheta = \xi_2 + h_1(\xi_1, \vartheta), \tag{2.152}$$

which suggests:

$$\begin{aligned} x_3 &= \frac{d}{dt}(\xi_2 + h_1(\xi_1, \vartheta)) - \phi_2^T(\xi_1, \xi_2 + h_1(\xi_1, \vartheta))\vartheta \\ &= \xi_3 + \frac{\partial h_1}{\partial \xi_1}(\xi_1, \vartheta)\xi_2 - \phi_2^T(\xi_1, \xi_2 + h_1(\xi_1, \vartheta))\vartheta \\ &= \xi_3 + h_2(\xi_1, \xi_2, \vartheta). \end{aligned} \tag{2.153}$$

Apply the same procedure recursively to yield the following relations:

$$\begin{aligned} x_1 &= \xi_1 \\ x_2 &= \xi_2 + h_1(\xi_1, \vartheta) \\ x_3 &= \xi_3 + h_2(\xi_1, \xi_2, \vartheta) \\ &\vdots \\ x_r &= \xi_r + h_{r-1}(\xi_1, \dots, \xi_{r-1}\vartheta) \\ u &= v + h_r(z, \xi, \vartheta), \end{aligned} \tag{2.154}$$

where h_i, $i \in \{1, \dots, r\}$ are continuously differentiable maps, due to the regularity assumptions imposed to the vector field. The right-inverse of system (2.77) can be thus represented by a model of the form

$$\begin{aligned} &\dot{z} = \psi_\vartheta(z, C_\xi \xi, \vartheta), \qquad C_\xi = \begin{pmatrix} 1 & 0 & \dots & 0 \end{pmatrix} \\ &\dot{\xi} = \left(\begin{array}{c|c} 0 & \\ \vdots & I_{r-1} \\ 0 & \\ \hline 0 & 0 \ \dots \ 0 \end{array}\right)\xi + \begin{pmatrix} 0 \\ \vdots \\ 0 \\ 1 \end{pmatrix} v = A_\xi \xi + B_\xi v \\ &x = \xi + M_\xi(\xi, \vartheta), \qquad u = v + h_r(z, \xi, \vartheta). \end{aligned} \tag{2.155}$$

This structure could be intuitively exploited as in Section 2.2, following a design for systems in normal form (requiring then to include an Explicit Reference Governor to ensure feasibility at all times). In this section, however, we intend to follow a different approach, based on the available robustness properties of the zero-dynamics. Indeed, recalling the properties deriving from Assumption 2.7, we have that the $\tilde{z}$-subsystem deriving from (2.155) (with $\tilde{z} = z - \pi_z(\xi_1, \vartheta)$) is ISS with respect to ξ_2. Indeed, from $V_z = (1/2)\tilde{z}^T P \tilde{z}$, it follows that

$$\dot{V}_z \leq -c_z V_z + d_z |P^{1/2}\tilde{z}||\xi_2|, \tag{2.156}$$

for some positive scalars c_z, d_z. Let $y_\mathrm{r} \in \mathcal{Y}_\mathrm{r}$ be a constant reference that the output of the system, y, is required to track, and suppose that an appropriate BLF of the form $W_\xi(\xi_1, y_\mathrm{r})$ was designed to achieve such regulation objective, as well as to ensure that the steady state configurations $(\pi_z(\xi_1, \vartheta), \xi_1, 0, \dots, 0)$ are feasible for the constraints (2.78). The above ISS bounds suggests that, intuitively, the right-inverse should always operate sufficiently close to the condition $(\xi_2, \dots, \xi_r) = 0$, i.e. in a "quasi-static" fashion. In particular, this indicates that ξ_2 should be designed to establish a slow gradient descent of the map $W_\xi(\xi_1, y_\mathrm{r})$. Following this idea, the next design steps propose a strategy to effectively address the trajectory generation problem. Note that such technique is currently under investigation, therefore only an outline is presented.

Because of the continuous differentiability of the map M_ξ, it is possible to factorize h_i as

$$h_i(\xi_1, \dots, \xi_i, \vartheta) = h_{Bi}(\xi_1, \vartheta) + \Delta_i^T(\xi_1, \dots, \xi_i, \vartheta) \begin{pmatrix} \xi_2 \\ \vdots \\ \xi_i \end{pmatrix}, \quad i = 2, \dots, r-1, \tag{2.157}$$

with in addition $h_1 = h_{B1}$. Then, v can be designed according to the following procedure:

- choose positive scalars X_π, X_1' satisfying $0 < X_\pi < X_1' < X_1$;
- for $i = 2, \dots, r$, choose X_{Bi}, X_i' such that $0 < X_{Bi} < X_i' < X_i$;
- following a backstepping procedure consider, in the first step, a BLF that incorporates the constraints $|\xi_1| \leq X_\pi$ and $|h_{Bi}(\xi_1, \vartheta)| \leq X_{Bi}$ $i \in \{1, \dots, r-1\}$, $\underline{Z}_j^\delta = \underline{Z}_j + \delta \leq \pi_{z,j}(\xi_1, \vartheta) \leq \overline{Z}_j - \delta = \overline{Z}_j^\delta$, $j \in \{1, \dots, n-r\}$, for some positive scalar δ ensuring that the resulting intervals are non-empty, considering the worst case scenario for $\vartheta \in \bar{\Theta}$;
- design the first virtual control action $\pi(\cdot)$ as a smooth map depending on the gradient of the BLF of the previous step, with a shape such that its derivatives can be chosen arbitrarily small. In particular, π has to be designed so that the maximal perturbation in (2.156) as $\xi_2 = \pi$, i.e. when $|\xi_2| = \max_{(\xi_1, \vartheta)} |\pi(\xi_1, \vartheta)|$, ensures that the residual trajectories of the z-subsystem are contained in the interval $[\underline{Z}_j + \delta_\pi, \overline{Z}_j - \delta_\pi]$, with $0 < \delta_\pi < \delta$;
- complete the backstepping design from the second to the r-th step in order to obtain linear error equations. In addition, design the virtual controller gains, together with the structure of $\pi(\cdot)$, so to ensure feasibility of the right-inverse with respect to the conditions $|\xi_i + h_{i-1}| \leq X_i'$, $i \in \{1, \dots, r\}$ (with $h_0 = 0$), $\underline{Z}_j + \delta_\xi \leq z_j \leq \overline{Z}_j - \delta_\xi$, $j \in \{1, \dots, n-r\}$, in an appropriate domain of attraction and for a positive scalar $0 < \delta_\xi < \delta_\pi$.

In other words, $\pi(\cdot)$ must be sufficiently smooth to guarantee that its derivatives, that arise during backstepping recursion, are sufficiently small to contain the virtual controllers within the desired bounds. The linear stabilizing gains are then used to ensure attraction of the manifold $\xi_2 = \pi$, this way ensuring that the nonlinearities arising from H_ξ are correctly dealt with the BLF. To appropriately confine the z-subsystem in the feasible set, we both exploit the boundedness properties of π and the gains of the backstepping controller. Note that in the full structure the feasibility margin of z has to account for both the off-manifold error $\xi_2 - \pi$ and the tracking error introduced by the robust stabilizer (handled with $\delta_\xi > 0$).

We briefly sketch this backstepping procedure, without intending to be exhaustive. Following an approach similar to the structure in (2.33) (or its Constrained-Inversion MRAC equivalent), consider:

$$W_\xi(\xi_1, y_r) := \frac{1}{2}\left(\omega(\xi_1) - y_r\right)^2 + k_B B(H(\xi_1)), \tag{2.158}$$

with k_B a positive scalar for tuning and $B(\cdot)$ such that

$$\begin{aligned}
B(H) &= -\ln\left(\frac{H}{1+H}\right), \\
H(\xi_1,\vartheta) &= \prod_{i=1}^{r-1}(h_{Bi,\mathrm{m}}(\xi_1)+X_{Bi})(X_{Bi}-h_{Bi,\mathrm{M}}(\xi_1))\prod_{j=1}^{n-r}(\pi_{\mathrm{m},j}(\xi_1)-\underline{Z}_j^{\delta})(\overline{Z}_j^{\delta}-\pi_{\mathrm{M},j}(\xi_1)), \\
h_{Bi,\mathrm{m}}(\xi_1) &= \min_{\hat\vartheta\in\bar\Theta} h_{Bi}(\xi_1)(\xi_1,\hat\vartheta), \qquad h_{Bi,\mathrm{M}}(\xi_1) = \max_{\hat\vartheta\in\bar\Theta} h_{Bi}(\xi_1,\hat\vartheta), \\
\pi_{\mathrm{m},i}(\xi) &= \min_{\hat\vartheta\in\bar\Theta} \pi_{z,j}(\xi_1,\hat\vartheta), \qquad \pi_{\mathrm{M},j}(\xi_1) = \max_{\hat\vartheta\in\bar\Theta} \pi_{z,j}(\xi_1,\hat\vartheta).
\end{aligned} \tag{2.159}$$

Suppose that a nonlinear map of the form

$$\pi = \pi_\kappa\left(\xi_1, y_{\mathrm{r}}, \frac{\partial W_\xi}{\partial \xi_1}\right) \tag{2.160}$$

exists and can be shaped, through a set of parameters $\kappa \in \mathcal{K}$ so that, for any set of positive scalars N_i, $i = 1,\dots,r$, there exists a set $\bar{\mathcal{K}} \subset \mathcal{K}$ such that, for any $\kappa \in \bar{\mathcal{K}}$ it holds:

$$\left|\frac{\partial^{i-1}\pi}{\partial \xi_1^{i-1}}\right| \le N_j. \tag{2.161}$$

Let $\tilde\xi_2 := \xi_2 - \pi$, it holds:

$$\dot{\tilde\xi}_2 = \xi_3 - \frac{\partial \pi}{\partial \xi_1}\tilde\xi_2 - \frac{\partial \pi}{\partial \xi_1}\pi, \tag{2.162}$$

and note that we could employ, as virtual controller, a feedback of the form

$$\alpha_2 = \frac{\partial \pi}{\partial \xi_1}\pi - \left(m_2 - \frac{\partial \pi}{\partial \xi_1}\right)\tilde\xi_2, \tag{2.163}$$

with m_2 a positive scalar for tuning. We can thus define the next tracking error as $\tilde\xi_3 := \xi_3 - \alpha_2$, and continue recursively, obtaining at last an error system of the form:

$$\begin{aligned}
\dot\xi_1 &= \pi + \tilde\xi_2 \\
\dot{\tilde\xi}_i &= -m_i\tilde\xi_i + \tilde\xi_{i+1}, \qquad i = 2,\dots,r-1, \\
\dot{\tilde\xi}_r &= -m_r\tilde\xi_r
\end{aligned} \tag{2.164}$$

which yields the desired input v. It can be shown that each virtual controller, α_i, can be bounded by proper selection of π_τ, the above bounds N_j, $j = 1,\dots,n$, and an appropriate selection of the initial conditions $(\tilde\xi_2,\dots,\tilde\xi_r)$, with associated gains $m_2,\dots,m_r$. This way, by means of (2.154), (2.157), it is possible to ensure that the trajectories of x and z, in conditions of perfect tracking, are feasible for the sets considered in the right-inverse design, as long as the initial conditions of $(\tilde\xi_2,\dots,\tilde\xi_r)$ and the gains $m_2,\dots,m_r$ are chosen appropriately.

We do not delve any further in this topic, as future efforts will be dedicated to fully explore this alternative strategy for right-inverse trajectory generation. To conclude this section, we will sketch the intuitive procedure to tune the stabilizer, in particular through the application of the presented techniques to a simple relative degree 1 system with input and state constraints.

2.4.5 Tuning Procedure to Enforce Constraint Feasibility: Scalar Relative Degree 1 Example

We consider a system of the form:

$$\dot{x} = \phi^T(x)\vartheta + u, \tag{2.165}$$

with constraints given by $|x| \le X$, $|u| \le U$. Firstly, we can perform an extension of the above system with an integral action:

$$\begin{aligned} \dot{x} &= \phi^T(x)\vartheta + u \\ \dot{\eta} &= \varphi, \end{aligned} \tag{2.166}$$

which yields a system of the form (2.79), with state constraints $|x| \le X$, $|\eta| \le U$. Consider a controller of the form:

$$\begin{aligned} &e_1 = x - \xi_1, \quad \alpha = -k_1 e_1 - d_1 \left| \frac{\phi(x) - \phi(\xi_1)}{e_1} \right|^2 e_1 - \phi^T(x)\hat{\vartheta}, \\ &e_2 = \eta - \xi_2 - \alpha, \qquad \dot{\xi}_1 = \xi_2 \qquad \dot{\xi}_2 = v \\ &\dot{\eta} = v - k_2 e_2 - w^T\hat{\vartheta} - \left(d_2 \left| \frac{\partial \alpha}{\partial x}\phi(x) \right|^2 + l \left| \frac{\partial \alpha}{\partial \hat{\vartheta}} \right|^2 \right) \frac{e_2}{\mu_2^2 - e_2^2} - e_1 \frac{\mu_2^2 - e_2^2}{\mu_1^2 - e_1^2} + \frac{\partial \alpha}{\partial x}\eta + \frac{\partial \alpha}{\partial x}\xi_2, \\ &\dot{\chi}^T = -\chi^T + \phi^T(x) \qquad \dot{\chi}_0 = -(\chi_0 + x) + \eta \\ &\dot{\hat{\vartheta}} = \operatorname*{Proj}_{\hat{\vartheta} \in \bar{\Theta}} \left\{ \Gamma\chi \frac{x + \chi_0 - \chi^T\hat{\vartheta}}{1 + \gamma_0 Tr(\chi^T\Gamma\chi)} \right\} \qquad w = -\frac{\partial \alpha}{\partial x}\phi(x), \end{aligned} \tag{2.167}$$

for some positive gains k_1, k_2, d_1, d_2, μ_1, μ_2, l, γ_0 and a positive-definite matrix Γ. In addition, let v be a control law to be designed to guarantee a feasible right-inverse. Denote for simplicity:

$$\Omega(\xi_1, e_1) = \frac{\phi(x) - \phi(\xi_1)}{e_1}, \tag{2.168}$$

which is well defined in $e_1 = 0$ due to the continuous differentiability of the map ϕ. It is easy to notice that x and u can be rewritten as:

$$\begin{aligned} x &= \xi_1 + e_1 \\ u &= \xi_2 - \phi^T(\xi_1)\hat{\vartheta} + e_2 + \left(-k_1 - d_1|\Omega|^2 - \Omega^T\hat{\vartheta} \right) e_1. \end{aligned} \tag{2.169}$$

The tuning procedure can be performed as follows. Let $0 < X' < X$, $0 < U' < U$, then we impose that the right-inverse satisfies

$$|\xi_1| \le X', \qquad |\phi^T(\xi_1)\hat{\vartheta}| \le U_B, \qquad |\xi_2 + \phi^T(\xi_1)\hat{\vartheta}| \le U'. \tag{2.170}$$

The selection of the gains must then satisfy the following set of inequalities:

$$\begin{aligned} \mu_1 - (X - X') &\le 0 \\ k_1^2 - k_1 \frac{R^2}{d_1} - 2\frac{\Xi^2}{\mu_1^2} &> 0 \\ \mu_2 + [k_1 + L(r_\vartheta + R) + d_1 L^2]\mu_1 - (U - U') &\le 0, \end{aligned} \tag{2.171}$$

where $R = \|\tilde{\vartheta}\|_\infty$, $\Xi = \|\phi^T\tilde{\vartheta}\|_\infty$, r_ϑ is the maximum value of $|\vartheta|$ and L is the Lipschitz constant of ϕ in the interval $[-X, X]$. Note that the first and third inequalities embed the boundedness of trajectories requirement, while the second is imposed to guarantee that the stabilizer is ISS with respect to $\tilde{\vartheta}$. As we can see, the constraints are then satisfied by tuning rules that only depend on the data of the system, and not its trajectories. This becomes possible only as long as the control problem is split into a trajectory planning module and a robust stabilizer.

Choose, and fix, arbitrary gains $d_1 > 0$ and $0 < \mu_2 < U - U'$. We investigate the conditions which ensure feasibility of the conditions (2.171) in the arguments k_1, μ_1. From the second inequality it follows that:

$$\mu_1 > \Xi\sqrt{\frac{2}{k_1\left(k_1 - \frac{R^2}{d_1}\right)}}, \tag{2.172}$$

while the third yields

$$\mu_1 \leq \frac{U - U' - \mu_2}{k_1 + L(r_\vartheta + R) + d_1 L^2}. \tag{2.173}$$

Note that this last inequality can be used to remove the constraint $\mu_1 - (X - X') \leq 0$. Combine these conditions, applying the bounds on μ_1^2:

$$\Xi^2 \frac{2}{k_1^2 - k_1\frac{R^2}{d_1}} < \frac{(U - U' - \mu_2)^2}{(k_1 + L(r_\vartheta + R) + d_1 L^2)^2}, \tag{2.174}$$

which also reads as

$$2\Xi^2(k_1 + L(r_\vartheta + R) + d_1 L^2)^2 < (U - U' - \mu_2)^2\left(k_1^2 - k_1\frac{R^2}{d_1}\right). \tag{2.175}$$

This last inequality finally provides the desired bound, obtained by inspection of the two polynomials in the decision variable k_1. The right-hand side is a parabola with one zero root and a positive root, while the left-hand side has two negative and coincident roots. As a consequence, the condition is violated for small k_1. In order to guarantee the existence of feasible values of k_1, we require then that the second derivative of the right-hand side is larger, i.e.:

$$\mu_2 + \sqrt{2}\Xi \leq U - U', \tag{2.176}$$

which can be satisfied with proper selection of the right-inverse constraints. This suggests that feasibility is inherently related to the design of the right-inverse. Therefore, even though (2.171) introduces nonlinear relations between the gains, the resulting tuning rule becomes relatively simple and can be performed with ease. We believe that the extension of such method to arbitrary relative degrees should become a simple recursive algorithm, which somehow resembles a nonlinear equivalent of linear matrix inequality (LMI).

Finally we outline how to proceed with the right-inverse module. Consider a Barrier Lyapunov Function $W_\xi(\xi_1, y_r)$ of the form (2.158), embedding the constraints $|\xi_1| \leq X_\pi < X_1'$, $|\phi^T(\xi_1)\hat{\vartheta}| \leq U_B < U'$. Then, choose

$$\pi = -N\sigma\left(\lambda(\xi_1)\frac{\frac{\partial W_\xi}{\partial \xi_1}}{1 + \left(\frac{\partial W_\xi}{\partial \xi_1}\right)^2}\right), \tag{2.177}$$

with σ a saturation function satisfying $|\sigma| \leq 1$, N a positive scalar and $\lambda(\xi_1) > 0$ a nonlinear gain used to adjust the shape of π and its derivatives. As a consequence, let $\tilde{\xi}_2 = \xi_2 - \pi$ and

$$v = \frac{\partial \pi}{\partial \xi_1}\pi - \left(m - \frac{\partial \pi}{\partial \xi_1}\right)\tilde{\xi}_2, \tag{2.178}$$

with m a positive scalar. This way, we finally obtain the error system

$$\begin{aligned} \dot{\xi}_1 &= \pi + \tilde{\xi}_2 \\ \dot{\tilde{\xi}}_2 &= -m\tilde{\xi}_2. \end{aligned} \tag{2.179}$$

Choose m and an appropriate range of $|\tilde{\xi}_2(0)|$ to ensure that the constraints in (2.170) are satisfied at all times.

2.5 Concluding Remarks

In this chapter, we presented a novel control architecture that combines adaptive control for nonlinear systems and hard constraint satisfaction. The proposed structure is based on the interconnection of a reference generation unit, designed so to impose a feasible right-inversion of the plant, and a robust adaptive stabilizer. Firstly, we showed that through two time scales arguments it is possible to completely solve the problem for systems that can be written in the canonical normal form, and we validated the approach by means of simulation tests on an Euler-Lagrange system. Then, we sketched a promising direction that can be pursued for systems in strict-feedback form, with a stabilizer structure that in principle does not require high-gain arguments to guarantee feasibility. Future activities will be devoted to consolidate this novel approach and extend it to larger classes of systems, as well as to deal with the problem of time-varying reference tracking and output feedback.

Part II

Observers for Nonlinear Systems on Manifolds

Chapter 3

Dynamical Systems and Observability on Manifolds

The previous part of the thesis focused on control systems with hard inequality constraints and parametric uncertainties. Such class of limitations is not however the only one that is faced in engineering applications, and indeed problems involving equality constraints or limits on the shape of the dynamics (e.g. nonholonomic constraints) are vastly reported as well in the literature. A relevant case is given in particular by dynamical systems bound to evolve on manifolds, which in general may not be convex, or even contractible. Notably, many complex behaviors are related to an inherently nonlinear state space domain, e.g. involving intensities and phases, which typically arise in engineering, biological, financial or social systems. We refer to this class of constraints as *topological constraints*. In this context, the main goal is to achieve global or semi-global results, regardless of the challenging structure of the state space, which only locally presents a classic vector space structure. These topological constraints are also connected to several engineering applications, related e.g. to attitude control (Tsiotras, 1996), estimation (Mahony, Hamel, and Pflimlin, 2008) and synchronization (Sarlette, Sepulchre, and Leonard, 2009), Kuramoto oscillators synchronization (Scardovi, Sarlette, and Sepulchre, 2007; Dorfler and Bullo, 2012; Bosso, Azzollini, and Baldi, 2019), inertial navigation (Farrell, 2008; Bosso et al., 2018), vehicle pose control (Bellens, De Schutter, and Bruyninckx, 2012) and synchronization (Igarashi et al., 2009).

The focus of this part of the thesis is on observation. In particular, given a dynamical system on a manifold, we are interested in an estimator which directly evolves on such manifold. This requirement is motivated by several reasons of practical interest, including robustness and in general a smaller number of required state variables, and for this reason it agrees with the objective of developing computational-effective algorithms. Clearly, imposing equality constraints of this form poses some challenges, and calls for special attention both in analysis and design. However, with these tools it is often possible to extend the analysis (and hopefully the convergence/stability properties) globally or semi-globally, a feature that is possibly hindered or severely complicated with the vector space formalism.

In this chapter, we begin recalling some basic mathematical elements related to manifolds and dynamical systems defined on them, without the purpose of being exhaustive. The content of the first sections does not include any novel material, but is intended as instrumental to clarify the following arguments and keep this thesis as much self-contained as possible. The introduction to manifolds is based on (Isidori, 2013; De Marco, 2017), while Lie groups and dynamical systems on them can be found e.g. in (Zhang, Sarlette, and Ling, 2015; Barrau and Bonnabel, 2016; De Marco, 2017) and references therein. In the following sections, the indistinguishable dynamics approach, based on the seminal work (Hermann and Krener, 1977), is presented as a valid method to yield global observability properties, and is thus shown to be fundamental to extend to inherently non-local approaches. Finally, some meaningful observer structures are recalled, and the main idea of the problem underlying the next chapter's developments is presented as a direction for future generalizations.

3.1 Dynamical Systems on Manifolds

We begin with a formal definition of smooth manifold, after a brief introduction of some basic topology notions.

Definition 3.1 (Topological Space)**.** *A topological space is a set $\mathcal{S}$ with a topology τ, i.e. a collection of subsets of $\mathcal{M}$ (referred to as open sets in the following) satisfying the following axioms:*

- *$\varnothing$ and $\mathcal{S}$ belong to τ;*
- *any arbitrary union of members of τ belongs to τ;*
- *any finite intersection of members of τ belongs to τ.*

A map between two topological spaces is called a homeomorphism if it is bijective, continuous and its inverse is continuous. Recall that, given a topological space $\mathcal{S}$, a basis is a collection of open sets, called basic open sets, such that $\mathcal{S}$ is the union of such sets and a nonempty intersection of two basic open sets is the union of basic open sets. For any point $p \in \mathcal{S}$, a neighborhood of p is any open set containing p. A Hausdorff topological space is a topological space $\mathcal{S}$ such that any $p_1, p_2 \in \mathcal{S}$, with $p_1 \neq p_2$, have disjoint neighborhoods.

Definition 3.2 (Manifold)**.** *A Hausdorff topological space $\mathcal{M}$ with countable basis is a manifold of dimension n if it is locally Euclidean of dimension n, that is, for all $p \in \mathcal{M}$, there exists a homeomorphism $\phi : \mathcal{U} \to \mathbb{R}^n$, for some neighborhood $\mathcal{U}$ of p.*

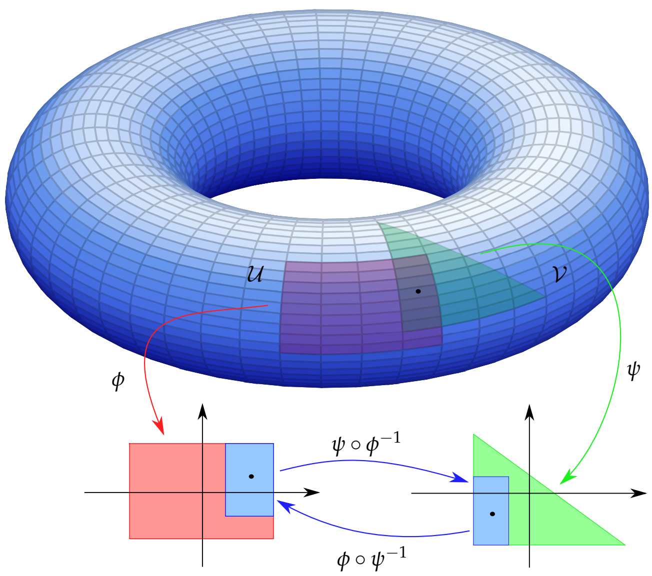

FIGURE 3.1: Example of a smooth manifold (2-torus).

A chart on a manifold $\mathcal{M}$ of dimension n is a pair $(\mathcal{U}, \phi)$, where $\mathcal{U}$ is an open subset of $\mathcal{M}$ and ϕ is a homeomorphism of $\mathcal{U}$ onto an open subset of $\mathbb{R}^n$. Two charts $(\mathcal{U}, \phi)$, $(\mathcal{V}, \psi)$ are called $\mathcal{C}^\infty$-compatible if, whenever $\mathcal{U} \cap \mathcal{V} \neq \emptyset$ the map $\psi \circ \phi^{-1} : \phi(\mathcal{U} \cap \mathcal{V}) \mapsto \psi(\mathcal{U} \cap \mathcal{V})$ is a diffeomorphism. A $\mathcal{C}^\infty$ atlas is a collection $\{(\mathcal{U}_i, \phi_i) : i \in A\}$ of pairwise $\mathcal{C}^\infty$-compatible charts on $\mathcal{M}$ satisfying $\cup_{i \in A} \mathcal{U}_i = \mathcal{M}$. An atlas is complete if it is maximal, i.e. it is not contained in any other atlas. Finally, we can formally define a smooth manifold.

Definition 3.3 (Smooth Manifold)**.** *A smooth manifold is a manifold with a $\mathcal{C}^\infty$ complete atlas.*

See Figure 3.1 for the representation of a manifold of dimension 2, along with a couple of compatible charts $(\mathcal{U}, \phi)$, $(\mathcal{V}, \psi)$. Given a smooth manifold $\mathcal{M}$, two differentiable curves $\gamma_1, \gamma_2 : \mathbb{R} \to \mathcal{M}$ are equivalent at $p \in \mathcal{M}$ if $\gamma_1(0) = \gamma_2(0) = p$ and $(d/dt)(\phi \circ \gamma_1)(0) = (d/dt)(\phi \circ \gamma_2)(0)$, for some chart $(\mathcal{U}, \phi)$. It follows that a tangent vector v at p is an equivalence class of all equivalent differentiable curves at p. Denote with $T_p\mathcal{M}$ the tangent space to the manifold at p. The tangent bundle of $\mathcal{M}$ is given by

$$T\mathcal{M} = \cup_{p \in \mathcal{M}} T_p\mathcal{M}. \tag{3.1}$$

Finally, a vector field on the manifold $\mathcal{M}$ is a map $f : \mathcal{M} \to T\mathcal{M}$ such that $f(p) \in T_p\mathcal{M}$, for all $p \in \mathcal{M}$.

With these instruments available, it is easy to introduce dynamics on manifolds. Indeed, a vector field f on a manifold $\mathcal{M}$ can be used to define the velocity of a system evolving on it. The simplest example of such systems takes the form

$$\dot{p} = f(p), \qquad p(t_0) = p_0 \in \mathcal{M}, \tag{3.2}$$

with $t_0 \in \mathbb{R}$ the initial time. Clearly, time-varying systems on manifolds can be defined with the same tools. Since $T\mathcal{M}$ is a smooth manifold of dimension $2n$, it is possible to define a vector field on it, assigning to each pair $(p, \dot{p})$ an element of $T_{(p,\dot{p})}T\mathcal{M}$. This way, the acceleration contained in $T_{(p,\dot{p})}T\mathcal{M}$ can be used similarly to the above differential equation. Note that the integration of these vector fields is well-defined. Particularly relevant in control applications is the concept of action, or transport map, which is used to map tangent vectors at different points. There are several possible ways to define transport maps, and we will show some canonical choices that arise in the context of Lie groups.

Finally, it is important to define the concept of distance between points on a manifold, since it can be used to appropriately define the tracking errors for control and observation schemes.

Definition 3.4 (Riemannian Metric)**.** *Consider a smooth manifold $\mathcal{M}$ of dimension n, then a Riemannian metric on $\mathcal{M}$ is a collection of inner products $(\langle \cdot, \cdot \rangle_p)_{p \in \mathcal{M}}$ (each satisfying $\langle \cdot, \cdot \rangle_p : T_p\mathcal{M} \times T_p\mathcal{M} \to \mathbb{R}$) such that the function that associates to each $p \in \mathcal{M}$ the element $\langle f(p), g(p) \rangle_p$ is smooth, for any smooth vector fields f, g defined on $\mathcal{M}$.*

A manifold equipped with a Riemannian metric is called Riemannian manifold. Notably, a Riemannian metric on $\mathcal{M}$ allows to naturally define the length of curves. Let $\gamma(t) \in \mathcal{M}$, $t \in [a, b]$ be a generic curve, with $\gamma'(t) \in T_{\gamma(t)}\mathcal{M}$ the associated tangent vector, for all $t \in [a, b]$, then we define the arc length as

$$L_a^b(\gamma) = \int_a^b \sqrt{\langle \gamma'(s), \gamma'(s) \rangle_{\gamma(s)}} ds, \tag{3.3}$$

and thus it follows that the distance between two points p, $q \in \mathcal{M}$ is $\mathrm{d}(p, q) = \inf_{\gamma \in \Gamma} L_a^b(\gamma)$, with Γ the set of all differentiable curves such that $\gamma(a) = p$ and $\gamma(b) = q$. Any such minimizing curve is referred to as geodesic.

3.1.1 Lie Groups

As a special case of the above structures, we consider the important class of Lie groups, which often appear in engineering applications, usually but not exlusively related to mechanical systems.

Definition 3.5 (Group). *A group is a set G equipped with a binary operation $\bullet$ satisfying the following group axioms:*

- *Closure: for all $a, b \in G$, then $a \bullet b \in G$;*

- *Associativity: for all $a, b, c \in G$, then $(a \bullet b) \bullet c = a \bullet (b \bullet c)$;*

- *Identity element: there exists a unique element $e \in G$ such that, for all $a \in G$, then $a \bullet e = e \bullet a = a$;*

- *Inverse element: for each $a \in G$ there exists an element of G, denoted with a^{-1}, such that $a^{-1} \bullet a = a \bullet a^{-1} = e$.*

Definition 3.6 (Lie Group). *A Lie group G is a smooth manifold such that G is a group with a smooth binary operation $\bullet$.*

For simplicity, for any two elements a, b belonging to a Lie group, we will use ab to denote the operation $a \bullet b$. We indicate with $\mathfrak{g} := T_e G$ the Lie algebra of G, which is used to define canonical actions from $T_g G$, for arbitrary $g \in G$, as we will show in the following. More in general, a Lie algebra is a vector space $\mathfrak{g}$ over some field $\mathbb{F}$ equipped with a binary operation $[\cdot, \cdot] : \mathfrak{g} \times \mathfrak{g} \to \mathfrak{g}$ (called Lie bracket) satisfying the following axioms:

- Bilinearity: for all $a, b \in \mathbb{F}$ and all $x, y, z \in \mathfrak{g}$, it holds

$$\begin{aligned} [ax + by, z] &= a[x, z] + b[y, z] \\ [x, ay + bz] &= a[x, y] + b[x, z]; \end{aligned} \tag{3.4}$$

- Alternativity: for all $x \in \mathfrak{g}$, $[x, x] = 0$;

- Jacobi identity: for all $x, y, z \in \mathfrak{g}$, it holds

$$[x, [y, z]] + [z, [x, y]] + [y, [z, x]] = 0. \tag{3.5}$$

We showed that to each Lie group uniquely corresponds a Lie algebra: similarly it can be proven (Lie's third theorem) that the converse holds true (with uniqueness up to finite coverings). This equivalence means that Lie groups can be globally characterized with linear tools, making them particularly attractive for analysis and design because of their simplicity.

Consider the maps $L_g : G \to G$ and $R_g : G \to G$, such that $L_g(h) = gh$ and $R_g(h) = hg$. These maps are usually referred to as left action and right action, and are clearly diffeomorphisms of G. Note that their differentials are naturally defined with tangent spaces as $(dL_g)_h : T_h G \to T_{gh} G$ and $DR_g(h) : T_h G \to T_{hg} G$. Indeed, to define the derivative of a smooth function between manifolds $F : \mathcal{M}_1 \to \mathcal{M}_2$, recall the definition of a tangent vector v in $p \in \mathcal{M}_1$ as an equivalence class and let a curve $\gamma : \mathbb{R} \to \mathcal{M}_1$ such that $\gamma(0) = p \in \mathcal{M}_1$ and $(d/dt)(\phi_1 \circ \gamma)(0) = v$, for some chart $(\mathcal{U}_1, \phi_1)$. Then, $(dF)_p v = (d/dt)(\phi_2 \circ F \circ \gamma)(0)$, for some chart $(\mathcal{U}_2, \phi_2)$ of

$\mathcal{M}_2$. Exploiting this definition, a vector field $f : G \to TG$ is called left (resp. right) invariant if it satisfies:

$$(dL_g)_h f(h) = f(gh) \qquad (\text{ resp. } (dR_g)_h f(h) = f(hg) \text{ }). \tag{3.6}$$

In particular, when considering dynamical systems on Lie groups, we denote the left and right invariant velocities as $\xi^{\mathrm{l}} = L_{g^{-1}}\dot{g}$ and $\xi^{\mathrm{r}} = R_{g^{-1}}\dot{g}$, respectively. Generally speaking, left and right actions can be defined on a generic smooth manifold $\mathcal{M}$ as a maps of the form $\mathcal{L} : G \times \mathcal{M} \to \mathcal{M}$, $\mathcal{R} : G \times \mathcal{M} \to \mathcal{M}$ such that (we express the properties for the left action, but the same can be trivially inferred for right actions):

- $\mathcal{L}(e, p) = p$, for all $p \in \mathcal{M}$;
- $\mathcal{L}(g, \mathcal{L}(h, p)) = \mathcal{L}(gh, p)$, for all $g, h \in G$ and all $p \in \mathcal{M}$.

A left (right resp.) action is transitive if, for any $p, q \in \mathcal{M}$ there exists $g \in G$ such that $\mathcal{L}(g, p) = q$ ($\mathcal{R}(g, p) = q$). Finally, we can define a homogeneous space as a smooth manifold equipped with a transitive action. Homogeneous spaces, similarly to Lie groups, are smooth manifolds with a symmetrical structure, but do not possess the very strong property of having a group structure (consider for instance a sphere with rotations as transitive action). As the last relevant object introduced in this section, we define the adjoint action. Let $\Psi_g : G \to G$ such that $\Psi_g(h) = R_{g^{-1}} \circ L_g(h)$, then the adjoint action is the map $\mathrm{Ad} : G \times \mathfrak{g} \to \mathfrak{g}$ such that, for $g \in G$ and $x \in \mathfrak{g}$, $\mathrm{Ad}_g(x) = (d\Psi_g)_e x$. In dynamical systems defined on Lie groups, the adjoint action is useful to relate left and right invariant velocities as $\xi^{\mathrm{r}} = \mathrm{Ad}_g\, \xi^{\mathrm{l}}$.

Finally, we recall that on Lie groups, apart from the aforementioned distance function originating from a Riemannian metric, it is possible to define errors as elements of the manifold. In particular, given $g, h \in G$, we denote with $\eta^{\mathrm{l}} = g^{-1}h$ and $\eta^{\mathrm{r}} = hg^{-1}$ the left and right invariant errors, respectively.

3.1.2 Notable Examples of Lie Groups

We conclude this introductory section with some examples that will be used in the following. In particular, the focus is on matrix Lie groups, which find wide application in control engineering, especially when considering mechanical systems involving rotations. For simplicity, we consider the entries of matrix Lie groups to be real valued, but in general they can be chosen to be complex valued as well.

The General Linear Group $GL(n, \mathbb{R})$

It is defined as the n^2 dimensional manifold given by $n \times n$ invertible matrices, equipped with the matrix multiplication as group operator.

Definition 3.7. *A real valued matrix Lie group is a closed subgroup of $GL(n, \mathbb{R})$.*

Therefore the following properties can be applied, with their opportune simplifications, to all other matrix Lie groups that we will see after $GL(n, \mathbb{R})$. Remarkably, any matrix Lie group G is related to its Lie algebra through the matrix exponential:

$$\mathfrak{g} = \{U : \exp(tU) \in G, t \in \mathbb{R}\} \tag{3.7}$$

and in particular:

$$\mathfrak{gl}_n = \{U : \exp(tU) \in GL(n, \mathbb{R}), t \in \mathbb{R}\}. \tag{3.8}$$

It can be proved that the Lie bracket becomes in this case the classic commutator operator, i.e. $[U, V] = UV - VU$, for $U, V \in \mathfrak{gl}_n$. From the above general definitions of left and right invariant velocities, it is clear that for $X \in GL(n, \mathbb{R})$ and $U \in \mathfrak{gl}_n$, then a left (resp. right) invariant system on $GL(n, \mathbb{R})$ is given by

$$\dot{X} = XU \qquad (\text{ resp. } \dot{X} = UX \text{ }). \tag{3.9}$$

Finally, the adjoint action is given by $\mathrm{Ad}_X U = XUX^{-1}$.

The Special Orthogonal Group $SO(n)$

It is defined as the $n(n-1)/2$ dimensional manifold of $n \times n$ orthogonal matrices with unitary determinant, that is:

$$SO(n) = \{R \in GL(n, \mathbb{R}) : RR^T = I_n,\ \det(R) = 1\}, \tag{3.10}$$

and equipped with the matrix multiplication as group operator. It can be proved that the Lie algebra associated to $SO(3)$ is given by the $n \times n$ antisymmetric matrices. We recall that $SO(n)$ is one of the two connected components of the orthogonal group $O(n)$ given by orthogonal matrices (the other connected component being the orthogonal matrices with determinant -1). Note in addition that $O(n)$ is the maximal compact subgroup of $GL(n, \mathbb{R})$. This fact has many implications from the control point of view, which will be reviewed in the following. Because of their practical interest, we focus in particular on the cases corresponding to $n = 2$ and $n = 3$.

To begin with $n = 2$, notice that $SO(2)$ represents the 1-dimensional manifold of planar rotations, with associated Lie algebra given by

$$\mathfrak{so}(2) = \left\{ \begin{pmatrix} 0 & -\omega \\ \omega & 0 \end{pmatrix} \in \mathbb{R}^{2\times 2}, \omega \in \mathbb{R} \right\} \tag{3.11}$$

Indeed, the exponential map yields the structure:

$$C = \exp \begin{pmatrix} 0 & -\omega t \\ \omega t & 0 \end{pmatrix} = \begin{pmatrix} \cos(\omega t) & -\sin(\omega t) \\ \sin(\omega t) & \cos(\omega t), \end{pmatrix} \in SO(2) \tag{3.12}$$

with $\vartheta = \omega t$ the angle of the planar rotation associated with C. For any $\omega \in \mathbb{R}$, indicate with $\omega_\times \in \mathfrak{so}(2)$ the correspondingly parameterized Lie algebra element, and let $\mathrm{vex}_2(\cdot) : \mathfrak{so}(2) \to \mathbb{R}$ represent the inverse operator of $(\cdot)_\times$. From direct verification, it follows that this Lie group is also abelian, and thus the adjoint action corresponds to the identity. Remarkably, an equivalent representation of this group is the unit circle, denoted with $\mathbb{S}^1$ in this thesis (also indicated in the literature as the 1-torus $\mathbb{T}^1$ or the unitary group $U(1)$). Note that the group multiplication in $\mathbb{S}^1$ is still given by rotation matrices. As a consequence, for a pair $\zeta_1, \zeta_2 \in \mathbb{S}^1$, the product is given by $\mathcal{C}[\zeta_1]\zeta_2 = \mathcal{C}[\zeta_2]\zeta_1$, where $\mathcal{C} : \mathbb{S}^1 \to SO(2)$ is the map that, to any element $\mathbb{S}^1$, associates the equivalent element in $SO(2)$. On $SO(2)$ (resp. $\mathbb{S}^1$), a generic system with angular speed ω is given by

$$\dot{C} = C\omega_\times = \omega_\times C, \quad C(t_0) \in SO(2) \qquad (\text{ resp. } \dot{\zeta} = \omega \mathcal{J} \zeta, \quad \zeta(t_0) \in \mathbb{S}^1 \text{ }), \tag{3.13}$$

with $t_0 \in \mathbb{R}$ the initial time and $\mathcal{J} = \exp((\pi/2)_\times) = \left(\begin{smallmatrix} 0 & -1 \\ 1 & 0 \end{smallmatrix}\right)$ the matrix associated with a counter-clockwise rotation by $\pi/2$ radians. This very simple representation of angular rotations will be exploited, in the next chapter, to yield a semi-global characterization of the stability properties of a sensorless observer for electric machines.

Moving to $SO(3)$, which is the manifold associated to 3D rotation matrices, we notice that the previous commutativity property is lost (this can be immediately shown by taking two $\pi/2$ rotations about two different orthonormal axes in $\mathbb{R}^3$). For $\omega \in \mathbb{R}^3$, indicate with $\omega_\times \in \mathfrak{so}(3)$ the corresponding Lie algebra parameterized element, while let $\text{vex}_3(\cdot) : \mathfrak{so}(3) \to \mathbb{R}^3$ be the inverse operator. In particular, for $\omega = (p, q, r)$, we have:

$$\omega_\times = \begin{pmatrix} 0 & -r & q \\ r & 0 & -p \\ -q & p & 0 \end{pmatrix}. \tag{3.14}$$

It follows that, for $\omega^{\mathrm{l}}_\times = \Omega^{\mathrm{l}} \in \mathfrak{so}(3)$, a left invariant system on $SO(3)$ is given by (again, denote with t_0 the initial time):

$$\dot{R} = R\Omega^{\mathrm{l}}, \quad R(t_0) = R_0 \in SO(3), \tag{3.15}$$

and similarly a right invariant system on $SO(3)$ is obtained by taking $\omega^{\mathrm{r}}_\times = \Omega^{\mathrm{r}} = \mathrm{Ad}_R\,\Omega^{\mathrm{l}} = R\Omega^{\mathrm{l}}R^T = (R\omega^{\mathrm{l}})_\times$. If R represents the relative rotation of a moving reference frame $\{B\}$ (e.g. the attitude of a vehicle) with respect to a fixed one $\{A\}$, then ω^{l} is angular velocity of $\{B\}$ with respect to $\{A\}$, expressed in the coordinates of the frame $\{B\}$. Similarly, ω^{r} is the angular velocity of $\{B\}$ with respect to $\{A\}$, expressed in the coordinates of the frame $\{A\}$. Notably, the compactness of the group leads to the preservation of the norm in the transformation between ω^{l} and ω^{r} (and vice-versa).

It can be shown that $SO(3)$ is equivalent to the real projective space of dimension 3 (indicated with $\mathbb{P}_3(\mathbb{R})$) given by the manifold of lines passing through the origin in $\mathbb{R}^4$. We recall that, in many engineering applications, the quaternions are used as well to denote $3D$ rotations. In particular, quaternions are elements of the 3-sphere $\mathbb{S}^3$ (also diffeomorphic to $SU(2) \subset GL(2, \mathbb{R})$), and generate a Lie group with quaternion multiplication as group operation. Interestingly, it can be proved that the 3-sphere is a double cover of $SO(3)$, that is, for any rotation there exist two quaternions corresponding to it. This is a crucial element to consider in control applications, since an algorithm processing quaternions may incur in the dangerous "unwinding" phenomenon. See (Mayhew, Sanfelice, and Teel, 2011) for a deep analysis of this issue in attitude control, as well as the introduction of a hybrid strategy to correctly account for it in the design. Finally, it is worth noting that the 2-sphere, given by $\mathbb{S}^2 = SO(3)/SO(2)$, and equipped with the left multiplication by rotations in $SO(3)$, is a homogeneous space and can thus be treated with the same tools that we presented before. In particular, a dynamical system on the 2-sphere features a similar structure to that used for $\mathbb{S}^1$ (i.e. $\dot{\zeta} = \omega_\times \zeta$), only in a higher dimensional setup.

The Special Euclidean Group $SE(n)$

It is defined as the manifold of pairs (R, p), with $R \in SO(n)$ and $p \in \mathbb{R}^n$, together with the group operation satisfying $(R_1, p_1) \bullet (R_2, p_2) = (R_1 R_2, R_1 p_2 + p_1)$. $SE(n)$ is again a matrix Lie group and then the previous arguments for dynamical systems on them still hold. Indeed, it is possible to define the Lie algebra through the exponential map and left/right invariant systems are naturally defined. As a special case, $SE(3)$ is usually employed to denote the 3D pose (position and attitude) of rigid bodies, and is a manifold of dimension 6. Usually, the elements of $SE(3)$ are represented with the so-called affine transformations, given by

$$\begin{pmatrix} R & p \\ 0_{1\times 3} & 1 \end{pmatrix} \in SE(3), \tag{3.16}$$

with corresponding Lie algebra represented as:

$$\begin{pmatrix} \omega_\times & v \\ 0_{1\times 3} & 0 \end{pmatrix} \in \mathfrak{se}(3), \tag{3.17}$$

with ω, $v \in \mathbb{R}^3$. It is relevant that in this case the mapping between right and left invariant velocities does not preserve the norm of (ω, v). Trivial extensions of this Lie group, such as $SE_n(3)$ (augmenting the translation part with n vectors in $\mathbb{R}^3$) are not treated here for brevity, but the previous arguments still apply with an increased notational burden.

3.2 Global Observability of Dynamical Systems on Manifolds

Taking advantage of the definitions of the previous section, some general observability and detectability concepts can be established. The definitions that are presented in this section are based on the fundamental paper (Hermann and Krener, 1977), of which we recall the introduction to the concept of indistinguishability. Let $\mathcal{M}$ be a smooth manifold of dimension n, equipped with a metric $\mathrm{d} : \mathcal{M} \times \mathcal{M} \to \mathbb{R}$, then consider a nonlinear system on $\mathcal{M}$ of the form

$$\begin{aligned} \dot{p} &= f(p, u), \qquad p(t_0) = p_0 \in \mathcal{M} \\ y &= h(p), \end{aligned} \tag{3.18}$$

where $u \in \mathbb{R}^m$ is the input, $y \in \mathbb{R}^l$ is the output vector, f is a smooth vector field and h is a smooth function. Consider a class of piecewise continuous signals over $(-\infty, \infty)$ with codomain $\mathbb{R}^m$, $\mathcal{U}$, and let $\bar{p}(t; t_0, p_0, u_{[t_0,t)})$ indicate a forward solution of system (3.18), for initial condition (t_0, p_0), input signal $u(\cdot) \in \mathcal{U}$, and with maximal interval of existence given by $[t_0, t_0 + \delta_{\max})$. For simplicity, suppose that system (3.18) is forward complete, that is $\delta_{\max} = \infty$, for all (t_0, p_0) and all $u(\cdot) \in \mathcal{U}$. This

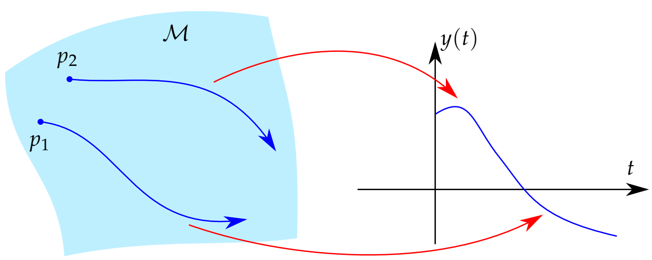

FIGURE 3.2: Graphical representation of two indistinguishable points, p_1 and p_2.

property is also instrumental in the definition of detectability, as shown in the following. We can thus formally introduce indistinguishability of initial conditions, also depicted in Figure 3.2.

Definition 3.8 ($u(\cdot)$-Indistinguishability)**.** *Let $t_0 \in \mathbb{R}$, and let p_1, $p_2 \in \mathcal{M}$. Consider an input $u(\cdot) \in \mathcal{U}$, and pick a positive scalar δ. Then, p_1 and p_2 are said to be $u(\cdot)$-indistinguishable in the interval $[t_0, t_0+\delta)$ if, for all $t \in [t_0, t_0+\delta)$, it holds*

$$h(\bar{p}(t; t_0, p_1, u_{[t_0,t)})) = h(\bar{p}(t; t_0, p_2, u_{[t_0,t)})). \tag{3.19}$$

For any interval of the form $[t_0, t_0+\delta)$, the points that are $u(\cdot)$-indistinguishable in such time interval represent an equivalence relation, denoted with $\mathcal{I}^{[t_0,t_0+\delta)}(p,u)$. Note that in general we can no longer establish such equivalence relation if system (3.18) is not forward complete, since the $u(\cdot)$-indistinguishability relation may not be transitive in such case (Hermann and Krener, 1977). To decrease the notational burden, let $\mathcal{I}^{[t_0,\infty)}(p,u) = \mathcal{I}(p,u)$.

Definition 3.9 (Observability)**.** *A state $p \in \mathcal{M}$ is observable in $[t_0, t_0+\delta)$ if, for all $u(\cdot) \in \mathcal{U}$, $\mathcal{I}^{[t_0,t_0+\delta)}(p,u) = \{p\}$.*

A state p will be called observable if it holds $\mathcal{I}(p,u) = \{p\}$, i.e. the interval of analysis is unbounded (note that observability in $[t_0, t_0+\delta)$, for bounded $\delta > 0$, implies observability in $[t_0, \infty)$). Similarly, from the analysis of the interval $[t_0, \infty)$ derives the definition of detectability.

Definition 3.10 (Detectability)**.** *A state $p \in \mathcal{M}$ is detectable if, for all $u(\cdot) \in \mathcal{U}$, it holds*

$$q \in \mathcal{I}(p,u) \subset \mathcal{M} \implies \lim_{t\to+\infty} \mathrm{d}(\bar{p}(t; t_0, p, u_{[t_0,t)}), \bar{p}(t; t_0, q, u_{[t_0,t)})) = 0. \tag{3.20}$$

Clearly, the above definitions of observability and detectability can be extended to system (3.18) when they hold for all $p \in \mathcal{M}$. Furthermore, the local equivalent of these properties holds in $p \in \mathcal{M}$ if the conditions are verified for some neighborhood $\mathcal{N}_p$ of p. We refer to (Ibarra-Rojas, Moreno, and Espinosa-Pérez, 2004) for related formulations (cf. observability and weak observability in Hermann and Krener, 1977). Notably, the above definitions do not require that the states can be distinguished in a certain amount of time (or with a given rate): the stronger definition based on the rank test is presented in detail in (Hermann and Krener, 1977) and, because of its features, we will not provide here further details about it. It is relevant to stress that the states of a system may be distinguished only for a subset of the class $\mathcal{U}$. Indeed, in many applications the observability/detectability properties are strongly connected with the input signals, which are often required to be sufficiently "rich" to excite the entire nonlinear dynamics. For this reason, we often consider the converse problem of characterizing $\mathcal{U}$ as the class of inputs displaying sufficient richness in order to yield global observability results.

Taking advantage of the previous discussion, it is easy to see that the global observability analysis can be recast into the study of the indistinguishable trajectories of (3.18), i.e. the set of all trajectories with initial conditions $q_0 \in \mathcal{M}$ s.t. $q_0 \in \mathcal{I}(p_0, u)$, for $p_0 \in \mathcal{M}$ and $u(\cdot) \in \mathcal{U}$. In particular, if such set coincides with the single trajectory for any possible $u(\cdot)$, p_0 is observable; if all trajectories converge to a single one for any possible $u(\cdot)$, it is detectable. In a more constructive sense, the indistinguishable dynamics is identified as follows.

Definition 3.11 (Indistinguishable Dynamics)**.** *The indistinguishable dynamics of system (3.18) is defined as a differential algebraic equation (DAE), composed of two instances* *of* (3.18)*, together with the algebraic condition that the outputs coincide for all* $t \in [t_0, \infty)$*:*

$$\begin{aligned} \dot{p} &= f(p,u) \qquad p(t_0) = p_0 \in \mathcal{M} \\ \dot{q} &= f(q,u) \qquad q(t_0) = q_0 \in \mathcal{M} \\ h(p) &= h(q), \end{aligned} \tag{3.21}$$

with $u(\cdot) \in \mathcal{U}$*.*

As a consequence, the observability analysis of a point p_0 coincides with the study of the trajectories of the above DAE, for all initial conditions of the form $(p_0, q_0) \in \mathcal{M} \times \mathcal{M}$, and all $u(\cdot) \in \mathcal{U}$. Note, in addition, that if it is possible to globally define an error between the two systems (e.g. if $\mathcal{M}$ is a Lie group), then a simpler analysis derives. For this reason, we consider in the following the dynamics of inertial navigation systems as case of study for global observability analysis. Due to the tools available for systems defined on Lie groups, we show that the treatment can be greatly simplified and collapsed to the study of a low-order system.

3.3 Global Observability of Inertial Navigation Systems

Inertial Navigation Systems (INS) have been a core element for several military and civilian applications for long time. Nowadays, the most popular architecture is based on Inertial Measurement Units (IMUs), mounted rigidly on the vehicle in a so-called strap-down configuration (Farrell, 2008). Typically, the low-cost inertial sensors that IMUs are equipped with suffer from noise and biases, affecting long term accuracy. For this reason, navigation is commonly aided by means of external instrumentation such as Global Navigation Satellite Systems (GNSS) and/or vision devices. Given the large number of autonomous vehicles expected in the near future, the quest for reliable navigation algorithms, exploiting the aforementioned sensor technologies to reconstruct the moving object state, is growing.

In this respect, regardless of the estimation method, a crucial aspect concerns observability analysis, as it provides rigorous results of what kinematic states can be reconstructed, despite measurement non-idealities. However, such study comes with some challenges, given by the nonlinear time-varying nature of system mechanization dynamics. Several approaches have been proposed in the literature. In (Cho et al., 2007; Gao et al., 2014) system linearization and particular conditions making it time invariant are considered for flying and land vehicle applications, respectively, and the standard observability matrix rank test is applied. In (Chung, Park, and Lee, 1996) linear time-varying dynamics, obtained neglecting position error, are handled with the study of an equivalent system. In (Hong et al., 2002), instantaneous observability of the time-varying dynamics of INS aided with multiple antenna GPS is investigated, while (Vu et al., 2012) studies the GPS-aided INS observability Gramian properties under specific working conditions. Additionally, recent use of the observability matrix rank test to INS can be found in (Huang, Song, and Zhang, 2017; Panahandeh et al., 2016) where vision-aided UAVs are considered (the latter exploiting a diffeomorphism to simplify the analysis).

The aforementioned frameworks focus on instantaneous/local observability. Studies concerning global properties have been presented in (Hong et al., 2005; Tang et al., 2008; Wu et al., 2012). However, less rigorous evaluations are performed, computing the time derivatives of the output and considering specific scenarios to draw analytical conclusions about system observability. For instance, (Tang et al.,

2008) and (Wu et al., 2012) provide conditions for trajectories with static/constant-attitude periods and phases with non-zero angular velocity. In (Hernandez, Tsotsos, and Soatto, 2015) a thoughtful observability analysis is presented for the case of vision-assisted INS, employing arguments closely related to the indistinguishable dynamics approach we presented here. In particular, the concept of unknown input observability is presented to account for the presence of input signals which, even though not available for observer design, are still informative in the analysis (cf. Definition 4.1 in the next chapter).

Using the previously presented tools, we can show how the observability analysis of INS can lead to simple and global results that do not depend on specific scenarios to hold. To correctly present this topic, we firstly review the INS dynamics and some of the typical sensors that are used in real applications. Then, we apply the indistinguishable dynamics approach to some relevant applications connected to recent works in the literature.

3.3.1 Inertial Navigation Equations

Consider, for simplicity, the kinematic equations of a rigid body moving in a 3D inertial reference frame. The state space representation of such dynamical system is the following:

$$\begin{aligned} \dot{p}^{\mathrm{n}} &= R_{\mathrm{nb}} v^{b} \\ \dot{v}^{\mathrm{b}} &= u^{\mathrm{b}} - (\omega^{\mathrm{b}}_{\mathrm{nb}})_{\times} v^{\mathrm{b}} \\ \dot{R}_{\mathrm{nb}} &= R_{\mathrm{nb}} (\omega^{\mathrm{b}}_{\mathrm{nb}})_{\times}, \end{aligned} \tag{3.22}$$

where $p^{\mathrm{n}} \in \mathbb{R}^3$ is the position in the navigation frame, $v^{\mathrm{b}} \in \mathbb{R}^3$ is the navigation velocity, represented in the body frame, and $R_{\mathrm{nb}} \in SO(3)$ is the attitude between the two reference frames. On the other hand, $u^{\mathrm{b}} \in \mathbb{R}^3$ and $\omega^{\mathrm{b}}_{\mathrm{nb}} \in \mathbb{R}^3$ are the total acceleration and the body angular velocity, respectively, represented in the body frame. We avoid for simplicity to include the non-ideal effects deriving from the use of a non-inertial frame as navigation frame (sometimes, this approximation is referred to as "flat Earth" navigation).

Several sensor choices are adopted in the field of inertial navigation, some of the most common are listed here. In particular, we begin with the typical "rate" sensors found on board the Inertial Measurement Units, i.e. accelerometers and gyroscopes. We choose not to cover magnetometers and altimeters, typically found as well in the IMUs, since they will not be exploited in our cases of study.

Accelerometer: it measures the acceleration (up to gravity) of the vehicle in the body frame:

$$u_{\mathrm{s}} = u^{\mathrm{b}} - R_{\mathrm{bn}} g + \tilde{u}, \tag{3.23}$$

where $g \in \mathbb{R}^3$ is the local gravity acceleration vector, represented in the navigation frame of reference, and is assumed known and constant, while $\tilde{u} \in \mathbb{R}^3$ is the sensor error, which is usually described as the sum of a bias and noise:

$$\tilde{u} = b_u + w_u, \tag{3.24}$$

with b_u a constant (or slowly-varying) parameter and w_u a white or colored noise, depending on the context. Note that the bias b_u, if present, cannot be always effectively estimated offline due to the high dependance on the device temperature and other disturbances. This leads to a slow drift of b_u during operation time, thus its online estimation is often a crucial element for high performance inertial navigation, in particular when low-cost commercial IMUs are employed.

Gyroscope: it measures the angular speed of the vehicle in the body frame:

$$\omega_{\mathrm{s}} = \omega_{\mathrm{nb}}^{\mathrm{b}} + \tilde{\omega}, \tag{3.25}$$

where $\tilde{\omega} \in \mathbb{R}^3$ is the sensor error, which is described, as for the accelerometer case, as the sum of a bias and noise:

$$\tilde{\omega} = b_\omega + w_\omega, \tag{3.26}$$

with b_ω a constant (or slowly-varying) parameter and w_ω a white or colored noise, depending on the context. Similarly to the accelerometer case, the gyro bias b_ω cannot be in general effectively estimated offline, and thus it often requires an appropriate estimation during the vehicle operation.

In addition to IMU measurements, a wide selection of devices is available to provide "external" readings of the system pose. In particular, we recall the following aiding sensors providing the vehicle's position and velocity.

Navigation Position Sensor (e.g. GNSS): it provides the position in navigation frame:

$$p_{\mathrm{s}} = p^{\mathrm{n}} + \tilde{p}, \tag{3.27}$$

where $\tilde{p}$ is the sensor error which can be (very roughly) represented as a white noise, even though it usually presents strong correlation. Apart from satellite systems, the same model is used for many other position sensors (e.g. indoor positioning systems).

Relative Position of Known Features: we consider in this case sensors (e.g. vision systems) that exploit a constellation of known (usually fixed) points in the navigation frame $p_1, \ldots, p_N$:

$$\begin{aligned} p_{\mathrm{s}1} &= R_{\mathrm{bn}}(p_1 - p) + \tilde{p}_1 \\ &\vdots \\ p_{\mathrm{s}N} &= R_{\mathrm{bn}}(p_N - p) + \tilde{p}_N. \end{aligned} \tag{3.28}$$

(Visual) Odometry: this class of sensors provides the vehicle navigation speed, expressed in body axes:

$$v_{\mathrm{s}} = v^{\mathrm{b}} + \tilde{v}. \tag{3.29}$$

An example of such sensor is given by visual odometry. Indeed, CMOS optical flow sensors are equipped with a sonar that rescales flow in a metric value and a gyroscope that compensates body rotation (Honegger et al., 2013), thus providing the above output measurement.

In the following, the subscripts and superscripts referring to reference frames will be omitted when clear from the context, in order to avoid heavy notation in the computations and thus enhance readability.

3.3.2 Example 1: 2D Car Navigation

As a special case of system (3.22), consider the unicycle model, equipped with an ideal odometer on each wheel and an ideal position sensor. Then, under the assumption of no slipping we have the following dynamics:

$$\begin{aligned}\frac{d}{dt}\begin{pmatrix} C & p \\ 0_{2\times1} & 1 \end{pmatrix} &= \begin{pmatrix} C & p \\ 0_{2\times1} & 1 \end{pmatrix}\begin{pmatrix} 0 & -\omega & v \\ \omega & 0 & 0 \\ 0 & 0 & 0 \end{pmatrix} \qquad \begin{pmatrix} C & p \\ 0_{2\times1} & 1 \end{pmatrix} \in SE(2) \\ y &= p,\end{aligned} \tag{3.30}$$

with $\omega \in \mathbb{R}$ and $v \in \mathbb{R}$ available as measurements: indeed, if we denote with v_{R}, v_{L} the speed of the right and the left wheel, respectively, it holds:

$$v = \frac{v_{\mathrm{R}} + v_{\mathrm{L}}}{2}, \qquad \omega = \frac{v_{\mathrm{R}} - v_{\mathrm{L}}}{d}, \tag{3.31}$$

where d corresponds to the the wheelbase, i.e. the distance between the two wheels. Interestingly, this system also embeds a nonholonomic constraint, which however does not represent an obstacle to global results, if the formalism of the present work is adopted.

Indicate with the overline notation a second copy of system (3.30), then setting $y = \bar{y}$ for all $t \geq t_0$ yields $C\begin{pmatrix} v \\ 0 \end{pmatrix} = \bar{C}\begin{pmatrix} v \\ 0 \end{pmatrix}$, which in turn allows to write:

$$\bar{C}^T C\begin{pmatrix} v \\ 0 \end{pmatrix} = \begin{pmatrix} v \\ 0 \end{pmatrix}. \tag{3.32}$$

Therefore, it follows $\bar{C}^T C = I_2$ as long as $|v| \neq 0$. As a consequence, we know that if the inputs belong to a class such that, for any $v(\cdot)$ in that class, there exists t satisfying $|v(t)| \neq 0$, then system (3.30) is observable. This condition can be made stronger requiring that $|v(t)| \geq v_0 > 0$, for all t. Indeed, the above observability property holds regardless of ω, and indeed this is a scenario where unknown input observability holds, with ω the unknown signal: this way, we have a formal guarantee that ω is not needed to yield a globally convergent observer. Since v_{R} and v_{L} are both available as measurements, this means that we can design an observer that is independent of the parameter d (or that can effectively used to estimate it). In the following chapter, we will show a complete design where this concept is exploited to yield an unknown input observer. Consider now the case $v(t) = 0$, for all $t \geq t_0$. Denote with $\tilde{C} = \bar{C}^T C$ the error between the frames $\bar{C}$ and C, then the indistinguishable dynamics is given by system (3.30) along with:

$$\dot{\tilde{C}} = \tilde{C}\omega_\times - \omega_\times \tilde{C} = 0, \tag{3.33}$$

since $\tilde{C} \in SO(2)$, with $SO(2)$ an abelian group. Therefore as expected the system is neither observable nor detectable under this condition. We refer to (Barrau and Bonnabel, 2016) for an example of an observer for system (3.30).

3.3.3 Example 2: 3D Vehicle Navigation - Calibrated Sensors

We want to study now the observability of a vehicle moving in a 3D space, equipped with an accelerometer, a gyroscope, a position sensor and an odometry system. The model of the system is given in $SE_2(3)$, and can be written as follows:

$$\frac{d}{dt}\chi = f(\chi, u, \omega), \qquad y = \begin{pmatrix} p \\ v \end{pmatrix},$$
$$f(\cdot, u, \omega) : \begin{pmatrix} R & v & p \\ 0_{1\times 3} & 1 & 0 \\ 0_{1\times 3} & 0 & 1 \end{pmatrix} \in SE_2(3) \to \begin{pmatrix} R\omega_\times & u - \omega_\times v + R^T g & Rv \\ 0_{1\times 3} & 0 & 0 \\ 0_{1\times 3} & 0 & 0 \end{pmatrix}, \tag{3.34}$$

with $u \in \mathbb{R}^3$ the acceleration in body axes and $\omega \in \mathbb{R}^3$ the angular velocity. Both u and ω are available from the accelerometer and gyroscope readings. Following the same arguments of the previous example, consider a copy of the above dynamics (indicated with the overline notation), and let $y = \bar{y}$, for all $t \geq 0$, then it holds $Rv = \bar{R}v$ and $R^T g = \bar{R}^T g$. Let $\tilde{R} = \bar{R}^T R$, then the following identities hold:

$$\tilde{R}v = v, \qquad \tilde{R}(R^T g) = R^T g. \tag{3.35}$$

It can be shown that, as long as v and $R^T g$ are not collinear, the above system of equations has the unique solution $\tilde{R} = I_3$. Indeed, consider an arbitrary rotation $\hat{R}$ such that $\hat{R}^T v = (\hat{v}, 0, 0)$, then it follows, for $\hat{v} \neq 0$, that:

$$(I_3 - \hat{R}^T \tilde{R} \hat{R}) \begin{pmatrix} \hat{v} \\ 0 \\ 0 \end{pmatrix} = \left(I_3 - \begin{pmatrix} 1 & 0_{1\times 2} \\ 0_{2\times 1} & C \end{pmatrix} \right) \begin{pmatrix} \hat{v} \\ 0 \\ 0 \end{pmatrix} = 0, \tag{3.36}$$

with $C \in SO(2)$ an unknown planar rotation about the velocity vector. Suppose that v and $R^T g$ are not collinear, then the previous rotation leads to:

$$\left(I_3 - \begin{pmatrix} 1 & 0_{1\times 2} \\ 0_{2\times 1} & C \end{pmatrix} \right) \hat{g} = 0, \tag{3.37}$$

with $\hat{g} = \hat{R}^T R^T g$, which is not collinear with $(\hat{v}, 0, 0)$ as both vectors were subject to the same rigid rotation. The resulting equation in the unknown C is exactly the same as in (3.32), with the vector $(\hat{g}_2, \hat{g}_3) \neq 0$ as a consequence of the previous arguments on v and $R^T g$. Hence system (3.34) is observable if the input class is such that for all resulting trajectories, for some t, the condition $v(t) = cR^T(t)g$ is violated for all $c \in \mathbb{R}$ (note that the zero velocity is included with $c = 0$). We aim to characterize a class of inputs guaranteeing this condition. Indeed, the same rotation $\hat{R}$ can be applied to the dynamics (3.34), considering the new variable $\hat{R}^T(v)v$, whose second and third components are zero at all times. Setting the corresponding derivatives to zero, we yield a relation of the form

$$\mu + \gamma - \xi\hat{v} = 0, \tag{3.38}$$

where μ, γ and $-\mathcal{J}\xi$ are the second and third components of $\hat{R}^T u$, $\hat{g}$ and $\hat{R}^T\omega + \hat{\omega}$, respectively, with $\dot{\hat{R}} = \hat{R}\hat{\omega}_\times$. Similarly, compute the derivative of $\hat{R}^T \tilde{R} \hat{R}$:

$$\frac{d}{dt}(\hat{R}^T \tilde{R} \hat{R}) = \begin{pmatrix} 1 & 0_{1\times 2} \\ 0_{2\times 1} & C \end{pmatrix} (\hat{R}^T\omega + \hat{\omega})_\times - (\hat{R}^T\omega + \hat{\omega})_\times \begin{pmatrix} 1 & 0_{1\times 2} \\ 0_{2\times 1} & C \end{pmatrix}, \tag{3.39}$$

which yields $C\xi = \xi$, by analyzing the algebraic equation derived from the off-diagonal terms. Since $C\gamma = \gamma$ due to (3.37), we have that $C\mu = \mu$, thus we obtained the following system of equations:

$$\begin{pmatrix} C & 0_{2\times 2} \\ 0_{2\times 2} & C \end{pmatrix} \begin{pmatrix} \mu \\ \xi \end{pmatrix} = \begin{pmatrix} \mu \\ \xi \end{pmatrix}, \tag{3.40}$$

which yields $C = I_2$ as long as at least one of the two vectors (ξ or μ) is non-zero, similarly to what was obtained in the example of the unicycle. Let ζ be the element in $\mathbb{S}^1$ associated with C, then we can rearrange the system of equations to

$$\Psi\left(\zeta - \begin{pmatrix} 1 \\ 0 \end{pmatrix}\right) = 0, \qquad \Psi = \begin{pmatrix} \mu & \mathcal{J}\mu \\ \xi & \mathcal{J}\xi \end{pmatrix}, \tag{3.41}$$

which compactly embeds the properties of the class of inputs ensuring observability.

Finally, it must be noted that the acceleration along the velocity direction is responsible for the vehicle's velocity norm, so the input class is not decoupled with the state configuration of the system. Note however that the remaining component (along the velocity vector) of both acceleration and angular velocity are not needed for full state reconstruction, thus in this context some form of unknown input observability property holds.

3.3.4 Example 3: 3D Vehicle Navigation - Biased Sensors

We finally consider the full observability problem. In addition to the above example of 3D Navigation, we suppose that the rate sensors (accelerometer, gyroscope) are affected by a constant (actually slowly-varying) unknown bias. It can be shown that in this case the resulting system to be analyzed takes the form:

$$\begin{aligned} &\frac{d}{dt}\chi = f(\chi, u, \omega), \qquad y = \begin{pmatrix} p \\ v \end{pmatrix}, \\ &f(\cdot, u, \omega) : \begin{pmatrix} R & v & p & b_u & b_\omega \\ 0_{1\times 3} & 1 & 0 & 0 & 0 \\ 0_{1\times 3} & 0 & 1 & 0 & 0 \\ 0_{1\times 3} & 0 & 0 & 1 & 0 \\ 0_{1\times 3} & 0 & 0 & 0 & 1 \end{pmatrix} \in SE_4(3) \to \\ &\begin{pmatrix} R(\omega - b_\omega)_\times & u - b_u - (\omega - b_\omega)_\times v + R^T g & Rv & 0_{3\times 1} & 0_{3\times 1} \\ 0_{1\times 3} & 0 & 0 & 0 & 0 \\ 0_{1\times 3} & 0 & 0 & 0 & 0 \\ 0_{1\times 3} & 0 & 0 & 0 & 0 \\ 0_{1\times 3} & 0 & 0 & 0 & 0 \end{pmatrix}, \end{aligned} \tag{3.42}$$

with $\chi \in SE_4(3)$. It can be easily shown that the same arguments of the previous case can be applied here, although the non-collinearity property for a single time t is not sufficient anymore to ensure observability. Indeed, let μ, $-\mathcal{J}\xi$ β_u, $-\mathcal{J}\beta_\omega$ be the second and third components of $\hat{R}^T(u - b_u)$, $\hat{R}^T(\omega - b_\omega) + \hat{\omega}$ (as before, $\dot{\hat{R}} = \hat{R}\hat{\omega}_\times$), $\hat{R}^T\tilde{b}_u$ and $\hat{R}^T\tilde{b}_\omega$, respectively (with $\tilde{b}_u = b_u - \bar{b}_u$, $\tilde{b}_\omega = b_\omega - \bar{b}_\omega$), then let b_v be the first component of $\hat{R}^T\tilde{b}_\omega$ and let $\hat{\omega} = (\omega_v, \lambda)$, with $\omega_v \in \mathbb{R}$ and $\lambda \in \mathbb{R}^2$. Then, it is possible to show that if $|v| \neq 0$ the indistinguishable dynamics in this case is given by system (3.42), together with the following DAE:

$$\begin{gathered}\dot{\zeta} = -b_v \mathcal{J} \zeta \qquad \dot{b}_v = -\lambda^T \beta_\omega \\ \frac{d}{dt}\begin{pmatrix}\beta_u \\ \beta_\omega\end{pmatrix} = -\omega_v \begin{pmatrix}\mathcal{J} & 0_{2\times 2} \\ 0_{2\times 2} & \mathcal{J}\end{pmatrix}\begin{pmatrix}\beta_u \\ \beta_\omega\end{pmatrix} + \begin{pmatrix}0_{2\times 1} \\ \lambda\end{pmatrix} b_v \\ \begin{pmatrix}\beta_u \\ \beta_\omega\end{pmatrix} = \Psi\left(\zeta - \begin{pmatrix}1 \\ 0\end{pmatrix}\right), \qquad \Psi = \begin{pmatrix}\mu & \mathcal{J}\mu \\ \xi & \mathcal{J}\xi\end{pmatrix}.\end{gathered} \tag{3.43}$$

This DAE highlights some important structural properties. Firstly, the algebraic equation is analogous to the previous equation (3.41), with the addition of the biases and their dynamics. This shows that Ψ is a coupling term between the attitude error and the biases errors which enhances the observability properties of the system. Indeed, suppose that the relative alignment of velocity in the body frame is constant, then it follows that β_u, β_ω and b_v are constant, and thus Ψ can be required to satisfy some persistency of excitation conditions to ensure global observability. We refer to (Bosso et al., 2018) for a detailed discussion on these properties, as well as the analysis trajectories either satisfying $|v| = 0$, or switching between the conditions $|v| = 0$ and $|v| \neq 0$.

3.4 Observer Design for Systems on Manifolds: State of the Art and Challenges

We conclude this chapter with a brief overview of some notable techniques from the recent literature that explicitly take the above topological constraints into account.

In (Barrau and Bonnabel, 2016) the authors consider the problem of Extended Kalman Filter design on matrix Lie Groups, considering in particular systems of the form $\dot{g} = f(g, u)$, $g \in G$ such that either the left or right invariant error has a dynamics that depends only on the error, that is (e.g. for the left invariant error):

$$\dot{\eta}^1 = \phi(\eta^1, u) = f(\eta^1, u) - f(e, u)\eta^1, \tag{3.44}$$

where recall that e denotes the identity element of G. Consider a set of (left invariant) observations

$$\begin{aligned} y_1 &= g x_1 \\ &\vdots \\ y_N &= g x_N, \end{aligned} \tag{3.45}$$

with $x_1, \ldots, x_N$ known vectors, and for $g \in G$ let $\xi \in \mathbb{R}^{\dim \mathfrak{g}}$ be such that $\mathcal{L}(\xi) \in \mathfrak{g}$ ($\mathcal{L}$ being a linear mapping) is the Lie algebra element linked to g through the exponential map, that is $g = \exp(\mathcal{L}(\xi))$. The corresponding (left invariant) Extended

Kalman Filter can be described as the following hybrid structure:

$$\begin{cases} \dot{\hat{g}} = f(\hat{g}, u) \\ \dot{P} = A(t)P + PA(t)^T + Q \qquad \rho \in [0,1] \\ \dot{\rho} = \Lambda \end{cases}$$
$$\begin{cases} \hat{g}^+ = \hat{g}\exp\left[K\begin{pmatrix} \hat{g}^{-1}y_1 - x_1 \\ \vdots \\ \hat{g}^{-1}y_N - x_N \end{pmatrix}\right] \qquad \rho = 1, \\ P^+ = (I - KC(t))P \\ \rho^+ = 0 \end{cases} \tag{3.46}$$
$$K = PC(t)[C(t)PC^T(t) + R]^{-1}$$
$$A(t), C(t) \text{ s.t.} \quad \begin{cases} \phi(\exp(\xi), u) = \mathcal{L}(A\xi) + O(|\xi|^2) \\ C\xi = \begin{pmatrix} -(\mathcal{L}(\xi)x_1)^T \\ \vdots \\ -(\mathcal{L}(\xi)x_N)^T \end{pmatrix} \end{cases}$$

with Q, R positive definite matrices to be designed according to the estimated (local on $\hat{g}$) input and output noise covariance, respectively. In (Barrau and Bonnabel, 2016) it was shown that if the local linearization around the true trajectory $g(t)$ admits a stable linear time-varying Kalman Filter, then the (left invariant) Extended Kalman Filter displays a local uniform asymptotic stability property. The same arguments can be equivalently applied to the right invariant counterpart.

It is clear that the aforementioned Extended Kalman Filter structure yields a very general result, which can be applied to a wide class of systems (entirely characterized by property (3.44)). However, the convergence/stability properties are guaranteed only locally, also in case the indistinguishable dynamics approach proved global observability, as for the inertial navigation case, used in (Barrau and Bonnabel, 2016) as numerical example to validate the effectiveness of invariant EKFs.

On the other hand, the complementary filters on $SO(3)$ shown in (Mahony, Hamel, and Pflimlin, 2008) are globally analyzed by means of the Lie group formalism. In particular, a problem of 3D attitude and gyro bias estimation is solved considering a dynamical system of the form

$$\begin{aligned} \dot{R} &= R(\omega - b_\omega)_\times \\ \dot{b}_\omega &= 0 \\ R_y &\simeq R, \end{aligned} \tag{3.47}$$

with the input ω available from the gyro readings and the output R_y (given by the knowledge of at least two unit vectors in the two reference frames) corrupted by noise. Interestingly, the so-called passive complementary filter, given in $SO(3)$ by:

$$\begin{aligned} \dot{\hat{R}} &= \hat{R}\left(\omega - \hat{b}_\omega + k_p \operatorname{vex}\left(\frac{\tilde{R} - \tilde{R}^T}{2}\right)\right) \\ \dot{\hat{b}}_\omega &= -\gamma \operatorname{vex}\left(\frac{\tilde{R} - \tilde{R}^T}{2}\right), \end{aligned} \tag{3.48}$$

with $\tilde{R} = \hat{R}^T R_y$, has a very simple and elegant Lyapunov analysis, which can be carried out with tools similar to those of adaptive systems theory. Indeed, it is possible to yield a global characterization of the observer trajectories with the Lyapunov function:

$$V(\tilde{R}, \tilde{b}_\omega) = \frac{1}{2}\,\mathrm{Tr}(I_3 - \tilde{R}) + \frac{1}{2\gamma}|\tilde{b}_\omega|^2, \tag{3.49}$$

with $\tilde{b}_\omega = \hat{b}_\omega - b_\omega$. In (Mahony, Hamel, and Pflimlin, 2008) it is shown, however, that the domain of attraction displays some peculiarities, as the trajectories are proven to converge almost globally, leaving out an unstable set of measure zero.

Generally speaking, it is known that if the manifold on which a dynamical system evolves is not diffeomorphic to any Euclidean space, it is impossible for a smooth vector field to globally asymptotically stabilize an equilibrium point (Mayhew, Sanfelice, and Teel, 2011). Notably, the attempt to break this kind of topological constraints with discontinous, memoryless feedback laws often leads to non-robust solutions, causing in practice chattering behaviors which can be only removed employing a dynamic hybrid feedback law (Sontag, 1999).We also refer to (Zhang, Sarlette, and Ling, 2015), where this issue is clearly appreciated in the fact that it is impossible to define, on a compact Lie group, a smooth potential function with a unique critical point.

In the next chapter, we will consider a well-known electric machines observation problem taking advantage for the first time, to the author's best knowledge, of an explicit Lie group formulation of the system's dynamics. The objective will be to yield a global characterization of the stability and convergence results, and validate the effectiveness and simplicity of the Lie group formalism also through experimental tests. From a more general point of view, the considered class of systems is quite peculiar, as it is given by the cascade between a dynamics on a non-contractible manifold, and a flat system evolving in a vector space (essentially, a chain of integrators), whose output is the only available measurement from the system. Specifically, such dynamics can be represented as

$$\begin{aligned} \dot{\xi}_1 &= \xi_2 \\ \dot{\xi}_2 &= \xi_3 \\ &\vdots \\ \dot{\xi}_n &= \varphi(\xi_1, \ldots, \xi_n, p, u, d) \\ \dot{p} &= f(\xi_1, \ldots, \xi_n, p, u, d) \\ y &= \xi_1, \end{aligned} \tag{3.50}$$

where $\xi_i \in \mathbb{R}^k$, $i \in \{1, \ldots, n\}$ are the states of the flat subsystem, u is a vector of inputs available for measurement, d is a vector of disturbances, while $p \in \mathcal{M}$, with $\mathcal{M}$ a smooth manifold. Here, it is assumed the smooth vector fields f, φ are such that observability is ensured with y and u the only available signals.

For what concerns the electro-mechanical systems of the next chapter, we have $n = 1$, $k = 2$ and $\mathcal{M} = \mathbb{S}^1 \times \mathbb{R}$, but the design can be easily generalized, also accounting for the aforementioned results on the complementary filters on $SO(3)$. Future works will be dedicated to fully explore the analysis and design strategies inspired by this particular class of systems with topological constraints.

Chapter 4

Sensorless Observers for PMSMs with no Mechanical Model

Sinusoidal Electric Machines, such as Induction Machines (IMs) and Permanent Magnet Synchronous Machines (PMSMs), are massively adopted in several industrial fields, for different applications and power ranges. The field orientation principle is commonly exploited to obtain accurate regulation (torque, speed and position) with simple decoupled controllers (Novotny and Lipo, 2010). To implement such algorithms, however, knowledge of the rotor angular position and speed is essential, and therefore expensive and complex mechanical sensors (e.g. encoders) are commonly employed. This clearly poses significant economic and reliability issues. As a consequence, considerable research effort has been spent to develop specific control solutions, referred to as sensorless control techniques, where rotor mechanical variables are reconstructed by suitable estimation methods, exploiting solely the available electrical measurements and knowledge about the system dynamics.

A vast literature exists on this topic, with several monographs devoted to it (Marino, Tomei, and Verrelli, 2010; Vas, 1998). Two main estimation approaches can be distinguished. Signal-based techniques, on the one hand, exploit high frequency current/voltage injection to reveal magnetic saliency, i.e. the machine anisotropies that relate the stator inductance with the rotor angular configuration. On the other hand, Model-based strategies use the machine nominal dynamics to define state observers and controllers. Notably, this class of algorithms does not rely on those anisotropies which are expected to be minimized, in many electric machines, by increasingly accurate manufacturing techniques.

Focusing on Model-based techniques, where control theory finds natural application, we can identify in the literature both sensorless observers (usually interconnected with standard controllers) and sensorless controllers (simultaneously solving the control and estimation problems). In this context, note that observers are usually preferred in sensorless drives, since it is possible to replace real measurements without changing the controllers, even if a formal stability analysis of the resulting interconnection is typically unavailable. Among the different control/observation techniques, apart from Extended Kalman Filters (Hilairet, Auger, and Berthelot, 2009) and Sliding Mode techniques (Lee and Lee, 2013), Adaptive Systems theory and High-Gain approaches have turned out particularly successful. In this respect, and without intending to be exhaustive, some relevant results of the early 2000s are (Marino, Tomei, and Verrelli, 2008; Khalil, Strangas, and Jurkovic, 2009; Montanari, Paresada, and Tilli, 2006) and references therein, mainly oriented to IMs with known parameters. Other recent results concern the estimation of the stator resistance and the translation of IMs controllers into PMSMs controllers (see Verrelli et al., 2017 and references therein).

A crucial requirement for the real world application of sensorless techniques is the capability of dealing with variable speed, without any (or very limited) knowledge about the mechanical model of the load coupled with the machine. For instance, nonlinear mechanisms with uncertain/variable parameters and load torque are often adopted in industrial automation. Similarly, in the field of electric-powered vehicles, such as Hybrid Electric Vehicles (HEVs) or electric Unmanned Aerial Vehicles (UAVs), strongly variable and unknown load torques combined with variable speed references are very common. From a theoretical point of view, the aforementioned control scenarios are very demanding and are usually faced assuming constant speed in the formal analysis, allowing to completely neglect the mechanical model. This approximation is generally supported by the fact that the resulting speed dynamics is usually slowly-varying with respect to the electromagnetic one, but such assumption becomes limiting for high performance observation, oriented to high-end control. Notably, the algorithm in (Bobtsov et al., 2015) moves in the direction of sensorless observation with variable speed and unknown mechanical model. That solution, however, suffers from integration issues and the use of a high number of auxiliary states. In this respect, our main contribution is to present a rigorous result on sensorless speed, position and rotor flux amplitude estimation for PMSMs, in the context of no information of the mechanical dynamics, without assuming constant speed and without any open-loop integration. The time-varying rotor speed and position, along with the rotor flux amplitude, are reconstructed with arbitrary accuracy, under some mild limiting conditions, with no information on the mechanical structure and its parameters. In our solution, we only require a priori knowledge of the stator resistance and inductance, along with the motor pole pairs, while solely the stator voltages and currents need to be available for measurement. As a significant extension of the main result, also the stator resistance will be shown to be unnecessary to achieve high reconstruction performance, even though signal injection (via an appropriate current controller) will be necessary to ensure full state observability.

The main characteristics of the proposed solution are the following. Exploiting and improving the approaches proposed in (Tilli et al., 2012; Tilli and Conficoni, 2016), where rotor speed was assumed constant, a reference frame adaptation is designed to achieve alignment with the back-ElectroMotive Force (back-EMF) vector. As a crucial difference from the aforementioned works, the structure that we propose here does not achieve speed estimation by means of parameter adaptation, but with arguments related to unknown input observers. In this respect, a large role is played by the Lie Groups formalism introduced in the previous chapter. Indeed, we consider here a compact and effective representation in $\mathbb{S}^1$ of the intrinsic rotation dynamics of PMSMs (in contrast with other approaches that employ $\mathbb{R}^2$, such as Ortega et al., 2010; Verrelli et al., 2017). A two time-scales behavior is imposed to the observation error, this way exploiting the stator current estimation error as an indirect measurement of the alignment mismatch with the back-EMF vector. Using Lyapunov-like arguments, we prove in our main result that the proposed observer is regionally practically asymptotically stable, with a wide domain of attraction in the estimation error state space, assuming that the speed is bounded away from zero, with a constant unknown sign and a bounded unknown derivative. The inherently non-global result originates from high-gain arguments and the topological constraints of $\mathbb{S}^1$. However, it will be shown that the properties of the domain of attraction can be improved with an additional hybrid policy, appropriately designed to structurally break the aforementioned constraints.

After a brief introduction to the PMSM electromagnetic model, we begin the development of the proposed solution with a simple global observability analysis, based on the same arguments introduced for the general setting in the previous chapter. Then, the problem statement and the observer structure are given, and a thorough stability analysis is then provided. In addition, it is shown that the domain of attraction of the regional stability is very close to semi-global and only needs to exclude a lower-dimensional unstable manifold. Afterwards, meaningful simulation and experimental results are presented to show the effectiveness of the designed observer in a meaningful case of study, given in particular by the high-performance control of UAV propeller motors. As a final step, we discuss two meaningful extensions of the proposed observer, formally proving their stability properties. In particular, we formally deal with the rather advanced problems of stator resistance estimation and hybrid redesign to yield semi-global practical stability. Both these extensions are validated by means of numerical results, in order to testify to their applicability in UAV motor control applications.

4.1 PMSM Dynamics and Observability Analysis

The PMSM electromagnetic model in a static bi-phase reference frame s (typically known as α-β frame) under nominal operation (that is, balanced working conditions, linear magnetic circuits and negligible iron losses) can be represented as follows:

$$\begin{aligned} \frac{d}{dt} i_s &= -\frac{R}{L} i_s + \frac{1}{L} u_s - \frac{\omega \varphi \mathcal{J} \zeta}{L} \qquad\qquad y = i_s, \\ \dot{\zeta} &= \omega \mathcal{J} \zeta \end{aligned} \tag{4.1}$$

where $i_s \in \mathbb{R}^2$ and $u_s \in \mathbb{R}^2$ are the stator currents and voltages, $\zeta \in \mathbb{S}^1$ is the angular configuration of the rotor magnetic flux vector, ω is the rotor (electrical) angular speed, $\varphi > 0$ is the constant finite amplitude of the rotor magnetic flux vector and R, L are the stator resistance and inductance, respectively. The only measurable signals in system (4.1) are the input voltage u_s and the output current y. For our initial analysis, we suppose that the signals u_s, ω are piecewise continuous signals for all $t \geq t_0$, where t_0 denotes the initial time. This property is sufficient to guarantee that the solutions of system (4.1) are forward complete, as a consequence of (Khalil, 2002), Theorem 3.2. We recall that the PMSM electromagnetic model is linked with the mechanical system through the mechanical speed, $\omega_{\mathrm{m}} = \omega / p$ and the electrical torque T_{el}:

$$T_{\mathrm{el}} = -\frac{3}{2} p \varphi \zeta^T \mathcal{J} i_s, \tag{4.2}$$

where $p \in \mathbb{Z}_{\geq 1}$ is a known integer used to indicate the motor pole pairs.

In the field of sinusoidal machines, it is common to represent (4.1) in rotating reference frames, as some of them (e.g. the so-called d-q frame) are particularly convenient for field-oriented control. In general, denoting with r a generic rotating frame, and with ζ_r, ω_r its angular orientation and speed, respectively, (4.1) becomes:

$$\begin{aligned} \frac{d}{dt} i_r &= -\frac{R}{L} i_r + \frac{1}{L} u_r - \frac{\omega \varphi \mathcal{J} \mathcal{C}^T[\zeta_r] \zeta}{L} - \omega_r J i_r \\ \dot{\zeta} &= \omega \mathcal{J} \zeta \qquad \dot{\zeta}_r = \omega_r \mathcal{J} \zeta_r, \end{aligned} \tag{4.3}$$

where $i_r := \mathcal{C}^T[\zeta_r] i_s$, $u_r := \mathcal{C}^T[\zeta_r] u_s$ are the stator current and voltage vectors, represented in the r frame. In the section dedicated to the observer design, this generic frame of reference will be specialized with some appropriate selections.

A different representation of the PMSM dynamics, based on the total flux vector, can be also found in the literature. Let $\lambda = \varphi\zeta + Li_s$ denote the stator (total) flux vector, then it is easy to verify that

$$\dot{\lambda} = \omega\varphi\mathcal{J}\zeta + u_s - Ri_s - \omega\varphi\mathcal{J}\zeta, \tag{4.4}$$

thus an alternative to systems (4.1) and (4.3) is given by:

$$\begin{aligned} \dot{\lambda} &= u_s - Ri_s \\ \dot{\zeta} &= \omega\mathcal{J}\zeta, \end{aligned} \tag{4.5}$$

or, considering λ and $i_\lambda = Li_s$ as state variables:

$$\begin{aligned} \dot{\lambda} &= u_s - \frac{R}{L}i_\lambda \\ \frac{d}{dt}i_\lambda &= u_s - \frac{R}{L}i_\lambda - \omega\mathcal{J}(\lambda - i_\lambda). \end{aligned} \tag{4.6}$$

These representations result particularly convenient because the right-hand-side of $\dot{\lambda}$ is a measurable signal (assuming perfect knowledge of R, which is rarely the case), thus a simple open-loop integration yields λ, up to the unknown initial conditions. The peculiar properties of system (4.5) or (4.6) have been exploited in many theoretical works in the literature. In (Ortega et al., 2010) the rotor flux knowledge (along with R and L) is used to enforce convergence of the estimate of λ on a circle, while in (Bernard and Praly, 2018; Bernard and Praly, 2019) related algorithms are presented for the estimation of φ and R, respectively. Notably, in (Bobtsov et al., 2015) open-loop integration is combined with appropriate filters to yield a linear regression form, thus allowing to estimate the flux initial conditions and the rotor flux amplitude.

4.1.1 Global Observability Analysis through the Indistinguishable Dynamics Approach

We perform the observability analysis following a similar procedure to the one presented in the previous chapter, considering for simplicity the stator currents representation of PMSMs. Consider system (4.1) with the dynamics augmented with the additional state φ:

$$\begin{aligned} \frac{d}{dt}i_s &= -\frac{R}{L}i_s + \frac{1}{L}u_s - \frac{\omega\varphi\mathcal{J}\zeta}{L} \\ \dot{\varphi} &= 0 \\ \dot{\zeta} &= \omega\mathcal{J}\zeta \end{aligned} \qquad y = i_s. \tag{4.7}$$

Here, the main difference in the observability analysis is the presence of the unmeasurable input ω, which requires a stronger form of observability, known as Unknown Input Observability. Following the same notation as in the previous chapter, we provide a definition for the so-called the Unknown Input Indistinguishability (cf. Martinelli, 2018, Definition 3).

Definition 4.1 ($u(\cdot)$-Unknown Input Indistinguishability)**.** *Consider a nonlinear system of the form*

$$\begin{aligned} \dot{p} &= f(p,u,\nu), \qquad p(t_0) = p_0 \in \mathcal{M} \\ y &= h(x), \end{aligned} \tag{4.8}$$

where $p \in \mathcal{M}$, with $\mathcal{M}$ a smooth manifold, while $u(\cdot) \in \mathcal{U}$ and $\nu(\cdot) \in \mathcal{V}$ are a known and an unknown input signal, respectively, with $\mathcal{U}$ and $\mathcal{V}$ some classes of piecewise continuous signals defined over $\mathbb{R}$. In addition, let f and h be a smooth vector field and a smooth map, respectively. For any initial condition $(t_0, p_0) \in \mathbb{R} \times \mathcal{M}$ and any $u(\cdot) \in \mathcal{U}$, $\nu(\cdot) \in \mathcal{V}$, denote the solution of (4.8), evaluated at time $t > t_0$, with $\bar{p}(t; t_0, p_0, u_{[t_0,t)}, \nu_{[t_0,t)})$. Suppose that system (4.8) is forward complete, that is for any $(t_0, p_0) \in \mathbb{R} \times \mathcal{M}$ and any $u(\cdot) \in \mathcal{U}$, $\nu(\cdot) \in \mathcal{V}$ the solution exists and is uniquely defined in the interval $[t_0, \infty)$. Let p_1, $p_2 \in \mathcal{M}$, then p_1 and p_2 are called $u(\cdot)$-unknown input indistinguishable in the interval $[t_0, t_0 + \delta)$, with δ a positive scalar, if there exists a pair $\nu_1(\cdot)$, $\nu_2(\cdot) \in \mathcal{V}$ such that, for all $t \in [t_0, t_0 + \delta)$, it holds:

$$h(\bar{p}(t; t_0, p_0, u_{[t_0,t)}, \nu_{[t_0,t)})) = h(\bar{p}(t; t_0, p_0, u_{[t_0,t)}, \nu_{[t_0,t)})). \tag{4.9}$$

A point $p \in \mathcal{M}$ is thus unknown input observable in the interval $[t_0, t_0 + \delta)$ if for every input $u(\cdot) \in \mathcal{U}$, then p is $u(\cdot)$-unknown input indistinguishable from every $q \in \mathcal{M}$. Unknown input observability of system (4.8) follows immediately as unknown input observability of every $p \in \mathcal{M}$. Note, in particular, that to ensure unknown input observability we require to check the indistinguishability condition for every unknown input belonging to the class $\mathcal{V}$.

Let $[t_0, \infty)$ be the interval of existence, considered for observability analysis, of the solutions of system (4.7). For simplicity, suppose that $\omega(\cdot)$ is such that $\omega(t) \neq 0$, for all $t \in [t_0, \infty)$. This assumption will be exploited in the next section to formally state the requirements for the observer design. Denote with the bar notation a second instance of system (4.7), driven by the unknown input $\bar{\omega}$. Simple computations yield, for $i_s = \bar{\imath}_s$ and all $t \in [t_0, \infty)$:

$$\omega \varphi \mathcal{J} \zeta = \bar{\omega} \bar{\varphi} \mathcal{J} \bar{\zeta}. \tag{4.10}$$

Since $|\zeta| = |\bar{\zeta}| = 1$, it follows that $|\omega| \varphi = |\bar{\omega}| \bar{\varphi} = \chi$, where $\chi(t) > 0$ for $t \in [t_0, \infty)$. Denote $\sigma = \operatorname{sgn}(\omega)$, $\bar{\sigma} = \operatorname{sgn}(\bar{\omega})$, then it holds:

$$\sigma \zeta = \bar{\sigma} \bar{\zeta}, \tag{4.11}$$

since $\chi > 0$ can be removed on both sides of the previous equality. Apply the time derivative on both sides to yield:

$$\omega \mathcal{J} \sigma \zeta = \bar{\omega} \mathcal{J} \bar{\sigma} \bar{\zeta}, \tag{4.12}$$

and the only case which is compatible with this equation is $\omega = \bar{\omega}$, which becomes the only scenario to analyze for indistinguishablity. From the above considerations, it follows directly that $\sigma = \bar{\sigma}$, so $\zeta = \bar{\zeta}$ and $\varphi = \bar{\varphi}$. This proves that the PMSM dynamics, for the class of unknown inputs satisfying $\omega(t) \neq 0$, for all $t \in [t_0, \infty)$, is unknown input observable. As a consequence, the next section is dedicated to the design of an observer which fully exploits this simple, yet significant, initial result.

4.2 A Sensorless Observer with Unknown Mechanical Model

4.2.1 Problem Statement

As a first step, we formally specify the standing assumptions for the observer design. We stress the fact that in the following the rotor speed ω is not regarded as the state of a given mechanical system, but as a generic exogenous signal: this choice is due to the fact that the mechanical model is completely unknown, and we want to impose only mild regularity conditions to simplify the problem and make it mathematically well-posed. For this purpose, the next Assumption is introduced.

Assumption 4.1. *Let t_0 denote the initial time, then $\omega(t)$ exists for $t \in [t_0, \infty)$ and satisfies the following properties:*

a) $\omega(t)$ is C^0 and piecewise C^1 in $[t_0; +\infty)$, i.e. $\dot{\omega}(\cdot)$ is defined and C^0 except at some points, t_j, such that, for every arbitrary finite time interval, the number of exception points is finite, and the limits from the right and from the left of $\dot{\omega}$ exist at each of them;

b) $|\omega(t)| \in [\omega_{\min}, \omega_{\max}]$ for all t in $[t_0; +\infty)$, with $0 < \omega_{\min} < \omega_{\max} < +\infty$, therefore $\omega(t)$ is bounded, with known limits, such that it cannot be null. Furthermore, combining this with the above continuity property, the sign of $\omega(t)$ is constant, but not a-priori known;

c) $|D^+\omega(t)| = \dot{\omega}_{\max} < +\infty$ for all t in $[t_0; +\infty)$, therefore the Dini derivative of $\omega(t)$ is bounded with known bounds, but without any restriction on its sign and minimum amplitude.

These hypotheses are considered to hold uniformly in the initial time, thus justifying, in the remainder, to set without loss of generality $t_0 = 0$. Note that Assumption 4.1 is much less restrictive than the common hypothesis of slowly-varying speed, that is in fact usually turned into constant speed in the mathematical analysis. In particular, conditions a)-c) cover almost all possible behaviors expected in high-performance applications, since they are satisfied under very mild physical and technological limitations. Condition b), on the other hand, introduces an important limitation and is clearly connected to observability. Compared to the general observability requirement of non-permanent zero speed, this assumption on ω is much more restrictive, since we assume constant sign, even if unknown. Indeed, according to well-known results on sinusoidal machines, non-permanent zero speed is sufficient to guarantee observability (we refer to Zaltni et al., 2010 for an observability analysis that shows this property). The relaxation of condition b) is out of the purpose of this chapter, and will be a relevant element to be considered for an extension of the present work. It is worth noting that the features of many relevant applications are already covered by Assumption 4.1. Some important examples are power control of electric generators and speed control of UAVs electrically-powered propellers.

According to the aforementioned definitions and considerations, the *sensorless observer problem for PMSMs with (restricted) variable speed and no mechanical model* can be formulated as follows. Consider the electromagnetic PMSM model (4.1) (or equivalently models (4.3)/(4.5)) with known parameters L and R, and let Assumption 4.1 hold for the rotor speed ω. Assuming that solely the stator voltages and currents are measurable, design an observer for ζ, ω and φ, providing suitable stability and convergence properties. In particular, the estimation error dynamics is required to satisfy some form of practical asymptotic stability, with in addition local exponential stability in the special case $D^+\omega = 0$. We will make this statement precise in the stability analysis.

4.2.2 Observer Definition

As a first important step to deal with the unknown sign of ω, we introduce the variables $\chi \in \mathbb{R}_{>0}$ and $\xi \in \mathbb{R}$ s.t. $\chi := |\omega|\varphi$ and $\xi := (1/\varphi)\,\mathrm{sgn}(\omega)$. Clearly, χ is time-varying, while ξ is constant, finite, non-null and with unknown sign, according to Assumption 4.1. In addition, we introduce $\zeta_\chi \in \mathbb{S}^1$ such that $\zeta_\chi := \zeta\,\mathrm{sgn}(\xi) = \zeta\,\mathrm{sgn}(\omega)$. With these definitions at hand, the term $\omega\varphi\mathcal{J}\mathcal{C}^T[\zeta_r]\zeta$ in (4.3) can be reformulated as $\chi\,\mathrm{sgn}(\omega)\mathcal{J}\mathcal{C}^T[\zeta_r]\zeta = \chi\mathcal{J}\mathcal{C}^T[\zeta_r]\zeta_\chi$, and it results $\dot{\zeta}_\chi = \chi\xi\mathcal{J}\zeta_\chi$. Then, replacing ζ with ζ_χ in (4.3), the PMSM dynamics reads as follows:

$$\begin{aligned} &\frac{d}{dt}i_r = -\frac{R}{L}i_r + \frac{1}{L}u_r - \frac{\chi\mathcal{J}\mathcal{C}^T[\zeta_r]\zeta_\chi}{L} - \omega_r J i_r \\ &\dot{\zeta}_\chi = \chi\xi\mathcal{J}\zeta_\chi \qquad \dot{\zeta}_r = \omega_r\mathcal{J}\zeta_r, \end{aligned} \tag{4.13}$$

As a consequence, it is immediate to note that the selection $\zeta_r = \zeta_\chi$ leads to a model of the form

$$\begin{aligned} &\frac{d}{dt}i_\chi = -\frac{R}{L}i_\chi + \frac{1}{L}u_\chi - \frac{\chi J}{L}\begin{pmatrix}1\\0\end{pmatrix} - \chi\xi\mathcal{J}i_\chi \\ &\dot{\zeta}_\chi = \chi\xi\mathcal{J}\zeta_\chi, \end{aligned} \tag{4.14}$$

where i_χ, u_χ are used to denote currents and voltages in this special reference. Clearly, (4.14) represents the dynamics of the machine in a reference frame aligned with the back-EMF vector, including the effect of the speed sign. In this respect, it is worth underlining that $\zeta_r = \zeta_\chi$ will be aligned with the rotor flux vector orientation ζ or its opposite $-\zeta$, depending on the sign of the speed or, equivalently, on the sign of ξ. Based on the results in (Tilli and Conficoni, 2016), where only the case of constant speed for Induction Motors was considered, the previous considerations are exploited as follows.

- An observer reference frame with $\zeta_r = \hat{\zeta}_\chi$ is introduced as an estimator of ζ_χ. Clearly, the latter frame is not directly available from measurements, and it is not possible to impose $\hat{\zeta}_\chi = \zeta_\chi$, therefore $\dot{\hat{\zeta}}_\chi$ has to be designed using the remaining observer states in order to make $\hat{\zeta}_\chi$ converge to ζ_χ.
- The current dynamics corresponding to the reference frame $\hat{\zeta}_\chi$ is introduced, highlighting the mismatch between $\hat{\zeta}_\chi$ and ζ_χ in (4.14). The resulting system is used to arrange a high-gain observer providing indirect information on the back-EMF error. Then, the reformulation of ω and φ in terms of χ and ξ is exploited to derive and utilize information on the variable amplitude of the back-EMF and, consequently, on the variable speed amplitude.

Denote with $i_{\hat{\chi}}$, $u_{\hat{\chi}}$ currents and voltages in the $\hat{\zeta}_\chi$ frame, and let $\eta := \mathcal{C}^T[\hat{\zeta}_\chi]\zeta_\chi \in \mathbb{S}^1$ be the misalignment between $\hat{\zeta}_\chi$ and ζ_χ, then the dynamics (4.14) represented in the $\hat{\zeta}_\chi$ frame becomes (let $\hat{\omega}_\chi$ be the angular velocity associated with $\hat{\zeta}_\chi$):

$$\begin{aligned} &\frac{d}{dt}i_{\hat{\chi}} = -\frac{R}{L}i_{\hat{\chi}} + \frac{1}{L}u_{\hat{\chi}} - \frac{\chi\mathcal{J}\eta}{L} - \hat{\omega}_\chi\mathcal{J}i_{\hat{\chi}} \\ &\dot{\eta} = (\chi\xi - \hat{\omega}_\chi)\mathcal{J}\eta \qquad \dot{\hat{\zeta}}_\chi = \hat{\omega}_\chi\mathcal{J}\hat{\zeta}_\chi \end{aligned} \tag{4.15}$$

In the following, denote for compactness of notation the (rescaled) back-EMF with $h := -\chi \mathcal{J} \eta$ (note that $|h| = \chi$). Clearly, the estimator to design is expected to make η converge to the identity element of $\mathbb{S}^1$, i.e. vector $\binom{1}{0}$. As a consequence, the proposed six-order observer is reported in the following:

$$\begin{aligned} \dot{\hat{\imath}} &= -\frac{R}{L}\hat{\imath} + \frac{1}{L}u_{\hat{\chi}} + \frac{\hat{h}}{L} - \left(|\hat{h}|\hat{\xi} + k_\eta \hat{h}_1\right)\mathcal{J} i_{\hat{\chi}} + k_{\mathrm{p}}\tilde{\imath} \\ \dot{\hat{h}} &= k_{\mathrm{i}}\tilde{\imath} \qquad \dot{\hat{\zeta}}_\chi = \left(|\hat{h}|\hat{\xi} + k_\eta \hat{h}_1\right)\mathcal{J}\hat{\zeta}_\chi \qquad \dot{\hat{\xi}} = \gamma \hat{h}_1 \\ \hat{\omega} &= |\hat{h}|\hat{\xi} \qquad \hat{\zeta} = \hat{\zeta}_\chi \operatorname{sgn}(\hat{\xi}) \qquad \hat{\varphi} = \operatorname{sat}(1/|\hat{\xi}|), \end{aligned} \tag{4.16}$$

where $\hat{\imath} \in \mathbb{R}^2$ is the reconstruction of $i_{\hat{\chi}}$, with estimation error $\tilde{\imath} := i_{\hat{\chi}} - \hat{\imath}$; $\hat{\xi} \in \mathbb{R}$ is the estimation of ξ and, as already stressed, $\hat{\zeta}_\chi \in \mathbb{S}^1$ is expected to be pushed toward ζ_χ. Note that the angular velocity of $\hat{\zeta}_\chi$ is specified as $\hat{\omega}_\chi = |\hat{h}|\hat{\xi} + k_\eta \hat{h}_1$. Furthermore, $\hat{h} \in \mathbb{R}^2$ is a vector $\hat{h} := (\hat{h}_1, \hat{h}_2)$ embedded in the current estimation dynamics in order to reconstruct the back-EMF contribution, while k_{p}, k_{i}, k_η and γ are positive scalars to tune the convergence and stability properties of the proposed solution. Finally, $\hat{\omega}$, $\hat{\zeta}$ and $\hat{\varphi}$ are the estimations of ω, ζ and φ, respectively: it is worth noting that these are not states of the proposed observer, but outputs related to other state variables: for this reason, they are not needed in the observer stability analysis. In addition, for $\hat{\varphi}$ a saturation has been introduced to prevent it from becoming infinite as $\hat{\xi}$ crosses zero, during its convergence transient. In particular, an upper bound $\varphi_{\max}$, employed in the saturation function, is always given in practice (actually, a positive lower bound is usually given as well).

4.2.3 A High-Gain Observer for Back-EMF Reconstruction

Let $\tilde{\xi} := \xi - \hat{\xi}$, $\tilde{h} := h - \hat{h}$ and, in addition, let $\tilde{h} = (\tilde{h}_1, \tilde{h}_2)$, $\eta = (\eta_1, \eta_2)$. The resulting error dynamics can be represented as follows (the Dini derivative is applied to $\tilde{h}$ to account for the non-differentiability of h):

$$\begin{aligned} \dot{\tilde{\imath}} &= -\left(\frac{R}{L} + k_{\mathrm{p}}\right)\tilde{\imath} + \frac{\tilde{h}}{L} \\ D^+\tilde{h} &= -k_{\mathrm{i}}\tilde{\imath} - \left[(D^+\chi)I + \chi\omega_\eta\left(h, \tilde{h}, \eta, \xi, \tilde{\xi}, \chi\right)\mathcal{J}\right]\mathcal{J}\eta \\ \dot{\eta} &= \omega_\eta\left(h, \tilde{h}, \eta, \xi, \tilde{\xi}, \chi\right)\mathcal{J}\eta \\ \dot{\tilde{\xi}} &= -\gamma\chi\eta_2 + \gamma\tilde{h}_1, \end{aligned} \tag{4.17}$$

where $\omega_\eta(h, \tilde{h}, \eta, \xi, \tilde{\xi}, \chi) = \chi\xi - \hat{\omega}_\chi = \chi\tilde{\xi} - k_\eta\chi\eta_2 + k_\eta\tilde{h}_1 + (\chi - |h - \tilde{h}|)(\xi - \tilde{\xi})$ is used to denote the angular speed of η. In the observer stability analysis, the error model (4.17) will be cast in a two-time-scales problem, exploiting high-gain arguments. Among several possible choices, select k_{p}, k_{i} such that, for a positive scalar ε, it holds:

$$\frac{R}{L} + k_{\mathrm{p}} = 2\varepsilon^{-1} \qquad k_{\mathrm{i}} = 2L\varepsilon^{-2}. \tag{4.18}$$

Consider a linear change of coordinates such that:

$$x_{\mathrm{f}} = \begin{pmatrix} \varepsilon^{-1} I_{2\times 2} & 0_{2\times 2} \\ -\varepsilon^{-1} I_{2\times 2} & L^{-1} I_{2\times 2} \end{pmatrix} \begin{pmatrix} \tilde{\imath} \\ \tilde{h} \end{pmatrix} \tag{4.19}$$

and define $x_s := (\eta, \tilde{\xi}) \in \mathbb{S}^1 \times \mathbb{R}$, then the dynamics of $(\tilde{\imath}, \tilde{h})$ in (4.17) can be replaced with:

$$D^+ x_f = \underbrace{\begin{pmatrix} -\varepsilon^{-1} I_{2\times 2} & \varepsilon^{-1} I_{2\times 2} \\ -\varepsilon^{-1} I_{2\times 2} & -\varepsilon^{-1} I_{2\times 2} \end{pmatrix}}_{\varepsilon^{-1} A_f} x_f + \underbrace{\begin{pmatrix} 0_{2\times 2} \\ L^{-1} I_{2\times 2} \end{pmatrix}}_{B_f} f_h(x_f, x_s, \chi, D^+\chi, \xi), \tag{4.20}$$

where $f_h(\cdot)$ denotes $\dot{h}$ as shown in (4.17). Clearly, the x_f-dynamics can be made arbitrarily fast as $\varepsilon > 0$ is selected sufficiently small. In (Tilli, Bosso, and Conficoni, 2019), standard singular perturbations arguments were exploited to guarantee practical asymptotic stability of the observer error dynamics. To improve the understanding of the observer stability properties, and to yield an explicit expression of ε, we provide a proof based on Lyapunov arguments. This way, not only can the scheme be extended to similar estimation problems, but improved performance can also be expected from a tighter bound on ε. Firstly, we develop the machinery employed to bound $|x_f|$, which shares some tools with (Bin, 2019).

Consider a linear change of coordinates $x_f = T(\varepsilon^{-1})(\tilde{\imath}, \tilde{h})$ such that the dynamics of x_f is given by:

$$D^+ x_f = \varepsilon^{-1} A_f x_f + B_f f_h(x_f, x_s, \chi, D^+\chi, \xi), \tag{4.21}$$

with A_f Hurwitz. Let $P = P^T > 0$ be a positive-definite matrix such that

$$P A_f + A_f^T P = -I, \tag{4.22}$$

and let the Lyapunov function

$$V_f = \sqrt{x_f^T P x_f}. \tag{4.23}$$

Clearly, it holds:

$$\sqrt{\lambda_{\min}} |x_f| \leq V_f \leq \sqrt{\lambda_{\max}} |x_f|, \tag{4.24}$$

with $\lambda_{\min}$ and $\lambda_{\max}$ the minimum and maximum eigenvalues of P, respectively, whereas the Dini derivative of V_f along the solutions of the system is:

$$\begin{aligned} D^+ V_f &= \frac{1}{2V_f} \left[\varepsilon^{-1} x_f^T (P A_f + A_f^T P) x_f + x_f^T P B_f f_h \right] \\ &\leq \frac{\varepsilon^{-1}}{2V_f} \left(-|x_f|^2 + \varepsilon |x_f| |P| |B_f| |f_h| \right) \\ &\leq \frac{\varepsilon^{-1}}{2} \left(-\frac{V_f}{\lambda_{\max}} + \frac{\varepsilon}{\sqrt{\lambda_{\min}}} |P| |B_f| |f_h| \right). \end{aligned} \tag{4.25}$$

For any compact sets $\mathcal{K}_f(\Delta) := \{x_f : |x_f| \leq \sqrt{\lambda_{\max}/\lambda_{\min}} \Delta + \gamma$, for some $\gamma > 0\}$, $\Delta > 0$, and $\mathcal{K}_s \subset \mathbb{S}^1 \times \mathbb{R}$ (we will later specify the structure of $\mathcal{K}_s$), if $x_f \in \mathcal{K}_f$, $x_s \in \mathcal{K}_s$, then $|f_h| \leq b$, for some positive scalar b. Note in addition that $D^+\omega = 0$ implies that f_h vanishes as $x_f \to 0$ and $x_s \to (1, 0) \times 0$. Fix Δ, $\mathcal{K}_f(\Delta)$, $\mathcal{K}_s$ and suppose $x_s(t) \in \mathcal{K}_s$ for all $t \geq 0$, then $D^+ V_f \leq 0$ as $V_f = \sqrt{\lambda_{\max}} \Delta$ is imposed as long as $0 < \varepsilon \leq \varepsilon^*$, with ε^* given by:

$$\varepsilon^* = \sqrt{\frac{\lambda_{\min}}{\lambda_{\max}}} \frac{\Delta}{|P| |B_f| b}. \tag{4.26}$$

As a consequence, it is possible to apply the Gronwall-Bellman Lemma to yield:

$$\begin{aligned} V_\mathrm{f}(t) &\leq \left(V_\mathrm{f}(0) - \frac{\varepsilon \lambda_\mathrm{max}}{\sqrt{\lambda_\mathrm{min}}} |P||B_\mathrm{f}||f_h| \right) \exp\left(-\frac{t}{2\varepsilon\lambda_\mathrm{max}} \right) + \frac{\varepsilon \lambda_\mathrm{max}}{\sqrt{\lambda_\mathrm{min}}} |P||B_\mathrm{f}||f_h| \\ &\leq V_\mathrm{f}(0) \exp\left(-\frac{t}{2\varepsilon\lambda_\mathrm{max}} \right) + \frac{\varepsilon \lambda_{max}}{\sqrt{\lambda_\mathrm{min}}} |P||B_\mathrm{f}|b. \end{aligned} \tag{4.27}$$

Exploiting the bounds on V_f, it is then possible to recover the bounds on $|x_\mathrm{f}|$:

$$\begin{aligned} |x_\mathrm{f}(t)| &\leq \sqrt{\frac{\lambda_\mathrm{max}}{\lambda_\mathrm{min}}} |x_\mathrm{f}(0)| \exp\left(-\frac{1}{2\lambda_\mathrm{max}} \frac{t}{\varepsilon} \right) + \varepsilon \frac{\lambda_\mathrm{max}}{\lambda_\mathrm{min}} |P||B_\mathrm{f}|b \\ &= \alpha_{1\mathrm{f}} \exp(-\alpha_{2\mathrm{f}} t/\varepsilon)|x_\mathrm{f}(0)| + \varepsilon\delta_\mathrm{f}, \end{aligned} \tag{4.28}$$

for some positive scalars δ_f, $\alpha_{1\mathrm{f}}$, $\alpha_{2\mathrm{f}}$. It is obvious that, as $\varepsilon \to 0^+$, the convergence rate becomes arbitrarily fast, while the residual error $\varepsilon\delta_\mathrm{f}$ becomes arbitrarily small.

4.2.4 Sensorless Observer with Unknown Mechanical Model: Complete Stability Analysis

Recall the conditions in Assumption 4.1, now rewritten for the notation given by χ, ξ:

a) $\chi(t)$ is $\mathcal{C}^0$ in $(0; +\infty)$, and piecewise $\mathcal{C}^1$ in $(0; +\infty)$;

b) $\chi_\mathrm{min} \leq \chi(t) \leq \chi_\mathrm{max}$, with $\chi_\mathrm{min} = \omega_\mathrm{min}\varphi$ and $\chi_\mathrm{max} = \omega_\mathrm{max}\varphi$;

c) $|D^+\chi(t)| \leq M$, with $M = \dot{\omega}_\mathrm{max}\varphi$.

Furthermore, it is possible to compactly rewrite the observer estimation error (4.17) as a feedback interconnection of two subsystems, parametrized in ξ and driven by the exogenous signals ω, $D^+\omega$:

$$\begin{aligned} D^+ x_\mathrm{f} &= \varepsilon^{-1} A_\mathrm{f} x_\mathrm{f} + B_\mathrm{f} f_h(x_\mathrm{f}, x_\mathrm{s}, \chi, D^+\chi, \xi) \\ \dot{x}_\mathrm{s} &= f_s(x_\mathrm{f}, x_\mathrm{s}, \chi, \xi). \end{aligned} \tag{4.29}$$

From Assumption 4.1, it holds that f_h, f_s are Lipschitz in $(x_\mathrm{f}, x_\mathrm{s})$ for any compact set in $\mathbb{R}^4 \times \mathbb{S}^1 \times \mathbb{R}$. We are ready to present the main result of this chapter.

Theorem 4.1. *Consider (4.29), and denote its solutions with $(x_\mathrm{f}(t), x_\mathrm{s}(t))$. Let $x_\mathcal{A} := x_{\mathcal{A},\mathrm{f}} \times x_{\mathcal{A},\mathrm{s}}$, with $x_{\mathcal{A},\mathrm{f}} = (0_{2\times 1}, 0_{2\times 1}) \in \mathbb{R}^4$ and $x_{\mathcal{A},\mathrm{s}} = ((1,0),0) \in \mathbb{S}^1 \times \mathbb{R}$. Let χ satisfy Assumption 4.1, then $x_\mathcal{A}$ is regionally practically asymptotically stable, that is, there exist:*

- *an open region $\mathcal{R}_\mathcal{A} \subset \mathbb{S}^1 \times \mathbb{R}$, not depending on χ, such that $x_{\mathcal{A},\mathrm{s}} \in \mathcal{R}_\mathcal{A}$;*
- *a proper indicator of $x_{\mathcal{A},\mathrm{s}}$ in $\mathcal{R}_\mathcal{A}$ denoted with σ, a class $\mathcal{KL}$ function β_s and positive scalars $\alpha_{1\mathrm{f}}$, $\alpha_{2\mathrm{f}}$;*

such that, for any positive Δ_s, Δ_f and δ, there exists ε' such that, for all $0 < \varepsilon < \varepsilon'$ (i.e. sufficiently large k_p and k_i) and all $x_\mathrm{f}(0)$, $x_\mathrm{s}(0)$ with $|x_\mathrm{f}(0)| \leq \Delta_\mathrm{f}$, $\sigma(x_\mathrm{s}(0)) \leq \Delta_\mathrm{s}$, the solutions exist, and satisfy:

$$\begin{aligned} |x_\mathrm{f}(t)| &\leq \alpha_{1\mathrm{f}} \exp(\alpha_{2\mathrm{f}} t/\varepsilon)|x_\mathrm{f}(0)| + \delta \\ \sigma(x_\mathrm{s}(t)) &\leq \beta_\mathrm{s}(\sigma(x_\mathrm{s}(0)), t) + \delta. \end{aligned} \tag{4.30}$$

Proof. In a singular perturbation perspective, the quasi-steady-state of system (4.29) (i.e. the equilibrium manifold with $\varepsilon = 0$) is given by $x_{\mathrm{f}} = 0$. The reduced order system related is then given as follows:

$$\begin{aligned} \dot{\eta} &= \left(\chi\tilde{\xi} - k_\eta \chi \eta_2\right) \mathcal{J}\eta \\ \dot{\tilde{\xi}} &= -\gamma\chi\eta_2. \end{aligned} \tag{4.31}$$

We collect some useful results regarding (4.31) in the following Lemma.

Lemma 4.1. *Consider system (4.31) and let Assumption 4.1 hold, then all its trajectories, denoted with $(\eta(t), \tilde{\xi}(t))$, converge either to $x_{\mathcal{A},\mathrm{s}}$ or to $x_{\mathcal{U},\mathrm{s}} := ((-1,0),0)$, furthermore, there exists an open set $\mathcal{R}_{\mathcal{A}} \subset \mathbb{S}^1 \times \mathbb{R}$ with $x_{\mathcal{A},\mathrm{s}} \in \mathcal{R}_{\mathcal{A}}$ such that $x_{\mathcal{A},\mathrm{s}}$ is uniformly asymptotically stable in $\mathcal{R}_{\mathcal{A}}$. On the other hand, $x_{\mathcal{U},\mathrm{s}}$ is unstable.*

Proof. Notice that the only trivial solutions of (4.31) are $x_{\mathcal{A},\mathrm{s}}$ and $x_{\mathcal{U},\mathrm{s}}$. We define the following (radially unbounded in $\tilde{\xi}$) Lyapunov candidate function for the equilibrium $x_{\mathcal{A},\mathrm{s}}$:

$$V_0(\eta, \tilde{\xi}) := 1 - \eta_1 + \frac{1}{2\gamma}\tilde{\xi}^2. \tag{4.32}$$

The derivative of V_0 along the solutions of (4.31) yields:

$$\dot{V}_0(\eta, \tilde{\xi}, \chi) = \left(\chi\tilde{\xi} - k_\eta\chi\eta_2\right)\eta_2 - \tilde{\xi}\chi\eta_2 = -k_\eta\chi\eta_2^2 \leq -k_\eta\chi_{\min}\eta_2^2. \tag{4.33}$$

Because of LaSalle-Yoshizawa's Theorem (see Theorem A.1), we infer that $x_{\mathcal{A},\mathrm{s}}$ is uniformly globally stable and, in addition, $\lim_{t\to\infty}\eta_2 = 0$. Consider $\dot{\eta}_2$, we have that:

$$\lim_{t\to+\infty}\int_0^t \dot{\eta}_2(s)ds = -\eta_2(0) \in [-1;1], \tag{4.34}$$

furthermore, the second derivative $\ddot{\eta}_2$ is bounded by direct verification, recall Assumption 4.1: applying Barabalăt's Lemma (see Lemma A.1) to $\dot{\eta}_2$ we infer then that $\lim_{t\to+\infty}(\chi\tilde{\xi} - k_\eta\chi\eta_2)\eta_1 = 0$, which in turn implies that $\lim_{t\to\infty}\tilde{\xi} = 0$. This way we conclude that, for all initial conditions, the trajectories converge (with no uniformity guarantee) to either $x_{\mathcal{A},\mathrm{s}}$ or $x_{\mathcal{U},\mathrm{s}}$. Consider the set $\hat{\mathcal{R}}_{\mathcal{A}} := \{x_{\mathrm{s}} : V_0(x_{\mathrm{s}}) < 2\}$, together with the proper indicator $\sigma_1 : x_{\mathrm{s}} \mapsto V_0(x_{\mathrm{s}})/(2 - V_0(x_{\mathrm{s}}))$, defined on $\hat{\mathcal{R}}_{\mathcal{A}}$. Any compact set $\{x_{\mathrm{s}} \in \hat{\mathcal{R}}_{\mathcal{A}} : \sigma_1(x_{\mathrm{s}}) \leq c, c > 0\}$ is forward invariant since $\partial\sigma_1/\partial x_{\mathrm{s}}(x_{\mathrm{s}})f_{\mathrm{s}}(0_{4\times1}, x_{\mathrm{s}}, \chi, 0) \leq 0$ at the boundary (the inequality is strict whenever $\eta_2 \neq 0$): because of this, for the proof of the Lemma, a simple choice is to take $\mathcal{R}_{\mathcal{A}} \equiv \hat{\mathcal{R}}_{\mathcal{A}}$. Actually, $\hat{\mathcal{R}}_{\mathcal{A}}$ is a very conservative choice, and in fact it is possible to extend the result of the Lemma to points s.t. $V_0 \geq 2$. However, to simplify the presentation, an in-depth characterization of $\mathcal{R}_{\mathcal{A}}$ beyond $\hat{\mathcal{R}}_{\mathcal{A}}$ will not be provided here, but in the next subsection, where it will be shown that the stability properties of the observer hold almost semi-globally. To show uniform attractivity of $x_{\mathcal{A},\mathrm{s}}$ in $\mathcal{R}_{\mathcal{A}}$ (in a $\mathcal{KL}$ sense), and thus its asymptotic stability, we apply Matrosov's Theorem (Loría et al., 2005), using the auxiliary function:

$$V_1 := -\chi\tilde{\xi}\eta_1\eta_2, \tag{4.35}$$

and exploiting compact sets given in terms of a proper indicator function on $\mathcal{R}_{\mathcal{A}}$ w.r.t. $x_{\mathcal{A},\mathrm{s}}$. Recall Assumption 4.1 on χ, then, defining $\psi := \chi\tilde{\xi}$:

$$D^+V_1 \leq -\psi^2\eta_1^2 + \left(M|\tilde{\xi}| + \gamma\chi_{\max}^2 + \psi^2 + 2k_\eta\chi_{\max}|\psi|\right)|\eta_2|, \tag{4.36}$$

and note that D^+V_1 is strictly negative whenever $\eta_2 = 0$ and $\tilde{\xi} \neq 0$.
To prove instability of $x_{\mathcal{U},s}$, we apply Chetaev's Theorem, indeed consider the function:

$$W := 1 + \eta_1 - \frac{1}{2\gamma}\tilde{\xi}^2, \tag{4.37}$$

we have that $\dot{W} = k_\eta \chi \eta_2^2 > k_\eta \chi_{\min} \eta_2^2$: for any initial condition arbitrarily close to $x_{\mathcal{U},s}$, $W > 0$ implies $\dot{W} > 0$, hence the statement holds. □

Owing to the previous results, consider a proper indicator $\sigma(\cdot)$ of $x_{\mathcal{A},s}$ on $\mathcal{R}_{\mathcal{A}}$ (for instance, with $\mathcal{R}_{\mathcal{A}} \equiv \hat{\mathcal{R}}_{\mathcal{A}}$, a proper selection is $\sigma_1(\cdot)$ as defined above). Lemma 4.1 implies there exists a function $\beta \in \mathcal{KL}$ such that the trajectories of the reduced order system satisfy:

$$\sigma(x_s(t)) \leq \beta(\sigma(x_s(0)), t), \qquad \forall x_s(0) \in \mathcal{R}_{\mathcal{A}}. \tag{4.38}$$

Before providing a detailed proof of the Theorem, we recall the arguments in (Tilli, Bosso, and Conficoni, 2019).

Teel - Moreau - Nešić Approach

Appealing to standard considerations from singular perturbations theory, or directly exploiting (4.28), it is possible to yield a bound for the trajectories of the boundary layer system, given by considering the time scale $\tau = t/\varepsilon$ and letting $\varepsilon \to 0^+$:

$$|x_f(\tau)| \leq \alpha_{1f} \exp(\alpha_{2f}\tau)|x_f(0)|. \tag{4.39}$$

Pick any positive scalars Δ_s, Δ_f, then consider the compact sets:

$$\begin{aligned} \bar{\mathcal{R}}_{\mathcal{A}}(\Delta_s) &:= \{x_s : \sigma(x_s) \leq \Delta_s\} \subset \mathcal{R}_{\mathcal{A}} \\ \mathcal{B}(\Delta_f) &:= \Delta_f \mathbb{B}^4 \subset \mathbb{R}^4. \end{aligned} \tag{4.40}$$

Due to the bounds (4.39) - (4.38), the regularity properties of (4.29) and in the light of Assumption 4.1, it can be inferred from (Teel, Moreau, and Nešić, 2003) that, for any $\delta > 0$, there exists $\varepsilon' > 0$ which satisfies (4.30) for all initial conditions in $\bar{\mathcal{R}}_{\mathcal{A}}(\Delta_s)$, $\mathcal{B}(\Delta_f)$. This result is yielded by inspection of the system's solutions and application of the Gronwall lemma.

Converse Lyapunov Function Approach

From (Teel and Praly, 2000, Corollary 2), we have that the robust $\mathcal{KL}$ stability of the reduced order stability implies the existence of class $\mathcal{K}_\infty$ functions $\underline{\alpha}$, $\overline{\alpha}$ and a continuously differentiable (actually smooth) function $V_s : \mathbb{R} \times \mathcal{R}_{\mathcal{A}} \to \mathbb{R}_{\geq 0}$ such that:

$$\begin{aligned} \underline{\alpha}(\sigma(x_s)) \leq V_s(t, x_s) &\leq \overline{\alpha}(\sigma(x_s)) \\ \frac{\partial V_s}{\partial t} + \frac{\partial V_s}{\partial x_s} f_s(0, x_s, \chi, \xi) &\leq -V_s(t, x_s). \end{aligned} \tag{4.41}$$

In addition, due to the regularity properties of f_s and continuity of $\partial V_s / \partial x_s$, there exists a continuous, positive and non-decreasing map μ such that:

$$\dot{V}_s = \frac{\partial V_s}{\partial t} + \frac{\partial V_s}{\partial x_s} f_s \leq -V_s(t, x_s) + \mu(\sigma(x_s))|x_f|. \tag{4.42}$$

Pick positive scalars Δ_s, Δ_f, δ, and suppose without loss of generality that $\delta \leq \min\{\Delta_s, \Delta_f\}$. Let $\eta \in (0,1)$, $\eta \leq \underline{\alpha}(\delta)/2$ and $\Omega_s = \underline{\alpha}^{-1}(\overline{\alpha}(\Delta_s) + 1)$. Define $\mathcal{K}_s(\Omega_s) := \{x_s \in \mathbb{S}^1 \times \mathbb{R} : \sigma(x_s) \leq \Omega_s\}$. We want to ensure that, for any $|x_f(0)| \leq \Delta_f$ and any $\sigma(x_s(0)) \leq \Delta_s$, the solutions are contained in the compact sets $\mathcal{K}_f(\Delta_f)$ and $\mathcal{K}_s(\Omega_s)$ and satisfy the bounds (4.30). For this purpose, let $[0, t_f)$ be a time interval such that the trajectories of system (4.29) are contained in the above compact sets. Let $b > 0$ be such that $|f_h| \leq b$, for all $(x_f, x_s) \in \mathcal{K}_f \times \mathcal{K}_s$, then let $\bar{\mu} = \mu(\Omega_s)$. Select ε_f, similarly to the choice in (4.26):

$$\varepsilon_f = \min\left\{\sqrt{\frac{\lambda_{\min}}{\lambda_{\max}}}\frac{\Delta_f}{|P||B_f|b}, \frac{\lambda_{\min}}{\lambda_{\max}}\frac{\delta}{|P||B_f|b}\right\}. \tag{4.43}$$

If $\varepsilon \leq \varepsilon_f$ then the trajectories are contained in $\{x_f : V_f(x_f) \leq \sqrt{\lambda_{\max}}\Delta_f\} \subset \mathcal{K}_f(\Delta_f)$ for all $t \in [0, t_f)$ and, in addition

$$|x_f(t)| \leq \alpha_{1f}\exp(-\alpha_{2f}t/\varepsilon)|x_f(0)| + \varepsilon\frac{\lambda_{\max}}{\lambda_{\min}}|P||B_f|b \leq \alpha_{1f}\exp(-\alpha_{2f}t/\varepsilon)|x_f(0)| + \delta. \tag{4.44}$$

Let $\delta_f = \lambda_{\max}/\lambda_{\min}|P||B_f|b$ It is thus possible to replace (4.44) in (4.42):

$$\dot{V}_s \leq -V_s + \bar{\mu}\left[\alpha_{1f}\exp(-\alpha_{2f}t/\varepsilon)|x_f(0)| + \varepsilon\delta_f\right]. \tag{4.45}$$

Let $U := V_s - \bar{\mu}\varepsilon\delta_f$, then it follows that:

$$\dot{U} \leq -U + \bar{\mu}\alpha_{1f}\exp(-\alpha_{2f}t/\varepsilon)|x_f(0)|. \tag{4.46}$$

In the following, let $\varepsilon < \alpha_{2f}$. Simple computations allow to show that (multiply both sides by $\exp(t)$ to yield $d/dt(\mathcal{U}\exp(t))$, then integrate):

$$\begin{aligned} U(t) &\leq U(0)\exp(-t) + \bar{\mu}\alpha_{1f}|x_f(0)|\int_0^t \exp\left(-(t-s) - \alpha_{2f}\frac{s}{\varepsilon}\right) ds \\ &= U(0)\exp(-t) + \bar{\mu}\alpha_{1f}|x_f(0)|\frac{\varepsilon}{\alpha_{2f} - \varepsilon}[\exp(-t) - \exp(-\alpha_{2f}t/(2\varepsilon))] \\ &\leq U(0)\exp(-t) + \bar{\mu}\alpha_{1f}|x_f(0)|\frac{\varepsilon}{\alpha_{2f} - \varepsilon}, \end{aligned} \tag{4.47}$$

for $t \in [0, t_f)$. As a consequence, it follows that:

$$V_s(t) \leq V_s(0)\exp(-t) + \varepsilon\bar{\mu}\left(\delta_f + \frac{\alpha_{1f}|x_f(0)|}{\alpha_{2f} - \varepsilon}\right) = V_s(0)\exp(-t) + \varepsilon\delta_s(\varepsilon). \tag{4.48}$$

Note that $\varepsilon\delta_s(\varepsilon) = 0$ as $\varepsilon = 0$ and is strictly increasing in $[0, \alpha_{2f})$. Recall the bounds (4.41) to yield:

$$\begin{aligned} \sigma(x_s(t)) &\leq \underline{\alpha}^{-1}\left[\overline{\alpha}(\sigma(x_s(0)))\exp(-t) + \varepsilon\delta_s(\varepsilon)\right] \\ &\leq \underline{\alpha}^{-1}\left[2\overline{\alpha}(\sigma(x_s(0)))\exp(-t)\right] + \underline{\alpha}^{-1}\left[2\varepsilon\delta_s(\varepsilon)\right]. \end{aligned} \tag{4.49}$$

The choice $\varepsilon \leq \min\{\varepsilon_f, \varepsilon_s\}$, where ε_s is such that $\varepsilon_s\delta_s(\varepsilon_s) = \eta$ leads to $\sigma(x_s(t)) \leq \underline{\alpha}^{-1}(\overline{\alpha}(x_s(0)) + \eta) < \Omega_s$. In addition, it holds:

$$\sigma(x_s(t)) \leq \underline{\alpha}^{-1}\left[2\overline{\alpha}(\sigma(x_s(0)))\exp(-t)\right] + \delta, \tag{4.50}$$

hence the selection $\beta_s(s,r) = \underline{\alpha}^{-1}[2\overline{\alpha}(s)\exp(-r)] \in \mathcal{KL}$ provides the second bound in (4.30). To conclude the proof, notice that we have shown that all trajectories satisfying $|x_f(0)| \leq \Delta_f$ and $\sigma(x_s(0)) \leq \Delta_s$ are strictly contained, for $t \in [0, t_f)$, in a compact set Ω. Clearly, $(x_f(t_f), x_s(t_f)) \in \mathrm{Int}(\Omega)$ and, by continuity, there exists $T > 0$ such that it is possible to extend the solution to $[0, t_f + T]$. Suppose that $(x_f(t_f + T), x_s(t_f + T)) \notin \Omega$, then there must be a time t', with $t_f < t' < t_f + T$, such that $(x_f(t'), x_s(t')) \in \partial\Omega$. For all $t \in [0, t')$ it is then possible to apply the previous bounds, in particular there exist positive scalars γ_f, γ_s such that $\{x_f : V_f(x_f) \leq \sqrt{\lambda_{\max}}\Delta_f + \gamma_f\} \subset \mathcal{K}_f(\Delta_f)$, $\sigma(x_s(t)) + \gamma_s < \Omega_s$. By continuity, these bounds apply for $t = t'$, hence by contradiction $(x_f(t), x_s(t)) \in \mathrm{Int}(\Omega)$, for all $t \in [0, t_f + T]$. Apply these arguments recursively to prove that the trajectories never leave Ω. See (Sanfelice and Teel, 2011) for similar arguments to extend solutions in the context of singular perturbations for hybrid systems. $\square$

In addition, we show that local exponential stability holds if $D^+\chi = 0$.

Proposition 4.1. *Let the hypotheses of Theorem 4.1 hold and, in addition, let $M = 0$ in Assumption 4.1, then there exists $\varepsilon'' > 0$ such that, for all $0 < \varepsilon < \varepsilon''$, $x_{\mathcal{A}}$ is locally exponentially stable.*

Proof. Note that, with $M = 0$, the fast subsystem becomes:

$$\dot{x}_f = \varepsilon^{-1} A_f x_f - B_f \chi \omega_\eta \eta, \tag{4.51}$$

which in turn implies that $x_{\mathcal{A}}$ is an equilibrium of (4.17) for all $\varepsilon > 0$, since ω_η is vanishing as $(x_f, x_s) \to x_{\mathcal{A}}$. To linearize the reduced order system (4.31), consider $\eta \simeq (1, y_1)$, $y_2 = \tilde{\xi}$, then ($y = (y_1, y_2)$):

$$\dot{y} = \chi \begin{pmatrix} -k_\eta & 1 \\ -\gamma & 0 \end{pmatrix} y. \tag{4.52}$$

Since $\chi \geq \chi_{\min} > 0$, $y = 0$ is exponentially stable, thus local exponential stability is implied for (4.31). Due to the fact that all sufficient conditions of (Khalil, 2002, Theorem 11.4) are satisfied, including twice differentiability of (4.29) in an open neighborhood of $x_{\mathcal{A}}$, then there exists ε'' such that the equilibrium is locally exponentially stable for $0 < \varepsilon < \varepsilon''$. $\square$

Theorem 4.1 and Proposition 4.1 can be combined, in the constant speed context, in order guarantee asymptotic stability from an arbitrarily large set of initial conditions (and local exponential stability), as long as it is ensured that $x_s \in \mathcal{R}_{\mathcal{A}}$ and ε is sufficiently small, that is $0 < \varepsilon < \min\{\varepsilon', \varepsilon''\}$, with ε' from Theorem 4.1 and ε'' from Proposition 4.1.

4.2.5 Sensorless Observer with Unknown Mechanical Model: Domain of Attraction

In the following, a detailed non-conservative characterization of $\mathcal{R}_{\mathcal{A}}$ of Theorem 4.1 is presented, thus providing practical indication of the almost semi-global behavior of the observer. This analysis is focused on the extension of the estimate given by $\hat{\mathcal{R}}_{\mathcal{A}}$ in Lemma 4.1, exploiting a precise analysis of the unstable point $x_{\mathcal{U},s}$, introduced there. Firstly, notice that $\hat{\mathcal{R}}_{\mathcal{A}} = \{x_s : V_0(x_s) < 2\}$ could be made arbitrarily large, along $\tilde{\xi}$, increasing γ, however this is not in general a profitable strategy, because of the decreased robustness due to the need to reduce ε to preserve the time-scale separation. To extend the analysis to points with $V_0 \geq 2$ (i.e. beyond $\hat{\mathcal{R}}_{\mathcal{A}}$), it is necessary to take $x_{\mathcal{U},\mathrm{s}}$ into account, since $V_0(x_{\mathcal{U},\mathrm{s}}) = 2$ and, therefore, points s.t. $V_0 \geq 2$ may not converge to $x_{\mathcal{A},\mathrm{s}}$. Moreover, the shape of the set collecting the points with $V_0 \geq 2$ converging to $x_{\mathcal{A},\mathrm{s}}$ could be dependent on the behavior of χ, while a region of attraction independent of time is requested. The discussion is therefore dedicated first to show that the two sets of points converging to $x_{\mathcal{A},\mathrm{s}}$ and $x_{\mathcal{U},\mathrm{s}}$, respectively, are time-invariant. Then, a characterization of the set of points converging to $x_{\mathcal{U},\mathrm{s}}$, named $\mathcal{R}_{\mathcal{U}}$, is provided. Thus, the largest $\mathcal{R}_{\mathcal{A}}$ for Thm.4.1 is derived as $\{\mathbb{S}^1 \times \mathbb{R}\} \backslash \mathcal{R}_{\mathcal{U}}$.

Note that (4.31) can be factorized as $\dot{x}_\mathrm{s} = f_0(x_\mathrm{s}, \chi) = f_0(x_\mathrm{s}, 1)\chi$, thus highlighting that the vector field is modified by the time-varying signal χ only in its amplitude. This fact suggests to employ a different time coordinate to make the analyzed vector field time-invariant. In particular, choose:

$$t' := \int_0^t \chi(s)ds, \tag{4.53}$$

which yields:

$$\dot{x}_\mathrm{s} = \frac{dx_\mathrm{s}}{dt'}\frac{dt'}{dt} = \frac{dx_\mathrm{s}}{dt'}\chi(t). \tag{4.54}$$

The map between t and t' is bijective, since the assumptions on χ imply its time integral is a strictly increasing function with no finite-escape time: this allows to consider the dynamics $(d/dt')x_\mathrm{s} = f_0(x_\mathrm{s}, 1)$ in order to thoroughly characterize the reduced order dynamics. Hence, several structural properties of the time-varying system are given by the geometric paths of the trajectories. In particular stable/unstable manifolds related to equilibria, their linearization eigenspaces, and the regions of attraction of $x_{\mathcal{A},\mathrm{s}}$ and $x_{\mathcal{U},\mathrm{s}}$ are all time invariant.

With the above result at hand, the analysis of the time-invariant region of attraction of $x_{\mathcal{U},\mathrm{s}}$, $\mathcal{R}_{\mathcal{U}}$, is carried out. We linearize around $x_{\mathcal{U},\mathrm{s}}$ using the t' variable, considering $\eta \simeq (-1, -y_1)$, $y_2 = \tilde{\xi}$ and $y = (y_1, y_2)$:

$$\frac{d}{dt'}y = \begin{pmatrix} k_\eta & 1 \\ \gamma & 0 \end{pmatrix} y, \tag{4.55}$$

therefore the unstable point is, more precisely, a saddle point. Since $x_{\mathcal{U},\mathrm{s}}$ is a hyperbolic equilibrium, owing to the Stable Manifold Theorem and Hartman-Grobman's Theorem (Hartman, 1963), we infer there exists, in a neighborhood of $x_{\mathcal{U},\mathrm{s}}$, a manifold of dimension 1, a separatrix, where trajectories converge to such equilibrium, while all other points belong to orbits escaping from it. Therefore, $\mathcal{R}_{\mathcal{U}}$ close to $x_{\mathcal{U},\mathrm{s}}$ is a line, i.e. the union of two trajectories, tangent to the stable eigenspace of (4.55) in $x_{\mathcal{U},\mathrm{s}}$, and both pointing to it, but opposite in direction. To extend the analysis of $\mathcal{R}_{\mathcal{U}}$ in a semi-global sense, consider the backward (in time t') solutions of (4.31) from the previously obtained manifold. For any level set of the Lyapunov function V_0, we have the guarantee of existence and uniqueness of forward solutions due to the vector field being Lipschitz in that level set. This way, the backward solutions imply that $\mathcal{R}_{\mathcal{U}}$, for any reached arbitrarily large level set of V_0, remains a manifold of dimension 1, i.e. a line given by the union of the backward extensions of the two aforementioned trajectories.

To further investigate the shape of line $\mathcal{R}_{\mathcal{U}}$, the (not globally invertible) change of coordinates $\tilde{\vartheta} = \mathrm{atan2}(\eta_2, \eta_1)$ is used to represent the vector field of (4.31) in $\mathbb{R}^2$

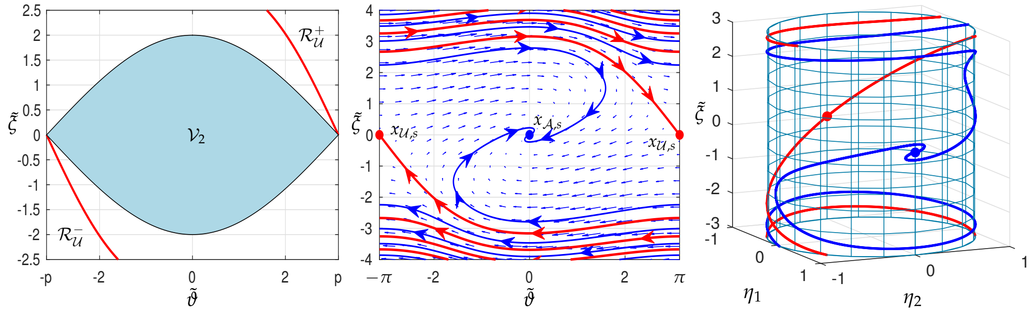

FIGURE 4.1: Representation of the domain of attraction of system (4.31), along with some meaningful sets and trajectories.

(in t and t'):

$$\begin{aligned} \dot{\tilde{\vartheta}} &= \chi(\tilde{\xi} - k_\eta \sin\tilde{\vartheta}) & \dot{\tilde{\xi}} &= -\chi\gamma\sin\tilde{\vartheta} \\ \frac{d}{dt'}\tilde{\vartheta} &= \tilde{\xi} - k_\eta \sin\tilde{\vartheta} & \frac{d}{dt'}\tilde{\xi} &= -\gamma\sin\tilde{\vartheta}. \end{aligned} \tag{4.56}$$

To clarify the following arguments, Figure 4.1 presents a numerical representation of the domain of attraction and some sample trajectories (blue lines) converging to $x_{\mathcal{A},s}$ (blue dot), for $\chi = 1$, $k_\eta = 1.5$, $\gamma = 1$. In the first and second images, the phase plane and portrait of (4.56) are reported (wrapped for $\tilde{\vartheta}$ within the interval $[-\pi;\pi)$), while the equivalent representation in cylindrical coordinates for (4.31) is depicted in the third image. In the left picture, $\mathcal{R}_{\mathcal{U}}$ (red line) close to $x_{\mathcal{U},s}$ (red dot) is reported and can be easily seen as the union of the two trajectories $\mathcal{R}_{\mathcal{U}}^+$, for $\tilde{\xi} \geq 0$, and $\mathcal{R}_{\mathcal{U}}^-$, for $\tilde{\xi} \leq 0$. In addition, the curve $V_0 = 2$ is depicted and the set $\mathcal{V}_2 = \{(\tilde{\vartheta}, \tilde{\xi}) \,|\, V_0 \leq 2\}$ can be easily identified. It is worth noting that the stable eigenspace of the linearization of (4.56) at $x_{\mathcal{U},s}$ is given by the span of $(1, -(k_\eta + \sqrt{k_\eta^2 + 4\gamma})/2)$, therefore $\mathcal{R}_{\mathcal{U}} \cap \mathcal{V}_2 = x_{\mathcal{U},s}$ and there will be a portion of $\mathcal{R}_{\mathcal{U}}$ close to $x_{\mathcal{U},s}$ where $V_0 > 2 + \delta$, with a sufficiently small $\delta > 0$. Moreover, according to Lemma 4.1, the set $\mathcal{V}_2$ is forward invariant, then the two sets $\mathcal{U}_2^+ = \overline{((\mathbb{S}^1 \times \mathbb{R}) \backslash \mathcal{V}_2) \cap \{\tilde{\xi} \geq 0\}}$ and $\mathcal{U}_2^- = \overline{((\mathbb{S}^1 \times \mathbb{R}) \backslash \mathcal{V}_2) \cap \{\tilde{\xi} \leq 0\}}$ are both backward invariant. Therefore, the two trajectories $\mathcal{R}_{\mathcal{U}}^+$ and $\mathcal{R}_{\mathcal{U}}^-$ will lie in $\mathcal{U}_2^+$ and $\mathcal{U}_2^-$, respectively. Bearing in mind such considerations, the unboundedness of $\mathcal{R}_{\mathcal{U}}$ can be inferred by contradiction. Focusing on $\mathcal{R}_{\mathcal{U}}^+$, in $\mathcal{U}_2^+$, assuming its boundedness implies that there exists a large enough $c > 0$ such that, defining $\mathcal{V}_c = \{(\tilde{\vartheta}, \tilde{\xi}) \,|\, V_0 \leq c\}$, the orbit $\mathcal{R}_{\mathcal{U}}^+$ is inside the compact set $\mathcal{U}_2^+ \cap \mathcal{V}_c$. Then, by Poincaré-Bendixson Theorem, $\mathcal{R}_{\mathcal{U}}^+$ is either an heteroclinic or homoclinic orbit, or it has an α-limit set given by a fixed point or a limit cycle. According to Lemma 4.1, no fixed point or limit cycle can be present in $\mathcal{U}_2^+$. In addition, $\mathcal{R}_{\mathcal{U}}^+$ cannot be an heteroclinic orbit because the only other fixed point in $\mathbb{S}^1 \times \mathbb{R}$ is $x_{\mathcal{A},s}$, in the interior of $\mathcal{V}_2$, where the orbit $\mathcal{R}_{\mathcal{U}}^+$ cannot enter. Moreover, it cannot be a homoclinic orbit since otherwise, according to the fact that $V_0 > 2 + \delta$ in a portion of $\mathcal{R}_{\mathcal{U}}^+$, the condition $\dot{V}_0 \leq 0$, derived in the proof of Lemma 4.1, would be violated. Then, the $\mathcal{R}_{\mathcal{U}}^+$ cannot be fully contained in any set $\mathcal{U}_2^+ \cap \mathcal{V}_c$ with arbitrary large $c > 0$. According to the above results, focusing on backward behavior, we can conclude that $\mathcal{R}_{\mathcal{U}}^+$ will leave any arbitrary large $\mathcal{V}_c$ exiting from its border just once, again thanks to the forward invariance of $\mathcal{V}_c$. The same arguments can be replicated for $\mathcal{R}_{\mathcal{U}}^-$, in $\mathcal{U}_2^-$. Therefore, recalling that, according to Lemma 4.1, $\mathcal{R}_{\mathcal{A}} = (\mathbb{S}^1 \times \mathbb{R}) \backslash \mathcal{R}_{\mathcal{U}}$, it can be easily seen, that for any arbitrarily large $c > 0$, all of the points of $\partial\mathcal{V}_c$, except two, will belong to $\mathcal{R}_{\mathcal{A}}$. This implies that $\mathcal{R}_{\mathcal{A}}$ is unbounded. Due to the above considerations the results of Thm.4.1 can be extended almost semi-globally, i.e. considering an arbitrarily large domain excluding an ever thinner stripe around $\mathcal{R}_{\mathcal{U}}$.

Finally, it is worth noting that, for a sufficiently large $|\tilde{\xi}|$, $\mathcal{R}_{\mathcal{U}}^{+}$ and $\mathcal{R}_{\mathcal{U}}^{-}$ "wrap around" with no sign change in $\dot{\tilde{\vartheta}}$. This can be easily inferred by (4.56) for any trajectory, when $|\tilde{\xi}| > |k_\eta|$. Moreover, the larger $|\tilde{\xi}|$ is, the closer the trajectory turns are, as depicted the central picture in Figure 4.1. Nevertheless, thanks to the previous results, it is guaranteed that the distance between the turns of $\mathcal{R}_{\mathcal{U}}^{+}$ and $\mathcal{R}_{\mathcal{U}}^{-}$ can tend to zero only when $|\tilde{\xi}| \to \infty$.

4.3 Advanced UAV Electric Propulsion

Electrically powered Unmanned Aerial Vehicles are becoming in the recent years an ever-growing source of interest for civil, military and industrial applications (Cox et al., 2004). On this topic, several works from different communities can be found (Valavanis, 2008), and a significant effort has been dedicated to improve the related technology, control accuracy, and effectiveness in numerous demanding scenarios. A crucial UAV design issue is flight endurance, which is typically assessed in the literature at the flight control level, e.g., considering trajectory optimization to minimize energy losses (Morbidi, Cano, and Lara, 2016). Alternative power sources, on purpose design (Driessens and Pounds, 2015), and energy harvesting systems (Sowah et al., 2017) have also been explored to enhance this feature. However, not only flight endurance but also tracking performance are critically affected by the propeller drives, since maneuvering is achieved by regulating the propeller speed/thrust (Pounds, Mahony, and Corke, 2007).

The typical driving technique for the considered UAV motors is sensorless Brushless DC (BLDC) control, which is very popular nowadays because of its parameter-free implementation and relatively simple position/speed reconstruction algorithms (for further details see (Acarnley and Watson, 2006) and references therein). Clearly, sensorless BLDC control is adequate if the motor back-EMF displays a trapezoidal shape, but it is sub-optimal in efficiency and accuracy whenever applied PMSMs. On the other hand, the optimal control technique for PMSMs, known as Field-Oriented Control (FOC), requires in general accurate knowledge of parameters and states, but theoretically allows to drive the motors at the highest torque-per-current ratio and lowest torque distortion. We refer to (Bosso, Conficoni, and Tilli, 2016; Bosso et al., 2020) for a thorough power losses comparison between BLDC control and FOC.

Relative to this UAV propeller control application, we present both simulation and experimental results. Firstly, some simple open-loop simulations are shown to further verify the stability properties that we proved before, and in particular some aggressive speed trajectories are used to test the algorithm in conditions which cannot be assimilated to the typical slowly-varying scenarios. Then, motivated by its promising theoretical properties, we show how the proposed sensorless observer can lead to a simple high-performance sensorless controller for UAV propellers. Such controller, first proposed in (Bosso et al., 2020), is sufficiently simple and easy to tune to make it an effective solution for several high-performance UAV applications, as demonstrated in the experimental validation tests. Because of the evident practical interest in showing the implementation details, we also include the quantitative arguments leading to the tuning procedure, based on the linearization of the dynamics about the operation points expected for adequate thrust generation.

TABLE 4.1: Simulation PMSM parameters

Stator resistance R $[\Omega]$	0.06	Stator inductance L $[\mu\text{H}]$	33.75
Nominal angular speed [rpm]	6000	Rotor magnetic flux φ [mWb]	1.9
Number of pole pairs p	7	Nominal RMS current [A]	20
Motor inertia J [Kgm^2]	2.5×10^{-6}		

4.3.1 Open Loop Simulation of the Observer

Firstly, we present some simulation tests that were specifically carried out to highlight the observer features. For this purpose, the results are shown without the observer in the control loop: instead, a standard sensored field-oriented controller with nested PIs is employed in order to yield the desired motor speed profile. To verify the stability and robustness properties, we impose in particular an aggressive amplitude-modulated sinusoid. In the next subsections, we will also present experimental results that validate the effectiveness of the proposed solution in realistic closed-loop scenario.

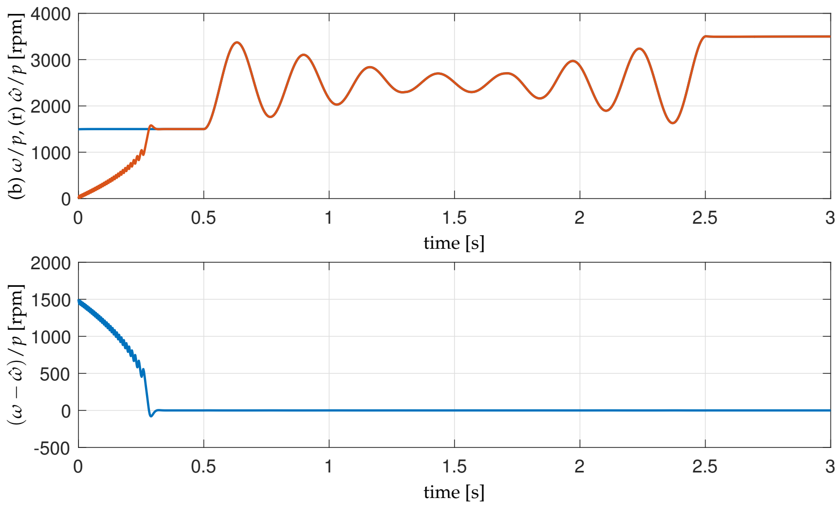

FIGURE 4.2: Speed estimation performance of the proposed sensorless observer.

The main simulation parameters are reported in Table 4.1, while the observer gains have been chosen imposing ε with (4.18) and considering the linearized reduced slow system in (4.52), in order to ensure the required time-scale separation. As a result, the following parameters have been set: $k_\text{p} = 2.18 \times 10^4$, $k_\text{i} = 9.34 \times 10^3$ ($\varepsilon = 85 \times 10^{-6}$) $\gamma = 4582$, $k_\eta = 95.7$ (corresponding to eigenvalues in $-(5/3)(1 \pm \text{i}) \times 10^2$ for the linearized system (4.52) with χ set according to nominal flux and mid-range speed for simulation, that is 2500rpm). For implementation convenience, a structure similar to (4.56) has been used, i.e. recovering the magnetization angle information as $\hat{\vartheta} = |\hat{h}|\hat{\xi} + k_\eta \hat{h}_1$ (cf. (4.16)), with an opportune wrap operation to contain $\hat{\vartheta}$ in the interval $[-\pi; \pi)$. The observer states have been initialized to zero, assuming no a-priori knowledge about the machine.

Figures 4.2-4.3-4.4 present the results obtained under the considered working scenario. In Figure 4.2 we show the speed profiles, while in Figures 4.3-4.4 the behavior of the main components of x_s and x_f is indicated, respectively. We omit the current prediction error waveforms for brevity. From the plot of $\hat{\omega}$ it can be noted how, after a transient where the effects of the angular "wraps" are clearly visible,

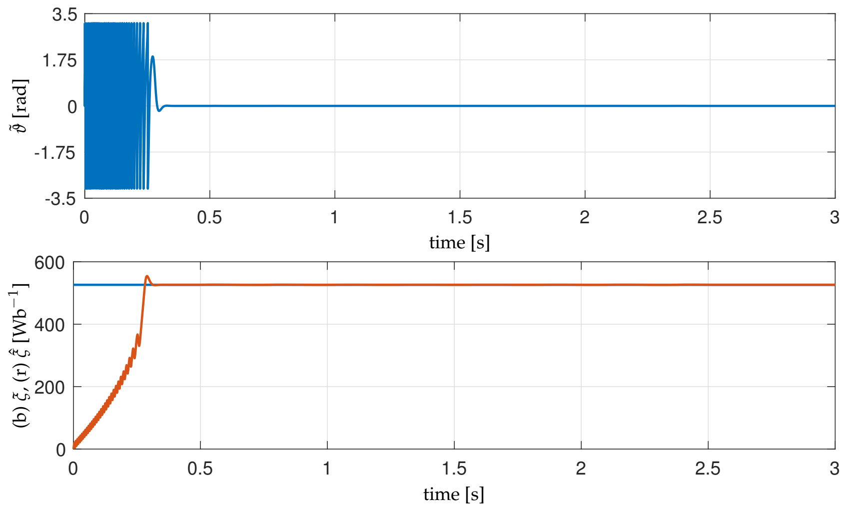

FIGURE 4.3: Position and rotor flux amplitude estimation performance of the proposed sensorless observer.

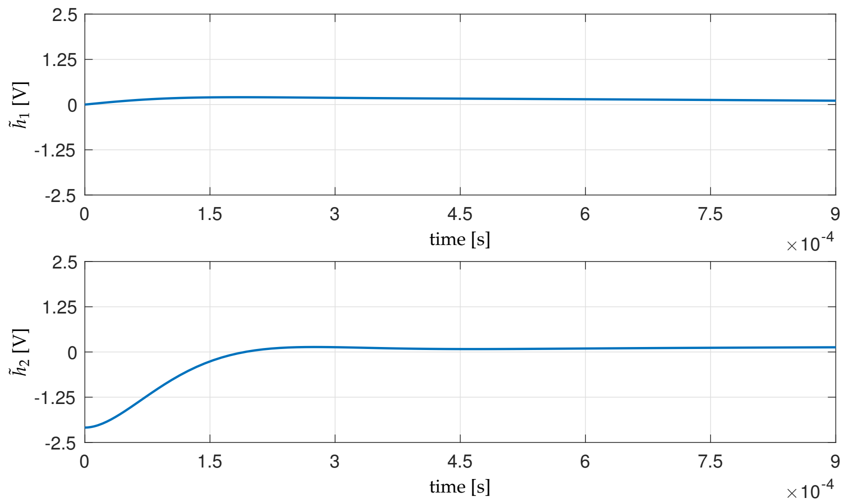

FIGURE 4.4: Back-EMF estimation performance of the proposed sensorless observer.

the speed estimate closely tracks the true signal, confirming the capability of the reconstruction scheme to deal with time-varying speed profiles, with no information about the system mechanical model. Alignment with the magnetization vector is ensured and kept throughout the test, as portrayed in Figure 4.3. Finally, Figure 4.4 highlights, with a proper choice of the time scale, how the estimate $\hat{h}$ is promptly steered towards the true back-EMF components, due to the robustness properties guaranteed by gains k_{p}, k_{i}. Note the residual error is caused by f_h (recall (4.30)), which cannot vanish if $D^+\omega \neq 0$, as is the case during most of the simulation (in the depicted time window, f_h is non-zero also because of large $\sigma(x_{\mathrm{s}})$ values).

4.3.2 A Computational-Effective Nested Speed Controller

We can finally introduce a computational-effective sensorless FOC strategy, based on the observer (4.16) and a nested stabilizer for current tracking and reference torque generation. The goal is to develop an output-feedback controller that regulates the rotor mechanical speed, $\omega/p =: \omega_{\mathrm{m}}$, to a reference ω_{m}^*, available for control design

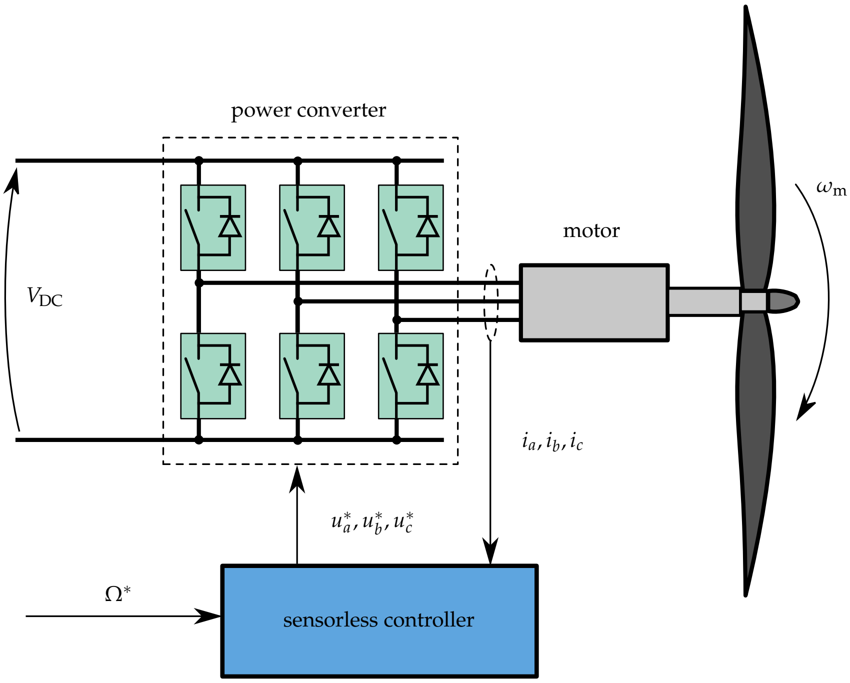

FIGURE 4.5: UAV actuator scheme for sensorless FOC.

along with its derivative $\dot{\omega}_{\mathrm{m}}^*$. In general, ω_{m}^*, $\dot{\omega}_{\mathrm{m}}^*$ may be generated by an opportune trajectory planner, processing a generic speed set-point Ω^*. In the present work, we considered a simple low-pass filter for trajectory planning, but such structure could be replaced with a more advanced scheme to include, e.g., constraint handling features.

Let i^*, p^* be a current reference and its derivative, respectively, then consider the estimated current mismatch $e = \hat{\imath} - i^*$. We can assign the input voltages in the estimated reference frame as follows:

$$\begin{aligned} u_{\hat{\chi}} &= -\hat{h} + L\left(\hat{\omega}_\chi \mathcal{J} i_{\hat{\chi}} + p^* - k_{\mathrm{p}e} e\right) + \sigma + R i^* \\ \dot{\sigma} &= -k_{\mathrm{i}e} e, \end{aligned} \tag{4.57}$$

with $k_{\mathrm{p}e}$, $k_{\mathrm{i}e}$ positive gains for tuning. The remaining design step involves torque reference generation, as well as the conversion of such reference into i^*, p^*. For, let

$$\hat{\varpi} = \frac{\hat{\xi}|\hat{h}|}{p} = \frac{\hat{\omega}}{p}, \quad \tilde{\omega}_{\mathrm{m}} = \hat{\varpi} - \omega_{\mathrm{m}}^*, \quad i^* = \begin{pmatrix} 0 \\ i_{\mathrm{q}}^* \end{pmatrix}, \quad p^* = \begin{pmatrix} 0 \\ p_{\mathrm{q}}^* \end{pmatrix}, \tag{4.58}$$

and consider the following PI controller:

$$\begin{aligned} T_{\mathrm{el}}^* &= -k_{\mathrm{p}\omega} \tilde{\omega}_{\mathrm{m}} + \sigma_\omega & i_{\mathrm{q}}^* &= \frac{2}{3p} \hat{\xi} T_{\mathrm{el}}^* \\ \dot{\sigma}_\omega &= -k_{\mathrm{i}\omega} \tilde{\omega}_{\mathrm{m}} & p_{\mathrm{q}}^* &= \frac{2}{3p}\left[\gamma \hat{h}_1 T_{\mathrm{el}}^* + \hat{\xi}\left(-k_{\mathrm{p}\omega}\dot{\hat{\varpi}} + k_{\mathrm{p}\omega}\dot{\omega}_{\mathrm{m}}^* - k_{\mathrm{i}\omega}\tilde{\omega}_{\mathrm{m}}\right)\right], \end{aligned} \tag{4.59}$$

with $k_{\mathrm{p}\omega}$ and $k_{\mathrm{i}\omega}$ positive scalars. We remark that we chose to represent estimated mechanical speed as $\hat{\varpi}$, that does not include the term $k_\eta \hat{h}_1$, in order to reduce sensitivity to measurement noise. Note that additional feedforward terms could be added in T_{el}^*, to account for the load or the reference derivative $\dot{\omega}_{\mathrm{m}}^*$: this clearly would come at the expense of an increased computational burden due to the inclusion of an opportune adaptation strategy. For simplicity, this direction is not explored here and left for future research activities. Finally, we recall the transformations involved in the conversion of signals from three-phase to rotating two-phase representations and vice-versa:

$$i_{\hat{\chi}} = \mathcal{C}^T[\hat{\zeta}_\chi] i_s = \mathcal{C}^T[\hat{\zeta}_\chi] \begin{pmatrix} i_\alpha \\ i_\beta \end{pmatrix}, \qquad u_{\hat{\chi}} = \mathcal{C}^T[\hat{\zeta}_\chi] u_s = \mathcal{C}^T[\hat{\zeta}_\chi] \begin{pmatrix} u_\alpha \\ u_\beta \end{pmatrix},$$
$$\begin{pmatrix} i_\alpha \\ i_\beta \end{pmatrix} = \frac{2}{3} \begin{pmatrix} 1 & -0.5 & -0.5 \\ 0 & \sqrt{3}/2 & -\sqrt{3}/2 \end{pmatrix} \begin{pmatrix} i_a \\ i_b \\ i_c \end{pmatrix}, \qquad \begin{pmatrix} u_a^* \\ u_b^* \\ u_c^* \end{pmatrix} = \begin{pmatrix} 1 & 0 \\ -0.5 & \sqrt{3}/2 \\ -0.5 & -\sqrt{3}/2 \end{pmatrix} \begin{pmatrix} u_\alpha \\ u_\beta \end{pmatrix}. \tag{4.60}$$

The typical structure of a UAV actuator, including the power converter and the controller, is summarized in Figure 4.5.

4.3.3 Error System Analysis and Tuning

In addition to the above structure, we provide some considerations to appropriately tune the controller, based on the simplifying assumption that $\dot{\omega}_{\mathrm{m}}^* = 0$. These arguments rely on the linearization of the error system and allow to draw a simple local stability analysis, with related formal guarantees when $\dot{\omega}_{\mathrm{m}}^* \neq 0$. For analysis, we include a generic propeller mechanical model, approximated for simplicity up to the quadratic dependence on the motor speed:

$$J\dot{\omega}_{\mathrm{m}} = -\frac{3}{2}\frac{p}{\xi}\eta^T \mathcal{J} i_{\hat{\chi}} - c_1\omega_{\mathrm{m}} - c_2|\omega_{\mathrm{m}}|\omega_{\mathrm{m}}, \tag{4.61}$$

where J is the total motor and load inertia, while c_1 and c_2 are positive load coefficients, including both the motor friction and the propeller aerodynamic torque. Note that a typical expression for c_2 is given by

$$c_2 = C_{\mathrm{M}} \frac{\rho D_{\mathrm{p}}^5}{4\pi^2}, \tag{4.62}$$

with C_{M} the propeller torque coefficient, D_{p} the propeller diameter and ρ the local air density.

We proceed by defining the error equations. Firstly, recall the current estimation error dynamics:

$$\dot{\tilde{\imath}} = -\left(\frac{R}{L} + k_{\mathrm{p}}\right)\tilde{\imath} + \frac{\tilde{h}}{L}, \qquad \dot{\tilde{h}} = -k_{\mathrm{i}}\tilde{\imath} + \dot{h}, \tag{4.63}$$

and the attitude observer reconstruction error, based on the $\mathbb{R}^2$ representation of the cylinder dynamics (we employ this model since we are interested in the linearization about the origin):

$$\dot{\tilde{\vartheta}} = \chi(\tilde{\xi} - k_\eta \sin(\tilde{\vartheta})) + \delta_1, \qquad \dot{\tilde{\xi}} = -\gamma\chi\sin(\tilde{\vartheta}) + \delta_2, \tag{4.64}$$

where both δ_1 and δ_2 vanish in $\tilde{h} = 0$. Here, we include the dynamics of the estimated current mismatch dynamics and of the speed tracking error, highlighting the shape of $\dot{h}$ in (4.63). Note that we can take the ordinary derivative of h instead of a generalized derivative due to the regularity of the mechanical model (4.61). From the definition of the stabilizer in (4.57), it follows:

$$\dot{e} = -\left(\frac{R}{L} + k_{\mathrm{pe}}\right) e + \frac{\sigma}{L} + k_{\mathrm{p}}\tilde{\imath}, \qquad \dot{\sigma} = -k_{\mathrm{ie}} e. \tag{4.65}$$

On the other hand, to compute the speed dynamics, we first factorize by Taylor expansion the speed estimation error, for $\omega > 0$ and $\tilde{h}$ sufficiently small:

$$\begin{aligned} p(\hat{\omega} - \omega_{\mathrm{m}}) &= \hat{\xi}|\hat{h}| - \xi|h| = (\xi - \tilde{\xi})|h - \tilde{h}| - \xi|h| \\ &= -p\frac{\tilde{\xi}}{\xi}\omega_{\mathrm{m}} + (\tilde{\xi} - \xi)\delta_3(h, \tilde{h}) \end{aligned} \tag{4.66}$$

where δ_3 vanishes in $\tilde{h} = 0$. Denote with $e_\omega = \omega_{\mathrm{m}} - \omega_{\mathrm{m}}^*$ the tracking error, then it holds ($\tilde{\omega}_{\mathrm{m}} = e_\omega + \hat{\omega} - \omega_{\mathrm{m}}$, $\dot{\omega}_{\mathrm{m}}^* = 0$):

$$\begin{aligned} J\dot{e}_\omega &= \frac{3p}{2\xi}\left[\cos(\tilde{\vartheta})i_{\mathrm{q}}^* + (\tilde{\imath}_2 + e_2)\cos(\tilde{\vartheta}) - (\tilde{\imath}_1 + e_1)\sin(\tilde{\vartheta})\right] - c_1(\omega_{\mathrm{m}}^* + e_\omega) - c_2(\omega_{\mathrm{m}}^* + e_\omega)^2 \\ &= \frac{\xi - \tilde{\xi}}{\xi}\cos(\tilde{\vartheta})\left[\sigma_\omega - k_{\mathrm{p}\omega}e_\omega + k_{\mathrm{p}\omega}\frac{\tilde{\xi}}{\xi}(\omega_{\mathrm{m}}^* + e_\omega)\right] - d_0 - d_1 e_\omega - c_2 e_\omega^2 + \\ &\quad + \frac{3p}{2\xi}(\tilde{\imath}_2 + e_2)\cos(\tilde{\vartheta}) - \frac{3p}{2\xi}(\tilde{\imath}_1 + e_1) + \delta_4(\xi, \tilde{\xi}, \tilde{\vartheta}, h, \tilde{h}), \end{aligned} \tag{4.67}$$

where d_0, d_1 are positive scalars and δ_4 is a map that vanishes in $\tilde{h} = 0$. Consider $\tilde{\sigma}_\omega = \sigma_\omega - d_0$, with associated dynamics:

$$\dot{\tilde{\sigma}}_\omega = -k_{\mathrm{i}\omega}e_\omega + k_{\mathrm{i}\omega}\frac{\tilde{\xi}}{\xi}(\omega_{\mathrm{m}}^* + e_\omega) + \delta_5(\xi, \tilde{\xi}, h, \tilde{h}), \tag{4.68}$$

with δ_5 vanishing in $\tilde{h} = 0$. Since $\chi = |h| = (p/\xi)(\omega_{\mathrm{m}}^* + e_\omega)$, we have

$$\dot{h} = \frac{p}{\xi}\dot{e}_\omega \begin{pmatrix} \sin(\tilde{\vartheta}) \\ -\cos(\tilde{\vartheta}) \end{pmatrix} + \frac{p}{\xi}(\omega_{\mathrm{m}}^* + e_\omega)\begin{pmatrix} \cos(\tilde{\vartheta}) \\ \sin(\tilde{\vartheta}) \end{pmatrix}(\omega - \hat{\omega}_\chi), \tag{4.69}$$

where in particular the second term vanishes in $\tilde{h} = 0$, $\tilde{\vartheta} = 0$, $\tilde{\xi} = 0$. This means that the error system (4.63)-(4.64)-(4.65)-(4.67)-(4.68) has an equilibrium in the origin, whose local stability analysis can be performed by means of the usual two time-scales arguments, writing the overall error system as an extended form of the structure (4.29). In particular, we impose the current dynamics (4.63)-(4.65) to be the fast subsystem, while we leave the attitude estimation error (4.64) and the speed tracking dynamics (4.67)-(4.68) as the slow subsystem. Following the same arguments as before, we select k_{p}, k_{i} by placing the roots of the polynomial

$$P_1(\lambda) = \lambda^2 + \left(\frac{R}{L} + k_{\mathrm{p}}\right)\lambda + \frac{k_{\mathrm{i}}}{L} \tag{4.70}$$

in $\varepsilon^{-1}\{\lambda_1, \lambda_2\}$, where the pair $\{\lambda_1, \lambda_2\}$ is a design choice and ε is a positive scalar. System (4.65) is cascade-interconnected to the previous one, hence we similarly choose k_{pe}, k_{ie} to place the roots of the polynomial

$$P_2(\lambda) = \lambda^2 + \left(\frac{R}{L} + k_{\mathrm{pe}}\right)\lambda + \frac{k_{\mathrm{ie}}}{L} \tag{4.71}$$

TABLE 4.2: T-Motor-Antigravity-4006-KV380 parameters

Stator resistance R [mΩ]	108	Stator inductance L [μH]	30.6
Number of pole pairs p	12	Rotor magnetic flux φ [mWb]	1.3

in $\varepsilon^{-1}\{\lambda_{1e}, \lambda_{2e}\}$. The boundary layer model can be then shown to be globally exponentially stable, with dynamics completely defined by the eigenvalues λ_1, λ_2, λ_{1e}, λ_{2e}.

The reduced-order model, which corresponds to the slow subsystem as $\tilde{\imath} = \tilde{h} = e = \sigma = 0$, is analyzed by linearization of the dynamics. The attitude estimation error corresponds to:

$$\dot{y} = \frac{p\omega_{\mathrm{m}}^*}{\xi} \begin{pmatrix} -k_\eta & 1 \\ -\gamma & 0 \end{pmatrix} y, \tag{4.72}$$

whose eigenvalues can be assigned as usual with k_η, γ, exploiting a priori flux information and the range of speed references for flight control. On the other hand, the linearization of the speed tracking error is given by:

$$\dot{z} = \begin{pmatrix} -\frac{k_{\mathrm{p}\omega}+d_1}{J} & \frac{1}{J} \\ -k_{\mathrm{i}\omega} & 0 \end{pmatrix} z + \frac{1}{\xi} \begin{pmatrix} \frac{k_{\mathrm{p}\omega}\omega_{\mathrm{m}}^* - d_0}{J} \\ k_{\mathrm{i}\omega}\omega_{\mathrm{m}}^* \end{pmatrix} \begin{pmatrix} 0 & 1 \end{pmatrix} y, \tag{4.73}$$

which is cascade-interconnected with (4.72), hence $k_{\mathrm{p}\omega}$, $k_{\mathrm{i}\omega}$ can be chosen independently from k_η, γ. With all these elements in place, we can finally summarize the local stability properties of the proposed controller.

Proposition 4.2. *Consider a constant reference ω_{m}^*, satisfying $0 < \underline{\Omega} \le \omega_{\mathrm{m}}^* \le \overline{\Omega}$, with positive scalars $\underline{\Omega}$, $\overline{\Omega}$. Pick, and fix, positive constants k_η, γ, $k_{\mathrm{p}\omega}$, $k_{\mathrm{i}\omega}$, and choose λ_1, λ_2, λ_{1e}, λ_{2e} such that the polynomials $P_1(\cdot)$ and $P_2(\cdot)$ are Hurwitz, for any $\varepsilon > 0$. Then, there exists $\varepsilon^* > 0$ such that, for all $0 < \varepsilon < \varepsilon^*$, the origin of the error system* (4.63)-(4.64)-(4.65)-(4.67)-(4.68) *is locally exponentially stable.*

Proof. The analysis is similar to Proposition 4.1. In particular, the boundary layer system is globally exponentially stable by design of $\lambda_1, \lambda_2, \lambda_{1e}, \lambda_{2e}$, while the reduced-order model is locally exponentially stable. Furthermore, the vector field and its partial derivatives, up to second order, are bounded in a neighborhood of the origin, since $\omega_{\mathrm{m}}^* \neq 0$ and thus $|\hat{h}|$ is twice differentiable in its arguments. It is then sufficient to notice that the origin of the error system is an isolated equilibrium, for any bounded $\varepsilon > 0$, to guarantee that all sufficient conditions of (Khalil, 2002, Theorem 11.4) hold. □

The practical relevance of this result is due to the inherent robustness to small perturbations (such as small values of $\dot{\omega}_{\mathrm{m}}^*$) ensured by the theorem of total stability (Isidori, 2012, Theorem 10.2.1). Notably, we can re-define the error of the speed integrator as $\tilde{\sigma}_\omega = \sigma_\omega - d_0 - J\dot{\omega}_{\mathrm{m}}^*$, thus indicating that weaker singular perturbations results (Khalil, 2002, Theorems 11.1-11.2), can be applied in time intervals such that $\underline{\Omega} \le \omega_{\mathrm{m}}^* \le \overline{\Omega}$ and $\ddot{\omega}_{\mathrm{m}}^*$ is continuous. This means that the proposed controller is also effective in time-varying scenarios, as long as $\varepsilon > 0$ is sufficiently small.

4.3.4 The Experimental Setup

In order to test the presented controller, we developed an experimental setup which is reported in Figure 4.6. The main components of the equipment are the following:

an Aim-TTi CPX400DP bench power supply, a LeCroy HDO4054 four-channel oscilloscope and an aluminum frame to suspend a T-Motor Antigravity-4006-KV380 (whose experimentally identified parameters are reported in Table 4.2), coupled with a T-Motor CFProp 13×4.4 L Propeller. In addition, we equipped the motor structure with a 14bit-resolution on-axis magnetic rotary encoder (AD5047D-EK-AB encoder evaluation kit and AS5000-MD6H-2 diametric magnet), in order to compare the sensorless control algorithms with a common speed-position information source (clearly, the encoder was only employed for analysis and not for feedback). For what concerns the electronic board for actuation and control implementation,

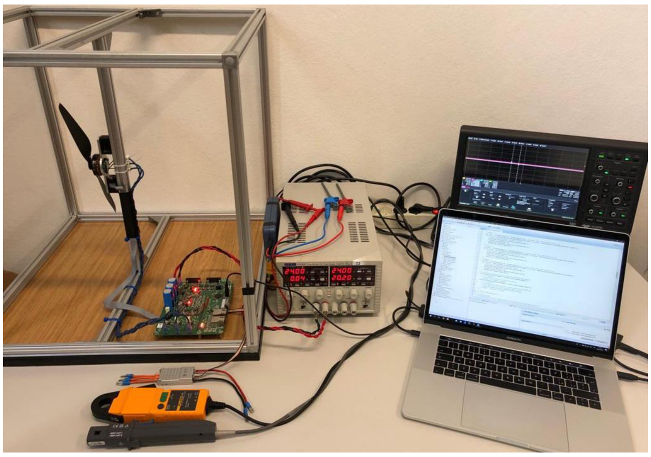

FIGURE 4.6: UAV propeller experimental setup.

we employed a custom power converter endowed with a Mosfet-Voltage Source Inverter and a Cortex-M4 digital controller. In particular, the MCU was operated with a custom-developed lightweight Hard Real-Time Operating System that was synchronized with the inverter PWM carrier. This board was used to host, apart from the main control algorithms, also a position/speed acquisition routine to elaborate the encoder data for analysis. It is worth noting that a filter (whose details are omitted for brevity) was introduced to improve the encoder speed/position readings.

The controller was converted into its discrete-time equivalent with forward Euler discretization, except for the current observer dynamics, that was obtained through matrix exponential. In addition, a state-variable filter was introduced to approximate $\dot{\hat{\omega}}$ in (4.59), instead of computing the required generalized derivative. Finally, we highlight that the algorithm was implemented in fixed-point C code by means of automatic code generation from Matlab/Simulink (see Bosso, 2016 for further details on this topic).

4.3.5 Closed Loop Experimental Results

For the validation of the presented control solution, we considered both filtered step signals and an aggressive amplitude-modulated sinusoid. The controller gains, obtained via the aforementioned arguments, are reported in Table 4.3. The perturbation parameter employed for time-scale separation was chosen as $\varepsilon = 1.5L/R = 4.24 \times 10^{-4}$, which proved effective in all the speed operating range. For the experimental validation of the proposed sensorless controller we consider, as reference trajectories, both some filtered step signals and an aggressive amplitude-modulated sinusoid. As we can appreciate in Figures 4.7-4.8, the encoder speed reconstruction

TABLE 4.3: Tuning Parameters of the Proposed Controller

k_{p}	1178	k_{i}	340	$k_{\mathrm{p}e}$	964	$k_{\mathrm{i}e}$	154.6
k_η	115.8	γ	6707	$k_{\mathrm{p}\omega}$	7.1×10^{-3}	$k_{\mathrm{i}\omega}$	41.7×10^{-3}

is particularly close to the observer estimate, up to noise and distortions due to filtering. Clearly, it is possible to appreciate a non-zero tracking error when the angular

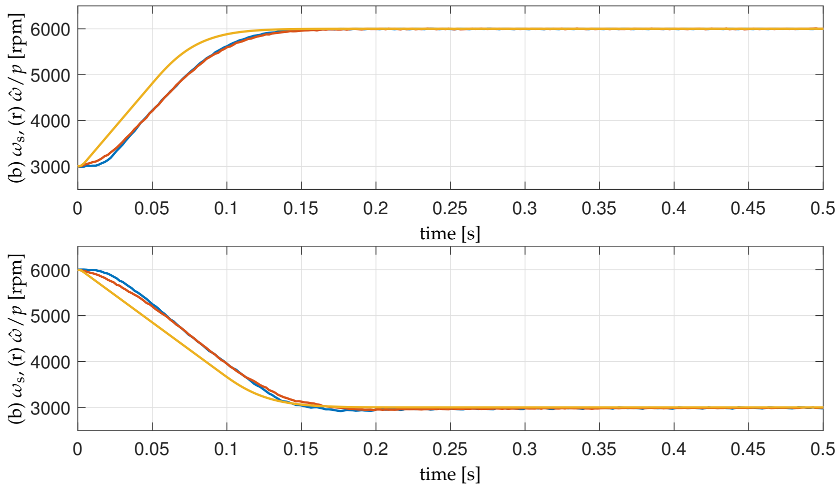

FIGURE 4.7: Sensorless controller response to some benchmark reference signals (yellow).

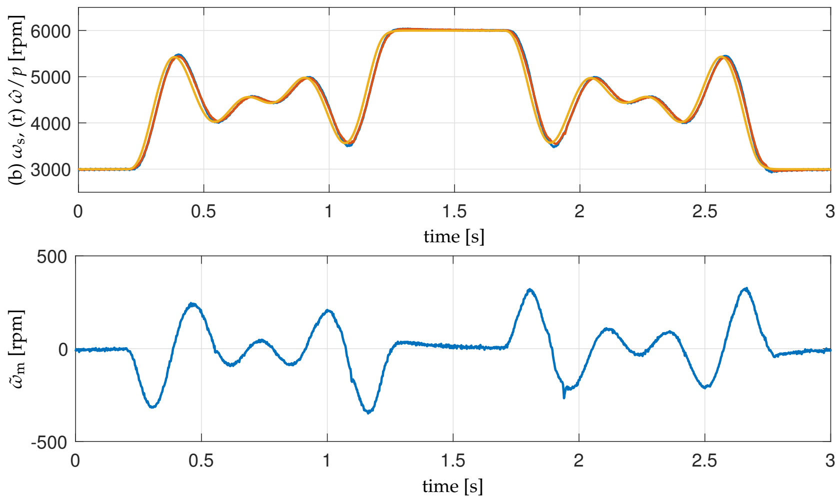

FIGURE 4.8: Sensorless controller response to an aggressive sinusoidal reference (yellow).

acceleration request is non-zero: as expected from the previous arguments, the controller is still capable to ensure boundedness of trajectories about the origin of the error system.

4.4 Advanced Topics

We conclude this chapter with two interesting extensions of the aforementioned baseline strategy, based on the works (Bosso, Tilli, and Conficoni, 2020; Bosso, Azzollini, and Tilli, 2020). In particular, we want to address two particularly important questions that arise: namely, how to address robustness with respect to an uncertain stator resistance, and how to make the stability properties semiglobal, thus removing the undesirable unstable manifold $\mathcal{R}_{\mathcal{U}}$. Even though these two topics are presented separately for simplicity, they could be naturally combined because of the modular nature of our observer. In fact, for the two cases, a stator resistance adaptation in the fast subsystem and a hybrid correction mechanism in the slow subsystem are introduced, respectively.

4.4.1 A Controller-Observer for Robust Resistance Estimation

In this subsection, we present a modification of the current high-gain observer, including in particular an adaptation strategy to provide appropriate estimate/compensation of the unknown stator resistance. Notably, to enforce observability of this additional unknown parameter, a non-permanently zero speed working scenario is not anymore sufficient. Indeed, it is known from the literature (see e.g. the observability analysis in Bernard and Praly, 2019) that additional excitation properties must be guaranteed by the behavior of the stator currents. Because of this, instead of simply solving an observation problem, we rather opt to co-design a position, speed, flux and resistance observer and a current controller capable of imposing an appropriate signal injection strategy. The design of the speed controller, on the other hand, is not the focus here, thus we assume that a structure similar to the simple proportional-integral controller (4.59) is already available, end ensures a desirable certainty-equivalence behavior. Clearly, the interconnection between the speed controller and the controller-observer of this section may destroy the PMSM observability properties and, ultimately, the whole closed loop stability. Therefore, to simplify the analysis and leave the overall stability discussion to future works, we assume that the speed behavior is compatible with the unknown input observability conditions that we showed above. Hence, we let Assumption 4.1 hold, even if in practice it must be imposed by appropriate selection of the gains of the structure and, of course, suitable initial conditions. For the formal result that we are going to provide, we suppose the existence of a torque reference T^*_{el}, whose regularity properties are given in the following Assumption.

Assumption 4.2. *The signal $T^*_{\mathrm{el}}(\cdot)$ is $\mathcal{C}^1$ in the interval $[t_0, \infty)$ and satisfies $\|T^*_{\mathrm{el}}(\cdot)\|_\infty \leq T^*_{\max}$, for some positive scalar $T^*_{\max}$. Furthermore $T^*_{\mathrm{el}}(\cdot)$ and its derivative, $\dot{T}^*_{\mathrm{el}}(\cdot)$, are available for measurement.*

As usual, we let $t_0 = 0$ in Assumptions 4.1-4.2, without loss of generality. Like for the baseline sensorless observer strategy, we consider an attitude observer on $\mathbb{S}^1$ of the form

$$
\begin{aligned}
\dot{\hat{\zeta}}_\chi &= (|\hat{h}|\hat{\xi} + k_\eta \hat{h}_1)\mathcal{J}\hat{\zeta}_\chi \\
\dot{\hat{\xi}} &= \gamma \hat{h}_1,
\end{aligned}
\tag{4.74}
$$

with $\hat{h}$ that now needs to be redefined as a consequence of the controller-observer co-design. Define the following signals, which represent a generalization of the signals in (4.59):

$$
\begin{aligned}
i_{\mathrm{q}}^{*} &= \frac{2}{3p}\hat{\xi}T_{\mathrm{el}}^{*} \\
p_{\mathrm{q}}^{*} &= \frac{2}{3p}\left(\dot{\hat{\xi}}T_{\mathrm{el}}^{*} + \hat{\xi}\dot{T}_{\mathrm{el}}^{*}\right).
\end{aligned}
\tag{4.75}
$$

We can summarize the proposed strategy as follows:

- an observer of the stator current $i_{\hat{\chi}}$ is designed, including a suitable adaptive law for R and h (both regarded in this step as constant parameters);
- the current estimate is imposed to track a reference $i_{\hat{\chi}}^{*}$, embedding the requests of both torque tracking and signal injection;
- the time scale separation is imposed by suitably choosing the gains of the structure, thus restoring the desirable behavior of the adaptive attitude observer.

For convenience, rewrite the current dynamics (4.15) as a linear regression form:

$$
\begin{aligned}
&\frac{d}{dt}i_{\hat{\chi}} = L^{-1}\Omega^{T}(i_{\hat{\chi}})\theta + L^{-1}u_{\hat{\chi}} - \hat{\omega}_{\chi}\mathcal{J}i_{\hat{\chi}} \\
&D^{+}\theta = f_{\theta}(\chi, D^{+}\chi, \eta, \omega_{\eta}) \\
&\theta = \begin{pmatrix} R \\ h \end{pmatrix}, \qquad \Omega^{T}(i_{\hat{\chi}}) = \begin{pmatrix} -i_{\hat{\chi}} & I_2 \end{pmatrix}.
\end{aligned}
\tag{4.76}
$$

If the map f_{θ} is identically zero, the above dynamics can be treated as in classic adaptive observer design, with θ an unknown parameter vector. With this idea in mind, consider an Immersion and Invariance observer of the form (see Astolfi and Ortega, 2003)

$$
\begin{aligned}
\dot{\hat{\imath}} &= L^{-1}\Omega^{T}(i_{\hat{\chi}})(\hat{\theta} + \beta(i_{\hat{\chi}})) + L^{-1}u_{\hat{\chi}} - \hat{\omega}_{\chi}\mathcal{J}i_{\hat{\chi}} + k_{\mathrm{p}}(i_{\hat{\chi}} - \hat{\imath}) \\
\dot{\hat{\theta}} &= -L^{-1}\frac{\partial\beta}{\partial i_{\hat{\chi}}}(i_{\hat{\chi}})\left[\Omega^{T}(i_{\hat{\chi}})(\hat{\theta} + \beta(i_{\hat{\chi}})) + u_{\hat{\chi}} - L\hat{\omega}_{\chi}\mathcal{J}i_{\hat{\chi}}\right],
\end{aligned}
\tag{4.77}
$$

where k_{p} is a positive scalar, while $\beta(i_{\hat{\chi}})$ is a map to be defined in the following. Let $\tilde{\imath} = i_{\hat{\chi}} - \hat{\imath}$, $z = \hat{\theta} + \beta(i_{\hat{\chi}}) - \theta$, so that the resulting error dynamics becomes

$$
\begin{aligned}
\dot{\tilde{\imath}} &= -L^{-1}\Omega^{T}(i_{\hat{\chi}})z - k_{\mathrm{p}}\tilde{\imath} \\
D^{+}z &= -L^{-1}\frac{\partial\beta}{\partial i_{\hat{\chi}}}(i_{\hat{\chi}})\Omega^{T}(i_{\hat{\chi}})z - f_{\theta}(\chi, D^{+}\chi, \eta, \omega_{\eta}),
\end{aligned}
\tag{4.78}
$$

thus suggesting the choice $\partial\beta/\partial i_{\hat{\chi}} = k_z\Omega$, with k_z a positive scalar, therefore

$$
\beta(i_{\hat{\chi}}) = k_z\begin{pmatrix} -\frac{|i_{\hat{\chi}}|^2}{2} \\ i_{\hat{\chi}} \end{pmatrix}.
\tag{4.79}
$$

It follows that the parameter estimation error takes the form

$$
D^{+}z = -(k_z L^{-1})\underbrace{\left[\Omega(i_{\hat{\chi}})\Omega^{T}(i_{\hat{\chi}})\right]}_{M(i_{\hat{\chi}})}z - f_{\theta}(\chi, D^{+}\chi, \eta, \omega_{\eta}),
\tag{4.80}
$$

which corresponds, for $f_\theta = 0$, to a classical gradient descent algorithm. The parameter estimates are then given by:

$$\begin{aligned}\hat{R} &= \begin{pmatrix}1 & 0_{1\times 2}\end{pmatrix}\hat{\theta} - (k_z/2)|i_{\hat{\chi}}|^2 \\ \hat{h} &= \begin{pmatrix}0_{2\times 1} & I_2\end{pmatrix}\hat{\theta} + k_z i_{\hat{\chi}}.\end{aligned} \tag{4.81}$$

Consider the exosystem

$$\frac{d}{dt}\begin{pmatrix}w_1\\ w_2\end{pmatrix} = \begin{pmatrix}0 & \lambda\\ -\lambda & 0\end{pmatrix}\begin{pmatrix}w_1\\ w_2\end{pmatrix}, \tag{4.82}$$

with λ a positive scalar for tuning, and the current reference given by

$$i^*_{\hat{\chi}}(w,t) = \begin{pmatrix}w_1\\ i^*_{\mathrm{q}}(t)\end{pmatrix}. \tag{4.83}$$

Similarly to the strategy in the above nested controller, we consider the estimated current mismatch $e = \hat{\imath} - i^*_{\hat{\chi}}$, suggesting for simplicity a proportional controller of the form:

$$u_{\hat{\chi}} = -\Omega^T(i_{\hat{\chi}})(\hat{\theta} + \beta(i_{\hat{\chi}})) + L\hat{\omega}_\chi \mathcal{J} i_{\hat{\chi}} - Lk_e e + L\begin{pmatrix}\lambda w_2\\ p^*_{\mathrm{q}}\end{pmatrix}, \tag{4.84}$$

which leads to the error dynamics:

$$\dot{e} = -k_e e + k_p \tilde{\imath}. \tag{4.85}$$

Let $x_{\mathrm{s}} := (\eta, \tilde{\xi})$ be the state variables associated with the slow subsystem. As a consequence, write the overall error dynamics as

$$\begin{aligned}\frac{d}{dt}\begin{pmatrix}w_1\\ w_2\end{pmatrix} &= \begin{pmatrix}0 & \lambda\\ -\lambda & 0\end{pmatrix}\begin{pmatrix}w_1\\ w_2\end{pmatrix}\\ \frac{d}{dt}\begin{pmatrix}e\\ \tilde{\imath}\end{pmatrix} &= \begin{pmatrix}-k_e I_2 & k_{\mathrm{p}} I_2\\ 0_{2\times 2} & -k_{\mathrm{p}} I_2\end{pmatrix}\begin{pmatrix}e\\ \tilde{\imath}\end{pmatrix} - \begin{pmatrix}0_{2\times 2}\\ L^{-1}I_2\end{pmatrix}\Omega^T(i^*_{\hat{\chi}} + e + \tilde{\imath})z\\ D^+ z &= -(k_z L^{-1})M(i^*_{\hat{\chi}} + e + \tilde{\imath})z - f_\theta(\chi, D^+\chi, \eta, \omega_\eta)\\ \dot{x}_{\mathrm{s}} &= f_0(x_{\mathrm{s}}, \chi) + N(x_{\mathrm{s}}, \tilde{h}, \chi, \xi),\end{aligned} \tag{4.86}$$

with f_0 the vector field associated with the reduced order dynamics (4.31) and N a continuous map vanishing in $\tilde{h} = 0$. Choose, and *fix*, some positive scalars $\bar{\kappa}_e$, $\bar{\kappa}_{\mathrm{p}}$, $\bar{\kappa}_z$. Appealing to classical singular perturbations arguments, denote with ε the perturbation parameter, let $\lambda = k_e/\bar{\kappa}_e = k_{\mathrm{p}}/\bar{\kappa}_{\mathrm{p}} = k_z/(L\bar{\kappa}_z) = \varepsilon^{-1}$ and let $t = t^* + \varepsilon\tau$, with τ indicating the fast time scale and $t^* \geq 0$. The boundary layer system can be then written as follows (denote with $(\cdot)'$ the time derivative in the fast scale):

$$\begin{aligned}\begin{pmatrix}w_1'\\ w_2'\end{pmatrix} &= -\mathcal{J}\begin{pmatrix}w_1\\ w_2\end{pmatrix}, \qquad i^*_{\hat{\chi}}(w,t^*) = \begin{pmatrix}w_1\\ i^*_q(t^*)\end{pmatrix}\\ \begin{pmatrix}e'\\ \tilde{\imath}'\end{pmatrix} &= \begin{pmatrix}-I_2\bar{\kappa}_e & I_2\bar{\kappa}_p\\ 0_{2\times 2} & -I_2\bar{\kappa}_{\mathrm{p}}\end{pmatrix}\begin{pmatrix}e\\ \tilde{\imath}\end{pmatrix} = A_{\mathrm{f}}\begin{pmatrix}e\\ \tilde{\imath}\end{pmatrix}\\ z' &= -\bar{\kappa}_z M(i^*_{\hat{\chi}}(w,t^*) + e + \tilde{\imath})z,\end{aligned} \tag{4.87}$$

and note that only ordinary derivatives can be used since f_θ is absent. Associated with (4.87) we have the following stability result.

Lemma 4.2. *Suppose that $|i_{\mathrm{q}}^*(t^*)| \leq I^*$, for a positive scalar I^*. Then, there exists a positive scalar W^* such that, for any $w(0)$ satisfying $|w(0)| \geq W^*$, the origin of system*

$$\frac{d}{d\tau}\begin{pmatrix} e \\ \tilde{\imath} \\ z \end{pmatrix} = \begin{pmatrix} -I_2\bar{\kappa}_e & I_2\bar{\kappa}_{\mathrm{p}} & 0_{2\times 3} \\ 0_{2\times 2} & -I_2\bar{\kappa}_{\mathrm{p}} & 0_{2\times 3} \\ 0_{3\times 2} & 0_{3\times 2} & -\bar{\kappa}_z M(i_{\hat{\chi}}^*(w,t^*)+e+\tilde{\imath}) \end{pmatrix}\begin{pmatrix} e \\ \tilde{\imath} \\ z \end{pmatrix} \tag{4.88}$$

is globally asymptotically stable and locally exponentially stable.

Proof. See Appendix B.1. □

Let $x_{\mathrm{f}} := (e, \tilde{\imath}, z)$, then we can state the following stability result, which allows to solve the presented mixed controller-observer problem.

Theorem 4.2. *Consider system (4.86), parameterized through the positive scalar ε as shown above. Denote with $(w(t), x_{\mathrm{f}}(t), x_{\mathrm{s}}(t))$ the trajectories of such system, when they exist, for initial conditions $(w(0), x_{\mathrm{f}}(0), x_{\mathrm{s}}(0))$. Let Assumptions 4.1-4.2 hold. Then, there exist:*

- *an open region $\mathcal{R} \subset \mathbb{S}^1 \times \mathbb{R}$, independent of $\chi(\cdot)$, $T_{\mathrm{el}}^*(\cdot)$, $\dot{T}_{\mathrm{el}}^*(\cdot)$, and such that $x_{\mathcal{A},\mathrm{s}} \in \mathcal{R}$;*
- *a proper indicator of $x_{\mathcal{A},\mathrm{s}}$ in $\mathcal{R}$, denoted with σ;*
- *class $\mathcal{KL}$ functions β_{s}, β_{f};*

such that, for any positive scalars Δ_{f}, Δ_{s}, δ, there exist $\varepsilon^* > 0$, $W^* > 0$ such that, for all $0 < \varepsilon < \varepsilon^*$ and all initial conditions satisfying $|w(0)| \geq W^*$, $|x_{\mathrm{f}}(0)| \leq \Delta_{\mathrm{f}}$, $\sigma(x_{\mathrm{s}}) \leq \Delta_{\mathrm{s}}$, the resulting trajectories are forward complete and satisfy, for all $t \geq 0$:

$$\begin{aligned} |x_{\mathrm{f}}(t)| &\leq \beta_f(|x_{\mathrm{f}}(0)|, t/\varepsilon) + \delta \\ \sigma(x_{\mathrm{s}}(t)) &\leq \beta_{\mathrm{s}}(\sigma(x_{\mathrm{s}}(0)), t) + \delta. \end{aligned} \tag{4.89}$$

Proof. From Lemma 4.1, it follows that there exist $\mathcal{R}$, σ and β_{s} defined above such that the trajectories of system (4.31) satisfy, for all $t \geq 0$ and all $x_{\mathrm{s}} \in \mathcal{R}$:

$$\sigma(x_{\mathrm{s}}(t)) \leq \beta_{\mathrm{s}}(\sigma(x_{\mathrm{s}}(0)), t). \tag{4.90}$$

Let $\mathcal{K} := \{x_{\mathrm{s}} : \sigma(x_{\mathrm{s}}) \leq \beta_{\mathrm{s}}(\Delta_{\mathrm{s}}, 0) + \delta\}$, then by the regularity properties of T_{el}^* stated in Assumption 4.2 it follows that, for all $x_{\mathrm{s}} \in \mathcal{K}$, there exists a positive scalar I^* such that $\|i_{\mathrm{q}}^*\|_\infty \leq I^*$. Apply Lemma 4.2 with the bound I^* to imply the existence of a positive scalar W^* such that, for all $|w(0)| \geq W^*$, the trajectories (4.87) satisfy, for a class $\mathcal{KL}$ function β_{f}:

$$|x_{\mathrm{f}}(\tau)| \leq \beta_{\mathrm{f}}(|x_{\mathrm{f}}(0)|, \tau). \tag{4.91}$$

Notably, the GAS + LES properties in Lemma 4.2 guarantee the existence, for any $c > 0$, of positive scalars $\alpha_{1\mathrm{f}}(c)$, $\alpha_{2\mathrm{f}}(c)$ such that, for all $|x_{\mathrm{f}}(0)| \leq c$:

$$|x_{\mathrm{f}}(\tau)| \leq \alpha_{1\mathrm{f}} \exp(\alpha_{2\mathrm{f}}\tau)|x_{\mathrm{f}}(0)|. \tag{4.92}$$

Due to the regularity properties of system (4.86), we can use same arguments of Theorem 4.1 (either methods can be applied) to imply the existence of a positive scalar ε^* which yields the bounds of the statement. □

It is important then to establish a connection between this stability result and the torque tracking behavior. Indeed, note that the electric torque is related to the

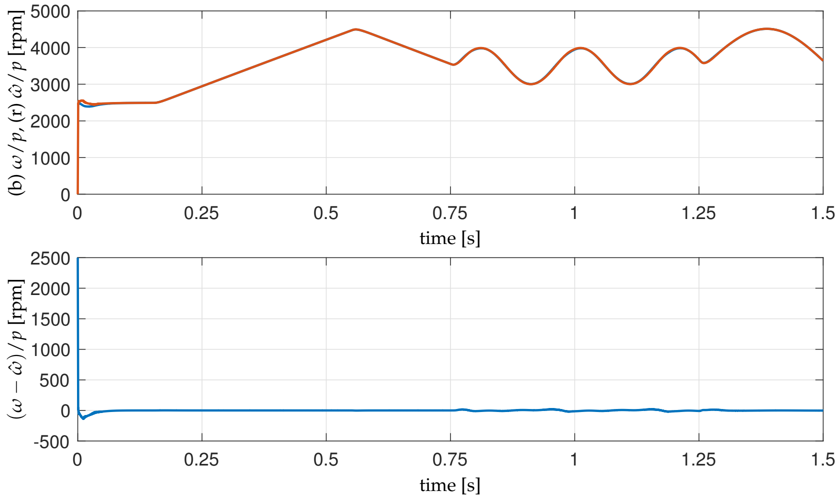

FIGURE 4.9: Speed estimation performance of the sensorless controller-observer.

currents, in the rotating frame $\hat{\zeta}_\chi$, as follows:

$$\zeta_\chi^T \mathcal{C}[\hat{\zeta}_\chi] \mathcal{J} i_{\hat{\chi}} = \eta^T \mathcal{J} i_{\hat{\chi}} = -\eta_1 i_{\hat{\chi}2} + \eta_2 i_{\hat{\chi}1} = -\frac{2}{3p} \xi T_{\text{el}}, \tag{4.93}$$

therefore, if the frames $\hat{\zeta}_\chi$ and ζ_χ achieve synchronization, it holds $i_{\hat{\chi}2} = (2/(3p))\xi T_{\text{el}}$. Clearly, appropriate choice of δ ensures an arbitrarily small residual torque tracking error. We finally summarize the overall controller-observer structure, to be interconnected with an opportune speed controller:

$$\begin{aligned}
\dot{\hat{\imath}} &= L^{-1}\Omega^T(i_{\hat{\chi}})(\hat{\theta} + \beta(i_{\hat{\chi}})) + L^{-1}u_{\hat{\chi}} - \hat{\omega}\mathcal{J} i_{\hat{\chi}} + k_{\text{p}}(i_{\hat{\chi}} - \hat{\imath}) \\
\dot{\hat{\theta}} &= -\frac{\partial \beta}{\partial i_{\hat{\chi}}}(i_{\hat{\chi}}) \left[L^{-1}\Omega^T(i_{\hat{\chi}})(\hat{\theta} + \beta(i_{\hat{\chi}})) + L^{-1}u_{\hat{\chi}} - \hat{\omega}_\chi \mathcal{J} i_{\hat{\chi}} \right] \\
\dot{\hat{\zeta}}_\chi &= (|\hat{h}|\hat{\xi} + k_\eta \hat{h}_1)\mathcal{J}\hat{\zeta}_\chi, \qquad \dot{\hat{\xi}} = \gamma \hat{h}_1 \\
\frac{d}{dt}\begin{pmatrix} w_1 \\ w_2 \end{pmatrix} &= \begin{pmatrix} 0 & \lambda \\ -\lambda & 0 \end{pmatrix} \begin{pmatrix} w_1 \\ w_2 \end{pmatrix} \qquad e = \hat{\imath} - \begin{pmatrix} w_1 \\ i_{\text{q}}^* \end{pmatrix} \\
\beta(i_{\hat{\chi}}) &= k_z \begin{pmatrix} -\frac{|i_{\hat{\chi}}|^2}{2} \\ i_{\hat{\chi}} \end{pmatrix}, \qquad \begin{aligned} \hat{R} &= \begin{pmatrix} 1 & 0_{1\times 2} \end{pmatrix} \hat{\theta} - (k_z/2)|i_{\hat{\chi}}|^2 \\ \hat{h} &= \begin{pmatrix} 0_{2\times 1} & I_2 \end{pmatrix} \hat{\theta} + k_z i_{\hat{\chi}} \end{aligned} \\
i_{\text{q}}^* &= \frac{2}{3p}\hat{\xi} T_{\text{el}}^* \qquad p_{\text{q}}^* = \frac{2}{3p}\left(\dot{\hat{\xi}} T_{\text{el}}^* + \hat{\xi} \dot{T}_{\text{el}}^* \right) \\
u_{\hat{\chi}} &= -\Omega^T(i_{\hat{\chi}})(\hat{\theta} + \beta(i_{\hat{\chi}})) + L\hat{\omega}_\chi \mathcal{J} i_{\hat{\chi}} - Lk_e e + L\begin{pmatrix} \lambda w_2 \\ p_{\text{q}}^* \end{pmatrix}.
\end{aligned} \tag{4.94}$$

We conclude the section with some simulation results, considering the usual UAV propeller control case of study. In Figures 4.9, 4.10 are depicted some relevant observer estimates, compared to the corresponding true values. In particular, we see that the stator resistance estimate presents the expected fast response, corresponding to the initial transient of the estimated speed, which is linked to the behavior of $\hat{h}$. On the other hand, it can be appreciated that the torque tracking performance is connected to the angular estimation error, see Figure 4.11. In particular, a high alignment error corresponds to torque oscillations, due to the coupling with the signal

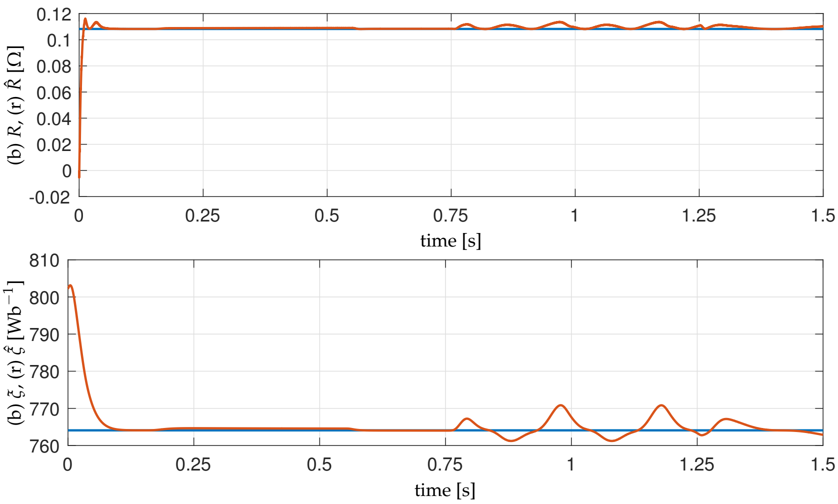

FIGURE 4.10: Stator resistance and rotor flux amplitude estimation performance of the proposed sensorless controller-observer.

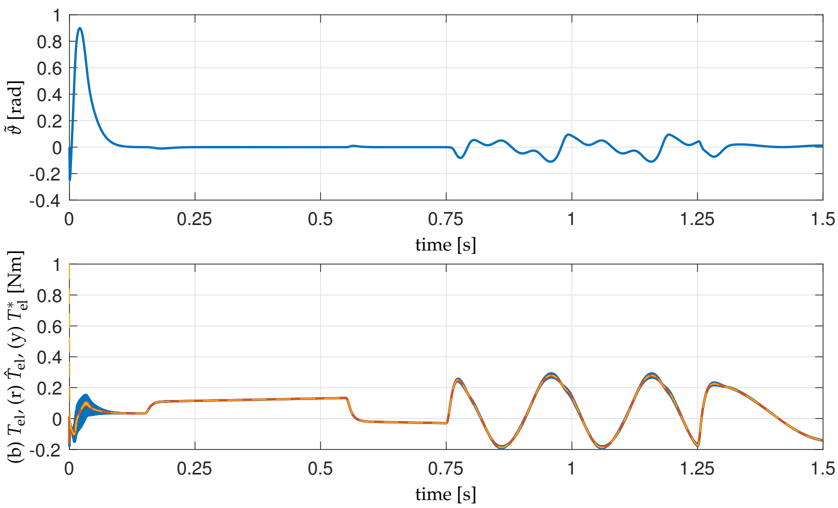

FIGURE 4.11: Torque tracking performance of the sensorless controller-observer, and relation with the position estimation error.

injection strategy. This is evident, apart from the initial transient, during periods of very aggressive acceleration, as we can see in the central/final part of the simulation. Finally, we present in Figure 4.12 the current controller tracking performance. In the top figure, we see how the currents, in the $\hat{\zeta}_\chi$ frame, are imposed to track a sinusoidal reference (the first component in blue) and a reference for torque generation (the second component in red). The tracking error e is then depicted in the bottom figure.

Finally, we refer for completeness to (Verrelli et al., 2017; Verrelli, Tomei, and Lorenzani, 2018; Bazylev, Pyrkin, and Bobtsov, 2018; Bernard and Praly, 2019) for other notable examples of sensorless control/observation with resistance estimation.

4.4.2 A Hybrid Sensorless Observer for Semi-Global Practical Stability

As expected, the proposed sensorless observer featured a regional stability property due to the use of a continuous vector field. Indeed the reduced order system, that

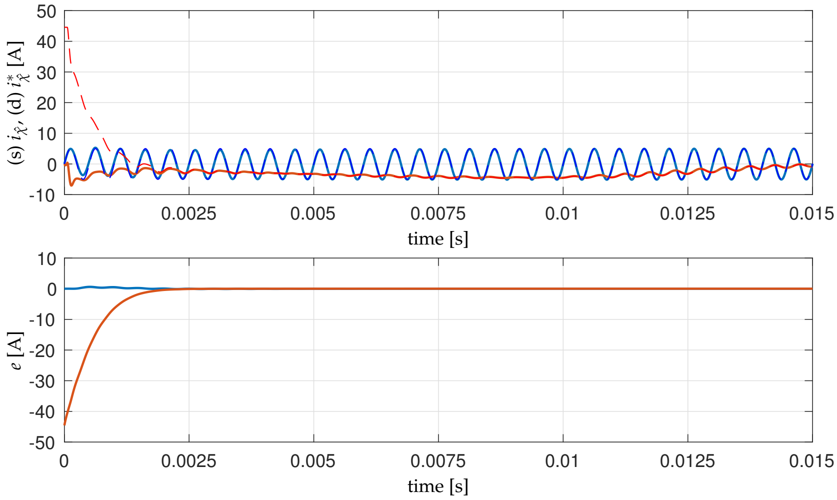

FIGURE 4.12: Stator currents tracking performance of the sensorless controller-observer.

we recall once again for convenience:

$$\begin{aligned} \dot{\eta} &= \left(\chi\tilde{\xi} - k_\eta \chi \eta_2\right) \mathcal{J}\eta \\ \dot{\tilde{\xi}} &= -\gamma\chi\eta_2, \end{aligned} \tag{4.95}$$

is defined on the cylinder, $\mathbb{S}^1 \times \mathbb{R}$, which is not contractible, and hence it is impossible to globally robustly stabilize the isolated equilibrium point $x_{\mathcal{A},s}$. In this subsection, we will present a hybrid strategy that removes the unstable manifold $\mathcal{R}_\mathcal{U}$. Following the insights provided by the continuous-time solution, we opt to modify the reduced order system (4.95) by enriching its dynamics with a jump policy, which corresponds to jumps of the estimates $\hat{\zeta}_\chi$, $\hat{\xi}$, while preserving the existent flows. To simplify the approach and allow easy implementation of the observer, we propose to augment the observer dynamics with a timer, that is

$$\begin{cases} \dot{\rho} = \Lambda & \rho \in [0,1] \\ \rho^+ = 0 & \rho = 1 \end{cases} \tag{4.96}$$

with Λ a positive scalar for tuning. Clearly, the timer dynamics can be used to enforce jumps of the angular estimate at regular times and thus break the cylinder topological constraint, but it seems also convenient as a way to embed additional desirable features. Among these, we propose a simple identifier structure to enhance the observer transient performance. Firstly, we introduce the baseline strategy with no identifier.

As we saw before, the high gain current observer contains an integral action providing an indirect measurement of the back-EMF, which contains the angular synchronization error. Therefore, it results convenient to design a jump policy such that, as soon as $\hat{h}$ becomes sufficiently close to $h = -\chi\mathcal{J}\eta$, the angle estimate $\hat{\zeta}_\chi$ is reset to a value closer to ζ_χ, corresponding to a smaller value of the cost function $1 - \eta_1$. In particular, we propose to divide the circle in two halves according to the sign of η_1: if the sign is positive the estimate does not require adjustment, while when the sign is negative, the angular error η is reset to the specular value $(-\eta_1, \eta_2)$. The dwell time imposed by the timer is in this context instrumental to guarantee that, if the high gain observer is made sufficiently fast, then the jumps will not introduce a destabilizing effect. The new reduced order system is then given as follows:

$$\mathcal{H}_0 : \begin{cases} \begin{pmatrix} \dot{\eta} \\ \dot{\tilde{\xi}} \\ \dot{\rho} \end{pmatrix} = \begin{pmatrix} \left(\chi\tilde{\xi} - k_\eta \chi \eta_2\right) \mathcal{J}\eta \\ -\gamma\chi\eta_2 \\ \Lambda \end{pmatrix} =: F_0(\eta, \tilde{\xi}, \rho, \chi) & \begin{pmatrix} \eta \\ \tilde{\xi} \\ \rho \end{pmatrix} \in C_\mathrm{s} \\ \begin{pmatrix} \eta^+ \\ \tilde{\xi}^+ \\ \rho^+ \end{pmatrix} \in \begin{pmatrix} \begin{cases} -F\eta, & \chi\eta_1 \leq 0 \\ \eta, & \chi\eta_1 \geq 0 \end{cases} \\ \tilde{\xi} \\ 0 \end{pmatrix} =: G_0(\eta, \tilde{\xi}, \rho, \chi) & \begin{pmatrix} \eta \\ \tilde{\xi} \\ \rho \end{pmatrix} \in D_\mathrm{s} \end{cases} \tag{4.97}$$

where $F = \mathrm{diag}\{1, -1\}$, while $C_\mathrm{s} = \mathbb{S}^1 \times \mathbb{R} \times [0, 1]$ and $D_\mathrm{s} = \mathbb{S}^1 \times \mathbb{R} \times \{1\}$. In this structure, the angle η is always reset to a value satisfying $\eta_1 \geq 0$, thus ensuring that the set $\bar{x}_\mathrm{u} \times [0, 1]$ is not an attractor compatible with the data of system (4.97). In fact, the next result confirms that the proposed hybrid strategy removes the unstable manifold $\mathcal{R}_\mathcal{U}$.

Lemma 4.3. *The set $\mathcal{A}_0 := \bar{x}_\mathrm{s} \times [0, 1] \subset \mathbb{S}^1 \times \mathbb{R}^2$ is a uniformly preasymptotically stable attractor for the hybrid system (4.97), with basin of preattraction given by $\mathbb{S}^1 \times \mathbb{R}^2$.*

Proof. It is a direct application of the Nested Matrosov Theorem for hybrid systems (Sanfelice and Teel, 2009, Theorem 4.1). Indeed, consider the following Matrosov functions (which are continuous in their arguments, and thus bounded in any compact set of the states $(\eta, \tilde{\xi}, \rho)$, by Assumption 4.1):

$$\begin{aligned} W_1(\eta, \tilde{\xi}, \rho, \chi) &= 1 - \eta_1 + \frac{1}{2\gamma}\tilde{\xi}^2 \\ W_2(\eta, \tilde{\xi}, \rho, \chi) &= -\chi\tilde{\xi}\eta_1\eta_2 \\ W_3(\eta, \tilde{\xi}, \rho, \chi) &= \exp(\rho)\left[\eta_2^2 + \tilde{\xi}^2\right] \\ W_4(\eta, \tilde{\xi}, \rho, \chi) &= \exp(-\rho)\left[1 - \eta_1\right]. \end{aligned} \tag{4.98}$$

Employing routine calculations and by means of by Assumption 4.1), it is possible to establish the bounds $\sup_{f \in F_0(\eta, \tilde{\xi}, \rho, \chi)} \langle \nabla W_i(\eta, \tilde{\xi}, \rho, \chi), (f, D^+\chi) \rangle \leq B_{\mathrm{c},i}(\eta, \tilde{\xi}, \rho)$, $i \in \{1, 2, 3, 4\}$, for all $(\eta, \tilde{\xi}, \rho) \in C_\mathrm{s}$:

$$\begin{aligned} B_{\mathrm{c},1} &= -k_\eta \chi_\mathrm{m} \eta_2^2 \leq 0 \\ B_{\mathrm{c},2} &= -\chi_\mathrm{m}^2 \eta_1^2 \tilde{\xi}^2 + \Delta_2(M, \chi_\mathrm{M}, \tilde{\xi}, \eta)|\eta_2| \\ B_{\mathrm{c},3} &= \Lambda W_2 + \exp(\rho)\Delta_3(\chi_\mathrm{M}, \tilde{\xi}, \eta)|\eta_2| \\ B_{\mathrm{c},4} &= -\Lambda \exp(-\rho)(1 - \eta_1) + \Delta_4(\chi_\mathrm{M}, \tilde{\xi}, \eta)|\eta_2|, \end{aligned} \tag{4.99}$$

with Δ_2, Δ_3, Δ_4 positive continuous functions in their arguments. Note that $B_{\mathrm{c},2} \leq -\chi_\mathrm{m}^2 \tilde{\xi}^2$ as $\eta_2 = 0$, thus in $B_{\mathrm{c},3}$ and $B_{\mathrm{c},4}$ the conditions 1)-2) of (Sanfelice and Teel, 2009, Theorem 4.1) must be checked in particular for $\eta_1 = -1$, $\eta_2 = 0$, $\tilde{\xi} = 0$, for any $\rho \in [0, 1]$. Similarly, it holds $\sup_{g \in G_0(\eta, \tilde{\xi}, \rho, \chi)} W_i(g) - W_i(\eta, \tilde{\xi}, \rho, \chi) \leq B_{\mathrm{d},i}(\eta, \tilde{\xi}, \rho)$, $i \in \{1, 2, 3, 4\}$, with the following bounds, for all $(\eta, \tilde{\xi}, \rho) \in D_\mathrm{s}$:

$$\begin{aligned} B_{\mathrm{d},1} &= \min\{0, 2\eta_1\} \leq 0 \\ B_{\mathrm{d},2} &= \max\{0, -2\chi_\mathrm{M}|\tilde{\xi}||\eta_2|\eta_1\}, \qquad (B_{\mathrm{d},2} > 0 \Rightarrow \eta_1 < 0) \\ B_{\mathrm{d},3} &= [\exp(0) - \exp(1)](\eta_2^2 + \tilde{\xi}^2) \leq 0 \\ B_{\mathrm{d},4} &= [\exp(0) - \exp(-1)](1 - |\eta_1|). \end{aligned} \tag{4.100}$$

It can be easily verified from the first three bounds that the conditions 1)-2) of (Sanfelice and Teel, 2009, Theorem 4.1) are satisfied for all $(\eta, \tilde{\xi}, \rho) \in D_s \backslash \mathcal{A}_0$. Finally, note that uniform global stability is easily established with $B_{c,1}$, $B_{d,1}$, in connection with the fact that W_1 is positive definite (considering a proper indicator function) with respect to the attractor $\mathcal{A}_0$, for all $(\eta, \tilde{\xi}, \rho) \in C_s \cup D_s \cup G_0(D_s)$. Since all sufficient conditions in (Sanfelice and Teel, 2009) are verified, the statement follows immediately. □

In order to implement the hybrid observer leading to the above reduced order system, we need to compute the jumps of $\hat{\zeta}_\chi$ corresponding to $\eta^+ = -F\eta$, using $\hat{h}$ as a proxy of $h = -\chi\mathcal{J}\eta$. For, note that

$$-F\eta = \mathcal{C}^T[\hat{\zeta}_\chi^+]\zeta_\chi = \mathcal{C}[\zeta_\chi]F\hat{\zeta}_\chi^+, \tag{4.101}$$

therefore it is possible to express $\hat{\zeta}_\chi^+$ as:

$$\hat{\zeta}_\chi^+ = -F\mathcal{C}^T[\zeta_\chi]F\eta = -\mathcal{C}[\zeta_\chi]\eta = -\mathcal{C}^T[\hat{\zeta}_\chi][\mathcal{C}[\zeta_\chi]\zeta_\chi]. \tag{4.102}$$

Furthermore, at each time a "fast" estimate of the rotor position (rescaled by $\chi > 0$) can be retrieved from $\hat{h}$ and $\hat{\zeta}_\chi$, since $\mathcal{J}h = \chi\eta$, and therefore $\chi\zeta_\chi = \mathcal{C}[\hat{\zeta}_\chi]\mathcal{J}h$. These considerations finally yield the complete jump map $G_\zeta : \mathbb{R}^2 \times \mathbb{S}^1 \rightrightarrows \mathbb{S}^1$:

$$\begin{aligned} G_\zeta(\hat{h}, \hat{\zeta}_\chi) &\in \begin{cases} -\mathcal{C}^T[\hat{\zeta}_\chi]\begin{pmatrix}\cos(2\theta_\chi(\hat{h}, \hat{\zeta}_\chi)) \\ \sin(2\theta_\chi(\hat{h}, \hat{\zeta}_\chi))\end{pmatrix} & \hat{h}_2 \geq 0 \\ \hat{\zeta}_\chi & \text{otherwise} \end{cases} \\ \theta_\chi &= \operatorname{atan2}(y_\chi, x_\chi) \subset [-\pi, \pi], \qquad \begin{pmatrix} x_\chi \\ y_\chi \end{pmatrix} = \mathcal{C}[\hat{\zeta}_\chi]\mathcal{J}\hat{h} \end{aligned} \tag{4.103}$$

where in particular we let $\operatorname{atan2}(0,0) = [-\pi, \pi]$ and $\operatorname{atan2}(y,x) = \{-\pi, \pi\}$, for all (x,y) in the set $S = \{(x,y) \in \mathbb{R}^2 : x < 0, y = 0\}$. For convenience, let the map $G_f(\hat{h}, \hat{\zeta}_\chi) = \mathcal{C}^T[G_\zeta(\hat{h}, \hat{\zeta}_\chi)]\mathcal{C}[\hat{\zeta}_\chi]$ indicate the change of coordinates from the $\hat{\zeta}_\chi$-frame to the $\hat{\zeta}_\chi^+$-frame. This map, which is available for observer design, is fundamental to describe the jumps that occur to both $i_{\hat{\chi}}$ and h, indeed:

$$i_{\hat{\chi}}^+ = \mathcal{C}^T[\hat{\zeta}_\chi^+]i_s = \mathcal{C}^T[G_\zeta(\hat{h}, \hat{\zeta}_\chi)]\mathcal{C}[\hat{\zeta}_\chi]\mathcal{C}^T[\hat{\zeta}_\chi]i_s = G_f i_{\hat{\chi}}, \qquad h^+ = -\chi\mathcal{J}\mathcal{C}^T[\hat{\zeta}_\chi^+]\zeta_\chi = G_f h \tag{4.104}$$

It follows that the overall observer structure is given by:

$$\begin{aligned} \begin{pmatrix} \dot{\hat{\imath}} \\ \dot{\hat{h}} \\ \dot{\hat{\zeta}}_\chi \\ \dot{\hat{\xi}} \\ \dot{\rho} \end{pmatrix} &= \begin{pmatrix} -\frac{R}{L}\hat{\imath} + \frac{1}{L}u_{\hat{\chi}} + \frac{\hat{h}}{L} - \hat{\omega}_\chi\mathcal{J}i_{\hat{\chi}} + k_p\tilde{\imath} \\ k_i\tilde{\imath} \\ \hat{\omega}_\chi\mathcal{J}\hat{\zeta}_\chi \\ \gamma\hat{h}_1 \\ \Lambda \end{pmatrix} & \rho \in [0,1] \\ \begin{pmatrix} \hat{\imath}^+ \\ \hat{h}^+ \\ \hat{\zeta}_\chi^+ \\ \hat{\xi}^+ \\ \rho^+ \end{pmatrix} &\in \begin{pmatrix} G_f(\hat{h}, \hat{\zeta}_\chi)\hat{\imath} \\ G_f(\hat{h}, \hat{\zeta}_\chi)\hat{h} \\ G_\zeta(\hat{h}, \hat{\zeta}_\chi) \\ \hat{\xi} \\ 0 \end{pmatrix} & \rho = 1 \end{aligned} \tag{4.105}$$

with $\hat{\omega}_\chi = |\hat{h}|\hat{\tilde{\xi}} + k_\eta \hat{h}_1$ as before. Let $x_{\mathrm{s}} := (\eta, \tilde{\xi}, \rho) \in \mathbb{S}^1 \times \mathbb{R} \times [0,1]$ and $x_{\mathrm{f}} := T(\tilde{\imath}, \tilde{h}) \in \mathbb{R}^4$, with T a change of coordinates matrix such that:

$$x_{\mathrm{f}} = T\begin{pmatrix}\tilde{\imath}\\ \tilde{h}\end{pmatrix} = \begin{pmatrix}\varepsilon^{-1}I_2 & 0_{2\times 2}\\ -\varepsilon^{-1}I_2 & L^{-1}I_2\end{pmatrix}\begin{pmatrix}\tilde{\imath}\\ \tilde{h}\end{pmatrix}, \tag{4.106}$$

with ε a positive scalar such that $R/L + k_{\mathrm{p}} = 2\varepsilon^{-1}$, $k_{\mathrm{i}} = 2L\varepsilon^{-2}$. We can then define the overall error dynamics as follows:

$$\begin{aligned}\begin{pmatrix}D^+ x_{\mathrm{f}}\\ \dot{x}_{\mathrm{s}}\end{pmatrix} &= \begin{pmatrix}\varepsilon^{-1}\underbrace{\begin{pmatrix}-I_2 & I_2\\ -I_2 & -I_2\end{pmatrix}}_{A_{\mathrm{f}}} x_{\mathrm{f}} + \underbrace{\begin{pmatrix}0_{2\times 2}\\ L^{-1}I_2\end{pmatrix}}_{B_{\mathrm{f}}} f_h\\ F_{\mathrm{s}}(x_{\mathrm{f}}, \chi, x_{\mathrm{s}})\end{pmatrix} & x_{\mathrm{s}} \in C_{\mathrm{s}}\\ \begin{pmatrix}x_{\mathrm{f}}+\\ x_{\mathrm{s}}^+\end{pmatrix} &\in \begin{pmatrix}\mathrm{diag}\{G_{\mathrm{f}}, G_{\mathrm{f}}\}x_{\mathrm{f}}\\ G_{\mathrm{s}}(x_{\mathrm{f}}, \chi, x_{\mathrm{s}})\end{pmatrix} & x_{\mathrm{s}} \in D_{\mathrm{s}}\end{aligned} \tag{4.107}$$

with F_{s}, G_{s} the flows and jumps of the attitude estimation error (which correspond to the data in (4.97) if $\tilde{h} = 0$), respectively. Note that it holds $A_{\mathrm{f}} + A_{\mathrm{f}}^T = -2I_4$, while the jump x_{f}^+ preserves the norm, indeed:

$$\begin{aligned}|x_{\mathrm{f}}^+|^2 &= |\varepsilon^{-1}\tilde{\imath}^+|^2 + |L^{-1}\tilde{h}^+ - \varepsilon^{-1}\tilde{\imath}^+|^2\\ &= |G_{\mathrm{f}}\varepsilon^{-1}\tilde{\imath}|^2 + |G_{\mathrm{f}}(L^{-1}\tilde{h} - \varepsilon^{-1}\tilde{\imath})|^2\\ &= |\varepsilon^{-1}\tilde{\imath}|^2 + |L^{-1}\tilde{h} - \varepsilon^{-1}\tilde{\imath}|^2 = |x_{\mathrm{f}}|^2.\end{aligned} \tag{4.108}$$

This means that on the one hand, during flows, the x_{f}-subsystem can be made arbitrarily fast by choosing ε sufficiently small, while on the other hand the jumps do not cause any increase of $|x_{\mathrm{f}}|$, and thus they do not represent an obstacle to time scale separation. We can summarize the stability properties of the above hybrid system with the following theorem, which is a hybrid counterpart of Theorem 4.1.

Theorem 4.3. *Consider system (4.107) with input $\chi(\cdot)$ satisfying Assumption 4.1, and denote its solutions with $(\psi_{\mathrm{f}}(\cdot), \psi_{\mathrm{s}}(\cdot))$, with initial conditions $(x_{\mathrm{f},0}, x_{\mathrm{s},0})$. Then the attractor $0_{4\times 1} \times \mathcal{A}_0$ is semiglobally practically asymptotically stable as $\varepsilon \to 0^+$, that is:*

- *there exists a proper indicator function σ_{s} of $\mathcal{A}_0$ in $\mathbb{S}^1 \times \mathbb{R}^2$;*
- *there exists a class $\mathcal{KL}$ function β_{s};*

such that, for any positive scalars Δ_{f}, Δ_{s}, δ, there exists a scalar $\varepsilon^* > 0$ such that, for all $0 < \varepsilon \leq \varepsilon^*$, all $(\psi_{\mathrm{f}}(\cdot), \psi_{\mathrm{s}}(\cdot))$ satisfying $\rho_0 = 0$, $|x_{\mathrm{f},0}| \leq \Delta_{\mathrm{f}}$ and $\sigma_{\mathrm{s}}(x_{\mathrm{s},0}) \leq \Delta_{\mathrm{s}}$, the following bounds hold, for all $(t, j) \in \mathrm{dom}(\psi_{\mathrm{f}}(\cdot), \psi_{\mathrm{s}}(\cdot))$:

$$\begin{aligned}|\psi_{\mathrm{f}}(t,j)| &\leq \exp(-t/\varepsilon)\,|x_{\mathrm{f},0}| + \delta\\ \sigma_{\mathrm{s}}(\psi_{\mathrm{s}}(t,j)) &\leq \beta_{\mathrm{s}}(\sigma_{\mathrm{s}}(x_{\mathrm{s},0}), t+j) + \delta.\end{aligned} \tag{4.109}$$

Proof. See Appendix B.2. □

Again, we highlight that the intuition behind this result is that $\varepsilon > 0$ has to be sufficiently small to guarantee that the the fast subsystem is, at the same time, sufficiently fast to guarantee boundedness along the flows of the slow subsystem, and such that the trajectories will reach a sufficiently small ball around the origin every time the jumps are triggered.

A Mini-Batch Identifier for Enhanced Initial Convergence

We conclude this section with a modification of the above strategy to ensure a faster observer response, obtained by means of a discrete-time identifier. The need to employ a higher number of state variables, in addition to performing the minimization of a cost function, clearly makes this method more computationally intensive. However, some strategies can be adopted to mitigate the online burden and enable implementation in embedded computing systems (e.g., moving the procedure in a lower priority/frequency task).

Firstly, recall that a perturbed estimate of $\chi\zeta_\chi$ can be computed as $\mathcal{C}[\hat{\zeta}_\chi]\mathcal{J}\hat{h}$. From the solutions of system (4.14) it can be noted that, for any positive scalar T, for all $t \geq T$:

$$\zeta_\chi(t) - \zeta_\chi(t-T) = \xi\mathcal{J}\int_{t-T}^{t} \chi(s)\zeta_\chi(s)ds. \tag{4.110}$$

Hence by multiplying both sides by $\chi(t-T)\chi(t)$ it follows (let $y(s) = \chi(s)\zeta_\chi(s)$):

$$\chi(t-T)y(t) - \chi(t)y(t-T) = \xi\chi(t-T)\chi(t)\mathcal{J}\int_{t-T}^{t} y(s)ds, \tag{4.111}$$

which can be constructed by means of division-free estimates, since χ can be replaced with $|\hat{h}|$ and y with $\mathcal{C}[\hat{\zeta}_\chi]\mathcal{J}\hat{h}$. Indeed, between jumps of the clock (4.96), we can compactly rewrite (4.111) as $X(t,j) + e_X(t,j) = (\Phi(t,j) + e_\Phi(t,j))\xi$, where X and Φ are only function of $\hat{h}$, $\hat{\zeta}_\chi$, their past values and their integrals, while e_X and e_Φ are disturbances depending on h and $\tilde{h}$. For $N \in \mathbb{N}_{\geq 1}$, let $\tau_N(\cdot)$ be a moving window operator such that, for a hybrid arc ψ satisfying jumps according to the clock (4.96) (with $\rho(0,0) = 0$), and for all $(t,j) \in \operatorname{dom}\psi$ such that $j \geq N$:

$$\tau(\psi)(t,j) = \begin{pmatrix} \psi\left((j-N+1)/\Lambda, j-N\right) \\ \vdots \\ \psi\left(j/\Lambda, j-1\right) \end{pmatrix}. \tag{4.112}$$

Choosing $T = 1/\Lambda$ as interval of integration in (4.111), we thus obtain a simple estimate of ξ through a batch least-squares algorithm as follows (see (Bin, Bernard, and Marconi, 2019) for the same structure in the context of output regulation):

$$\begin{aligned} \xi^*(t,j) &= \operatorname{argmin}_{\theta\in\mathbb{R}} J_N(\theta)(t,j) \\ J_N(\theta)(t,j) &:= |\tau_N(X)(t,j) - \tau_N(\Phi)(t,j)\theta|^2. \end{aligned} \tag{4.113}$$

To implement the above strategy, the hybrid observer in (4.105) is augmented with an identifier based on the shift register variables $Y^\mu = (Y_0^\mu, \ldots, Y_N^\mu) \in \mathbb{R}^{2(N+1)}$, $Z^\mu = (Z_0^\mu, \ldots, Z_N^\mu) \in \mathbb{R}^{N+1}$, $\Phi^\mu = (\Phi_1^\mu, \ldots, \Phi_N^\mu) \in \mathbb{R}^{2N}$, related to the moving window operator as $\tau_N(\Phi) = \Phi^\mu$, $\tau_N(X) = (X_1^\mu, \ldots, X_N^\mu)$, $X_i^\mu = Z_{i-1}^\mu Y_i^\mu - Z_i^\mu Y_{i-1}^\mu$,

$i \in \{1, \ldots, N\}$):

$$\begin{cases} \dot{\nu} = \mathcal{C}[\hat{\zeta}_X]\mathcal{J}\hat{h} \\ \dot{Y}^\mu = 0 \\ \dot{Z}^\mu = 0 \\ \dot{\Phi}^\mu = 0 \end{cases} \qquad \rho \in [0,1]$$
$$\begin{cases} \nu^+ = 0 \\ (Y_i^\mu)^+ = Y_{i+1}^\mu, \quad i \in \{0, \ldots, N\} \\ (Y_N^\mu)^+ = \mathcal{C}[\hat{\zeta}_X]\mathcal{J}\hat{h} \\ (Z_i^\mu)^+ = Z_{i+1}^\mu, \quad i \in \{0, \ldots, N\} \qquad \rho = 1 \\ (Z_N^\mu)^+ = |\hat{h}| \\ (\Phi_i^\mu)^+ = \Phi_{i+1}^\mu, \quad i \in \{1, \ldots, N\} \\ (\Phi_N^\mu)^+ = \mathcal{J}\nu|\hat{h}|Z_N^\mu \end{cases} \tag{4.114}$$
$$\xi^*(t,j) = \mathcal{G}[Y^\mu, Z^\mu, \Phi^\mu](t,j) = \text{argmin}_{\theta \in \mathbb{R}} J_N(\theta)(t,j),$$

where the standard Moore-Penrose pseudoinverse can be used to minimize J_N. The jump map of $\hat{\xi}$ can be then modified as a function of $\hat{\xi}(t,j)$ and $\xi^*(t,j)$. Without intending to provide a formal stability result for this modification, which will be the topic of future research activity, we propose to jump according to two criteria, which are the "readiness" of the shift register and the error $\hat{\xi} - \xi^*$:

$$\hat{\xi}^+ = \begin{cases} \hat{\xi} & j \leq N+1 \text{ or } |\hat{\xi} - \xi^*| \leq 4\sqrt{\gamma} \\ \xi^* & \text{otherwise.} \end{cases} \tag{4.115}$$

This way it is possible to ensure that, if the regression errors e_X, e_Φ are sufficiently small, the above jump improves the estimate $\hat{\xi}$ by guaranteeing x_s^+ to be close to the set $W_1 \leq 2$ in (4.98) (where $4\sqrt{\gamma}$ was employed to account for the worst case scenario). Within such set, the local behavior of the attitude observer becomes dominant, guaranteeing a desirable residual behavior. Finally, note that the errors e_X, e_Φ can be made arbitrarily small, for any jump of the overall system. This is possible because e_X, e_Φ vanish as $\tilde{h} \to 0$ and, by proper selection of the gains of the fast subsystem, $\tilde{h}$ can be forced to converge during flows in an arbitrarily small ball, before the first jump occurs.

Numerical Comparison of the Proposed Observers

Here we provide some comparative simulation results, in order to show how the hybrid sensorless observer modifies the transient behavior of the system. As we did before, we tested the observers in open loop to highlight the transient behavior of the estimation error. The chosen parameters for the presented results are the same as in Table 4.1, with the same choice of gains for the continuous time part of the observer. For what concerns the discrete-time half of the observers, we chose $\Lambda = 200$, $N = 2$. Notably, it is possible to appreciate that the hybrid observer (4.105), with no batch identifier, already provides a convergence speedup. This is motivated by the intuition that the jumps, for Λ sufficiently large, impose the position estimation error to be close, during transients, either to $\eta = (0,1)$, or to $\eta = (0,-1)$: these configurations are associated with the maximal value of $\dot{\hat{\xi}}$. For this reason, we can expect

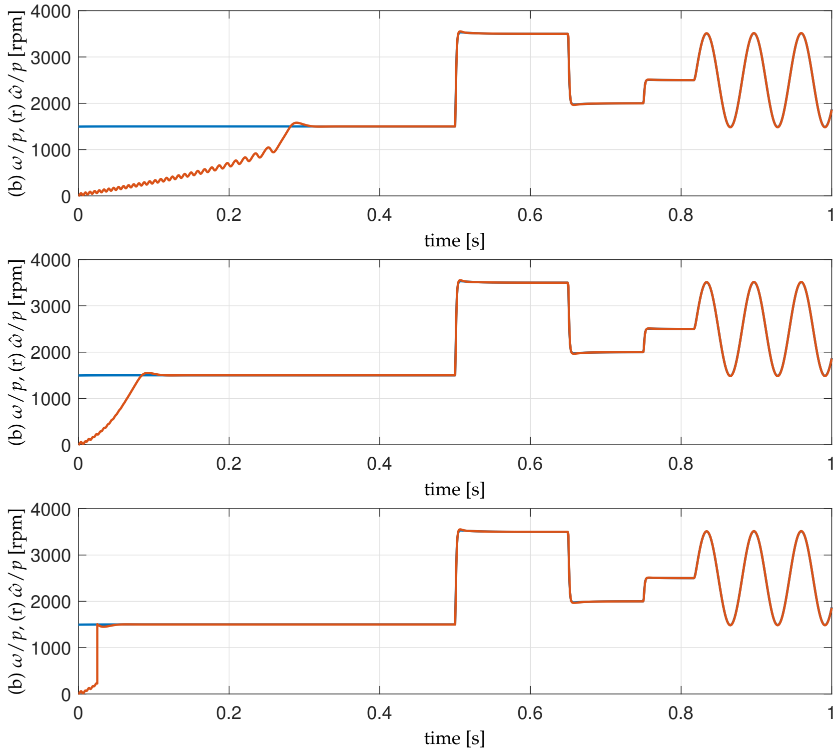

FIGURE 4.13: Speed estimation comparison. (Top): continuous-time observer. (Center): hybrid observer (4.105). (Bottom): hybrid observer with mini-batch identifier.

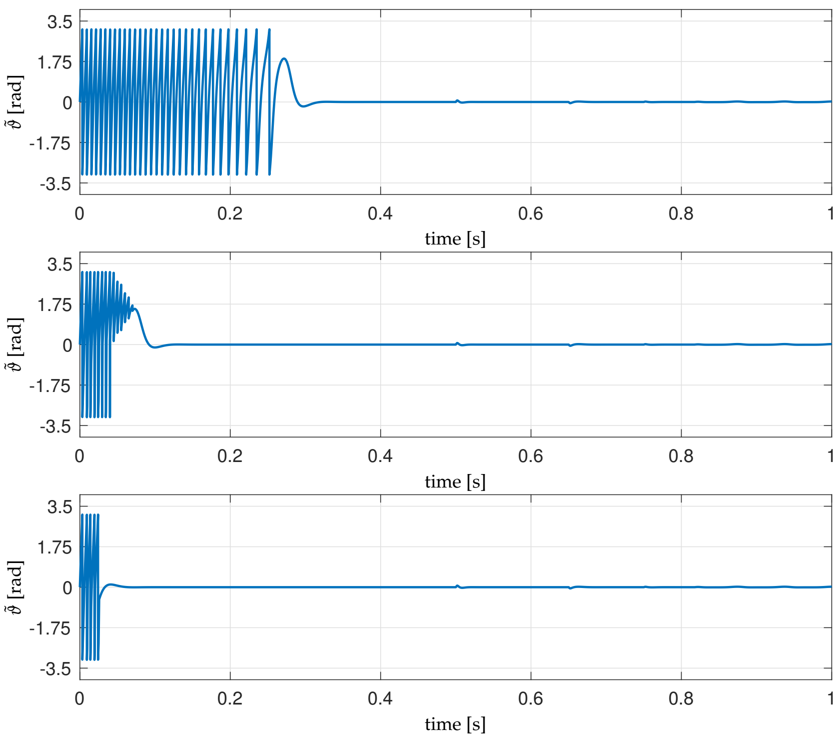

FIGURE 4.14: Position estimation error comparison. (Top): continuous-time observer. (Center): hybrid observer (4.105). (Bottom): hybrid observer with mini-batch identifier.

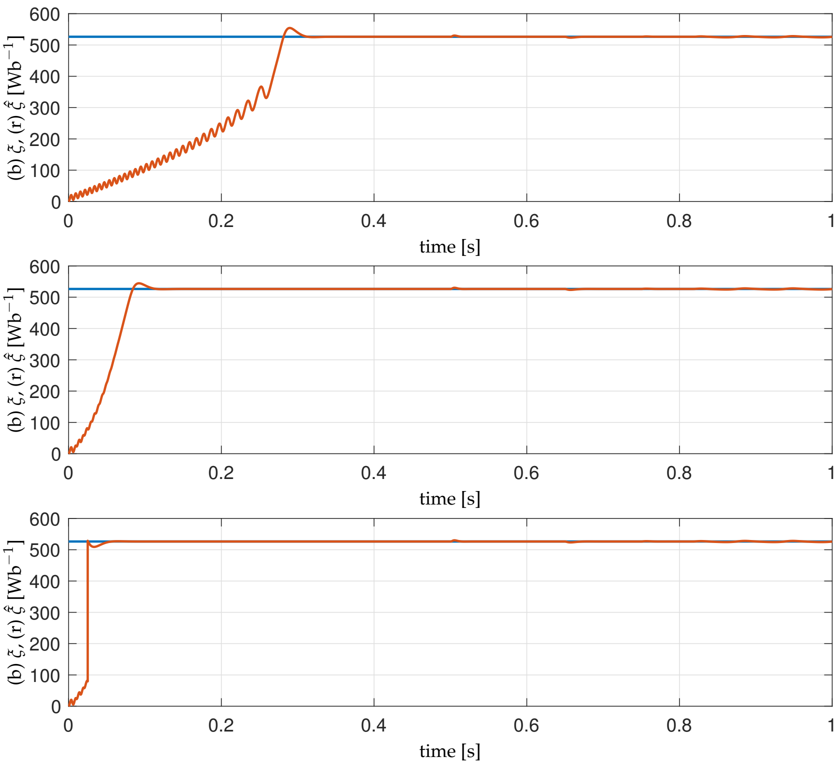

FIGURE 4.15: Inverse flux estimation comparison. (Top): continuous-time observer. (Center): hybrid observer (4.105). (Bottom): hybrid observer with mini-batch identifier.

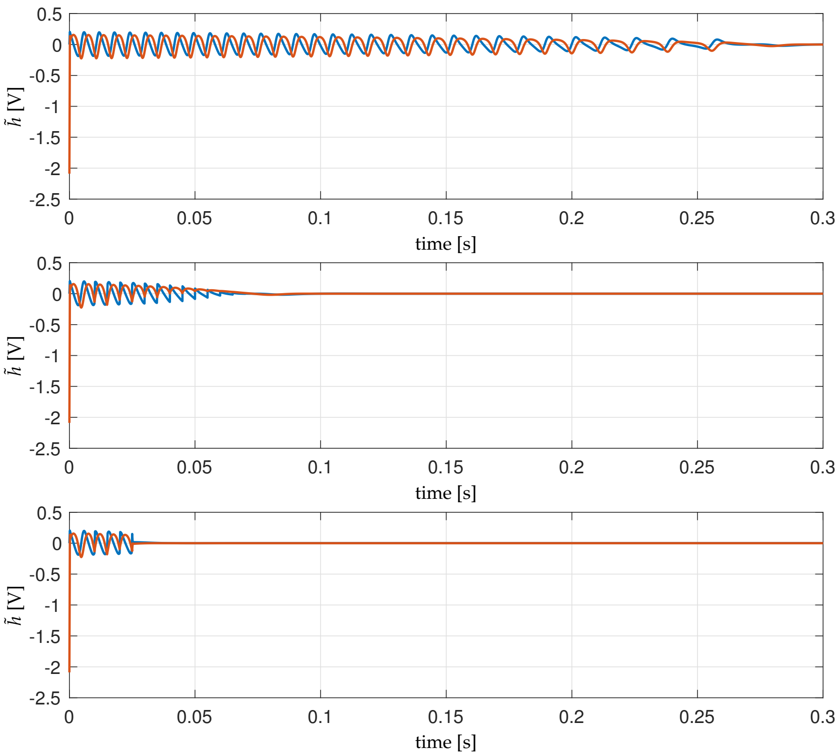

FIGURE 4.16: Back-EMF estimation error comparison. (Top): continuous-time observer. (Center): hybrid observer (4.105). (Bottom): hybrid observer with mini-batch identifier.

that there exists a range for initial conditions of $|\tilde{\xi}|$ where the convergence properties of this observer are optimized. In particular, this range is expected to be between very large initial errors, where the continuous time angular "wraps" dominate the behavior, and small initial errors, where jumps do not cause an estimation correction. Finally, note how the mini-batch identifier significantly boosts the convergence properties, even when a very small sample window is used.

4.5 Future Directions

Several research directions can be pursued from the results of this work. Without aiming to be exhaustive, we indicate some challenges that are currently of interest for further investigation.

Firstly, it will be essential to include robust strategies to account for saturations, constraints and power converter uncertainties. In particular, a significant source of performance deterioration (both from the estimation and actuation viewpoints) is caused by the so-called dead-times, an undesirable feature adopted in power converter driving strategies to avoid short circuits, and which corresponds to an unmeasurable time-varying disturbance for the current dynamics. We refer to (Tilli, Conficoni, and Bosso, 2017) for a recent work on sensorless observation with estimation and compensation of dead-time disturbances.

Furthermore, an inherently non-local stability analysis of closed loop control operation, with the related connections with constrained control, should be investigated to provide solid guarantees in several demanding applications. In this context it will also be crucial to relax the assumptions on the speed profile, handling in particular the low/very low speed scenarios.

The proposed resistance estimation scheme looks promising not only for its performance enhancement features, but also as a possible instrument to perform diagnosis of incipient faults (see Atamuradov et al., 2017; Nandi, Toliyat, and Li, 2005 and references therein). Notably, interesting connections could be established with the so-called Model-of-Signals approach presented e.g. in (Barbieri et al., 2018; Barbieri, Diversi, and Tilli, 2020).

Finally, future work will be dedicated to the extension of this approach to other classes of electric machines including, among the others, Induction Motors and Interior Permanent Magnets Electric Machines (IPMSMs), which are becoming increasingly relevant in several application domains.

Appendix A

Elements of Lyapunov Stability Theory for Time-Varying Systems

In this Appendix, we briefly review for completeness some important stability results related to time-varying systems, focusing on invariance-like results. These are of critical importance when dealing with adaptive systems. For a basic introduction on Lyapunov stability theory for time-invariant systems, we refer to (Khalil, 2002, Chapter 4).

We begin with the classical result by Barbalăt, which is ubiquitous in adaptive control literature, followed by the stronger result provided by LaSalle and Yoshizawa.

Lemma A.1 (Barbalăt's Lemma)**.** *Let $\phi : \mathbb{R} \to \mathbb{R}$ be a uniformly continuous function defined on $[0, \infty)$. Suppose that the limit*

$$\lim_{t\to\infty} \int_0^t \phi(s)ds \tag{A.1}$$

exists and is finite. Then, it holds

$$\lim_{t\to\infty} \phi(t) = 0. \tag{A.2}$$

Proof. See (Khalil, 2002, Lemma 8.2) or (Krstic, Kanellakopoulos, and Kokotovic, 1995, Lemma A.6) for the same steps. Suppose (A.2) does not hold, then there exists $\varepsilon > 0$ such that, for every $T > 0$, there exists $T' > T$ with $|\phi(T')| > \varepsilon$. By uniform continuity, there exists $\delta > 0$ such that $|\phi(t+\tau) - \phi(t)| < \varepsilon/2$, for all $t' > 0$ and all $t \in [0, \delta]$. Therefore

$$\begin{aligned} |\phi(t)| &= |\phi(t) - \phi(T') + \phi(T')| \\ &\geq |\phi(T')| - |\phi(t) - \phi(T')| \\ &> \varepsilon - \frac{\varepsilon}{2} = \frac{\varepsilon}{2}, \qquad t \in [T', T' + \delta]. \end{aligned} \tag{A.3}$$

This means that (the sign of $\phi(t)$ is preserved in the interval $[T', T' + \delta]$):

$$\left| \int_{T'}^{T'+\delta} \phi(t)dt \right| = \int_{T'}^{T'+\delta} |\phi(t)|\, dt > \delta \frac{\varepsilon}{2}. \tag{A.4}$$

For this reason (A.1) does not hold, hence we have a contradiction. □

Note that Barabalăt's Lemma does not provide any indication about the convergence rate, and indeed this result is non-uniform thus, inherently, non-robust.

Consider a time-varying system of the form

$$\dot{x} = f(t, x), \tag{A.5}$$

where f is piecewise continuous in $[0,\infty)$ and locally Lipschitz in $x \in \mathbb{R}^n$, uniformly in t. We suppose that the origin $x = 0$ is an equilibrium for system (A.5) if it holds $f(t,0) = 0$, for all $t \geq 0$.

Theorem A.1 (LaSalle-Yoshizawa). *Consider system (A.5) and let $V : \mathbb{R}_{\geq 0} \times \mathbb{R}^n \to \mathbb{R}_{\geq 0}$ be a continuously differentiable function satisfying*

$$\begin{aligned} &\underline{\alpha}(|x|) \leq V(t,x) \leq \overline{\alpha}(|x|) \\ &\frac{\partial V}{\partial t} + \frac{\partial V}{\partial x} f(t,x) \leq -W(x), \end{aligned} \tag{A.6}$$

for all $t \geq 0$ and all $x \in \mathbb{R}^n$, where $\underline{\alpha}(\cdot)$, $\overline{\alpha}(\cdot)$ are class $\mathcal{K}_\infty$ functions, and $W : \mathbb{R}^n \to \mathbb{R}_{\geq 0}$ is a continuous positive semi-definite function. Then, the origin of system (A.5) is uniformly globally stable and, in addition:

$$\lim_{t\to\infty} W(x(t)) = 0. \tag{A.7}$$

Proof. Consider an arbitrary initial condition $(t_0, x_0) \in \mathbb{R}_{\geq 0} \times \mathbb{R}^n$, and indicate with $x(t) = x(t; t_0, x_0)$ the corresponding solution. By basic results on existence and uniqueness of solutions, there exists a maximal interval $[t_0, t_0 + \delta)$ such that the solution $x(t)$ is uniquely defined. Let $V(t) = V(t, x(t; t_0, x_0))$, then $\dot{V}(t) \leq 0$ and hence $V(t, x(t; t_0, x_0)) \leq V(t_0, x_0)$, which means that:

$$|x(t)| \leq (\underline{\alpha}^{-1} \circ \overline{\alpha})(|x_0|) = B(x_0). \tag{A.8}$$

It follows that $\delta = \infty$, since for finite δ $x(t)$ would leave any compact set as $t \to t_0$, but this is in contradiction with the bound $B(x_0)$. Let $\rho = (\underline{\alpha}^{-1} \circ \overline{\alpha})(\cdot)$, therefore:

$$|x(t; t_0, x_0)| \leq \rho(|x_0|), \qquad \forall t_0 \geq 0, \forall t \geq t_0, \tag{A.9}$$

which proves uniform global stability of the origin. Note that

$$\int_{t_0}^{t} W(x(s))ds \leq V(t_0, x_0) - V(t), \tag{A.10}$$

while $\lim_{t\to\infty} V(t) = V_\infty$ exists and is finite since $V(t)$ is non-increasing and bounded from below. As a consequence $\lim_{t\to\infty} \int_{t_0}^{t} W(x(s))ds$ exists and is finite. Recall that

$$x(t_2; t_0, x_0) = x(t_1; t_0, x_0) + \int_{t_1}^{t_2} f(s, x(s))ds, \qquad t_2 \geq t_1 \geq t_0, \tag{A.11}$$

and by Lipschitz continuity it holds:

$$|f(t,x)| \leq L|x|, \qquad t \geq t_0, |x| \leq B(x_0), \tag{A.12}$$

for some positive scalar $L > 0$. Hence we have that

$$|x(t_2) - x(t_1)| \leq \int_{t_1}^{t_2} L|x(s)|ds \leq LB(x_0)|t_1 - t_2|, \tag{A.13}$$

for all $t_2 \geq t_1 \geq t_0$. For any $\varepsilon > 0$, let $\delta_\varepsilon = \varepsilon/(LB(x_0))$, so that

$$|t_1 - t_2| < \delta_\varepsilon \implies |x(t_1) - x(t_2)| < \varepsilon. \tag{A.14}$$

therefore $x(t)$ is uniformly continuous. In addition, since $W(x)$ is continuous, it is also uniformly continuous in the compact set $\{x : |x| \leq B(x_0)\}$. From uniform continuity of $W(x(t))$, all sufficient conditions of Barbalăt's Lemma, hence $W(x(t)) \to 0$ as $t \to \infty$. □

Instrumental to establishing asymptotic stability in the context of adaptive systems are the following theorems.

Theorem A.2 (Anderson and Moore). *Consider system (A.5) and let $V : \mathbb{R}_{\geq 0} \times \mathbb{R}^n \to \mathbb{R}_{\geq 0}$ be a continuously differentiable function satisfying*

$$\begin{aligned} &\underline{\alpha}(|x|) \leq V(t,x) \leq \overline{\alpha}(|x|) \\ &\frac{\partial V}{\partial t} + \frac{\partial V}{\partial x} f(t,x) \leq 0, \end{aligned} \tag{A.15}$$

for all $t \geq 0$ and all $x \in \mathbb{R}^n$, where $\underline{\alpha}(\cdot)$, $\overline{\alpha}(\cdot)$ are class $\mathcal{K}_\infty$ functions. Assume, in addition, that there exist $\delta > 0$ and $\lambda \in (0,1)$ such that

$$\int_t^{t+\delta} \dot{V}(s, \chi(s;t,x))ds \leq -\lambda V(t,x) \tag{A.16}$$

for all $t \geq 0$ and all $x \in \mathbb{R}^n$, where $\chi(s;t,x)$ is the solution of system (A.5), at time τ, originated from the initial condition (t,x). Then, the equilibrium $x = 0$ is uniformly globally asymptotically stable. Furthermore, if for some positive scalars a_1, a_2 and ρ the comparison functions $\underline{\alpha}(\cdot)$, $\overline{\alpha}(\cdot)$ satisfy

$$\underline{\alpha}(s) \geq a_1 s^2, \qquad \overline{\alpha}(s) \leq a_2 s^2 \tag{A.17}$$

for all $s \in [0, \rho)$, then the equilibrium $x = 0$ is uniformly globally asymptotically stable and locally exponentially stable.

Proof. This proof can be found, e.g., in (Khalil, 2002, Theorem 8.5). Following the proof of Theorem A.1, we have that

$$|x(t)| \leq (\underline{\alpha}^{-1} \circ \overline{\alpha})(|x_0|) = B(x_0). \tag{A.18}$$

For all $t \geq t_0$, it holds

$$V(t+\delta, x(t+\delta;t_0,x_0)) \leq V(t, x(t;t_0,x_0)) - \lambda V(t, x(t;t_0,x_0)) = (1-\lambda)V(t, x(t;t_0,x_0)), \tag{A.19}$$

and note in addition that

$$V(s, x(s;t_0,x_0)) \leq V(t, x(t;t_0,x_0)), \qquad s \in [t, t+\delta]. \tag{A.20}$$

For $t \geq t_0$, let N be the smallest positive integer such that $t \leq t_0 + N\delta$. Divide the interval $[t_0, t_0 + (N-1)\delta]$ into $N-1$ subintervals of length δ. It holds:

$$\begin{aligned} V(t, x(t;t_0,x_0)) &\leq (1-\lambda)^{N-1} V(t_0, x_0) \\ &\leq \frac{(1-\lambda)^{\frac{t-t_0}{\delta}}}{1-\lambda} V(t_0, x_0) \\ &\leq m \exp(-\alpha(t-t_0)) V(t_0, x_0), \quad m = \frac{1}{1-\lambda}, \quad \alpha = \frac{1}{\delta} \log \frac{1}{1-\lambda}, \end{aligned} \tag{A.21}$$

hence we have that

$$|x(t;t_0,x_0)| \leq \underline{\alpha}^{-1}\left(m\exp(-\alpha(t-t_0))\overline{\alpha}(|x_0|)\right) =: \beta(|x_0|, t-t_0), \tag{A.22}$$

where $\beta(\cdot,\cdot)$ is a class $\mathcal{KL}$ function. Thus the origin is uniformly globally asymptotically stable. Replace $\underline{\alpha}(\cdot)$, $\overline{\alpha}(\cdot)$ with their local quadratic bounds to yield local exponential stability. □

Similar to Theorem A.2 we also find (Sastry and Bodson, 2011, Theorem 1.5.2), where in particular only the quadratic bounds for exponential stability are considered.

Consider a linear time-varying system of the form:

$$\begin{aligned} \dot{x} &= A(t)x \\ y &= C(t)x \end{aligned} \tag{A.23}$$

with $x \in \mathbb{R}^n$, $y \in \mathbb{R}^m$ and $A : \mathbb{R}_{\geq 0} \to \mathbb{R}^{n\times n}$, $C : \mathbb{R}_{\geq 0} \to \mathbb{R}^{m\times n}$ piecewise continuous and bounded functions. Denote with Φ the transition matrix associated with A, then define the observability Gramian as follows:

$$W(t_1,t_2) = \int_{t_1}^{t_2} \Phi^T(s,t_1)C^T(s)C(s)\Phi(s,t_1)ds. \tag{A.24}$$

Proposition A.1. *Suppose that the pair (C, A) of system (A.23) is uniformly completely observable (UCO), that is, there exist positive scalars δ, k such that*

$$W(t, t+\delta) \geq kI, \qquad \forall t \geq 0. \tag{A.25}$$

Furthermore, suppose that there exists a continuously differentiable and symmetric map $P : \mathbb{R} \to \mathbb{R}^{n\times n}$, solution of the differential equation

$$\dot{P}(t) + A^T(t)P(t) + P(t)A(t) \leq -C^T(t)C(t), \qquad c_1 I \leq P(t) \leq c_2 I, \tag{A.26}$$

for all $t \geq 0$ and for some positive scalars c_1, c_2. Then, the origin is uniformly globally asymptotically stable.

Proof. Consider the Lyapunov function

$$V(t,x) = x^T P(t) x, \tag{A.27}$$

then it holds, along the solutions of system (A.23):

$$\dot{V}(t,x) \leq -x^T C^T(t) C(t) x \leq 0. \tag{A.28}$$

By Theorem A.1, system (A.23) is uniformly globally stable and, in addition, $y(t) \to 0$ as $t \to \infty$. Let

$$\begin{aligned} H(t,x) &= \int_t^{t+\delta} \dot{V}(s, \chi(s;t,x))ds \\ &\leq -x^T \int_t^{t+\delta} \Phi^T(s,t)C^T(s)C(s)\Phi(s,t)dsx, \end{aligned} \tag{A.29}$$

which yields

$$H(t,x) \leq -k|x|^2 \leq \frac{k}{2}V(t,x). \tag{A.30}$$

By Theorem A.2, it follows that the origin of system (A.23) is uniformly globally asymptotically stable. □

The above result is fundamental for several adaptive and continuous-time identification results. Given a piecewise continuous and bounded function $\psi : \mathbb{R}_{\geq 0} \to \mathbb{R}^n$, we say that ψ is persistently exciting (PE) if the pair $(\psi^T, 0_{n\times n})$ is uniformly completely observable. Furthermore, it is known that uniform complete observability is invariant to output injection, as formally shown in the following result.

Proposition A.2. *Suppose that, for all $\delta > 0$, there exists a non-negative scalar k such that, for all $t \geq 0$:*

$$\int_t^{t+\delta} |K(s)|^2 ds \leq k. \tag{A.31}$$

Then, the pair (C, A) is uniformly completely observable if and only if the system $(C, A + KC)$ is uniformly completely observable. Furthermore, if the observability gramian of (C, A), W, satisfies

$$\alpha_1 I \leq W(t, t+\delta) \leq \alpha_2 I, \tag{A.32}$$

then the observability gramian of $(C, A + KC)$ satisfies a similar condition with the same δ, and the bounds given by

$$\alpha_1' = \frac{\alpha_1}{(1 + \sqrt{k\alpha_2})^2}, \qquad \alpha_2' = \alpha_2 \exp(k\alpha_2). \tag{A.33}$$

We also recall an important equivalence between uniform asymptotic stability and exponential stability when dealing with linear time-varying systems (Sastry and Bodson, 2011, Proposition 1.5.5).

Proposition A.3. *The origin of system (A.23) is globally exponentially stable if and only if it is uniformly globally asymptotically stable.*

All the above tools are instrumental to prove crucial results such as the following, arising in continuous-time system identification (Sastry and Bodson, 2011, Theorem 2.5.1).

Theorem A.3. *Suppose that the piecewise continuous and bounded function $\psi : \mathbb{R}_{\geq 0} \to \mathbb{R}^n$ is persistently exciting, then the origin of system*

$$\dot{x} = -\gamma \psi(t) \psi^T(t) x, \tag{A.34}$$

with γ a positive scalar, is globally exponentially stable.

Proof. Since ψ is PE, then by Proposition A.2, the pair $(\psi^T, -\gamma\psi\psi^T)$ is uniformly completely observable (we chose $K = -\gamma\psi$). To prove global exponential stability of the origin of the above system, apply Theorem A.2 to system

$$\begin{aligned} \dot{x} &= \gamma \psi(t) \psi^T(t) x \\ y &= \psi^T(t) x, \end{aligned} \tag{A.35}$$

with $V = |x|^2/(2\gamma)$, $P(t) = I/(2\gamma)$. □

We refer e.g. to (Barabanov and Ortega, 2017) for works analyzing the convergence properties of the above system when ψ is not persistently exciting.

Appendix B

Proofs

B.1 Proof of Lemma 4.2

See Appendix A for all the definitions and basic results employed in the following. Due to the upper triangular structure of system (4.88), we have that the $(e, \tilde{\imath})$-subsystem is globally exponentially stable, hence there exist positive scalars $a_{1\mathrm{f}}$, $a_{2\mathrm{f}}$ such that:

$$\left|\begin{matrix} e(\tau) \\ \tilde{\imath}(\tau) \end{matrix}\right| \leq a_{1\mathrm{f}} \exp\left(-a_{2\mathrm{f}}\tau\right) \left|\begin{matrix} e(0) \\ \tilde{\imath}(0) \end{matrix}\right| \tag{B.1}$$

The proof collapses then to the stability analysis of the z-subsystem, which is written as:

$$\begin{aligned} \frac{d}{dt}z &= -\bar{\kappa}_z(\underbrace{\Omega_w\Omega_w^T}_{M_w(w,e,\tilde{\imath})} + \underbrace{\Omega_t\Omega_t^T}_{M_t(e,\tilde{\imath},t^*)})z \\ \Omega_w &= \begin{pmatrix} -w_1 - e_1 - \tilde{\imath}_1 \\ 1 \\ 0 \end{pmatrix} \qquad \Omega_t = \begin{pmatrix} -i_{\mathrm{q}}^* - e_2 - \tilde{\imath}_2 \\ 0 \\ 1 \end{pmatrix} \end{aligned} \tag{B.2}$$

with $\Omega = \begin{pmatrix} \Omega_w(w, e, \tilde{\imath}) & \Omega_t(e, \tilde{\imath}, t^*) \end{pmatrix}$. The main idea is to exploit the richness properties of w, regardless of the fact that both Ω_w and Ω_t are not individually persistently exciting (PE). Firstly, we want to prove that, for any bounded $e(0)$, $\tilde{\imath}(0)$, the pair $(\Omega^T, 0_{3\times 3})$ is uniformly completely observable (UCO), i.e.:

$$\alpha_1 \leq \int_\tau^{\tau+\delta} \underbrace{x^T M(i_{\hat{\chi}}^*(w(s), t^*) + e(s) + \tilde{\imath}(s))x}_{x^T\Omega_w\Omega_w^T x + x^T\Omega_t\Omega_t^T x}\, ds \leq \alpha_2, \tag{B.3}$$

for some positive scalars α_1, α_2, δ, for all $x = \begin{pmatrix} x_1 & x_2 & x_3 \end{pmatrix}^T \in \mathbb{R}^3$ satisfying $|x| = 1$. Let $\Omega_0(\tau) = \Omega(i_{\hat{\chi}}^*(w(\tau), t^*))$ and $M_0(\tau) = \Omega_0(\tau)\Omega_0^T(\tau)$, then it follows that (for $\delta = 2\pi$)

$$\begin{aligned} \int_\tau^{\tau+\delta} x^T M_0(s) x ds = & \int_\tau^{\tau+\delta} [x_1^2 w_1^2(s) - 2x_1 x_2 w_1(s)] ds \\ & + \delta(x_1^2(i_{\mathrm{q}}^*)^2 - 2x_1 x_3 i_{\mathrm{q}}^* + x_2^2 + x_3^2) \\ \geq & \ \pi|w(0)|^2 x_1^2 + 2\pi(x_2^2 + x_3^2) \\ & + 2\pi x_1^2(i_{\mathrm{q}}^*)^2 - 4\pi|x_1||x_3|I^* \\ \geq & \ \pi|w(0)|^2 x_1^2 + 2\pi(x_2^2 + x_3^2) \\ & + 2\pi x_1^2(i_{\mathrm{q}}^*)^2 - \frac{2\pi}{\rho}(x_1 I^*)^2 - \rho 2\pi x_3^2, \end{aligned} \tag{B.4}$$

for any positive scalar ρ. Choose $\rho \in (0,1)$ and W^* sufficiently large to enforce that all coefficients multiplying x_i, $i \in \{1,2,3\}$, are positive. Hence the pair $(\Omega_0^T, 0_{3\times 3})$ is UCO. Denote with β_1 the UCO lower bound of $(\Omega_0^T, 0_{3\times 3})$, and let $\Omega = \Omega_0 + \Delta\Omega(e,\tilde{\imath})$, with $\Delta\Omega = \begin{pmatrix}\Delta\Omega_w & \Delta\Omega_t\end{pmatrix}$ Note that the following chain of inequalities holds, for $i \in \{1,2\}$:

$$\begin{aligned} |e(\tau)+\tilde{\imath}(\tau)| \leq |e(\tau)| + |\tilde{\imath}(\tau)| \leq 2\left|\begin{matrix} e(\tau) \\ \tilde{\imath}(\tau)\end{matrix}\right| \\ \leq 2a_{1\mathrm{f}} \exp\left(-a_{2\mathrm{f}}\tau\right)\left|\begin{matrix} e(0) \\ \tilde{\imath}(0)\end{matrix}\right|. \end{aligned} \tag{B.5}$$

Following (Sastry and Bodson, 2011, Lemma 6.1.2), apply the triangle inequality to yield:

$$\begin{aligned} \sqrt{\int_\tau^{\tau+\delta} x^T M x ds} &= \sqrt{\int_\tau^{\tau+\delta} \left|\begin{pmatrix}\Omega_w^T \\ \Omega_t^T\end{pmatrix} x\right|^2 ds} \\ &= \sqrt{\int_\tau^{\tau+\delta} \left|\Omega_0^T x + \begin{pmatrix}\Delta\Omega_w^T \\ \Delta\Omega_t^T\end{pmatrix} x\right|^2 ds} \\ &\geq \sqrt{\beta_1} - \sqrt{\int_\tau^{\tau+\delta} |e+\tilde{\imath}|^2 ds} \\ &\geq \sqrt{\beta_1} - 2\sqrt{\delta}\max_{s\geq\tau}\left|\begin{matrix} e(s) \\ \tilde{\imath}(s)\end{matrix}\right| \\ &\geq \sqrt{\beta_1} - 2\sqrt{\delta} a_{1\mathrm{f}} \exp\left(-a_{2\mathrm{f}}\tau\right)\left|\begin{matrix} e(0) \\ \tilde{\imath}(0)\end{matrix}\right|. \end{aligned} \tag{B.6}$$

Therefore, it is sufficient that

$$\left|\begin{matrix} e(0) \\ \tilde{\imath}(0)\end{matrix}\right| < \frac{1}{2a_{1\mathrm{f}}}\sqrt{\frac{\beta_1}{2\pi}} \tag{B.7}$$

in order to yield $(\Omega^T, 0_{3\times 3})$ UCO, with lower bound denoted with α_1. If the initial conditions do not satisfy (B.7), clearly it is sufficient to wait a finite time T such that

$$T > \frac{1}{a_{2\mathrm{f}}}\log\left(\left|\begin{matrix} e(0) \\ \tilde{\imath}(0)\end{matrix}\right| 2a_{1\mathrm{f}}\sqrt{\frac{2\pi}{\beta_1}}\right) \tag{B.8}$$

to recover the previous UCO property, with the same lower bound, a possibly higher upper bound, and $\delta = T + 2\pi$. Indeed, it is sufficient to note that:

$$\begin{aligned} \int_\tau^{\tau+T+2\pi} x^T M x ds &= \int_\tau^{\tau+T} x^T M x ds + \int_{\tau+T}^{\tau+T+2\pi} x^T M x ds \\ &\geq \int_{\tau+T}^{\tau+T+2\pi} x^T M x ds \geq \alpha_1. \end{aligned} \tag{B.9}$$

Pick an arbitrary positive scalar $c > 0$, and choose any initial condition satisfying $|(e(0),\tilde{\imath}(0))| \leq c$, with arbitrary $|z(0)|$. We have that $(\Omega^T, 0_{3\times 3})$ is UCO, with bounds depending on c. By classic identification results, $(\Omega^T, 0_{3\times 3})$ UCO if and only if so is

$(\Omega^T, -\Omega\Omega^T)$. Consider $V = z^T z/(2\bar{\kappa}_z)$, then:

$$\int_{\tau}^{\tau+\delta} \frac{d}{ds} V(s) ds = \int_{\tau}^{\tau+\delta} -z(s)^T \Omega\Omega^T z(s) ds \leq -\alpha |z(\tau)|^2, \tag{B.10}$$

for some α such that $0 < 1 - 2\bar{\kappa}_z \alpha < 1$. From (Sastry and Bodson, 2011, Theorem 1.5.3) we have:

$$|z(\tau)| \leq \sqrt{\frac{1}{1 - 2\bar{\kappa}_z \alpha}} \exp\left(-\frac{1}{2\delta} \log\left(\frac{1}{1 - 2\bar{\kappa}_z \alpha}\right) \tau\right) |z(0)|. \tag{B.11}$$

See also Theorem A.2 for a generalized form of these bounds.

Since α and δ are fixed, once c is selected, and the exponential decay holds uniformly in the specified initial conditions, it follows that the origin of (4.88) is locally exponentially stable. We cannot infer global exponential stability, though, because these parameters change once a larger (compact) set of initial conditions is selected. However, note that $\delta \to \infty$ only if $c \to \infty$, therefore the convergence rate becomes increasingly smaller as the initial conditions grow in norm, but it is always non-zero in any compact set. From these arguments, and the fact that the bounds hold uniformly in time, it follows that the origin of (4.88) is globally asymptotically stable.

B.2 Proof of Theorem 4.3

As a consequence of Assumption 4.1, we can define a hybrid system that admits, as possible solution, the signal $\chi(\cdot)$, that is:

$$\mathcal{H}_\chi : \quad \begin{cases} \dot{\chi} \in F_\chi(\chi), & (\chi, \rho) \in \Omega_\chi \times [0, 1], \\ \chi^+ = \chi, & (\chi, \rho) \in \Omega_\chi \times \{1\}, \end{cases} \tag{B.12}$$

with $\Omega_\chi = [\chi_{\min}, \chi_{\max}]$ and $F_\chi(\cdot)$ a convex, outer semicontinuous map satisfying $\max_{f \in F_\chi(\chi)} |f| \leq M$, for all $\chi \in \Omega_\chi$. The interconnection $\mathcal{H}_\chi$ - $\mathcal{H}_0$ is well-posed, and it follows from Lemma 4.3 that the compact set $\mathcal{A}_s = \Omega_\chi \times \mathcal{A}_0$ is uniformly preasymptotically stable, with basin of preattraction given by $\mathbb{R} \times \mathbb{S}^1 \times \mathbb{R}^2$. From (Cai, Teel, and Goebel, 2008, Theorem 3.14), it follows that for any proper indicator function σ of $\mathcal{A}_s$ in $\mathbb{R} \times \mathbb{S}^1 \times \mathbb{R}^2$, there exist class $\mathcal{K}_\infty$ functions $\underline{\alpha}$, $\overline{\alpha}$ and a smooth function $V_s : \mathbb{R} \times \mathbb{S}^1 \times \mathbb{R}^2 \to \mathbb{R}_{\geq 0}$ such that:

$$\begin{aligned} &\underline{\alpha}(\sigma(\chi, x_s)) \leq V_s(\chi, x_s) \leq \overline{\alpha}(\sigma(\chi, x_s)) \\ &\left\langle \nabla V_s(\chi, x_s), \begin{pmatrix} f_1 \\ f_2 \end{pmatrix} \right\rangle \leq -V_s(\chi, x_s), \quad \begin{cases} (\chi, x_s) \in \Omega_\chi \times C_s \\ f_1 \in F_\chi(\chi) \\ f_2 \in F_0(x_s, \chi) \end{cases} \\ &V_s(\chi, g) \leq \exp(-1) V_s(\chi, x_s), \quad \begin{cases} (\chi, x_s) \in \Omega_\chi \times D_s \\ g \in G_0(x_s, \chi). \end{cases} \end{aligned} \tag{B.13}$$

In particular, choose σ such that $\sigma(\chi, x_s) = \sigma_s(x_s)$, for all $\chi \in \Omega_\chi$. Note that we can write

$$\begin{aligned} F_s(x_f, \chi, x_s) &= F_0(x_s, \chi) + \tilde{F}(x_f, \chi, x_s) x_f \\ G_s(x_f, \chi, x_s) &= G_0(x_s, \chi) + \tilde{G}(x_f, \chi, x_s) x_f, \end{aligned} \tag{B.14}$$

and in particular it can be proved that:

$$\begin{aligned}&\left\langle \nabla V_{\mathrm{s}}(\chi, x_{\mathrm{s}}), \begin{pmatrix} f_1 \\ f_2 \end{pmatrix} \right\rangle \leq -V_{\mathrm{s}}(\chi, x_{\mathrm{s}}) + \mu(\sigma(\chi, x_{\mathrm{s}}))|x_{\mathrm{f}}| \\ &(x_{\mathrm{f}}, \chi, x_{\mathrm{s}}) \in \mathbb{R}^4 \times \Omega_\chi \times C_{\mathrm{s}}, f_1 \in F_\chi(\chi), f_2 \in F_{\mathrm{s}}(x_{\mathrm{f}}, \chi, x_{\mathrm{s}}),\end{aligned} \tag{B.15}$$

for some class $\mathcal{K}$ function $\mu(\cdot)$, and similarly for the jumps:

$$\begin{aligned}&V_{\mathrm{s}}(\chi, g) \leq \exp(-1) V_{\mathrm{s}}(\chi, x_{\mathrm{s}}) + \nu(x_{\mathrm{f}}, \chi, x_{\mathrm{s}})|x_{\mathrm{f}}| \\ &(x_{\mathrm{f}}, \chi, x_{\mathrm{s}}) \in \mathbb{R}^4 \times \Omega_\chi \times C_{\mathrm{s}}, g \in G_{\mathrm{s}}(x_{\mathrm{f}}, \chi, x_{\mathrm{s}}),\end{aligned} \tag{B.16}$$

with $\nu(\cdot)$ a positive continuous map. On the other hand, the flows of the fast subsystem are given by:

$$\dot{x}_{\mathrm{f}} \in \varepsilon^{-1} A_{\mathrm{f}} x_{\mathrm{f}} + B_{\mathrm{f}} f_h(x_{\mathrm{f}}, x_{\mathrm{s}}, \chi, F_\chi(\chi), \xi) = F_{\mathrm{f}}(x_{\mathrm{f}}, \chi, x_{\mathrm{s}}), \tag{B.17}$$

with A_{f} such that $A_{\mathrm{f}} + A_{\mathrm{f}}^T = -2I_4$. Consider the Lyapunov function

$$V_{\mathrm{f}}(x_{\mathrm{f}}) = |x_{\mathrm{f}}|, \tag{B.18}$$

whose derivative along the solutions of the system is given by

$$\begin{aligned} D^+ V_{\mathrm{f}} &\leq -\frac{\varepsilon^{-1}}{2V_{\mathrm{f}}} \left(2V_{\mathrm{f}}^2 - 2\varepsilon |B_{\mathrm{f}}| V_{\mathrm{f}} \max_{\chi \in \Omega_\chi} |f_h(\cdot)| \right) \\ &\leq -\varepsilon^{-1} \left(V_{\mathrm{f}} - \varepsilon |B_{\mathrm{f}}| \max_{\chi \in \Omega_\chi} |f_h(\cdot)| \right). \end{aligned} \tag{B.19}$$

Let $\max_{\chi \in \Omega_\chi} |f_h(\cdot)| \leq \bar{f}_h(x_{\mathrm{f}}, x_{\mathrm{s}})$, with $\bar{f}_h$ a continuous function. Note that it holds $V_{\mathrm{f}}^+ = V_{\mathrm{f}}$ for all jumps, as it was shown in the above discussion. Pick arbitrary positive scalars Δ_{s} and Δ_{f} and, without loss of generality, $\delta \leq \min\{\Delta_{\mathrm{f}}, \Delta_{\mathrm{s}}\}$. Choose $\eta \in (0,1)$, $\eta \leq \underline{\alpha}(\delta)/2$, $\Omega_{\mathrm{s}} = \underline{\alpha}^{-1}(\overline{\alpha}(\Delta_{\mathrm{s}}) + 1)$, $\lambda_D \in (\exp(-1), 1)$, then define the following compact sets:

$$\begin{aligned} \mathcal{K}_{\mathrm{s}} &= [\Omega_\chi \times (C_{\mathrm{s}} \cup D_{\mathrm{s}})] \cap \{(\chi, x_{\mathrm{s}}) : V(\chi, x_{\mathrm{s}}) \leq \Omega_{\mathrm{s}}\} \\ \mathcal{K}_{\mathrm{f}} &= \{x_{\mathrm{f}} : V_{\mathrm{f}}(x_{\mathrm{f}}) \leq \Delta_{\mathrm{f}} + \gamma, \text{ for some } \gamma > 0\}. \end{aligned} \tag{B.20}$$

It is possible then to define the following positive quantities, which exist and are bounded by continuity of the arguments and compactness of $\mathcal{K}_{\mathrm{f}}$, $\mathcal{K}_{\mathrm{s}}$:

$$\begin{aligned} \delta_{\mathrm{f}} &= \max_{\substack{x_{\mathrm{f}} \in \mathcal{K}_{\mathrm{f}}, \\ (\chi, x_{\mathrm{s}}) \in \mathcal{K}_{\mathrm{s}}}} |B_{\mathrm{f}}| \bar{f}_h(x_{\mathrm{f}}, x_{\mathrm{s}}), \\ \overline{\mu} &= \max_{(\chi, x_{\mathrm{s}}) \in \mathcal{K}_{\mathrm{s}}} \mu((\chi, x_{\mathrm{s}})) \\ R &= \frac{\eta/2}{\max\limits_{\substack{x_{\mathrm{f}} \in \mathcal{K}_{\mathrm{f}}, \\ (\chi, x_{\mathrm{s}}) \in \mathcal{K}_{\mathrm{s}} \cap (\omega_\chi \times D_{\mathrm{s}})}} \nu(x_{\mathrm{f}}, \chi, x_{\mathrm{s}})}, \\ r &= \min\{2\Delta_{\mathrm{f}}, (\lambda_D - \exp(-1))R\}, \\ \lambda_C &= \frac{1}{\Lambda \log\left(2\frac{\Delta_{\mathrm{f}} + \gamma}{r}\right)} \end{aligned} \tag{B.21}$$

Pick $0 < \varepsilon^* < 1$ such that:

$$\begin{aligned} \varepsilon^* &< \min\left\{\lambda_C, \frac{r}{2\delta_{\mathrm{f}}}, \frac{\delta}{\delta_{\mathrm{f}}}, \frac{\eta}{2\overline{\mu}\delta_{\mathrm{f}}}\right\}, \\ \varepsilon^*\delta_{\mathrm{s}}(\varepsilon^*) &\leq \eta, \quad \delta_{\mathrm{s}}(y) = 2\left(\frac{\overline{\mu}\Delta_{\mathrm{f}}}{1-y}\frac{1}{1-\lambda_D}\right) \end{aligned} \tag{B.22}$$

then choose, and fix, a positive scalar $\varepsilon \leq \varepsilon^*$.
Define a hybrid system, $\mathcal{H}_{\mathcal{K}}$, described by:

$$\begin{aligned} \begin{pmatrix} \dot{z}_{\mathrm{f}} \\ \dot{\phi} \\ \dot{z}_{\mathrm{s}} \end{pmatrix} &\in \begin{pmatrix} F_{\mathrm{f}}(z_{\mathrm{f}}, \phi, z_{\mathrm{s}}) \\ F_\chi(\phi) \\ F_{\mathrm{s}}(z_{\mathrm{f}}, \phi, z_{\mathrm{s}}) \end{pmatrix}, \quad \begin{pmatrix} z_{\mathrm{f}} \\ \phi \\ z_{\mathrm{s}} \end{pmatrix} \in \begin{pmatrix} \mathcal{K}_{\mathrm{f}} \\ \mathcal{K}_{\mathrm{s}} \cap (\omega_\chi \times C_{\mathrm{s}}) \end{pmatrix} \\ \begin{pmatrix} z_{\mathrm{f}}^+ \\ \phi^+ \\ z_{\mathrm{s}}^+ \end{pmatrix} &\in \begin{pmatrix} \mathrm{diag}\{G_{\mathrm{f}}, G_{\mathrm{f}}\} z_{\mathrm{f}} \\ \phi \\ G_{\mathrm{s}}(z_{\mathrm{f}}, \phi, z_{\mathrm{s}}) \end{pmatrix}, \quad \begin{pmatrix} z_{\mathrm{f}} \\ \phi \\ z_{\mathrm{s}} \end{pmatrix} \in \begin{pmatrix} \mathcal{K}_{\mathrm{f}} \\ \mathcal{K}_{\mathrm{s}} \cap (\omega_\chi \times D_{\mathrm{s}}) \end{pmatrix} \end{aligned} \tag{B.23}$$

which agrees with the solutions of the original error dynamics, except with the solutions restricted to $\mathcal{K}_{\mathrm{f}}$, $\mathcal{K}_{\mathrm{s}}$. With a slight abuse of notation, use $(z_{\mathrm{f}}, \phi, z_{\mathrm{s}})$ to indicate the solutions of $\mathcal{H}_{\mathcal{K}}$. Firstly, note that it is possible to apply the Gronwall-Bellman Lemma to yield, for any $(t, j) \in \mathrm{dom}((z_{\mathrm{f}}, \phi, z_{\mathrm{s}}))$:

$$|z_{\mathrm{f}}(t, j)| \leq \exp\left(-t/\varepsilon\right)|z_{\mathrm{f}}(0,0)| + \varepsilon\delta_{\mathrm{f}}. \tag{B.24}$$

From the bounds (B.22), it follows that:

$$|z_{\mathrm{f}}(t, j)| \leq \exp\left(-t/\varepsilon\right)|z_{\mathrm{f}}(0,0)| + \min\left\{\delta, \frac{r}{2}, \frac{\eta}{2\overline{\mu}}\right\}, \tag{B.25}$$

and in addition we have $|x_{\mathrm{f}}(1/\Lambda, 0)| \leq r$, therefore every jump of the slow subsystem satisfies, for $V_{\mathrm{s}}(\phi, z_{\mathrm{s}}) \geq \eta/2$:

$$\begin{aligned} V_{\mathrm{s}}(\phi, g) &\leq \exp(-1)V_{\mathrm{s}}(\phi, z_{\mathrm{s}}) + \frac{\eta}{2}(\lambda_D - \exp(-1)) \\ &\leq \lambda_D V_{\mathrm{s}}(\phi, z_{\mathrm{s}}) \\ (z_f, \phi, z_{\mathrm{s}}) &\in \mathcal{K}_{\mathrm{f}} \times \mathcal{K}_{\mathrm{s}} \cap (\Omega_\chi \times C_{\mathrm{s}}), g \in G_{\mathrm{s}}(z_{\mathrm{f}}, \phi, z_{\mathrm{s}}). \end{aligned} \tag{B.26}$$

Hence, we obtain the following system, defined for $V_{\mathrm{s}}(\phi, z_{\mathrm{s}}) \geq \eta/2$:

$$\begin{aligned} \dot{V}_{\mathrm{s}} &\leq -V_{\mathrm{s}} + \overline{\mu}|z_{\mathrm{f}}(t, j)|, \quad (\chi, x_{\mathrm{s}}) \in \mathcal{K}_{\mathrm{s}} \cap (\omega_\chi \times C_{\mathrm{s}}) \\ V_{\mathrm{s}}^+ &\leq \lambda_D V_{\mathrm{s}} \quad (\chi, x_{\mathrm{s}}) \in \mathcal{K}_{\mathrm{s}} \cap (\omega_\chi \times D_{\mathrm{s}}). \end{aligned} \tag{B.27}$$

Note that $V_{\mathrm{s}}(\phi, z_{\mathrm{s}}) \leq \eta$ implies $\sigma(\phi, z_{\mathrm{s}}) \leq \delta$. Define $U = V_{\mathrm{s}} - \eta/2$, then we obtain (the constant term of $\overline{\mu}z_{\mathrm{f}}$ is bounded by $\eta/2$):

$$\begin{aligned} \dot{U} &\leq -U + \overline{\mu}\exp\left(-\frac{t}{\varepsilon}\right)|z_{\mathrm{f}}(0,0)|, \quad (\chi, z_{\mathrm{s}}) \in \begin{matrix} \mathcal{K}_{\mathrm{s}} \cap \\ (\omega_\chi \times C_{\mathrm{s}}) \end{matrix} \\ U^+ &\leq \lambda_D U, \qquad (\chi, z_{\mathrm{s}}) \in \mathcal{K}_{\mathrm{s}} \cap (\omega_\chi \times D_{\mathrm{s}}). \end{aligned} \tag{B.28}$$

It can be shown that the solutions of the above system are bounded by:

$$U(t, j) \leq \lambda^j \exp(-t)U(0,0) + \frac{\overline{\mu}|z_{\mathrm{f}}(0,0)|\varepsilon}{1-\varepsilon}\sum_{i=0}^{j}\lambda_D^i \exp(-t). \tag{B.29}$$

Clearly, the sum on the right is a geometric series, with ratio $\lambda_D \in (0,1)$, hence it is upper bounded by the sum of the corresponding infinite series:

$$U(t,j) \leq \lambda_D^j \exp(-t) U(0,0) + \frac{\overline{\mu}|z_\mathrm{f}(0,0)|\varepsilon}{1-\varepsilon} \frac{\exp(-t)}{1-\lambda_D}, \tag{B.30}$$

therefore:

$$\begin{aligned} V_\mathrm{s}(t,j) &\leq \lambda_D^{t+j} V_\mathrm{s}(0,0) + \varepsilon \left(\frac{\overline{\mu}|z_\mathrm{f}(0,0)|}{1-\varepsilon} \frac{1}{1-\lambda_D} \right) + \frac{\eta}{2}, \\ &\leq \lambda_D^{t+j} V_\mathrm{s}(0,0) + \eta. \end{aligned} \tag{B.31}$$

This bound can be readily converted into one on z_s as follows:

$$\sigma(\phi(t,j), z_\mathrm{s}(t,j)) \leq \underline{\alpha}^{-1} \left(2\lambda_D^{t+j} \overline{\alpha}(\sigma(\phi(0,0), z_\mathrm{s}(0,0))) \right) + \delta, \tag{B.32}$$

where we can pick $\beta_\mathrm{s}(s,r) = \underline{\alpha}^{-1}(2\lambda_D^r \overline{\alpha}(s))$. Thus, we have proved the desired bounds for $\mathcal{H}_\mathcal{K}$, which can be summarized as:

$$\begin{aligned} |z_\mathrm{f}(t,j)| &\leq \exp(-t/\varepsilon) |z_\mathrm{f}(0,0)| + \delta \\ \sigma(\phi(t,j), z_\mathrm{s}(t,j)) &\leq \beta_\mathrm{s}(\sigma(\phi(0,0), z_\mathrm{s}(0,0)), t+j) + \delta. \end{aligned} \tag{B.33}$$

To conclude the proof, apply the same considerations in (Sanfelice and Teel, 2011) to show that, if the trajectories of the original system agree with those of $\mathcal{H}_\mathcal{K}$, they cannot leave the compact sets $\mathcal{K}_\mathrm{f}$, $\mathcal{K}_\mathrm{s}$ by contradiction. We omit the details here for brevity. Finally, the bounds in the statement of the theorem are recovered noticing that $\chi(t)$ is defined for all t and always belongs to Ω_χ, therefore $\sigma = \sigma_\mathrm{s}$ for all solutions of the original system.

Bibliography

Acarnley, Paul P and John F Watson (2006). "Review of position-sensorless operation of brushless permanent-magnet machines". In: *IEEE Transactions on Industrial Electronics* 53.2, pp. 352–362.

Ames, Aaron D., Jessy W. Grizzle, and Paulo Tabuada (2014). "Control barrier function based quadratic programs with application to adaptive cruise control". In: *53rd IEEE Conference on Decision and Control*. IEEE, pp. 6271–6278.

Ames, Aaron D., Xiangru Xu, Jessy W. Grizzle, and Paulo Tabuada (2017). "Control Barrier Function Based Quadratic Programs for Safety Critical Systems". In: *IEEE Transactions on Automatic Control* 62.8, pp. 3861–3876.

Astolfi, Alessandro and Romeo Ortega (2003). "Immersion and invariance: A new tool for stabilization and adaptive control of nonlinear systems". In: *IEEE Transactions on Automatic control* 48.4, pp. 590–606.

Atamuradov, Vepa, Kamal Medjaher, Pierre Dersin, Benjamin Lamoureux, and Noureddine Zerhouni (2017). "Prognostics and health management for maintenance practitioners-review, implementation and tools evaluation". In: *International Journal of Prognostics and Health Management* 8.060, pp. 1–31.

Barabanov, Nikita and Romeo Ortega (2017). "On global asymptotic stability of $\dot{x} = -\phi(t)\phi^T(t)x$ with ϕ not persistently exciting". In: *Systems & Control Letters* 109, pp. 24–29.

Barbieri, Matteo, Roberto Diversi, and Andrea Tilli (2020). "Condition monitoring of electric-cam mechanisms based on Model-of-Signals of the drive current higher-order differences". In: *Submitted to the 21st IFAC World Congress*.

Barbieri, Matteo, Alessandro Bosso, Christian Conficoni, Roberto Diversi, Matteo Sartini, and Andrea Tilli (2018). "An Onboard Model-of-signals Approach for Condition Monitoring in Automatic Machines". In: *Enterprise Interoperability: Smart Services and Business Impact of Enterprise Interoperability*, pp. 263–269.

Barrau, Axel and Silvère Bonnabel (2016). "The invariant extended Kalman filter as a stable observer". In: *IEEE Transactions on Automatic Control* 62.4, pp. 1797–1812.

Bazylev, Dmitry, Anton Pyrkin, and Alexey Bobtsov (2018). "Position and speed observer for PMSM with unknown stator resistance". In: *2018 European Control Conference (ECC)*. IEEE, pp. 1613–1618.

Bellens, Steven, Joris De Schutter, and Herman Bruyninckx (2012). "A hybrid pose/wrench control framework for quadrotor helicopters". In: *2012 IEEE International Conference on Robotics and Automation (ICRA)*. IEEE, pp. 2269–2274.

Bernard, Pauline and Laurent Praly (2018). "Convergence of gradient observer for rotor position and magnet flux estimation of permanent magnet synchronous motors". In: *Automatica* 94, pp. 88–93.

— (2019). "Estimation of position and resistance of a sensorless PMSM: a nonlinear Luenberger approach for a non-observable system". In: *HAL*.

Bin, Michelangelo (2019). "Adaptive Output Regulation For Multivariable Nonlinear Systems Via Hybrid Identification Techniques". PhD thesis. alma.

Bin, Michelangelo, Pauline Bernard, and Lorenzo Marconi (2019). "Approximate Nonlinear Regulation via Identification-Based Adaptive Internal Models". In: *arXiv preprint arXiv:1907.05050*.

Blanchini, Franco and Stefano Miani (2000). "Any domain of attraction for a linear constrained system is a tracking domain of attraction". In: *SIAM Journal on Control and Optimization* 38.3, pp. 971–994.

Bobtsov, Alexey A., Anton A. Pyrkin, Romeo Ortega, Slobodan N. Vukosavic, Aleksandar M. Stankovic, and Elena V. Panteley (2015). "A robust globally convergent position observer for the permanent magnet synchronous motor". In: *Automatica* 61, pp. 47–54.

Bosso, Alessandro (2016). "Osservatore e Controllore Sensorless ad Elevate Prestazioni per Propulsione Elettrica di Unmanned Aerial Vehicles". MA thesis. University of Bologna.

Bosso, Alessandro, Ilario A. Azzollini, and Simone Baldi (2019). "Global Frequency Synchronization over Networks of Uncertain Second Order Kuramoto Oscillators via Distributed Adaptive Tracking". In: *58th IEEE Conference on Decision and Control*.

Bosso, Alessandro, Ilario A. Azzollini, and Andrea Tilli (2020). "A Semi-global Hybrid Sensorless Observer for Permanent Magnets Synchronous Machines with Unknown Mechanical Model". In: *arXiv preprint arXiv:2002.03635*.

Bosso, Alessandro, Christian Conficoni, and Andrea Tilli (2016). "Multirotor UAV flight endurance and control: the drive perspective". In: *IECON 2016-42nd Annual Conference of the IEEE Industrial Electronics Society*. IEEE, pp. 1839–1845.

Bosso, Alessandro, Andrea Tilli, and Christian Conficoni (2020). "A Robust Sensorless Controller-Observer Strategy for PMSMs with Unknown Resistance and Mechanical Model". In: *arXiv preprint arXiv:2002.01823*.

Bosso, Alessandro, Nicola Mimmo, Christian Conficoni, and Andrea Tilli (2018). "Global Observability Analysis of Aided-INS for UAVs Equipped with Visual Odometry Systems". In: *2018 European Control Conference (ECC)*. IEEE, pp. 2909–2916.

Bosso, Alessandro, Andrea Serrani, Christian Conficoni, and Andrea Tilli (2019). "Constrained-Inversion MRAC: An Approach Combining Hard Constraints and Adaptation in Uncertain Nonlinear Systems". In: *58th IEEE Conference on Decision and Control*.

Bosso, Alessandro, Christian Conficoni, Davide Raggini, and Andrea Tilli (2020). "A Computational-Effective Field-Oriented Control Strategy for Accurate and Efficient Electric Propulsion of Unmanned Aerial Vehicles". In: *Submitted to IEEE/ASME Transactions on Mechatronics*.

Boyd, Stephen and Lieven Vandenberghe (2004). *Convex optimization*. Cambridge university press.

Burger, Mathias and Martin Guay (2010). "Robust Constraint Satisfaction for Continuous-Time Nonlinear Systems in Strict Feedback Form". In: *IEEE Transactions on Automatic Control* 55.11, pp. 2597–2601.

Byrnes, Christopher I and Alberto Isidori (2003). "Limit sets, zero dynamics, and internal models in the problem of nonlinear output regulation". In: *IEEE Transactions on Automatic Control* 48.10, pp. 1712–1723.

Cai, Chaohong, Andrew R Teel, and Rafal Goebel (2008). "Smooth Lyapunov functions for hybrid systems part II:(pre) asymptotically stable compact sets". In: *IEEE Transactions on Automatic Control* 53.3, pp. 734–748.

Cai, Zhijun, Marcio S de Queiroz, and Darren M Dawson (2006). "A sufficiently smooth projection operator". In: *IEEE Transactions on Automatic Control* 51.1, pp. 135–139.

Camacho, Eduardo F and Carlos Bordons (2007). "Nonlinear model predictive control: An introductory review". In: *Assessment and future directions of nonlinear model predictive control*. Springer, pp. 1–16.

Cho, Seong Yun, Byung Doo Kim, Young Su Cho, and Wan Sik Choi (2007). "Observability analysis of the INS/GPS navigation system on the measurements in land vehicle applications". In: *2007 International Conference on Control, Automation and Systems*. IEEE, pp. 841–846.

Chowdhury, Dhrubajit and Hassan K. Khalil (2017). "Funnel control of higher relative degree systems". In: *2017 American Control Conference*. IEEE, pp. 598–603.

Chung, Dohyoung, Chan Gook Park, and Jang Gyu Lee (1996). "Observability analysis of strapdown inertial navigation system using Lyapunov transformation". In: *35th IEEE Conference on Decision and Control*. IEEE, pp. 23–28.

Cox, Timothy H, Christopher J Nagy, Mark A Skoog, Ivan A Somers, and Ryan Warner (2004). "Civil UAV capability assessment". In: *NASA, Tech. Rep.*

De Marco, Simone (2017). "Output regulation for systems with symmetry". PhD thesis. alma.

Dorfler, Florian and Francesco Bullo (2012). "Synchronization and transient stability in power networks and nonuniform Kuramoto oscillators". In: *SIAM Journal on Control and Optimization* 50.3, pp. 1616–1642.

Driessens, Scott and Paul Pounds (2015). "The triangular quadrotor: a more efficient quadrotor configuration". In: *IEEE Transactions on Robotics* 31.6, pp. 1517–1526.

Farrell, Jay (2008). *Aided navigation: GPS with high rate sensors*. McGraw-Hill.

Freeman, Randy and Petar V. Kokotovic (1996). "Inverse optimality in robust stabilization". In: *SIAM Journal on Control and Optimization* 34.4, pp. 1365–1391.

Freeman, Randy and Laurent Praly (1998). "Integrator Backstepping for Bounded Controls and Control Rates". In: *IEEE Transactions on Automatic Control* 43.2, pp. 258–262.

Galeani, Sergio, Sophie Tarbouriech, Matthew Turner, and Luca Zaccarian (2009). "A tutorial on modern anti-windup design". In: *European Journal of Control* 15.3-4, pp. 418–440.

Gao, Shesheng, Wenhui Wei, Yongmin Zhong, and Zhihua Feng (2014). "Rapid alignment method based on local observability analysis for strapdown inertial navigation system". In: *Acta Astronautica* 94.2, pp. 790–798.

Garone, Emanuele, Stefano Di Cairano, and Ilya Kolmanovsky (2017). "Reference and command governors for systems with constraints: A survey on theory and applications". In: *Automatica* 75, pp. 306–328.

Garone, Emanuele and Marco M. Nicotra (2015). "Explicit reference governor for constrained nonlinear systems". In: *IEEE Transactions on Automatic Control* 61.5, pp. 1379–1384.

Gayaka, Shreekant, Lu Lu, and Bin Yao (2012). "Global stabilization of a chain of integrators with input saturation and disturbances: A new approach". In: *Automatica* 48.7, pp. 1389–1396.

Gilbert, Elmer G, Ilya Kolmanovsky, and Kok Tin Tan (1995). "Discrete-time reference governors and the nonlinear control of systems with state and control constraints". In: *International Journal of robust and nonlinear control* 5.5, pp. 487–504.

Goebel, R, Ricardo G Sanfelice, and Andrew R Teel (2012). *Hybrid dynamical systems: modeling stability, and robustness*. Princeton University Press, Princeton, NJ.

Goebel, Rafal, Ricardo G. Sanfelice, and Andrew R. Teel (2009). "Hybrid dynamical systems". In: *IEEE Control Systems Magazine* 29.2, pp. 28–93.

Grimm, Gene, Jay Hatfield, Ian Postlethwaite, Andrew R Teel, Matthew C Turner, and Luca Zaccarian (2003). "Antiwindup for stable linear systems with input saturation: an LMI-based synthesis". In: *IEEE Transactions on Automatic Control* 48.9, pp. 1509–1525.

Hartman, Philip (1963). "On the local linearization of differential equations". In: *Proceedings of the American Mathematical Society* 14.4, pp. 568–573.

Hatanaka, Takeshi and Kiyotsugu Takaba (2005). "Output feedback reference governor for nonlinear systems". In: *Transactions of the Society of Instrument and Control Engineers* 41.10, pp. 803–812.

Hauser, John and Alessandro Saccon (2006). "A barrier function method for the optimization of trajectory functionals with constraints". In: *45th IEEE Conference on Decision and Control*. IEEE, pp. 864–869.

Hermann, Robert and Arthur Krener (1977). "Nonlinear controllability and observability". In: *IEEE Transactions on Automatic Control* 22.5, pp. 728–740.

Hernandez, Joshua, Konstantine Tsotsos, and Stefano Soatto (2015). "Observability, identifiability and sensitivity of vision-aided inertial navigation". In: *2015 IEEE International Conference on Robotics and Automation (ICRA)*. IEEE, pp. 2319–2325.

Hilairet, M., F. Auger, and E. Berthelot (2009). "Speed and rotor flux estimation of induction machines using a two-stage extended Kalman filter". In: *Automatica* 45.1, pp. 1819–1827.

Honegger, Dominik, Lorenz Meier, Petri Tanskanen, and Marc Pollefeys (2013). "An open source and open hardware embedded metric optical flow cmos camera for indoor and outdoor applications". In: *2013 IEEE International Conference on Robotics and Automation (ICRA)*. IEEE, pp. 1736–1741.

Hong, Sinpyo, Man Hyung Lee, Jose A Rios, and Jason L Speyer (2002). "Observability analysis of INS with a GPS multi-antenna system". In: *KSME International Journal* 16.11, pp. 1367–1378.

Hong, Sinpyo, Man Hyung Lee, Ho-Hwan Chun, Sun-Hong Kwon, and Jason L Speyer (2005). "Observability of error states in GPS/INS integration". In: *IEEE Transactions on Vehicular Technology* 54.2, pp. 731–743.

Hopfe, Norman, Achim Ilchmann, and Eugene P. Ryan (2010). "Funnel Control With Saturation: Nonlinear SISO Systems". In: *IEEE Transactions on Automatic Control* 55.9, pp. 2177–2182.

Huang, Lan, Jianmei Song, and Chunyan Zhang (2017). "Observability analysis and filter design for a vision inertial absolute navigation system for UAV using landmarks". In: *Optik* 149, pp. 455–468.

Ibarra-Rojas, Sebastian, Jaime Moreno, and Gerardo Espinosa-Pérez (2004). "Global observability analysis of sensorless induction motors". In: *Automatica* 40.6, pp. 1079–1085.

Igarashi, Yuji, Takeshi Hatanaka, Masayuki Fujita, and Mark W Spong (2009). "Passivity-based attitude synchronization in $SE(3)$". In: *IEEE Transactions on Control Systems Technology* 17.5, pp. 1119–1134.

Ioannou, Petros A and Jing Sun (2012). *Robust adaptive control*. Courier Corporation.

Isidori, Alberto (2012). *Nonlinear control systems II*. Springer Science & Business Media.

— (2013). *Nonlinear control systems*. Springer Science & Business Media.

Isidori, Alberto and Christopher I Byrnes (1990). "Output regulation of nonlinear systems". In: *IEEE Transactions on Automatic Control* 35.2, pp. 131–140.

Jankovic, Mrdjan (2018). “Robust control barrier functions for constrained stabilization of nonlinear systems”. In: *Automatica* 96, pp. 359–367.

Kalman, Rudolf Emil et al. (1960). “Contributions to the theory of optimal control”. In: *Boletin Sociedad Matematica Mexicana* 5.2, pp. 102–119.

Kanellakopoulos, I, Petar V. Kokotovic, and A. S. Morse (1991). “Systematic design of adaptive controllers for feedback linearizable systems”. In: *IEEE Transactions on Automatic Control* 36.11, pp. 1241–1253.

Kapasouris, Petros, Michael Athans, and Günter Stein (1990). “Design of feedback control systems for stable plants with saturating actuators”. In: *Proc. IFAC symposium on nonlinear control system design*, pp. 302–307.

Khalil, Hassan K. (2002). *Nonlinear Systems, third ed.* Prentice-Hall.

Khalil, Hassan K., E. G. Strangas, and S. Jurkovic (2009). “Speed Observer and Reduced Nonlinear Model for Sensorless Control of Induction Motors”. In: *IEEE Transactions on Control Systems Technology* 17.4, pp. 327–339.

Kimmel, Melanie, Christoph Jähne, and Sandra Hirche (2016). “Augmented invariance control for systems with smoothness constraints”. In: *55th IEEE Conference on Decision and Control*. IEEE, pp. 4867–4873.

Kolmanovsky, Ilya V and Jing Sun (2006). “Parameter governors for discrete-time nonlinear systems with pointwise-in-time state and control constraints”. In: *Automatica* 42.5, pp. 841–848.

Krstic, Miroslav, Ioannis Kanellakopoulos, and Petar V. Kokotovic (1995). *Nonlinear and adaptive control design*. Wiley New York.

Krstic, Miroslav and Petar V. Kokotovic (1995). “Adaptive nonlinear design with controller-identifier separation and swapping”. In: *IEEE Transactions on Automatic Control* 40.3, pp. 426–440.

Lee, H. and J. Lee (2013). “Design of Iterative Sliding mode Observer for Sensorless PMSM Control”. In: *IEEE Transactions on Control Systems Technology* 21.4, pp. 1394–1399.

Löfberg, Johan (2012). “Oops! I cannot do it again: Testing for recursive feasibility in MPC”. In: *Automatica* 48.3, pp. 550–555.

Loría, Antonio, Elena V. Panteley, Dobrivoje Popovic, and Andrew R. Teel (2005). “A nested Matrosov theorem and persistency of excitation for uniform convergence in stable nonautonomous systems”. In: *IEEE Transactions on Automatic Control* 50.2, pp. 183–198.

Lozier, J (1956). “A steady state approach to the theory of saturable servo systems”. In: *IRE Transactions on Automatic Control* 1.1, pp. 19–39.

Mahony, Robert, Tarek Hamel, and Jean-Michel Pflimlin (2008). “Nonlinear complementary filters on the special orthogonal group”. In: *IEEE Transactions on Automatic Control* 53.5, pp. 1203–1217.

Marino, R., P. Tomei, and C. M. Verrelli (2008). “An adaptive tracking control from current measurements for induction motors with uncertain load torque and rotor resistance”. In: *Automatica* 44.2, pp. 2593–2599.

— (2010). *Induction Motor Control Design*. Springer, London (UK).

Martinelli, Agostino (2018). “Nonlinear unknown input observability: Extension of the observability rank condition”. In: *IEEE Transactions on Automatic Control* 64.1, pp. 222–237.

Mayhew, Christopher G., Ricardo G. Sanfelice, and Andrew R. Teel (2011). “Quaternion-based hybrid control for robust global attitude tracking”. In: *IEEE Transactions on Automatic Control* 56.11, pp. 2555–2566.

Mayne, David Q, James B Rawlings, Christopher V Rao, and Pierre OM Scokaert (2000). “Constrained model predictive control: Stability and optimality”. In: *Automatica* 36.6, pp. 789–814.

Mazenc, Frédéric and Samuel Bowong (2004). “Backstepping with bounded feedbacks for time-varying systems”. In: *SIAM Journal on Control and Optimization* 43.3, pp. 856–871.

Mazenc, Frédéric and Abderrhaman Iggidr (2004). “Backstepping with bounded feedbacks”. In: *Systems & Control Letters* 51.3-4, pp. 235–245.

Mazenc, Frédéric and Laurent Praly (1996). “Adding Integrations, Saturated Controls, and Stabilization for Feedforward Systems”. In: *IEEE Transactions on Automatic Control* 41.11, pp. 1559–1578.

Montanari, M., S. Paresada, and Andrea Tilli (2006). “A speed-sensorless indirect field-oriented control for induction motors based on high gain speed estimation”. In: *Automatica* 42.10, pp. 1637–1650.

Morbidi, Fabio, Roel Cano, and David Lara (2016). “Minimum-energy path generation for a quadrotor UAV”. In: *2016 IEEE International Conference on Robotics and Automation (ICRA)*. IEEE, pp. 1492–1498.

Nandi, Subhasis, Hamid A Toliyat, and Xiaodong Li (2005). “Condition monitoring and fault diagnosis of electrical motors—A review”. In: *IEEE transactions on energy conversion* 20.4, pp. 719–729.

Ngo, Khoi B, Robert Mahony, and Zhong-Ping Jiang (2005). “Integrator Backstepping using Barrier Functions for Systems with Multiple State Constraints”. In: *44th IEEE Conference on Decision and Control*. IEEE, pp. 8306–8312.

Nicotra, Marco M. and Emanuele Garone (2018). “The explicit reference governor: A general framework for the closed-form control of constrained nonlinear systems”. In: *IEEE Control Systems Magazine* 38.4, pp. 89–107.

Novotny, D. W. and T. A. Lipo (2010). *Introduction to Electric Machines and Drives*. University of Winsconsin.

Ortega, Romeo, Laurent Praly, Alessandro Astolfi, Junggi Lee, and Kwanghee Nam (2010). “Estimation of rotor position and speed of permanent magnet synchronous motors with guaranteed stability”. In: *IEEE Transactions on Control Systems Technology* 19.3, pp. 601–614.

Panahandeh, Ghazaleh, Seth Hutchinson, Peter Händel, and Magnus Jansson (2016). “Planar-based visual inertial navigation: Observability analysis and motion estimation”. In: *Journal of Intelligent & Robotic Systems* 82.2, pp. 277–299.

Pavlov, A, Nathan Van De Wouw, and Henk Nijmeijer (2007). “Global nonlinear output regulation: convergence-based controller design”. In: *Automatica* 43.3, pp. 456–463.

Pavlov, Alexey and Nathan van de Wouw (2017). “Convergent systems: nonlinear simplicity”. In: *Nonlinear Systems*. Springer, pp. 51–77.

Pavlov, Alexey, Alexander Pogromsky, Nathan van de Wouw, and Henk Nijmeijer (2004). “Convergent dynamics, a tribute to Boris Pavlovich Demidovich”. In: *Systems & Control Letters* 52.3-4, pp. 257–261.

Pounds, Paul, Robert Mahony, and Peter Corke (2007). “System identification and control of an aerobot drive system”. In: *2007 Information, Decision and Control*. IEEE, pp. 154–159.

Primbs, James A, Vesna Nevistic, and John C Doyle (2000). “A receding horizon generalization of pointwise min-norm controllers”. In: *IEEE Transactions on Automatic Control* 45.5, pp. 898–909.

Propoi, A. I. (1963). “Use of linear programming methods for synthesizing sampled-data automatic systems”. In: *Automation and Remote Control* 24.7, pp. 837–844.

Ren, Beibei, Shuzi Sam Ge, Keng Peng Tee, and Tong Heng Lee (2009). "Adaptive control for parametric output feedback systems with output constraint". In: *48th IEEE Conference on Decision and Control held jointly with 2009 28th Chinese Control Conference*. IEEE, pp. 6650–6655.
— (2010). "Adaptive neural control for output feedback nonlinear systems using a barrier Lyapunov function". In: *IEEE Transactions on Neural Networks* 21.8, pp. 1339–1345.
Richalet, Jacques, A Rault, JL Testud, and J Papon (1978). "Model predictive heuristic control". In: *Automatica (Journal of IFAC)* 14.5, pp. 413–428.
Sanfelice, Ricardo G and Andrew R Teel (2009). "Asymptotic stability in hybrid systems via nested Matrosov functions". In: *IEEE Transactions on Automatic Control* 54.7, pp. 1569–1574.
Sanfelice, Ricardo G. and Andrew R. Teel (2011). "On singular perturbations due to fast actuators in hybrid control systems". In: *Automatica* 47.4, pp. 629–701.
Sarlette, Alain, Rodolphe Sepulchre, and Naomi Ehrich Leonard (2009). "Autonomous rigid body attitude synchronization". In: *Automatica* 45.2, pp. 572–577.
Sastry, Shankar and Marc Bodson (2011). *Adaptive control: stability, convergence and robustness*. Courier Corporation.
Scardovi, Luca, Alain Sarlette, and Rodolphe Sepulchre (2007). "Synchronization and balancing on the N-torus". In: *Systems & Control Letters* 56.5, pp. 335–341.
Serrani, Andrea and Michael A. Bolender (2016). "Addressing limits of operability of the scramjet engine in adaptive control of a generic hypersonic vehicle". In: *55th IEEE Conference on Decision and Control*. IEEE, pp. 7567–7572.
Serrani, Andrea, Alberto Isidori, and Lorenzo Marconi (2001). "Semi-global nonlinear output regulation with adaptive internal model". In: *IEEE Transactions on Automatic Control* 46.8, pp. 1178–1194.
Slotine, Jean-Jacques E, Weiping Li, et al. (1991). *Applied nonlinear control*. Vol. 199. 1. Prentice hall Englewood Cliffs, NJ.
Sontag, Eduardo D (1989). "A 'universal' construction of Artstein's theorem on nonlinear stabilization". In: *Systems & Control Letters* 13.2, pp. 117–123.
— (1999). "Clocks and insensitivity to small measurement errors". In: *ESAIM: Control, Optimisation and Calculus of Variations* 4, pp. 537–557.
Sowah, Robert A, Moses Amoasi Acquah, Abdul R Ofoli, Godfrey A Mills, and Koudjo M Koumadi (2017). "Rotational energy harvesting to prolong flight duration of quadcopters". In: *IEEE Transactions on Industry Applications* 53.5, pp. 4965–4972.
Tang, Yonggang, Yuanxin Wu, Meiping Wu, Wenqi Wu, Xiaoping Hu, and Lincheng Shen (2008). "INS/GPS integration: Global observability analysis". In: *IEEE Transactions on Vehicular Technology* 58.3, pp. 1129–1142.
Tee, Keng Peng and Shuzi Sam Ge (2009). "Control of nonlinear systems with full state constraint using a barrier Lyapunov function". In: *48th IEEE Conference on Decision and Control held jointly with 2009 28th Chinese Control Conference*. IEEE.
— (2011). "Control of nonlinear systems with partial state constraints using a barrier Lyapunov function". In: *International Journal of Control* 84.12, pp. 2008–2023.
— (2012). "Control of State-Constrained Nonlinear Systems Using Integral Barrier Lyapunov Functionals". In: *51st IEEE Conference on Decision and Control*. IEEE, pp. 3239–3244.
Tee, Keng Peng, Shuzi Sam Ge, and Eng Hock Tay (2009). "Barrier Lyapunov Functions for the control of output-constrained nonlinear systems". In: *Automatica* 45.4, pp. 918–927.

Tee, Keng Peng, Beibei Ren, and Shuzi Sam Ge (2011). “Control of nonlinear systems with time-varying output constraints”. In: *Automatica* 47.11, pp. 2511–2516.

Teel, Andrew R. (1992). “Global stabilization and restricted tracking for multiple integrators with bounded controls”. In: *Systems & Control Letters* 18.3, pp. 165–171.

Teel, Andrew R., Luc Moreau, and Dragan Nešić (2003). “A unified framework for input-to-state stability in systems with two time scales”. In: *IEEE Transactions on Automatic Control* 48.9, pp. 1526–1544.

Teel, Andrew R. and Laurent Praly (2000). “A smooth Lyapunov function from a class-KL estimate involving two positive semidefinite functions”. In: *ESAIM: Control, Optimisation and Calculus of Variations* 5, pp. 313–367.

Tilli, Andrea, Alessandro Bosso, and Christian Conficoni (2019). “Towards sensorless observers for sinusoidal electric machines with variable speed and no mechanical model: A promising approach for PMSMs”. In: *Systems & Control Letters* 123, pp. 16–23.

Tilli, Andrea and Christian Conficoni (2016). “Semiglobal Uniform Asymptotic Stability of an Easy-to-Implement PLL-Like Sensorless Observer for Induction Motors”. In: *IEEE Transactions on Automatic Control* 61.11, pp. 3612–3618.

Tilli, Andrea, Christian Conficoni, and Alessandro Bosso (2017). “A UGAS Sensorless Observer for Permanent Magnets Synchronous Machines including Estimation and Compensation of Dead-Times Effects”. In: *IFAC-PapersOnLine* 50.1, pp. 1891–1897.

Tilli, Andrea, Giovanni Cignali, Christian Conficoni, and Carlo Rossi (2012). “A synchronous coordinates approach in position and speed estimation for permanent magnet synchronous machines”. In: *20th Mediterranean Conference on Control & Automation (MED)*. IEEE, pp. 487–492.

Tsiotras, Panagiotis (1996). “Stabilization and optimality results for the attitude control problem”. In: *Journal of Guidance, Control, and Dynamics* 19.4, pp. 772–779.

Valavanis, Kimon P (2008). *Advances in unmanned aerial vehicles: state of the art and the road to autonomy*. Vol. 33. Springer Science & Business Media.

Vas, P. (1998). *Sensorless Vector and Direct Torque Control*. Oxford Press.

Verrelli, C. M., P. Tomei, Emilio Lorenzani, Giovanni Migliazza, and Fabio Immovilli (2017). “Nonlinear tracking control for sensorless permanent magnet synchronous motors with uncertainties”. In: *Control Engineering Practice* 60, pp. 157–170.

Verrelli, Cristiano Maria, Patrizio Tomei, and Emilio Lorenzani (2018). “Persistency of excitation and position-sensorless control of permanent magnet synchronous motors”. In: *Automatica* 95, pp. 328–335.

Vu, Anh, Arvind Ramanandan, Anning Chen, Jay A Farrell, and Matthew Barth (2012). “Real-time computer vision/DGPS-aided inertial navigation system for lane-level vehicle navigation”. In: *IEEE Transactions on Intelligent Transportation Systems* 13.2, pp. 899–913.

Wolff, J. and M. Buss (2004). “Invariance control design for nonlinear control affine systems under hard state constraints”. In: *IFAC Proceedings Volumes* 37.13, pp. 555–560.

Wu, Yuanxin, Hongliang Zhang, Meiping Wu, Xiaoping Hu, and Dewen Hu (2012). “Observability of strapdown INS alignment: A global perspective”. In: *IEEE Transactions on Aerospace and Electronic Systems* 48.1, pp. 78–102.

Xu, Xiangru, Paulo Tabuada, Jessy W. Grizzle, and Aaron D. Ames (2015). “Robustness of control barrier functions for safety critical control”. In: *IFAC-PapersOnLine* 48.27, pp. 54–61.

Zaccarian, Luca and Andrew R Teel (2011). *Modern anti-windup synthesis: control augmentation for actuator saturation*. Vol. 36. Princeton University Press.

Zaltni, Dalila, Malek Ghanes, Jean Pierre Barbot, and Mohamed Naceur Abdelkrim (2010). "Synchronous motor observability study and an improved zero-speed position estimation design". In: *49th IEEE Conference on Decision and Control*. IEEE, pp. 5074–5079.

Zhang, Zhifei, Alain Sarlette, and Zhihao Ling (2015). "Integral control on Lie groups". In: *Systems & Control Letters* 80, pp. 9–15.